8-2023

Acceleration profiles of adolescent soccer players across a season

Jake A. Melaro
University of Tennessee, Knoxville, jmelaro@vols.utk.edu

To the Graduate Council:

I am submitting herewith a dissertation written by Jake A. Melaro entitled "Acceleration profiles of adolescent soccer players across a season." I have examined the final electronic copy of this dissertation for form and content and recommend that it be accepted in partial fulfillment of the requirements for the degree of Doctor of Philosophy, with a major in Kinesiology.

Joshua T. Weinhandl, Major Professor

We have read this dissertation and recommend its acceptance:

Joshua T. Weinhandl, Songning Zhang, Dawn P. Coe, Louis M. Rocconi

Accepted for the Council:

Dixie L. Thompson

Vice Provost and Dean of the Graduate School

(Original signatures are on file with official student records.)

ACCELERATION PROFILES OF ADOLESCENT SOCCER PLAYERS ACROSS A SEASON

A Dissertation Presented for the
Doctor of Philosophy
Degree
The University of Tennessee, Knoxville

Jake Anthony Melaro
August 2023

DEDICATION

I'd like to dedicate this to my mom and dad, Jenna, Cami, and Noah for their unending support and love.

ACKNOWLEDGMENT

I'd like to thank Dr. Weinhandl for his excellent tutelage, patience, and support throughout my time here in Knoxville. Words cannot express the gratitude I have being your student, colleague, and friend. I would also like to extend my heartfelt thanks towards Shelby, Lauren, Josh, Sean, and the countless other graduate students who I would now consider some of my best friends.

I would like to thank Dr. Zhang, Dr. Coe, and Dr. Rocconi for putting up with lame jokes in my presentations and making the committee process a painless endeavor.

I would like to thank my previous mentors, Dr. Paquette and Dr. Powell, for providing me with a memorable experience in Memphis and helping lay the foundation for my biomechanical journey. I'd also like to Alex and the rest of my University of Memphis cohort for making that experience way more fun than it should have been.

Finally, I would like to acknowledge all of the other people I've met along the way. It's been a wild ride.

ABSTRACT

The injury risk inherent to soccer can be affected by external training loads and intrinsic factors. These intrinsic factors (sex, mass, strength, coordination, etc.) in young athletes can be rapidly altered the near their peak height velocity (PHV) during puberty, modifying their movement complexity and, potentially, their injury risk. While quantification of movement complexity through multiscale entropy analysis have been used in past biomechanical investigations, no studies have incorporated this analysis on tibial accelerometry signals collected in these maturing athletes. The purpose of this study is to collect tibial acceleration data from youth soccer athletes during several discrete drills and determine discrete acceleration metrics or signal complexity differs across athletes based on their relation to PHV, sex, or over the course of a season. Chapter 3 lays out the methodology behind our studies regarding population criteria, experimental protocol, PHV estimation, raw data processing and cleaning, entropy analysis details, and the regression models used to analyze our data. Chapter 4 examines how PHV, sex, and time affects tibial acceleration complexity across youth soccer players while Chapter 5 examines these effects on acceleration peaks and integrals.

Chapter 4 showed some limited significant time effects on tibial movement complexity during only two drills in our protocol. Chapter 5 showed significant effects for PHV, sex, and time on acceleration peaks and integrals across several drills. However, in the case of both complexity and discrete acceleration statistical analyses, model trends suggest that the predictive power of our independent variables is limited.

The findings of this dissertation pave the way for future research focused on injury prevention and its relationship to the growth associated with puberty in adolescent soccer players. It also highlights areas for improvement and expansion in subsequent studies.

TABLE OF CONTENTS

LIST OF TABLES

LIST OF FIGURES

NOMENCLATURE

3D	Three-dimensional
ACL	Anterior cruciate ligament
ACTH	Adrenocorticotropic hormone
AE	Athletic Exposure
ApEn	Approximate entropy
BW	Body weight
CEn	Control entropy
CoM	Center of mass
DHEA	dehydroepiandrosterone
DHT	Dihydrotestosterone
DOF	Degrees of freedom
deg/s	Degrees per second
FEn	Fuzzy entropy
FFM	Fat-free mass
FSH	Follicle stimulating hormone
GRF	Ground reaction force
IMU	Inertial measurement unit
LEFS	Lower Extremity Functional Scale
LH	Luteinizing hormone
LMER	Linear mixed effects regression
ms	Millisecond
MsEn	Multiscale entropy

N	Newton
OSD	Osgood-Schlatter's disease
PHV	Peak height velocity
SEn	Sample entropy
yrs	Years old

Chapter 1: Development of the Problem

Background and Rationale

Almost seven million children and adolescents (6-17 years old) played soccer, or American soccer, in the United States in 2019 (SFIA 2020). Survey data collected by the National Federation of State High School Associations (NFHS) shows that more than 850,000 athletes participated competitively at the high school level that same year (NFHS 2019). Unfortunately, the boon of soccer popularity amongst youth athletes is marred by the injuries that accompany such a dynamic sport. Not including injuries sustained by players on youth and private club rosters, over 400,000 injuries befell high school boys and girls playing or practicing soccer in 2018 (Comstock and Pierpoint 2020). Between youth and high school soccer athletics, the rate per 1,000 athletic exposures is approximately 2.43-17.0 injuries and 2.50-10.60 injuries for boys and girls, respectively (Powell and Barber-Foss 1999; Radelet et al. 2002; Kucera et al. 2005; Comstock and Pierpoint 2020). Further, the rates of injury seem to be elevated at and immediately after peak height velocity (PHV), the pubertal "growth spurt", compared to the time just prior to PHV (Van der Sluis et al. 2013; Van der Sluis et al. 2015). Identifying and preventing the risk factors inherent to child and adolescent soccer training and competition could prevent time lost to injury in this young population.

Musculoskeletal or connective tissue injuries to athletes commonly occur via one of two scenarios: a) an external load acutely exceeds the maximal material tolerance of the tissue and failure occurs or b) repetitive exposure to submaximal loading causes gradual microtrauma to the tissue that can eventually compromise the integrity of the biological structure (Renström and Johnson 1985; DiFiori 2010; DiFiori et al. 2014). External loads placed on youth soccer athletes over the course of a match stem from covering distances of several kilometers, periods of maximum effort sprints, and rapid changes of direction via accelerations and decelerations.

Further, these external load demands only scale upwards as youth athletes graduate to larger fields and physical maturation drives increases in training load intensity.

Researchers cannot examine the evolution of external loading on developing youth athletes without considering the physical changes due to puberty. While it is understood that the fastest rates of human growth occur *in utero*, this rate declines linearly throughout childhood until puberty and a "growth spurt" occurs (Wood et al. 2019). Periodic release of gonadotrophin hormone from the pituitary gland leads to the production of sex steroid hormones (i.e., androgens and oestrogens) which increase mineral content in bone and muscle mass (Saggese et al. 2002; Wood et al. 2019). Apart from these changes, young athletes undergoing puberty also show increases in muscular strength, power, sprint speed, and endurance (Rowland et al. 1991; Seger and Thorstensson 2000; Van Praagh and Doré 2002; Papaiakovou et al. 2009). Access to these elevated physical attributes, body and segmental mass, and muscle contractility means that dynamic soccer tasks performed as young children now produce greater external and internal loading on these adolescent athletes. Monitoring of these loads could be of utmost importance in preventing these players from being exposed to abnormal and injurious loading patterns, both acutely and chronically.

While motion capture camera systems and force plates are the 'gold standard' in biomechanics research when assessing these loads, these systems do not lend themselves to unfettered field-based tasks. Inertial measurement units (IMUs), however, provide estimates of biomechanical loading on body segments via embedded triaxial accelerometers, gyroscopes, and magnetometers. Specifically, when considering the large majority of soccer injuries occur in the lower extremities (Comstock and Pierpoint 2020), metrics derived from IMUs placed on the shank during training (Nedergaard et al. 2017; de Moraes et al. 2018; Willy 2018) seem to be

promising potential indicators of leg injury risk in these adolescent athletes. Commonly reported metrics from these sensors include peak resultant accelerations, binned frequencies of accelerations, and other discrete variables (Armitage et al. 2021), though other analyses are available to analyze the collected IMU signals.

The 'complexity' of biological signals (i.e., heart rate variability, electroencephalograms, etc.) has been previously used to delineate healthy and diseased systems (Lake et al. 2002; Costa et al. 2005; Abásolo et al. 2006). The signal complexity is determined via entropy analyses which utilize information theory to calculate the expectation of observing a series of data points in the biological signal based on previous data points (Shannon Claude Elwood 1948). It has been postulated that, relative to unhealthy biological systems, healthy systems exhibit greater signal complexity (i.e., higher entropy) as they are capable of greater adaptation and less system constraint (Costa et al. 2002). Previous work has shown that untrained runners exhibit lower center of mass (CoM) acceleration complexity than trained runners (Parshad et al. 2012) and that CoM acceleration complexity decreases before fatigue onset during a long run (McGregor et al. 2009). Further, a prospective proof-of-concept investigation by Gruber et al. (2021) on a small sample of collegiate runner long runs reported that CoM acceleration complexity increased from baseline to immediately pre-injury. Though the complexity differences reported were not statistically significant, the moderate to large group-difference effect sizes between the injured and non-injured runners suggest that entropy analyses could still prove to be a useful tool in identifying injury risk during similar tasks.

Statement of the Problem

Previous investigations have monitored youth soccer athlete training loads in a one-dimensional manner, i.e., by simply reporting global positioning system (GPS) distances

covered, binned and absolute CoM acceleration peaks, total accelerations and decelerations, etc. However, a paucity of shank-mounted IMU or accelerometer data from these athletes exists, particularly data accounting for the effects of pubertal development. Further, entropy analyses of these data may show that the movement complexity of these athletes differs between athletes in various pubertal stages or at different time points in their training. If such differences existed and could be characterized, coaches and researchers could potentially use such analyses to monitor these athletes and potentially prevent injury.

Statement of Purpose

The purpose of this study is to collect IMU linear acceleration data from adolescent soccer athletes and determine if derived linear acceleration metrics (discretized peak accelerations, cumulative acceleration loading, etc.) or overall signal complexity differs between athletes based on relation to peak height velocity, sex, or over the course of a season. We propose to accomplish this purpose with two specific aims. Specific aim 1 is to determine if peak height velocity and sex differences exist in shank acceleration signal peaks and integrals and if those acceleration measures change over a competitive season. Specific aim 2 is to compare shank acceleration complexity measures across peak height velocity and sex to determine if complexity changes over the course of a season.

Research Hypotheses

This investigation is novel in its methodology and population, therefore directed hypotheses are difficult to form. However, as the literature has made clear that puberty affects a multitude of physical attributes, it is hypothesized that youth soccer athletes at different points of pubertal development and of varying sex will exhibit differing shank-mounted acceleration profiles and complexity metrics. Additionally, to increase the resolution of these time-dependent

pubertal changes and consider the effects of training and competition on this data, we hypothesize that the acceleration complexity will differ when measured at the beginning as compared to after a competitive season.

Significance of the Study

This study will utilize a sample that is under-represented in the biomechanics literature and analytical methods that have yet to be employed in said population. Complexity analysis of athlete movement during training and drills could provide a robust metric for determining movement complexity evolution in this population over the course of a season and longitudinally over adolescence. Further, by characterizing the profiles of these acceleration data for this population, deviations from these data could serve as indicators of an unhealthy and potentially at-risk system. Therefore, it is vital that the acceleration profiles of these adolescent soccer players be collected and analyzed.

Independent Variables

- Offset in years from peak height velocity (PHV)
- Session – pre-season, post-season
- Sex – female, male

Dependent Variables

- Linear acceleration
    - Resultant linear acceleration peaks
    - Resultant linear acceleration integral
        - "Cumulative acceleration loading"
- Complexity Measures
    - Multiscale Entropy

    - Complexity Index

Limitations of the Study

- Participant relation to pubertal stages will be carried out via cross-sectional anthropometric measurements used to estimate peak height velocity, a surrogate measure, rather than the gold standard of longitudinally collected radiographic measurements.

Delimitations of the Study

- Participants will be between the ages of 9 to 17 years old.
- Any participant who experiences a lower extremity injury in the 6 months prior to the initial testing session will be excluded.
- Any participant who experiences pain on the days of testing will be excluded.

Assumptions of the Study

- Participants will be truthful when answering screening questions regarding lower extremity injury history and weekly soccer participation.
- Participants will be truthful when completing the Lower Extremity Functional Scale and fitness activity questionnaire forms.
- Participants will give maximal effort during the experimental tasks.
- The dual-g IMU sensors (IMeasureU Blue Trident, Vicon Motion Systems Ltd., Oxford, UK) will be accurately calibrated for each data collection throughout the study.

Operational Definition of Terms

Complexity: "… the amount of nonlinear information that a time series conveys over time." Highly complex signals (i.e., biological signals) exhibit patterns of 'structure' and regularity across frequency components and temporal scales. (Omidvarnia et al. 2018)

Entropy: the mean quantity of “surprise” or “uncertainty” produced by a random variable, i.e., the average amount of information expressed by a random trial for a variable.

Information: knowledge that allows for a signal, input, or the entire state of a system to be differentiated from the available potential states, or the “resolution of uncertainty”.

Puberty: “… the attainment of reproductive capability and the acquisition of adult body composition and habitus. The pubertal growth spurt and the appearance of secondary sex characteristics are the most visible manifestations of puberty.” (Abbassi 1998)

Regularity: the ability of a signal to be locally approximated via a polynomial, i.e., the predictability of a signal.

Chapter 2: Review of the Literature

Introduction

Many sports and the training regimens associated with them dictate that the participating athletes cover a range of distances at moderate to maximal speeds. Ignoring the biomechanical impact of factors like fatigue, coordination, and object manipulation, the vertical ground reaction forces and loading rates experienced during sprinting can surpass 3-5x bodyweight and 100x bodyweight per second, respectively (Udofa et al. 2017; Yu L et al. 2021). Other commonly performed sporting maneuvers (e.g., accelerating, decelerating, and cutting) further increase the internal loading response within the biological structures of the lower extremity. These facts explain why almost 50-70% of sports-related musculoskeletal overuse injuries are predominantly occurring in the lower extremities (Stracciolini A. et al. 2014; Roos et al. 2015). Repeated loading cycles of the musculoskeletal and connective tissues, even sub-maximal relative to their failure point, can lead to injurious damage and potential failure (i.e., tearing and rupture) if adequate recovery and repair does not follow. In the absences of invasive methods, tracking "external loads" such as total distance covered, number of sprints at certain intensities, and accelerometry has become common metrics used to identify athletes potentially at risk of overuse injuries (Gabbett 2016; Bourdon et al. 2017).

Tracking and managing these loading patterns could alleviate substantial financial burdens (Cumps et al. 2008; Ryan JL et al. 2019) and prevent arduous rehabilitation protocols, surgical or otherwise. Small, minimally invasive IMUs have become popular devices for tracking either athlete center of mass or segmental accelerations as a surrogate measure of external loading. The use of accelerometry metrics derived from IMUs have been used to monitor training workloads at the acute and chronic level in efforts to reduce overuse injury in youth and professional athletes (Bowen et al. 2017; Sampson et al. 2018; Izzo et al. 2022; Nobari et al.

2022). As puberty has been shown to drastically alter musculoskeletal strength and power, movement coordination, and fatiguability (Papaiakovou et al. 2009; Perroni et al. 2018; Almeida-Neto et al. 2020), data accounting for the interaction between pubertal status and these IMU metrics during training could be beneficial to the public. Further, the magnitudes, profiles, and rate of change of data collected via IMUs in rapidly developing adolescents is currently not available. Insights from the analysis of such data collected over the course of a season in maturing soccer athletes could, thus, provide insights that could prevent overuse injuries and add to the paucity of IMU external loading literature in this population.

The purpose of this study is to investigate the discrete IMU acceleration metrics and complexity differences between soccer players at different pubertal stages before and after a competitive season. The current literature explored in this chapter includes: the expected aging effects through late childhood and puberty on performance in young athletes; the epidemiology of sports injuries in developing athletes; measurement of external loading via IMUs; and the use of dynamical systems theory to analyze continuous IMU data for injury prevention.

Adolescent Development

Infancy

If humans continued developing at the same *in utero* growth rate once born then we each would achieve our full stature before we were two years old. A variety of factors affect this prenatal rate of growth, notably maternal carbohydrate intake during pregnancy (Scholl et al. 2004), toxic exposure to smoked tobacco or alcohol (Bird et al. 2017), gene expression (Weedon et al. 2005), and hormone regulation (Evain-Brion 1994; Gicquel and Le Bouc 2006; Belkacemi et al. 2010). Peak gestational growth rate is approximately 2.5 cm per week around weeks 20-24 (Kappy et al. 2005) and prenatal androgen profile may not be as influential to birth size as

thyroid hormone concentrations (Miles et al. 2010; Shields et al. 2011). The postnatal growth pattern, however, is predictable and split into infancy, childhood, and puberty (ICP) stages (Appendix U) by the Karlberg model of growth (Karlberg 1989). While primarily dependent upon nutritional content and uptake, the average height velocity over infancy is 25 cm per year (Benyi and Sävendahl 2017). Bone diaphyses have ossified by birth but epiphyses are still cartilaginous (Anderson 1996). Bone mineral density rises rapidly over the first 4 years, subsides, and spikes again at puberty (Cech 2011). Over the first 2 years, the brain reaches 80% of adult size during development (Knickmeyer et al. 2008). Myelination of the sensory, then motor and association areas of the brain proceeds rapidly, reaching the frontal lobes within the first year of birth (Barkovich et al. 1988; Barnea-Goraly et al. 2005). Muscle mass, at birth, accounts for roughly 25% total body mass (Cech 2011) and the contractile and relaxation times of certain muscles slow until around age 3 (Gatev et al. 1977). 50% and 95% of infants begin walking by 12 and 15 months, respectively (WHO 2006), yet the literature demonstrates that motor milestones like walking are more due to cerebral maturation instead of via experience (Savelsbergh et al. 2013). This point is supported by a case-study involving a 6-month-old presenting with bilateral hip dysplasia who was placed in a spica cast and immobilized for 12 months, yet she was able to walk within a day of cast removal (Peiper 1963, pp. 233).

Childhood

In the brain, the zona reticularis within the adrenal cortex produces and secretes dehydroepiandrosterone (DHEA), the most abundant circulating steroid hormone, at a very high rate during fetal development (Bech et al. 1969; Belgorosky et al. 2008). DHEA and its sulfate ester metabolite (DHEAS) provide more than 50% and 70% of the androgens and estrogens, respectively, in premenopausal women and men as a precursor to androgen production (Maggio

et al. 2015). DHEA production and levels decrease immediately following birth before rising again and marking the beginning of adrenarche, the period of increased adrenal androgen production preceding puberty, peaking in late adolescence (Babalola and Ellis 1985; Havelock et al. 2004; Castellano et al. 2006). Adrenarche typically occurs between ages 6-8 in parallel with skeletal age increase (dePeretti and Forest 1976; Ibáñez et al. 2000), though cases demonstrate it can be observed as early as 3 years of age (Palmert et al. 2001; Remer et al. 2005). Though it is unknown exactly how adrenarche is modulated, nutritional status and paracrine function of adrenocorticotropic (ACTH) hormone production are known contributors to this pubertal phase (Hinson 1990; Ibáñez et al. 2000; Suzuki et al. 2000).

Brain growth slows after age 2 as 90% of adult size is not achieved until year 5 (Dekaban and Sadowsky 1978). This is accompanied by a lifespan peak rate of brain metabolism and white matter development until age 10 (Barnea-Goraly et al. 2005; Snook et al. 2005) thought to be a product of energy demands related to synaptic remodeling and myelination (Tau and Peterson 2010). Bone mass reaches 50% and 60% of adult mass via linear growth rate before puberty in men and women, respectively (Whiting et al. 2004; Ondrak and Morgan 2007). Up to 85% of the fully developed height of an individual can be reached by the end of childhood prior to puberty (Prader 1984; Bogin 1999). Isometric strength increases from ages 3 to 6 proportionally with physiological cross-sectional area (PCSA) and volume increases (Tonson et al. 2008). Before age 10, average cross-sectional area of skeletal muscle is slightly greater in men compared to women (Kanehisa et al. 1994; Deighan et al. 2006). Muscle strength, volume, and PCSA increases up to 19%, 14%, and 11% have been reported, respectively, in 7-8 year old children over just 6 months (Pitcher et al. 2012). As myelination continues and androgen production has not yet peaked, long-term athlete development models have suggested that skill-related training (e.g., speed,

agility, coordination, and flexibility training) should take priority over solely resistance training during childhood to maximize future motor performance (Kraemer et al. 1989; Myer et al. 2011). However, the current literature regarding optimal training windows is conflicting (Sañudo et al. 2019).

Only 14% of all children can skip by year 4 (Cech 2011), though by year 4 and 5 approximately 60% of men and women, respectively, have become proficient at running (Seefeldt and Haubenstricker 1982). An adult walking pattern has been established by age 5 (Malina 2004) and no differences in lower extremity landing stiffness strategies has emerged yet by age 10 (Hamstra-Wright et al. 2006).

Puberty

Gonadarche, signaled by the production of follicle-stimulating hormone (FSH) and luteinizing hormone (LH) in the anterior pituitary (Witchel and Topaloglu 2019), marks the beginning of central puberty. FSH and LH promote maturation of the gonads via secretion of testosterone, estrogen and estradiol (Reardon et al. 2009). DHEA and testosterone are converted to dihydrotestosterone (DHT) which stimulates epiphyseal growth in long bones (Nilsson et al. 2005; Zhou and Glowacki 2018). More than 20% of bone density and mineral content is accumulated over puberty (Anderson 1996; Ondrak and Morgan 2007) and differences in testosterone levels contribute to the steady rate of bone mineral content accrual in men compared to the plateauing in women following PHV (Whiting et al. 2004). Men and women reach 90% and 95% of their adult peak bone mass by age 20 following the pubertal growth spurt (Anderson 1996), at which time differences in bony structure geometry appear that will persist across the lifespan (Lauretani et al. 2008).

It has been suggested that DHEA and DHEAS molecules affect neurite growth (Grube et al. 2018; Schverer et al. 2018), catalyzing brain development by fueling neuroplasticity during adrenarche (Greaves et al. 2019). These adrenarchal changes have been posited as a contributor to changes in documented behavior throughout puberty (Del Giudice 2009; Campbell 2011). Further reports suggest that increased intra-adrenal cortisol levels and macro-level growth frequently resets ACTH homeostasis concentrations in the presence of normal cortisol production relative to body size during puberty, leading to PHV (Topor et al. 2011; Majzoub and Topor 2018).

Several reports show that almost all strength increases over puberty can be explained by increases in muscle size when normalized to either muscle volume, PCSA, or fat-free mass (FFM) (Pitcher et al. 2012; Fukunaga et al. 2014). Further, peak power output in age 12 children assessed via Wingate tests is greater in men compared to women (Van Praagh et al. 1990) with a similar divergence in strength also presenting following the pubertal growth spurt (Malina et al. 2004, pp.219). In men, specifically, elevated testosterone levels are directly correlated with improvements in upper limb and squat jump power production (Almeida-Neto et al. 2020). Even when separated by less than one chronological year, strength and muscle volume have been reported to differ by 40-50% between pubertal men and their pre-pubertal counterparts (Tonson et al. 2008; Fukunaga et al. 2014).

Speed has been shown to improve with age across puberty, though when normalized to strength and muscle volume this relationship is no longer significant (Yoshimoto Takaya et al. 2012; Yoshimoto T et al. 2014). As with strength, peak running speed increases at a faster rate following PHV in men compared to women (Papaiakovou et al. 2009). Maximum oxygen uptake increases from infancy to adulthood (Armstrong and Welsman 1994; Viru et al. 1999), though

much variation in total aerobic work capacity exists between reports. Adults have been shown to run more economically than children and adolescents (Åstrand 1952; Daniels et al. 1978; Krahenbuhl et al. 1985), yet this relationship does not hold when running at speeds relative to leg length (Maliszewski and Freedson 1996). Aerobic capacity relative to mass remains constant in boys and decreases in girls (Åstrand 1952; Krahenbuhl et al. 1985), dooming children participating in endurance events to operate closer to their maximal oxygen uptake at any speed (Bar-Or 1983; Morgan et al. 1989).

Altered movement strategies also emerge as lower extremity joint stiffness during jump landings increases following puberty (Wang et al. 2004), though neuromuscular components of performance differ based on sport and sex (Quatman et al. 2006; DiCesare et al. 2019). Knee biomechanics during drop vertical jumps are similar between pubertal men and women but only women exhibit an increase in knee abduction angles and moments immediately following puberty (Ford et al. 2010). During a stop-jump task, post-pubertal women soccer players also exhibit greater knee abduction angles compared to pre-pubertal women (Yu B et al. 2005). The next section will cover how the combination of these anthropometric and musculoskeletal changes impart substantial influence on injury risk.

Adolescent Injury Overview

Intrinsic Injury Risk Factors

Across puberty, peak muscle accretion rates and PHV supersede peak bone mineral content accrual (Blimkie et al. 1993; Ruff 2003; Forwood et al. 2004; Rauch et al. 2004). Periosteal modelling and geometric expansion do not take place until bone elongation and muscle hypertrophy, an explanation posed for the greater rate of fractures occurring during puberty (Cooper et al. 2004). A retrospective pediatric clinical study found that adolescents (11-

17 years old) experienced a higher incidence rate of epiphyseal fractures than younger children with the majority occurring at the distal epiphysis of the tibia and fibula (Joeris et al. 2017). Osgood-Schlatter's Disease (OSD), or irregular ossification occurring at the tibial tubercle, is experienced by ~10% of adolescent athletes (Kujala et al. 1985; de Lucena et al. 2011). Sever's disease (calcaneal apophysitis) commonly occurs in athletes between 8 and 15 years as tension in Achilles tendon leads to avulsion of the calcaneal attachment (Ramponi and Baker 2019).

Biological sex is another known risk factor for non-contact injuries during dynamic movements, as women have been reported to be between 2-8x more likely to injure their anterior cruciate ligament (ACL) (Agel et al. 2005; Yu Bing and Garrett 2007). Interestingly, it is unclear if a sex-related difference in ACL injury rates in children or pre-pubertal athletes exists as it does in post-pubertal or adult populations (Andrish 2001; Shea K et al. 2004). In high school sports, women playing soccer, basketball, and softball experience higher ACL injury rates than men (Shea KG et al. 2011). ACL injury rates increase with age for both men and women, but these rates are greater in women immediately following PHV (Tursz and Crost 1986). Sport-related high school injury rates peak during freshman year for women before declining but increase for men until peaking senior year (Comstock and Pierpoint 2020). The rapid increase in stature and weight accompanying PHV may alters center of mass location and may lead to altered movement patterns that predispose women athletes to non-contact lower extremity injuries (Hewett et al. 2005). Men tend to experience OSD most frequently 1-1.5 years preceding PHV and at greater rates than women (Kujala et al. 1985). In fact, men tend to experience apophyseal, cartilaginous, and tendon overuse injuries more frequently than women between ages 5 to 18 (Valasek et al. 2019).

Non-Contact and Overuse Lower Extremity Injury Mechanisms

Across all sports, injury rates are greater in competition compared to practice and more frequently occur in the lower extremities (Sheu et al. 2016; Comstock and Pierpoint 2020). Playing sports exposes athletes to movements during training and competition that stress the structural integrity of the musculoskeletal system to varying degrees. Acute musculoskeletal injuries can occur when internal forces in the tissues exceed failure points due to instantaneous application or propagation of energy (Finch CF 1997). Conversely, the onset of overuse injuries is not typically linked with a specific event but rather repetitive microtrauma being applied to the tissues in the absence of adequate recovery (Finch C 2011). These injuries can culminate in non-contact injuries that are the product of progressively weakened tissue rather than acute application of traumatic force. Repeated bouts of intense training and sport is a risk factor for tendinopathy, particularly if jumping is involved (Ferretti et al. 1984; Warden and Brukner 2003; Gisslèn et al. 2005). One of the most common and debilitating injuries, ACL sprains, have been estimated to be the result of non-contact mechanisms in approximately 70% of reported cases (Gianotti et al. 2009). Overtraining and inadequate recovery between competitions and training increase the risk of musculoskeletal, non-contact injury (Gabbett 2004, 2010, 2016).

During dynamic tasks, athletes can position their joints in ways that forces propagating from the ground through the lower extremity may overload the material strength of soft tissue. Despite the Achilles tendon being the thickest, strongest tendon in the human body, it is the most frequently injured via acceleration-deceleration events associated with rapid ankle dorsiflexion or a lunging motion (Aicale et al. 2017; Tarantino et al. 2020). Lower extremity muscle strains are also more likely to occur during intense deceleration movements (i.e., late swing of gait cycle) when muscles are eccentrically producing more contractile force (Chumanov et al. 2007;

Kary 2010; Chumanov et al. 2012). 30% of ankle sprains experienced by both men and women high school soccer players during 2019 had non-contact mechanisms (Comstock and Pierpoint 2020). Video evaluation has shown that the deceleration phase of sprinting, landing, or changing direction is when most ACL non-contact injuries occur (McLean et al. 1999; Boden et al. 2000). Cadaveric benchtop testing has shown internal rotation of the hip and extension and adduction of the knee induce the most strain and load on the ACL (Bates NA et al. 2015; Bates NA et al. 2019). Indeed, a prospective study found that knee frontal plane angles and moments during dynamic tasks are considered a risk factor for ACL injury (Hewett et al. 2005). ACL injured athletes demonstrated greater knee abduction angles (>8°) and moments (>150%) at initial contact during a jump landing task than uninjured controls while abduction moments could predict ACL injury with 73% specificity and 78% sensitivity.

Sport-specific Injury Prevalence

Sport demands entailing intense, coordinated movements of the lower extremities (i.e., soccer, football, basketball, etc.) increase non-contact ACL injury risk (Noyes and Barber Westin 2012). Considering injury risk with respect to non-contact ACL injury risk, it is not surprising that ACL injury rates in high school women's sports are higher than those in sex-comparable sports (i.e., basketball and soccer) (Shea KG et al. 2011; Tirabassi et al. 2016). More than 1/3rd of Achilles tendon ruptures reported between 2012-2016 in those less than 18 years old played such sports (i.e., basketball, football, and soccer) and 80% of all AT ruptures over this period were sport-related (Lemme et al. 2018).

Sport specialization may also play a role in overuse injury, particularly for athletes playing year-round with no offseason. Athletes who exhibit a combination of training more than 8 months per year, quitting other sports to focus on a primary sport, or compete more than 60

times per year have 50-80% greater lower extremity injury rates than generalized athletes (McGuine et al. 2017). Adolescent baseball pitchers are 5x more likely to require surgery stemming from overuse injury if they compete more than 8 months out of the year (Olsen et al. 2006). While athletes who participate in sport specialization earlier are more likely to receive collegiate athletic scholarships, they are also more likely to sustain more injuries and miss a greater amount of time due to injuries than those who did not (Ahlquist et al. 2020).

ACL injuries are one of the most serious injuries that occur frequently across all sports, though ACL injury rates are relatively higher in soccer (Shea KG et al. 2011). High school women's soccer injury rates are only eclipsed by those in football (Shea KG et al. 2011; Comstock and Pierpoint 2020). Overall injury rates in high school women soccer players are 50% greater but also 30% and 50% more likely to incur knee and ankle sprains compared to men, respectively, though women are less likely to fracture a bone during competition or practice (Comstock and Pierpoint 2020). An analysis from 2010 demonstrated that women's soccer produced the highest ACL injury rate (13.87 injuries per 100,000 AEs) among the 9 most commonly played high school sports by women and men (Shea KG et al. 2011). The greatest non-football ACL injury rates (4.6 injuries per 100,000 AEs) for men also occurred playing soccer (Shea KG et al. 2011). Men had higher ACL injury rates in practice compared to women (1.04 vs 0.85 injuries per 1000 AEs, respectively), though these rates were below the national average for contact sports (1.51 injuries per 1000 AEs) (Montalvo et al. 2019).

Wearable Sensors

Over the past decade, more than 22 review papers have been published on wearables used to combat musculoskeletal injury in athletes (Preatoni et al. 2022). Almost 75% of these studies used these sensors to measure loading of the lower extremities and pelvis (Preatoni et al. 2022)

as these constitute the majority of overuse injuries at all levels of competition (Roos et al. 2015; Schroeder et al. 2015; Stracciolini Andrea et al. 2015). Most of these studies employed IMUs, small housings containing 3 sensors: an accelerometer, gyroscope, and a magnetometer (Ahmad et al. 2013). IMUs were initially designed almost 70 years ago as ground-position indicators in jets before the field exploded with the need for more advanced and accurate guidance systems in missiles and aircraft (Lambert and Kenneth 1952; Robot Navigator Guides Jet Pilots 1954; MacKenzie 1990), but have become popularized in health and sport monitoring in recent decades. The following section will detail the individual components of the IMUs and the principles on which they function; their use cases as they pertain to health monitoring, injury prevention and sport performance; and the use of signals obtained from IMUs in non-linear analyses.

Inertial Measurement Units

The size, processing requirements, and cost of the first IMUs rendered them inappropriate for consumer-application (MacKenzie 1990). 3D optical motion capture systems have been the golden standard for analyzing human kinematics for several decades (Muro-De-La-Herran et al. 2014; Van der Kruk and Reijne 2018), yet the validity and reliability afforded by these systems is overshadowed by their costs, fixed location requirements, and the need for extensive technical training to operate and process captured data. It was not until advancement in micro-fabrication techniques that micro-electromechanical systems (MEMS) made the manufacturing of wearable, research-grade IMU sensors for tracking human motion a possibility (Xu et al. 2019; Bukhari et al. 2020). Following this manufacturing breakthrough, IMUs can now provide athletes, coaches, and researchers the ability to track athlete motion in the field during training and competition in a way that traditional marker motion capture cannot, solidifying a strong basis for their recent

popularization. IMUs are small, lightweight, and relatively cheap in comparison to motion capture systems while still measuring linear and angular motion (Boddy et al. 2019).

A review of biomechanical studies over the past decade employing IMUS for examining musculoskeletal health found that over 60% only used 1D or 3D accelerometers in their experiments (Preatoni et al. 2022). The first accelerometer was devised in the late 1700s by George Atwood before the more modern spring mass system or piezoelectric accelerometers were commercialized in the 1900s (Greenslade Jr 1985; Walter 1997). Atwood's machine consisted of two unequal masses m_1 and m_2 connected by string or rope over a pulley, whereby both masses would experience uniform acceleration due to Earth's gravity (assuming massless, inextensible string and pulley):

$$a = g\frac{m_1 - m_2}{m_1 + m_2} \qquad \text{Eq. (1)}$$

In the 1920s, the first resistance-bridge accelerometers were commercially developed by McCollum and Peters in a Wheatstone half-bridge configuration for use in bridges, dynamometers, and aircraft (McCullom and Peters 1924; Stein 1996). This iteration weighed over a pound and was more than 8 inches long. It was not until the invention of the strain gauge that the form factor could be reduced (to less than 2 grams) and the strain gauge accelerometer was created more than 15 years later by J. Hans Meier while working for Douglas Aircraft (Starr et al. 1988). Piezoelectric accelerometers developed en masse at the midpoint of the 1900s improved on resonant frequency response, dynamic signal ranges, and apparatus size, which shortly thereafter led to the introduction of modern integrated circuits to combat cable noise due to static electricity interference (Walter 1997). The first silicon, micromachined MEMS accelerometer was proposed by Lynn Roylance in his dissertation at Stanford University prior to its funding and development through a NASA grant in 1979 (Lee et al. 2005; Bimm 2018).

These devices use inertia and a combination of free-moving and stationary electrodes or piezoelectric strain gauges that create differential capacitance via their displacement proportional to linear accelerations experienced by the system (Aydemir et al. 2016). The mechanism is similar to vestibular function in the human inner ear used for balance and orientation within the world coordinate frame (Day and Fitzpatrick 2005; Fortenberry et al. 2012). Skin-mounted accelerometers have been used to quantify human segment kinematics and energy transfer during walking, running, and other dynamic tasks (Lafortune et al. 1995; Whittle 1999; Mercer et al. 2002; Coventry et al. 2006; Simons and Bradshaw 2016; Brennan et al. 2017) and provide a less invasive alternative to bone-pin accelerometers. However, skin-mounted accelerometers move relative to the bone motion we are trying to measure due to subcutaneous tissue deformation during movement (Cappozzo et al. 1996). The mechanical properties of soft-tissue exhibit high inter-subject variability regarding movement artefact of skin-mounted accelerometers (Ziegert and Lewis 1979; Fuller et al. 1997; Holden et al. 1997), though this issue can be addressed by modelling the soft-tissue attachment as a second-order mass-spring-damper system (Kim et al. 1993; Luo et al. 2002). Researchers and coaches should be cognizant of the effects of sensor placement at the proximal or distal portion of the segment of interest as segment angular velocity will affect results (Mathie et al. 2004; Schwartz et al. 2004; Clark et al. 2010). Accelerometers have been used to quantify stride length, running velocity, tibial acceleration, vertical stiffness, and other biomechanical variables (Eggers et al. 2018; Mitschke et al. 2018), though the accuracy of these measures can be improved by combining accelerometer and gyroscope results (Boonstra et al. 2006).

Gyroscopes have also become more prominent in wearables to measure angular motion due to advances in MEMS technology (Yazdi et al. 1998) yet they are typically used in

conjunction with at least accelerometers when measuring biomechanical variables (Norris et al. 2014; Preatoni et al. 2022). Like accelerometers, MEMS gyroscopes contain a moving mass whose displacements produce measurable voltage differences that are proportional to the rate of angular velocity experienced by the system (Passaro et al. 2017). However, this mass is constantly oscillating or vibrating so applying principles of gyroscopic procession and the Coriolis effect in conjunction with Newton's 2nd Law of motion allow us to determine angular velocity (Maenaka et al. 1996; Xie and Fedder 2003). The first MEMS gyroscopes were designed by Draper Laboratory in the 1980s for military and space inertial navigation applications (Greiff et al. 1991) as they can measure inclination and heading with less interference than magnetometers alone (Fan et al. 2017). Gyroscope scale factor and bias stability (i.e., resolution of measurement and drift, respectively) are susceptible to error, however, in the presence of extreme temperatures or internal friction and vibration (Yoon et al. 2012; Jiang et al. 2014; Chong et al. 2016). More sophisticated ring laser and fiber optic gyroscopes can achieve bias stability of less than .0001°/hour drift while most commercially available MEMS equivalents are 4-7x less precise (Passaro et al. 2017). Bias stability can be improved via sensor fusion algorithms including correction inputs from magnetometers (Chang et al. 2008; Fan et al. 2017).

The magnetometer was first invented by Gauss in 1832 to measure the absolute value of Earth's magnetic field strength from a given location (Gauss 1832, 1877). MEMS magnetometers are designed with magnetoresistive conductive plates to measure heading and inclination using principles of the Hall effect and Lorentz force to measure voltage differentials based on deflection of electrons due to strength and direction of an external magnetic field (Smith et al. 1991; Tumanski 2001; Ramsden 2011). Magnetometers have been used in

applications ranging from early compass navigation to geospace and military projectile applications (Rogers et al. 2011; Brown P et al. 2012). Exclusive use of magnetometers in biomechanical investigations is unusual, though for less-dynamic tasks requiring fewer DOFs removing accelerometer input may improve accuracy by removing inertial error (Bonnet and Heliot 2007). Magnetometers vulnerability to ferromagnetic disturbances is well-documented, especially when deployed indoors (Bachmann et al. 2004; De Vries et al. 2009). In recent years, though, the accuracy obtained from IMUs using magnetometers for orientation drift-correction in gyroscope and accelerometer measurements has improved beyond magnetometer use alone (Han and Wang 2011; Wittmann et al. 2019; Preatoni et al. 2022).

Sport-Specific Implementation for IMUs

Early uses of IMUS were predominantly for navigation and industrial applications. MEMS IMUs have been used in recent years by coaches and researchers across sports to quantify and monitor impact loads athletes experience performing dynamic movements during training and competition in athletes (Wilkerson et al. 2016; Jaspers et al. 2018; Mehta 2019; de Leeuw et al. 2022; Miltko et al. 2022). Some previous reviews have covered best practices for sensor placement, fixation techniques, and data capture and processing based on the task being analyzed (Camomilla et al. 2018; Sheerin et al. 2019). Special consideration should be given to sensor mass and the need for all 3 internal sensors as the derived metrics from some dynamic tasks may sacrifice accuracy with more massive IMUs instead of a single sensor (i.e., an accelerometer) (Forner-Cordero et al. 2008).

As most sports-related injuries involve the lower extremity, the most common site of IMU fixation is the tibia (Preatoni et al. 2022). Tibial shock is the most common reported variable when study participants play sports involving considerable distance running for its link

to tibial stress fractures (Mathie et al. 2004; Zifchock et al. 2006; Crowell et al. 2010). Researchers should be wary of comparing study results in which different tibial sites of attachment (proximal or distal) were used as results will vary (Lucas-Cuevas et al. 2017). Further, the greater intensity of dynamic movements in the field relative to lab protocols show that IMU data collected in the field produces higher peak tibial accelerations compared to lab-based testing (Milner et al. 2020; Slaughter and Adamczyk 2020). The effects of fatigue, surface-interaction, and potentially other factors dictate that athletic loading measures collected on IMUs should be measured *in situ* during training or competition sessions (Boey et al. 2017; Johnson et al. 2020). Entropy analyses (see *IMUs and Non-linear Entropy Analysis* section) derived from accelerometer data have been used to quantify movement complexity and regularity in runners (Moe-Nilssen and Helbostad 2004; McGregor et al. 2009; Parshad et al. 2012; Schütte Kurt H et al. 2018; Rojas-Valverde et al. 2019). Nonlinear measures of movement regularity and complexity have been linked with pathophysiological conditions (Lamoth et al. 2010; Tochigi et al. 2012; Quirino et al. 2021; Gates et al. 2022) and may be suitable for injury forecasting in other athletic populations.

IMUs and similar global positioning system (GPS) units have been used to monitor athlete workloads in adults (i.e., (Arrones et al. 2014; Kempton et al. 2015; Gallo et al. 2016; Fox et al. 2018; Allard et al. 2022; Mamon et al. 2022) and youth athletes (Langendam et al. 2017; Ryan MR et al. 2021; Pino-Ortega et al. 2022) across soccer, football, rugby, basketball, and others. Commonly tracked variables include segment and whole-body accelerometry, speed, total distance covered, frequency and intensity of change-in-directions, proprietary workload metrics, etc.). Training loads can be categorized into 2 groups: external loads that are measures of the work done by the athlete (i.e., those listed in the previous paragraph) and internal loads

which are biological stress responses to the external loads (Bourdon et al. 2017). The overarching purpose of these load monitoring investigations is to reduce overuse injury due to overtraining by optimizing athlete intra- and inter-session recovery.

Recently, these load monitoring paradigms are being applied to youth and adolescent soccer athletes (Barron et al. 2014; Castillo et al. 2020a, 2020b; Marynowicz et al. 2020; Nobari et al. 2021; Nobari et al. 2022; Salter et al. 2022). Adolescent athletes experiencing the effects of puberty are prone to inadequate recovery bouts between training and competition due to increases in training volume in conjunction with typical age-related academic and recreational activities (Phibbs et al. 2018). Additionally, adolescents are commonly subjected to training modalities that influence movement strategies and coordination (Venturelli et al. 2008; Rumpf et al. 2013; Deprez DN et al. 2015; Trecroci et al. 2015). Changes in the movement coordination of youth soccer players have been examined (Deprez D et al. 2014; Rommers et al. 2019) using a movement battery scoring system to measure gross motor coordination (Vandorpe et al. 2011; Iivonen et al. 2016). However, entropy-related measures of movement complexity have yet to be deployed on a population of developing (i.e., pubertal) soccer athletes.

Dynamical Systems Theory

Variability is inherent to human movement and motor performance across repetitions of dynamic tasks (Stergiou et al. 2006). In the field of motor control, the generalized motor program theory (Schmidt 1975) and uncontrolled manifold hypotheses (Schoner 1995) offer frameworks for explaining the systemic variability in our movement patterns. While these theories suggest that movement variability can be considered error in the face of a discrete movement outcome, dynamical systems theory (DST) focuses on the motor system behavior rather than the outcome (Kamm et al. 1990; Thelen et al. 1991; Thelen 1995). Specifically, DST states that, once a

threshold of variability and system instability is created, a more stable movement pattern ("attractor state") is adopted to achieve a movement outcome (Stergiou and Decker 2011). This postulate suggests that trained, healthy individuals can execute a simple movement with any number of movement patterns and that naïve, unhealthy individuals will be forced to adopt more stable patterns out of necessity (Stergiou and Decker 2011).

While the blueprint outlining the cause for many overuse sports injuries has not yet been elucidated, many researchers have sought to characterize the different parameters that precede them so that future injuries can be forecast and potentially circumvented. Modelling the complex systems and elements producing these injuries is a difficult task. More sensitive and specific injury forecast models requiring the identification of "… factors that would prevent the state of the system from desired to undesired state shifts as a result of perturbations" (Tu et al. 2021, p.1). Many non-linear systems analyses aiming to prevent injury operate via holistic interpretation of the system's resilience and behavior both in the long-term and within attractor states. These goals require metrics that accurately reflect the behavior of the physiological signals measured in the system, a purpose served well by information theory and entropy.

Entropy

In the context of information theory, entropy is the loss of information in a time series and quantifies the probability of the next state of a system given a current state (Yentes 2018). A completely random, white noise signal would exhibit maximum entropy (in arbitrary units) compared to its reciprocal, a predictable sine wave or similar function. In his seminal paper, Shannon (1948) was trying to optimally design the framework for telephone communications, introducing the "bit" as the most basic unit of information and how it could be quantified in a signal. His work led to the invention of Huffman encoding and lossless data compression

(Huffman 1952) through the paradigm that source information contained redundancy and could be recreated by a signal containing fewer bits. In essence, Shannon viewed any chaotic process as a source of information and developed his entropy statistic as a metric to measure the amount of uncertainty in that process (Shannon Claude Elwood 1948).

Almost 40 years later, Approximate entropy (ApEn) (Pincus SM 1991) was created to quantify the rate of regularity in a time data series:

$$\text{ApEn}\ (m, r, N) = \lim_{N \to \infty} [\phi^m(r) - \phi^{m+1}(r)] \qquad \text{Eq. (2)}$$

and

$$\Phi^{\mathrm{m}}(\mathrm{r}) = (\mathrm{N} - \mathrm{m} + 1)^{-1} \sum_{i=1}^{N-m+1} ln\ \mathrm{C}_m^i(r) \qquad \text{Eq. (3)}$$

whereby *m* is the embedding template dimension, *r* is the resolution threshold, and *N* is the length of the time-series vector. The ApEn algorithm divides the series into vector templates of length *m* for comparison. Blocks are considered possible matches if the difference between all the corresponding block elements is ≤ *r*. Once that condition is met, if the subsequent point difference is also ≤ *r* then the blocks are a match and conditional probabilities calculated (template matches divided by possible matches). In layman's terms, ApEn is the "…(logarithmic) likelihood that runs of patterns that are close for *m* observations remain close on next incremental comparisons" and ApEn values approach zero for patterns in which successive points remain close with regularity (Pincus SM and Goldberger 1994, pp.H1644). A thorough explanation and interpretation is provided by Pincus & Goldberger (1994).

Sample entropy (SampEn) (Richman and Moorman 2000) was developed to address the regularity bias present from self-counting template matches in ApEn and sensitivity to smaller time series:

$$\text{SampEn}\ (m, r, N) = -ln\left(\frac{A}{B}\right) \qquad \text{Eq. (4)}$$

whereby *B* and *A* are defined as the total number of template matches of length *m* and total number of forward matches of length *m+1*, respectively:

$$A = \left\{\frac{[(N-m-1)(N-m)]}{2}\right\} A^m(r),\ \ B = \left\{\frac{[(N-m-1)(N-m)]}{2}\right\} B^m(r) \qquad \text{Eq. (5)}$$

Multiscale entropy (MSE) (Costa et al. 2002) was introduced to address the inconsistencies that the traditional ApEn and SampEn algorithms exhibited between random noise and physiologically complex signals. Some pathologies (i.e., cardiac arrythmias) have statistical properties associated with uncorrelated noise because of the erratic fluctuations in the original signal (Zeng and Glass 1996; Hayano et al. 1997; Di Rienzo 1998). MSE accounts for these complex temporal fluctuations by working across temporal scales via coarse-graining the original time series:

$$y_j^{(\tau)} = \frac{1}{\tau} \sum_{i=(j-1)\tau+1}^{j\tau} x_i, \qquad 1 \leqslant j \leqslant N/\tau \qquad \text{Eq. (6)}$$

before employing another entropy algorithm (typically SampEn) on the coarse-grained time series. Unlike ApEn and SampEn, MSE employs a 3rd parameter, τ, which signifies the number of time scales computed during the coarse-graining procedure prior to the execution of whichever base entropy analysis is preferred, ApEn or the more common SampEn. The area under the curve of the ApEn or SampEn values plotted across time scales, known as the complexity index (C_I), is defined as:

$$\mathrm{C}_I = \sum_{i=1}^{\tau} \text{SampEn}(i) \qquad \text{Eq. (7)}$$

whereby we need only sum the entropy values (in this case, SampEn values) across the time scales of interest.

Previous studies have claimed that constant parameters *m* and *r* are suitable for analyzing physiological time series (Pincus SM 1991; Pincus SM and Huang 1992). Chon et al. (2009) developed equations to estimate maximum values for *r* by fitting multiple nonlinear least squares to Monte-Carlo simulations and normalizing *r* to the short-term (sd_1) and long-term (sd_2) variability of the signal based on the embedding dimension *m*:

$$\begin{aligned} m = 2: \hat{r}_{max} &= \left(-0.036 + 0.26\sqrt{\mathrm{sd}_1/\mathrm{sd}_2}\right)/\sqrt[4]{N/1{,}000} \\ m = 3: \hat{r}_{max} &= \left(-0.08 + 0.46\sqrt{\mathrm{sd}_1/\mathrm{sd}_2}\right)/\sqrt[4]{N/1{,}000} \\ m = 4: \hat{r}_{max} &= \left(-0.12 + 0.62\sqrt{\mathrm{sd}_1/\mathrm{sd}_2}\right)/\sqrt[4]{N/1{,}000} \\ m = 5: \hat{r}_{max} &= \left(-0.16 + 0.78\sqrt{\mathrm{sd}_1/\mathrm{sd}_2}\right)/\sqrt[4]{N/1{,}000} \\ \mathrm{m} = 6: \hat{r}_{max} &= \left(-0.19 + 0.91\sqrt{\mathrm{sd}_1/\mathrm{sd}_2}\right)/\sqrt[4]{N/1{,}000} \\ m = 7: \hat{r}_{max} &= \left(-0.2 + 1.0\sqrt{\mathrm{sd}_1/\mathrm{sd}_2}\right)/\sqrt[4]{N/1{,}000} \end{aligned} \qquad \text{Eq. (8)}$$

Where for a sequence $x(n) = \{x(1), x(2), \ldots, x(N)\}$:

$$sd_1 = \{x(2) - x(1), x(3) - x(4), \ldots, x(N) - x(N-1)\} \qquad \text{Eq. (9)}$$

and sd_2 is simply the standard deviation of *x(n)*. This method results in *r* values that increase with sample size, however, and may be inappropriate for nonlinear signals (Castiglioni and Di Rienzo 2008; Liu et al. 2010). For most entropy analyses and datasets, *r* can be set between 10-30% of the standard deviation of the signal (Yentes et al. 2013).

Complexity

A complex system is one composed of many interwoven subunits whose constant interactions provide feedback to many of the individual subunits and drive the behavior of the system (Rickles et al. 2007). In the context of an athlete performing a movement task, the complex system entails the cellular and biochemical processes interacting to liberate energy for muscular fiber contraction to the central nervous system integrating sensory information to formulate further responses to environmental constraints. Patterns of complex behavior are dynamic and self-organizing, meaning that the state of the system at a given time point depends

on the previous states and determines future states (Adami 2002). The human body is a complex system in that it operates within certain physiological constraints yet still exhibits variability in how it accomplishes most homeostatic processes.

Dynamical Systems in Injury Prevention and Sport Performance

The resilience of a complex system is operationally defined as its ability to maintain its operational status in the presence of perturbations, whereby the duration of the system response to the perturbation is inversely proportional to the resiliency of the system (Arnoldi et al. 2016; May 2019). Attractor states are defined as a system's convergence towards or divergence from a set of states, and in this biomechanical context an example could be the coordination patterns between joints used to navigate the demands imposed by the system (Hill et al. 2018). Injuries are the undesirable attractor to which the system is moved towards by specific biomechanical perturbations (excessive tissue loading during dynamic movements, initial joint contact angles, lack of tissue recovery, joint coordination, etc.). Previous biomechanics investigations have quantified complexity differences within human movement and trends delineating variation between groups (e.g., pathological and non-pathological) in measured biological signals via entropy analyses (Costa et al. 2002; Costa et al. 2003; McGregor et al. 2009; Bisi and Stagni 2016; Gruber et al. 2021; Gates et al. 2022).

ApEn has been used to quantify the regularity of postural sway in concussed athletes (Cavanaugh et al. 2006), minimal toe clearance in elderly adults during treadmill walking (Karmakar et al. 2007), and knee kinematics during walking between legs in ACLR patients (Georgoulis et al. 2006). Currently (for reasons outlined in the next paragraph), there is a paucity of ApEn analyses deployed on IMU-derived data. However, some investigations have used this approach to validate IMU and force plate postural sway comparisons (Soangra and Lockhart

2013); to examine the influence of fatigue on trunk acceleration variability during walking (Soangra et al. 2017); and as a correlate with other external load indicators of musculoskeletal injury in trail running (Rojas-Valverde et al. 2019). SampEn used in conjunction with IMU-based signals have been correlated with VO_2, blood lactate, energy cost, and medial tibial stress syndrome during running (Murray AM et al. 2017; Schütte K. H. et al. 2018; Schütte Kurt H et al. 2018). With IMUs, MSE has been used to highlight differences between fallers and non-fallers in elderly walkers (Howcroft et al. 2016; Bizovska et al. 2017), as well as comparisons of stride variability between treadmill and overground running (Lindsay et al. 2014).

Conclusion

Prevention of overuse and non-contact injuries is paramount in youth sports as injured individuals are at risk of re-injury and complications when returning to play or later in life (Taylor et al. 1993; Barber-Westin and Noyes 2011; Friel and Chu 2013; Herzog et al. 2019). While training load monitoring is becoming more common in youth soccer, movement complexity has not yet been considered for quantifying movement complexity during puberty nor for assessing injury risk. This population of athletes experiences physiological changes at rates which predispose them to certain sports-related injuries and monitoring movement complexity via IMUs in the field may provide insight into how these injuries may be prevented.

Chapter 3: Methodology

The purpose of this study is to collect IMU linear acceleration data from adolescent soccer athletes and determine if derived linear acceleration metrics (discretized peak accelerations, binned acceleration frequencies, etc.) or overall signal complexity differs between groups stratified by pubertal status or over the course of a season.

Participants

Participants were recruited via word of mouth, fliers, social media, and emails. If participants are recruited via word of mouth, flyer (Appendix D), or social media, an email containing a pre-approved email script (Appendix C) will be sent to the participant's guardian to ensure they are still interested and qualified to participate in the study. Healthy adolescent soccer players between 9 and 17 years will be asked to participate in the study. Due to the paucity of literature regarding mixed-model statistical entropy comparisons, we planned for medium effect sizes between groups. An *a priori* power analysis for a mixed model repeated measures ANOVA with an *alpha* of 0.05, statistical power of 0.80, and effect size (*f*) of 0.20 indicated that a minimum of 66 participants (22 per group) are needed.

Each participant and their guardian provided written informed assent and consent, respectively, as well as complete the Lower Extremity Functional Scale (LEFS)(Binkley et al. 1999) and a musculoskeletal health history questionnaire. Participants were excluded from testing if they had not been participating in club soccer training or play at least twice per week. Inclusion criteria includes the following: no history of lower extremity surgical repair, no lower extremity injuries within the past six months, and no lower extremity pain on the day of testing.

Experimental Procedures

Data collections were preceded by the informed consent and assent process prior to any testing. Participants and their guardian(s) met with the primary investigator to give consent and assent before filling out the LEFS and musculoskeletal questionnaire. Height and seated height

were measured via stadiometer and mass via digital scale. Sex-specific equations (Mirwald et al. 2002) utilizing standing height, seated height, leg length, and age were used to estimate the time offset (in years) of each participant from their PHV:

$$\begin{aligned}\text{Male Maturity Offset (years)} \\ &= -9.236 + 0.0002708 \times (\text{Leg Length} \times \text{Sitting Height}) \\ &- 0.001663 \times (\text{Age} \times \text{Leg Length}) + 0.007216 \times (\text{Age} \times \text{Sitting Height}) \\ &+ 0.02292 \times ((\text{Weight}/\text{Height}) \times 100)\end{aligned} \quad \text{Eq. (10)}$$

$$\begin{aligned}\text{Female Maturity Offset (years)} \\ &= -0.376 + 0.0001882 \times (\text{Leg Length} \times \text{Sitting Height}) \\ &+ 0.0022 \times (\text{Age} \times \text{Leg Length}) + 0.005841 \times (\text{Age} \times \text{Sitting Height}) \\ &- 0.002658 \times (\text{Age} \times \text{Weight}) + 0.07693 \times (\text{Weight}/\text{Height} \times 100)\end{aligned} \quad \text{Eq. (11)}$$

All experimental testing (Appendix G) took place on either grass or artificial turf surfaces (depending where the team practice was held) following a brief dynamic warm-up. Due to time constraints rendering a counterbalanced study design impractical, each drill was completed one (1) time successfully (i.e., no slipping, maximal effort, etc) and in the same order for each testing group to fit within team practice schedules. Participants were fitted consistently by the same researcher with small inertial measurement units (IMUs) on their mediodistal tibia just superior to the medial malleolus using molded straps from the manufacturer per their recommendation. Data collection began with an “easy pace” jog for approximately 80 meters by all participants. Following the jog, each subsequent drill except for the broad jump was completed individually, beginning with a 40-yard (36.6 meters) dash. Then, participants completed an M-cone drill in which they sprinted and changed direction rapidly around a series of cones in both directions. Then participants completed a 5-10-5 shuffle drill where they began by straddling a central cone

and then laterally shuffling between cones placed 5 meters from the middle cone. Finally, participants performed a broad jump for maximum horizontal displacement. Following the broad jump, each participant had completed testing. The participants were then asked to complete the experimental protocol again on the same surface type (i.e., grass or turf) following the end of their season (~3 months later, i.e., February through May).

Instrumentation

A fixed stadiometer (SECA, Birmingham, UK) was be used to measure participant standing height and then seated height and leg length, respectively, to the nearest millimeter. An IMU with high-g accelerometer (1600 Hz; Vicon Blue Trident, Vicon Motion Systems Ltd, Oxford, UK) was used to measure 3D linear accelerations at the mediodistal tibia during testing. These data were then imported into Python v3.10.4 (Python Software Foundation, Beaverton, OR, USA) computing software for subsequent data processing and analysis and R 4.2.1 (R Foundation for Statistical Computing, Vienna, AUST) for visualization.

Data Reduction & Analysis

Raw data was imported from the IMU sensors for data conditioning (Appendix I) and entropy analysis (Appendix J). Due to the fixation and orientation of the IMUs upon the mediodistal tibia, an aggressive digital lowpass filter (4th order Butterworth with 0.2 Hz cutoff frequency) was used to separate any constant offset due to gravity. That gravitational component was then subtracted from each accelerometer signal component (Van Hees et al. 2013; Bayat et al. 2014) before another similar lowpass filter with a cutoff frequency of 50 Hz was used to reduce signal noise before further analysis. The more resolute onboard “low-g” accelerometer saturates at 16 units gravity (G’s) and the “high-g” sensor does not saturate prior to 200 G’s. Therefore, raw low-g acceleration signal component time-points that had plateaued at 16 G’s

were substituted with high-g component time-points. Then, the signal duration was cropped via manual inspection to remove data corresponding to movement performed before and after the drills (Appendix I). The EntropyHub toolkit (Flood and Grimm 2021) has functions native to both Python and was used to analyze the acceleration time series for each experimental task (jog, 40-yard dash, M-cone drill, 5-10-5 shuffle drill, and broad jump). For each resultant acceleration-time series, we calculated the Multiscale Entropy (MSE) of the signal (Costa et al. 2002; McGregor et al. 2009; Parshad et al. 2012). MSE values are unitless and used to examine signal regularity on different temporal scales by coarse-graining the original time series via:

$$y_j^{(\tau)} = \frac{1}{\tau} \sum_{i=(j-1)\tau+1}^{j\tau} x_i, \qquad 1 \leqslant j \leqslant N/\tau \qquad \text{Eq. (12)}$$

Once the time series has been "coarse-grained," Sample Entropy (SampEn) is then calculated for each new time scale:

$$\text{SampEn}\ (m, r, N) = -ln\left(\frac{A}{B}\right) \qquad \text{Eq. (13)}$$

whereby *B* and *A* are defined as the total number of template matches of length *m* and total number of forward matches of length *m+1*, respectively:

$$A = \left\{\frac{[(N-m-1)(N-m)]}{2}\right\} A^m(r),\ \ B = \left\{\frac{[(N-m-1)(N-m)]}{2}\right\} B^m(r) \qquad \text{Eq. (14)}$$

This allows for SampEn values to be plotted at each time scale and, by calculating the area under this curve, complexity index (CI) may be reported. CI values were used for statistical analyses as opposed to the individual SampEn values used to calculate CI for each trial. A visualization of the MSE workflow can be found in Appendix J.

Further, discrete peak resultant acceleration magnitudes and cumulative acceleration were reported. Peak resultant accelerations were the greatest magnitude resultant acceleration in each trial. Integrated acceleration was calculated as the area under the resultant acceleration curve.

Both can be respectively thought of as the peak and cumulative loading experienced during each task.

Statistical Analysis

Linear mixed effects regression (LMER) was chosen for this study over traditional repeated measures ANOVA due to its ability to account for variability originating from both participants and the independent variables, preservation of statistical power, and robustness to sphericity violations (Brown VA 2021). The 'lme4' package (Bates D et al. 2014) in R was used to conduct all LMER tests and all assumption tests (i.e., linearity, homoscedasticity (equal variances), and normality of residuals) carried out with the R 'performance' package (Lüdecke et al. 2021). Diagnostic plots were used to visually inspect residuals against predicted values (linearity), across levels of the independent variables (homoscedasticity), and against a normal distribution (Q-Q plot for normality).

An iterative method was used to develop the LMER models, initiated with a null model and successively incorporating fixed effects until a complete model was achieved. The process began with the formation of a null model only including random effects, providing a benchmark for subsequent model performance. Subsequent to the formation of the null model, fixed effects were methodically added one at a time (PHV offset followed by sex and then testing session) to determine their effect on modelling the relationship with CI. With the addition of each new fixed effect, the current model was compared to its predecessor. The comparison aimed to assess the model using Akaike (AIC) and Bayesian (BIC) Information Criterion, marginal and conditional R^2, intraclass correlation coefficients (ICC), and root-mean-square error (RMSE) values as guides. The iterative process continued until all fixed effects had been integrated, thus arriving at the full model. An essential consideration throughout this process was to maintain a balance

between model complexity and model fit, ensuring the final model was neither underfitted nor overfitted. This systematic, iterative approach enabled a robust and quantitative evaluation of the contribution of each fixed effect and facilitated the construction of a model that optimally represented the data.

Chapter 4: Relationship between multiscale entropy measures, accelerometry, and peak height velocity in adolescent soccer players

Abstract

Physiological changes due to puberty are drastic and happen over different timeframes based on biological sex. Both boys and girls, however, exhibit concomitant changes in movement variability and injury rates during puberty, particularly surrounding the occurrence of peak height velocity (PHV). Non-linear time-series analyses, such as multiscale entropy, have been used in previous biomechanical investigations to quantify changes in movement complexity based on wearable sensor signals. None of these studies have examined the relationship between PHV, sex, and time in youth athletes. The purpose of this study is to investigate the impact of pubertal status, sex, and time on the biomechanics of movement in adolescent soccer players using multiscale entropy analysis. A sample of 55 male and 52 female soccer players performed six drills before and after a competitive club season. Tibial impacts were collected via inertial measurement units and the 3D resultant acceleration signals were analyzed using multiscale entropy analysis to calculate complexity index. Linear mixed effects regression was used on each drill separately to determine the effects of PHV, sex, and time of testing on complexity index. Complexity significantly increased from pre- to post-season for only the Broad and M-R drills, though model evaluation metrics and sparsity of results across drills suggest that our models did not accurately capture the relationship between our predictor variables and complexity in this context. Further research is needed to elucidate how pubertal status, sex, and time affects tibial movement complexity.

Introduction

Puberty is a critical period of growth and development characterized by rapid changes in body composition, physical attributes, and hormonal levels. These changes can significantly influence competitive performance and injury risk in adolescent athletes. In sports such as soccer, puberty-related changes can affect the biomechanics of movement, potentially leading to an increased risk of injuries (Ford et al. 2010; Bergeron et al. 2015). Overuse injuries are particularly common in children and adolescents who participate in sports. These injuries occur because of repetitive submaximal loading of the musculoskeletal system, which can lead to microtrauma and eventual tissue damage (Myer et al. 2011; Valovich McLeod et al. 2011). The risk of overuse injuries is further increased during puberty, due to the rapid growth and changes in body composition that occur during this period (Ford et al. 2010; Myer et al. 2013). This risk may also differ between sexes as girls typically begin exhibiting puberty-related changes before boys (Hewett et al. 2006; Ford et al. 2010). Between ages 5-18, boys experience more tendinous, apophyseal, and cartilaginous overuse injuries than girls (Valasek et al. 2019), including greater rates of Osgood-Schlatter's disease (OSD – ossification of the tibial tubercle) typically being diagnosed 1-1.5 years pre-PHV (Kujala et al. 1985). Conversely, girls experience greater rates of ACL injury during their freshman year of high school (post-PHV) (Tursz and Crost 1986) before these rates decrease, the opposite trend that occurs in boys (Comstock and Pierpoint 2020).

Current methods for tracking external loading factors associated with injury risk in adolescent athletes include the use of global positioning system (GPS) distances covered, center of mass (CoM) acceleration peaks, total accelerations and decelerations, etc. (Hartwig et al. 2011; Malone et al. 2015; Haddad et al. 2017; Jones et al. 2017; McLaren et al. 2018). However, these methods provide a one-dimensional view of the biomechanical loads experienced by the

athletes. Multiscale entropy (MSE) analysis is a powerful tool that allows for the examination of the complexity of biological signals over multiple temporal scales. This method has been used to analyze various biological signals, including heart rate variability and gait dynamics, providing insights into the health and function of the system under study (Bosl et al. 2011; Bravi et al. 2011; Riva et al. 2013). The use of MSE analysis in the context of adolescent athletes is justified by the potential insights it can provide into how puberty-related changes affect movement patterns and injury risk. Specifically, changes in movement complexity, as measured by MSE, could be indicative of altered biomechanics and increased injury risk. Therefore, the purpose of this study is to investigate the impact of pubertal status, sex, and time on the biomechanics of movement in adolescent soccer players using MSE analysis. Our primary hypothesis is that puberty-related changes and sex will result in altered movement complexity and our secondary hypothesis is that movement complexity will also be different at post-season testing compared to pre-season.

Methods

Participants

Participants were recruited via word of mouth, fliers, social media, and emails. If participants were recruited via word of mouth, flyer (Appendix D), or social media, an email containing a pre-approved email script (Appendix C) was sent to the participant's guardian to ensure they were still interested and qualified to participate in the study. Healthy adolescent soccer players between 9 and 17 years were asked to participate in the current study and their anthropometric data can be found in Appendix V. Due to the paucity of literature regarding mixed-model statistical entropy comparisons, we planned for medium effect sizes between groups. An a priori power analysis for a mixed model repeated measures ANOVA with an *alpha*

of 0.05, a *beta* of 0.80, and effect size (*f*) of 0.20 indicated that a minimum of 66 participants were needed.

Once guardian consent had been obtained, each participant provided written informed assent and completed the Lower Extremity Functional Scale (LEFS) (Binkley et al. 1999) and a musculoskeletal health history questionnaire. Participants were excluded from testing if they had not been participating in club soccer training or play at least twice per week. Inclusion criteria included the following: no history of lower extremity surgical repair, no lower extremity injuries within the past six months, and no lower extremity pain on the day of testing.

Experimental Procedures

Data collections were preceded by the informed consent and assent process prior to any testing. Participants and their guardian(s) met with the primary investigator to give consent and assent before filling out the LEFS and musculoskeletal questionnaire. Standing height was measured via stadiometer and mass via digital scale. Then the participant sat up straight on a stool so seated height could be obtained and leg length calculated. All measurements were performed by the same investigator three times with the median measurement being reported. Once the investigator had obtained all IRB documents and anthropometric measurements, sex-specific equations (Mirwald et al. 2002) utilizing mass, standing height, leg length, and age were used to estimate the time offset (in years) of each participant from their peak height velocity (PHV):

$$\begin{aligned}\text{Male Maturity Offset (years)} &= -9.236 + 0.0002708 \times (\text{Leg Length} \times \text{Sitting Height}) \\ &- 0.001663 \times (\text{Age} \times \text{Leg Length}) + 0.007216 \times (\text{Age} \times \text{Sitting Height}) \\ &+ 0.02292 \times ((\text{Weight}/\text{Height}) \times 100)\end{aligned} \quad \text{Eq. (10)}$$

$$\text{Female Maturity Offset (years)} = -0.376 + 0.0001882 \times (\text{Leg Length} \times \text{Sitting Height}) + 0.0022 \times (\text{Age} \times \text{Leg Length}) + 0.005841 \times (\text{Age} \times \text{Sitting Height}) - 0.002658 \times (\text{Age} \times \text{Weight}) + 0.07693 \times (\text{Weight/Height} \times 100) \quad \text{Eq. (11)}$$

All experimental testing (Appendix G) took place on either grass or artificial turf surfaces (depending on where the team practice was held) following a brief dynamic warm-up. Due to time constraints rendering a counterbalanced study design impractical, each drill was completed one (1) time successfully (i.e., no slipping, maximal effort, etc.) and in the same order for each testing group to fit within team practice schedules. Participants were fitted consistently by the same researcher with small inertial measurement units (IMUs) on their mediodistal tibia just superior to the medial malleolus using molded straps from the manufacturer per their recommendation. Data collection began with an “easy pace” jog approximately 80 meters lengthwise down the field and back (DNB). Following the jog, each subsequent drill was completed once by each participant, beginning with a 40-yard (40yd; 36.6 meters) dash. Then, participants completed an M-cone drill (M-R, M-L) twice, once in which they sprinted and changed direction rapidly around a series of cones starting with a cut off of the right foot, and then again where the first cut was off of the left foot. Then participants completed a 5-10-5 shuffle drill where they began by straddling a central cone and then laterally shuffled between cones placed 5 meters from the middle cone. Finally, participants performed a broad jump (Broad) for maximum horizontal displacement. Following the broad jump, each participant had completed testing and were then asked to complete the experimental protocol again on the same surface type (i.e., grass or turf) following the end of their season (~3 months later, i.e., February through May).

Instrumentation

An IMU (1600 Hz; Vicon Blue Trident, Vicon Motion Systems Ltd, Oxford, UK) was used to measure 3D linear accelerations at the tibia during testing. These data were then imported into Python v3.10.4 (Python Software Foundation, Beaverton, OR, USA) computing software for subsequent data processing and analysis and R 4.2.1 (R Foundation for Statistical Computing, Vienna, AUST) for visualization.

Data Reduction & Analysis

Prior to any entropy analysis, the raw data had to be clipped and filtered prior to analysis (Appendix I). Offset of the IMU axes due to bony geometry of the tibia required that the constant gravitational bias in the 3D accelerometer components be removed with an aggressive digital lowpass filter (4th order Butterworth with 0.2 Hz cutoff frequency). That gravitational bias was then subtracted from each accelerometer component (Van Hees et al. 2013; Bayat et al. 2014) before another similar lowpass filter with a cutoff frequency of 50 Hz was used to reduce signal noise before further analysis. Two onboard sensors ("high-g" – 1600Hz; "low-g" – 1125Hz) were aligned via resampling before the higher bit resolution "low-g" data points with a range of ±16 units gravity (G's) were substituted with "high-g" data if sensor saturation had occurred. The resulting signal duration was then manually assessed and cropped via to remove data not occurring during the drill (Appendix I). The EntropyHub toolkit (Flood and Grimm 2021) has native Python functions and was used to analyze the acceleration time series for each experimental task (jog, 40-yard dash, M-cone drill, 5-10-5 shuffle drill, and broad jump). For each resultant acceleration-time series, we calculated the Multiscale Entropy (MSE) of the signal (Costa et al. 2002; McGregor et al. 2009; Parshad et al. 2012). MSE values are unitless and used

to examine signal regularity on different temporal scales by coarse-graining the original time series:

$$y_j^{(\tau)} = \frac{1}{\tau} \sum_{i=(j-1)\tau+1}^{j\tau} x_i, \qquad 1 \leqslant j \leqslant N/\tau \qquad \text{Eq. (12)}$$

Once the time series has been coarse-grained, Sample Entropy (SampEn) is then calculated for each new time scale:

$$\text{SampEn}\ (m, r, N) = -ln\left(\frac{A}{B}\right) \qquad \text{Eq. (13)}$$

whereby *B* and *A* are defined as the total number of template matches of length *m* and total number of forward matches of length *m+1*, respectively:

$$A = \left\{\frac{[(N-m-1)(N-m)]}{2}\right\} A^m(r),\ \ B = \left\{\frac{[(N-m-1)(N-m)]}{2}\right\} B^m(r) \qquad \text{Eq. (14)}$$

This allows for SampEn (m = 2, r = 0.2*SD, τ = 16) values (determined a priori via pilot testing and parameterization) to be plotted at each time scale and, by calculating the area under this curve, complexity index (CI) may be reported. CI values were used for statistical analyses as opposed to the individual SampEn values used to calculate CI for each trial.

Statistical Analysis

Linear mixed effects regression (LMER) was chosen for this study due to its ability to handle repeated measures and non-independence in the data. The ‘lme4’ package (Bates D et al. 2014) in R was used to conduct all LMER tests. Before conducting the analysis, the assumptions of the linear mixed model were checked (i.e., linearity, homoscedasticity (equal variances), and normality of residuals) using the R ‘performance’ package (Lüdecke et al. 2021). Diagnostic plots were used to visually inspect these assumptions. Linearity was checked by plotting the residuals against the predicted values. Homoscedasticity was assessed by looking at the spread of

residuals across levels of the independent variables. Normality of residuals was checked using a Q-Q plot, where the residuals are plotted against a normal distribution.

An iterative method was used to develop the LMER models (Appendix K), initiated with a null model and successively incorporating fixed effects until a complete model was achieved. The process began with the formation of a null model only including random effects, providing a benchmark for subsequent model performance. Subsequent to the formation of the null model, fixed effects were methodically added one at a time (PHV offset followed by sex and then testing session) to determine their effect on modelling the relationship with CI. With the addition of each new fixed effect, the current model was compared to its predecessor and this process was continued until all fixed effects had been integrated, thus arriving at the full model. The comparison aimed to assess the model using Akaike (AIC) and Bayesian (BIC) Information Criterion to assess model fit; marginal and conditional R^2 to quantify influence of only fixed effects and the combination of random and fixed effects, respectively; intraclass correlation coefficients (ICC) to see how grouping structure of predictors explains variance; and root-mean-square error (RMSE) values to quantify predictive error. An essential consideration throughout this process was to maintain a balance between model complexity and model fit, ensuring the final model was neither underfitted nor overfitted. This systematic, iterative approach enabled a robust and quantitative evaluation of the contribution of each fixed effect and facilitated the construction of a model that optimally represented the data.

Results

CI results parsed by drill, session, and sex can be found in Appendix V. Model comparisons for CI by drill are accompanied by scatterplots can also be found in Appendix V. A total of 130 athletes were tested initially, though only 109 completed both pre- and post-season

testing (13.5% attrition rate - Appendices N & O). All drill data for two participants were excluded due to sensor error during testing. Two participants' data were excluded only from the 40yd and DNB drill analyses due to file corruption.

Interestingly, the null LMER models, which only incorporated random effects, consistently matched the fit of the more complex models which also considered PHV, sex, and testing session. After controlling for PHV and sex, broad jump (β = 0.291, SE = 0.141) and right M-drill (β = 0.187, SE = 0.084) complexity were the only drills where complexity significantly increased compared to pre-season testing. However, no other fixed effect session differences for the other drills nor any differences for fixed sex effects across models was found. Overall, sparse significance of fixed session effects and a lack of any fixed sex effects, coupled with poor improvements across model iterations, suggests that the models are not capturing the relationship with CI in this context.

Discussion

In the realm of sports science, the biomechanics of movement in adolescent athletes has been a topic of growing interest. The onset of puberty introduces a myriad of physiological changes that can significantly impact an athlete's performance and injury risk. The purpose of this study was to investigate the impact of pubertal status, sex, and time on the biomechanics of movement in adolescent soccer players using MSE analysis. Our primary hypothesis that puberty- and sex-related differences would result in altered movement complexity was not supported. Our secondary hypothesis that complexity differences would be observed between testing sessions was only partially supported. Despite an adequately powered study design and careful measurement of key variables such as PHV, sex, and testing session, we found limited

significant effects of these variables on the complexity index (CI) calculated from 3D resultant tibial accelerometer signals.

The lack of significant findings could potentially be attributed to the true absence of an effect rather than a lack of power. This could suggest that the variables we studied may not have a significant impact on the calculated CI in the context of adolescent soccer players performing these discrete drills. Our study was adequately powered as stated in the methods section. However, it's important to note that statistical power is not a guarantee of significant results but merely increases the likelihood of detecting a true effect if one exists. Two drills (the broad jump and right M-drill) showed increased complexity at post-season testing, though the lack of significance in the other M-drill (M-L), fixed sex estimates, and non-existent improvements from null- to full-LMER models suggest that PHV, sex, and testing session are not strong linear predictors of tibial-mounted resultant acceleration CI.

Our primary predictor variable, PHV, was estimated from chronological age, height, weight, and leg length based on sex-specific equations. This is a common, non-invasive method used to estimate the timing of PHV (Van der Sluis et al. 2013; Van der Sluis et al. 2015), especially in field settings where more invasive measures are not feasible. However, it's worth noting that this method provides an estimate and not an exact measure of PHV, which itself is only a highly correlated surrogate measure of pubertal development (Kelly et al. 2014; Granados et al. 2015). Furthermore, the impact of puberty on biomechanics is complex and may not be fully captured by PHV alone. Our study included children aged 9-17, a range that encompasses the typical age of pubertal onset and progression (Appendix Q). Previously used arbitrary PHV-cutoffs (Van der Sluis et al. 2013; Van der Sluis et al. 2015) classified athletes as either pre- (-1.5 to -0.5 years PHV), circa- (-0.5 to +0.5 years PHV), and post-pubertal (+0.5 to +1.5 years PHV).

This means that our sample included children at various stages of pubertal development, from 4+ years pre-pubertal to 2+ years post-pubertal that were not evenly distributed between boys and girls (Appendix P). Puberty is a time of significant physiological changes, including changes in body composition, muscle development, and motor control, all of which could potentially impact biomechanics. However, not all of these changes are linear and they can vary greatly between individuals, particularly when the range of PHV offset is so wide and puberty may have not started or even run its course in some participants.

Movement complexity, an already nebulous concept, has yet to find consensus in the biomechanics literature regarding whether it more or less complexity and regularity in movement coordination is beneficial (Negahban et al. 2010; Hamill et al. 2012; Gruber et al. 2021; Quirino et al. 2021). Pubertal athletes are undergoing rapid changes to their neural and musculoskeletal physiology that affects movement quality. This led to our hypothesis that movement complexity could, via dynamical systems theory, be an indicator of critical phase transitions around the time of PHV that could precede injury (Pol et al. 2019; Fonseca et al. 2020). The CI, a novel and complex measure in this context, was calculated from 3D resultant tibial accelerometer signals. However, it's possible that the CI may not be sensitive to the variables we studied. In other words, factors such as age, sex, and PHV may not have a significant impact on movement complexity as captured by the CI.

LMER was the appropriate statistical approach for our study design, which included repeated measures and random effects. However, like any statistical test, LMER has certain assumptions and limitations. One key assumption based on the terms in our model equation is that the relationship between the predictors and the outcome variable is linear. If this assumption is violated, the results of the LMER may not be valid. In our case, it's possible that the

relationship between our predictors and the CI is not linear, which could explain our lack of significant findings. Stature, weight, and timing of pubertal-related changes in these PHV-predictors has been posited to hold a non-linear relationship (Marceau et al. 2011), as well as the possibility that alterations to brain function (Gracia-Tabuenca et al. 2021) could potentially affect movement complexity in a non-linear fashion.

One limiting factor in collecting data on boys in the PHV to post-PHV range was that local high school teams were in-season, diverting available athletes from their club competition and practice. Including more boys at this point in their pubertal growth would have brought the gap in average PHV offset between them and the female participants closer together and potentially revealed more significant results. Another limitation could potentially be testing on two different surfaces (i.e., grass and turf) and their respective conditions on the day of testing (e.g., dew and moisture, etc.). However, CI and acceleration peaks and integrals do not seem to differ between those who were tested on dissimilar surfaces (Appendix Q). Another plausible explanation is that other unknown sources of noise were present and exacerbating the variability of the accelerometer signals used in our calculations. Whether these noise sources would be biological in nature or the product of some measurement error or both is unclear, but their presence would unduly influence our statistical results. Further, only one trial of each drill was analyzed from both testing sessions. This was necessary due to logistical constraints but not ideal as collecting several trials could have allowed for more stable metric calculations following averaging of trials.

In conclusion, our hypothesis that PHV and other associated factors were predictive of movement complexity in adolescent soccer players was not wholly supported by our findings. However, future directions could focus on other variables (i.e., tibial acceleration metrics

associated with lower extremity loading), explore alternate accelerometer placements, and investigate whether rate of change in PHV contributes to changes in movement complexity.

Chapter 5: Relationship between peak height velocity and tibial acceleration metrics in adolescent soccer players

Abstract

Frequency, intensity, and time of training are all critical components impacting injury risk in athletes. Injury rates in youth soccer players have been shown to increase during and immediately following peak height velocity (PHV) during puberty. External load monitoring of impact magnitudes via tibial accelerometry has been used to mitigate and study lower-extremity injury risk. To date, no previous study has examined the relationship between PHV, sex, and time with cumulative tibial accelerations and peak acceleration magnitudes in youth athletes. The purpose of this study is to investigate the impact of pubertal status, sex, and time on these acceleration metrics in adolescent soccer players. Six drills were performed by 55 male and 52 female soccer before and after a competitive club season. 3D resultant acceleration peaks and the integral of these signals from tibial-mounted sensors were collected. These metrics for each separate drill were predicted using linear mixed effects regression models to determine the effects of PHV, sex, and time of testing on acceleration peaks and integrals. Significant PHV, sex, and time effects were found for estimates for each drill except the 40yd dash. However, comparisons with our null model suggest that the addition of our predictor variables to subsequent regression models do not increase the explained variance in acceleration peaks and integrals. These findings suggest that the relationship between cumulative and absolute loading of the lower-extremity during these drills with PHV, sex, and time is nuanced and requires further investigation.

Introduction

Athlete load monitoring has become a popular topic with regards to managing external loading on biological tissues to reduce injury rates (West et al. 2021). Of note, accelerometers have been garnering favor over gold-standards biomechanical motion capture systems for the fact that they can be used to collect impact and loading data during practice and games (Cummins et al. 2013; Dalen et al. 2016). Though many of the loads and impacts placed on tissues during dynamic movements (i.e., landing, cutting, accelerating and decelerating, etc.) are submaximal, the magnitude of the loading in relation to the failure point of the tissues and the cumulative effects of exposure to cycles of these loads can lead to overuse injuries in these athletes, particularly in adolescent athletes (Myer et al. 2011; Valovich McLeod et al. 2011). The confounding rapid physiological changes accompanying puberty in these athletes affects tissue morphology and distribution, which further impacts movement coordination and biomechanics that increases injury risk (Ford et al. 2010; Myer et al. 2013). Reports from Van der Sluis et al. have shown that injury rates in youth soccer athletes are greater during and immediately following peak height velocity (PHV) (Van der Sluis et al. 2013; Van der Sluis et al. 2015). Overuse injury risk in pubertal athletes is also modified by sex due to the differential timing in puberty onset as girls experience its effects on average two years before boys (Ford et al., 2010; Hewett, Myer, Ford, & Slauterbeck, 2006. Further, while normal puberty-related tissue changes (e.g., epiphyseal bone remodeling) will predispose these athletes to certain overuse injuries, fatigue-related damage through excessive training intensities and volumes over the course of a competitive season should also be taken into account (Drew and Finch 2016; Murray A 2017).

While the predominant method for accelerometry-based load monitoring has been either global positioning system (GPS) based (Rago et al. 2020; de Dios-Álvarez et al. 2023) or utilized

an accelerometer fixed near the center-of-mass (CoM) (Aristizábal Pla et al. 2021) in athletic populations, little to no data on this adolescent cohort has been collected at the site of most sport-related injuries: the lower-extremity. Tibial-mounted accelerometry in adults has used measured accelerations as a surrogate measure for impact loading during running and other dynamic tasks (Butler et al. 2007; García-Pérez et al. 2014; McGinnis et al. 2016; Sandrey et al. 2019). Some have also integrated metrics over the duration of tasks and movements for the purpose of quantifying 'cumulative loading effects' on tissues (Miller et al. 2015; Kiernan et al. 2018), though none have examined anything resembling cumulative tibial loading in this younger population in a longitudinal context.

Therefore, the purpose of this study was to investigate the impact of pubertal status, sex, and testing session on the peak and cumulative tibial accelerations in adolescent soccer players. We primarily hypothesize that puberty-related changes and sex will result in altered peaks and cumulative acceleration metrics. Our secondary hypothesis is that differences in peaks and cumulative accelerations will also present as a function testing session.

Methods

Participants

Participants were recruited via fliers, social media posts, word of mouth, and email. If participants were recruited via word of mouth, flyer (Appendix D), or social media, an email containing a pre-approved email script (Appendix C) was sent to the participant's guardian to ensure they were still interested and qualified to participate in the study. Healthy youth soccer players between 9 and 17 years were asked to participate in the study. An *a priori* power analysis for a mixed model repeated measures ANOVA with an *alpha* of 0.05, power of 0.80, and effect size (*f*) of 0.20 indicated that of 66 participants were needed at minimum. We planned for small

effect sizes between groups due to the novelty of our study design regarding mixed-model statistical entropy comparisons in this youth population. Participant anthropometric characteristics have previously been reported (Appendix V).

Each participant provided assent only after guardian consent was obtained, as well as Lower Extremity Functional Scale (LEFS) (Binkley et al. 1999) and musculoskeletal health history questionnaires. Exclusion criteria included participation in club soccer training or play less than twice per week; major lower extremity surgical repair history; lower extremity injuries within the past six months; and localized lower extremity pain the day of testing.

Experimental Procedures

Data collections were preceded by the informed consent and assent process prior to any testing. Participants and their guardian(s) met with the primary investigator to give consent and assent before filling out the LEFS and musculoskeletal questionnaire. Stature and mass were obtained via portable stadiometer and digital scale on site. Seated height was also calculated from the difference between standing height and seated height obtained from the participant sitting up straight on a stool. All measurements were performed by the same investigator three times with the median measurement being reported. Once the investigator had obtained all IRB documents and anthropometric measurements, sex-specific equations (Mirwald et al. 2002) utilizing standing height, mass, leg length, and age were used to estimate the time offset (in years) of each participant from their PHV:

$$\begin{aligned}\text{Male Maturity Offset (years)} \\ &= -9.236 + 0.0002708 \times (\text{Leg Length} \times \text{Sitting Height}) \\ &- 0.001663 \times (\text{Age} \times \text{Leg Length}) + 0.007216 \times (\text{Age} \times \text{Sitting Height}) \\ &+ 0.02292 \times ((\text{Weight}/\text{Height}) \times 100)\end{aligned} \qquad \text{Eq. (10)}$$

$$\text{Female Maturity Offset (years)} = -0.376 + 0.0001882 \times (\text{Leg Length} \times \text{Sitting Height}) + 0.0022 \times (\text{Age} \times \text{Leg Length}) + 0.005841 \times (\text{Age} \times \text{Sitting Height}) - 0.002658 \times (\text{Age} \times \text{Weight}) + 0.07693 \times (\text{Weight/Height} \times 100) \quad \text{Eq. (11)}$$

A full description of the testing protocol can be found in Chapter 4. The participants completed the experimental protocol consisting of six drills during their first testing session and again following the end of their season (~3 months later, e.g., February through May) on the same surface (i.e., grass or turf) that they were originally tested.

Instrumentation

An IMU with onboard low-g (1125 Hz; 16 G's range) and high-g (1600 Hz; 200 G's range) accelerometers (Vicon Blue Trident, Vicon Motion Systems Ltd, Oxford, UK) was used to measure 3D linear accelerations at the tibia during testing. These data were then imported into Python v3.10.4 (Python Software Foundation, Beaverton, OR, USA) computing software for subsequent data processing and analysis and R 4.2.1 (R Foundation for Statistical Computing, Vienna, AUST) for visualization.

Data Reduction & Analysis

A full description of how IMU sensor data were processed can be found in Chapter 4. Data processing preceded 3D resultant peak acceleration and acceleration integrals calculations for each experimental task (jog, 40-yard dash, M-cone drill, 5-10-5 shuffle drill, and broad jump). Each axial component (Figure 3) of the accelerometer signal at each time point within a trial was used to calculate the 3D resultant acceleration:

$$A_R = \sqrt{{A_x}^2 + {A_y}^2 + {A_z}^2} \quad \text{Eq. (15)}$$

Acceleration integrals were calculated as the area under the resultant acceleration curve for all drills from their beginning to end (except for the broad jump as it consisted of only one ground impact upon landing). Both dependent variables can be respectively thought of as the peak and cumulative loading experienced during each task.

Statistical Analysis

Due to the longitudinal component of this study and uneven distribution of PHV among sexes, linear mixed effects regression (LMER) was used for our statistical analyses. All LMER tests were carried out using the 'lme4' package (Bates D et al. 2014) in R after checking assumptions using the R 'performance' package (Lüdecke et al. 2021). Diagnostic plots were used to visually inspect: normality of residuals, via Q-Q plot where residuals are plotted against a normal distribution; linearity, by visualizing residuals against predicted values; and homoscedasticity by comparing the spread of residuals across independent variable levels.

The full process for building and assessing LMER models can be found in Appendix K. It consists of establishing a baseline "null" model only containing random effect terms before iteratively adding fixed effect terms (i.e., PHV, sex, and then testing session) until a complete model is built. The features of each new model is compared to the previous model using the following criteria: model fit using Akaike (AIC) and Bayesian (BIC) Information Criterion; fixed effects only and the combined influence of random and fixed effects via marginal and conditional R^2, respectively; intraclass correlation coefficients (ICC) to quantify the proportion of variance explained by the grouping structure of predictors; and model prediction error via root-mean-square error (RMSE).

Results

Acceleration peak and integral results parsed by drill, session, and sex can be found in Appendix W. Model comparisons for acceleration peaks by drill are detailed further in Appendix W along with acceleration integral model comparisons.

Models 2 (random subject effects, fixed PHV and sex effects) and 3 (random subject effects, fixed PHV, sex, and session effects) for the DNB drill (β = -1.511, SE = 0.428) exhibited significant PHV fixed effects for peak accelerations. Significant sex fixed effects on peak accelerations were found for the M-L (β = 3.733, SE = 1.314), M-R (β = 3.182, SE = 1.400), and DNB (β = -5.361, SE = 1.435) drills via models 2 and 3. Finally, models 2 and 3 for M-R (β = -1.322, SE = 0.576) revealed the only significant fixed effects for testing session.

For acceleration integrals, significant PHV fixed effects were found in model 1 (random subject effects, fixed PHV effects) for M-L (β = -670.475, SE = 251.883), M-R (β = -942.901, SE = 221.175), and DNB (β = -569.907, SE =263.467); and models 2 and 3 for M-R (β = -744.896, SE = 328.708) and DNB (β = -2095.469, SE = 343.002). Sex fixed effect significance for acceleration integrals was only found in models 2 and 3 for DNB (β = -6843.672, SE = 1149.294) and the only session effects were found in the 5-10-5 (β = -2413.302, SE = 668.440) and M-R (β = -1607.198, SE = 684.014) full models.

However, the null model results were consistently indistinguishable from the complex models for both peaks and integrals and fixed effects estimates and standard errors were identical between models 2 and 3. These observations and their potential underlying causes (which will be discussed in the following section) suggest we should be wary of each model's predictive power.

Discussion

The findings from our study offer insights into the acceleration profiles of adolescent soccer players. The purpose of this study was to investigate the impact of pubertal status, sex, and time on the tibial acceleration metrics in adolescent soccer players. Our primary hypothesis that puberty- and sex-related differences would change acceleration peaks and integrals was partially supported. Our secondary hypothesis that complexity differences would be observed between testing sessions was also only partially supported. These hypotheses were based on the understanding that puberty, a period of rapid growth and development, could lead to changes in loading on the lower extremity during a host of discrete drills. Unfortunately, conflicting results suggest that the physiological changes that occur during puberty may not directly translate into changes in acceleration profiles during the performance of our experimental tasks.

The only PHV fixed effects found suggested that the lower PHV is associated with lower peak tibial accelerations during the DNB but greater cumulative tibial loading (acceleration integral) during the DNB and both M-drills. Significant sex fixed effects convey that the boys produce greater peak tibial accelerations during both M-drills, but lower peaks and cumulative tibial loading during the DNB drill. Finally, the only session fixed effect for peak tibial accelerations suggest M-R increased at post-season while cumulative loading decreased for M-L and the 5-10-5 shuffling drill. The inconsistent trends and lack of similar significance among similar drill make interpretations of our models with any certainty very difficult. Indeed, this lack of confidence in the predictive power of the models is echoed by the null models, which only incorporated random effects, consistently matched the fit of the more complex models that also considered PHV, sex, and testing session. This finding is particularly interesting as it suggests that the additional fixed effects in the subsequent models did not significantly explain the

variability within acceleration peaks and integrals in this context. This could potentially indicate that the variables under study, while important in the context of growth and development, may not significantly impact the calculated acceleration metrics in the context of adolescent soccer players performing these discrete drills. In the progression of our mixed models, we also observed a recurring pattern: the addition of the session fixed effect in model 3 did not alter the estimates for existing fixed effects from model 2. This could imply that these variables independently influence the outcome variable without significant multicollinearity and are orthogonal to each other (Christensen 2002; Cohen et al. 2013). This consistency might be attributed to the nature of the data, wherein a limited variability in the predictors or minimal group differences might have resulted in consistent estimates and standard errors across models.

It is also possible that other factors not considered in our study may play a more significant role in determining acceleration profiles. The largest limiting factor in our methods was the constraining nature of the data collection process as only one trial of each drill could be collected at both pre- and post-season testing sessions. Due to the volatile nature of the outside sources of influence on accelerometer signal (i.e., site of fixation, sensor fixation method, etc.) (Brayne et al. 2018; Cabarkapa et al. 2023), collection of multiple trials and averaging these signals prior to peak and integral calculations would most likely have stabilized a large portion of noise present in the signals. It is also worth noting that the drills used in our study, while common in soccer training, may not fully extrapolate to actual gameplay due to their discrete nature. This could potentially limit the generalizability of our findings to the biomechanical demands of competitive matches.

The non-linear processes occurring during puberty such as body segment growth, tissue development, and coordination changes (without considering covariates such as sex) could also

alter tibial biomechanics in a way that our linear statistical model could not robustly measure (Fleury et al. 2001; Papaiakovou et al. 2009; Rudroff et al. 2013). Our study encompassed children aged 9-17, a range that includes the typical age of pubertal onset and progression (Granados et al. 2015), meaning our sample was comprised of youth athletes at various stages of pre-, mid-, and post-pubertal development (Appendix P). Most of our male participants had not yet hit their estimated growth spurt while the opposite was true for our female cohort. Considering how rapidly puberty can affect neural and musculoskeletal development and function, the imbalance in PHV distribution amongst our male and female participants could have led to our inconclusive results. Should non-linear effects of puberty on acceleration metrics from our predictor variables exist, then our models would fail to capture these complex relationships as our current LMER models were created.

The method of estimating PHV from chronological age, height, weight, and leg length based on sex-specific equations is a common, non-invasive method used in field settings (Mirwald et al. 2002; Van der Sluis et al. 2013; Van der Sluis et al. 2015). This method provides an estimate of the timing of the adolescent growth spurt, which is a crucial period of rapid growth and changes to motor development and performance during puberty (Yagüe and De La Fuente 1998; Nicholson et al. 2015; Tsutsui et al. 2022). However, it is important to note that this method provides an estimate of PHV which is not only a surrogate measure for pubertal stage but highly dependent on the sample demographics relative to the population that the estimation method was modeled upon (Mills et al. 2017). The impact of puberty on biomechanics is multifaceted and may not be fully encapsulated by PHV alone, particularly when considering the independence between our selected predictors found in our models.

One limitation of the study was the timing of the local boy's high school soccer season as it prevented us from including more post-PHV males in our sample. Further, while max effort was expected during testing and participants were encouraged by present researchers, gauging max effort compared to near-max effort is nigh impossible and could have impacted some of our acceleration metrics. Further, due to a limited number of IMU pairs, groups of participants were tested sequentially over the course of a practice. This introduces the possibility of a fatigue effect for groups tested later in the session, though rest between drills was adequately given if needed. Finally, all athletes were not tested on the same surface as practices took place where availability dictated. Even though some were tested on turf and others grass, however, breakdowns of acceleration impacts and cumulative loading from this study cohort (Appendix R) and pilot data (Appendix S) suggests that it doesn't produce differences in our measured dependent variables.

In conclusion, while our study did not find convincing significant effects of PHV, sex, and testing session on acceleration peaks and integrals, it underscores the complexity of the relationship between biomechanical loading and physiological changes during puberty. The lack of significant findings in our study should not be interpreted as evidence of no effect, but rather as an indication of the complexity of these relationships. Future research should consider a more comprehensive approach to capture the multifaceted nature of puberty and its impact on acceleration profiles in adolescent athletes. This could include the use of non-linear or interaction terms in future models, the use of more precise measures of pubertal development, or the inclusion of a wider range of drills that potentially include object manipulation (i.e., dribbling a ball) or other tasks to mimic demands seen in competition.

Chapter 6: Conclusion

This research study has only broached the surface of the complex interplay between multiscale entropy measures as a tool to understand loading regularity on the lower extremity in adolescent soccer players. The findings, while not supporting either of our hypotheses, suggest that puberty-related changes on the tibial loading biomechanics in these athletes may have a more nuanced relationship with our chosen predictor variables than we suspected. The precise nature and extent of these effects, as well as the context in which they are most optimally measured, remain to be fully understood. However, further research is needed to refine this approach and to validate the effectiveness of multiscale entropy analysis in different populations and settings. The potential of this method to serve as a predictive tool for injury risk is particularly worthy of further exploration. Similarly, the use of commercial IMUs in tracking injury risk factors in adolescent athletes represents an exciting avenue for future research. While traditional methods such as GPS systems provide valuable external loading insights, IMUs may serve as a more robust option in the appropriate context. The integration of IMUs with multiscale entropy analysis could potentially offer a more comprehensive view of these external loads, although more work is needed to realize this potential. In light of these findings, it is clear that there is much to be learned about the biomechanics of movement in adolescent athletes. The use of advanced analytical tools such as entropy analysis and IMUs, coupled with a comprehensive consideration of factors such as puberty-related changes, sex, and testing session, could greatly enhance our understanding of these issues. Nonetheless, this is a complex and multifaceted field, and future research will need to build on the foundations laid by this study to develop more effective strategies for monitoring and preventing injuries in adolescent athletes experiencing structural and function puberty-related changes in external loading.

References

Abásolo D, Hornero R, Espino P, Alvarez D, Poza J. 2006. Entropy analysis of the EEG background activity in Alzheimer's disease patients. Physiological measurement. 27(3):241.

Abbassi V. 1998. Growth and normal puberty. Pediatrics. 102(Supplement_3):507-511.

Adami C. 2002. What is complexity? BioEssays. 24(12):1085-1094.

Agel J, Arendt EA, Bershadsky B. 2005. Anterior cruciate ligament injury in national collegiate athletic association basketball and soccer: a 13-year review. The American journal of sports medicine. 33(4):524-531.

Ahlquist S, Cash BM, Hame SL. 2020. Associations of early sport specialization and high training volume with injury rates in national collegiate athletic association division I athletes. Orthopaedic Journal of Sports Medicine. 8(3):2325967120906825.

Ahmad N, Ghazilla RAR, Khairi NM, Kasi V. 2013. Reviews on various inertial measurement unit (IMU) sensor applications. International Journal of Signal Processing Systems. 1(2):256-262.

Aicale R, Tarantino D, Maffulli N. 2017. Basic science of tendons. Bio-orthopaedics. Springer; p. 249-273.

Allard P, Martinez R, Deguire S, Tremblay J. 2022. In-season session training load relative to match load in professional ice hockey. Journal of Strength and Conditioning Research. 36(2):486-492.

Almeida-Neto PFd, de Matos DG, Pinto VCM, Dantas PMS, Cesário TdM, da Silva LF, Bulhões-Correia A, Aidar FJ, Cabral BGdAT. 2020. Can the neuromuscular performance of young athletes be influenced by hormone levels and different stages of puberty? International journal of environmental research and public health. 17(16):5637.

Anderson JJ. 1996. Calcium, phosphorus and human bone development. The Journal of nutrition. 126(suppl_4):1153S-1158S.

Andrish J. 2001. Anterior cruciate ligament injuries in the skeletally immature patient. American Journal of Orthopedics (Belle Mead, NJ). 30(2):103-110.

Aristizábal Pla G, Hollville E, Schütte K, Vanwanseele B. 2021. The use of a single trunk-mounted accelerometer to detect changes in center of mass motion linked to lower-leg overuse injuries: a prospective study. Sensors. 21(21):7385.

Armitage M, Beato M, McErlain-Naylor SA. 2021. Inter-unit reliability of IMU Step metrics using IMeasureU Blue Trident inertial measurement units for running-based team sport tasks. Journal of Sports Sciences. 39(13):1512-1518.

Armstrong N, Welsman JR. 1994. Assessment and interpretation of aerobic fitness in children and adolescents. Exercise and sport sciences reviews. 22(1):435-476.

Arnoldi J-F, Loreau M, Haegeman B. 2016. Resilience, reactivity and variability: A mathematical comparison of ecological stability measures. Journal of theoretical biology. 389:47-59.

Arrones LS, Torreno N, Requena B, De Villarreal E, Casamichana D, Carlos J, Barbero-Alvarez D. 2014. Match-play activity profile in professional soccer players during official games and the relationship between external and internal load. J Sports Med Phys Fitness. 55:1417-1422.

Åstrand P-O. 1952. Experimental studies of physical working capacity in relation to sex and age. Munksgaard Forlag.

Aydemir A, Terzioglu Y, Akin T. 2016. A new design and a fabrication approach to realize a high performance three axes capacitive MEMS accelerometer. Sensors and Actuators A: Physical. 244:324-333.

Babalola A, Ellis G. 1985. Serum dehydroepiandrosterone sulfate in a normal pediatric population. Clinical biochemistry. 18(3):184-189.

An investigation of the effects of magnetic variations on inertial/magnetic orientation sensors. IEEE International Conference on Robotics and Automation, 2004 Proceedings ICRA'04 2004; 2004: IEEE.

Bar-Or O. 1983. Physiologic responses to exercise of the healthy child. Pediatric sports medicine for the practitioner. Springer; p. 1-65.

Barber-Westin SD, Noyes FR. 2011. Objective criteria for return to athletics after anterior cruciate ligament reconstruction and subsequent reinjury rates: a systematic review. The Physician and sportsmedicine. 39(3):100-110.

Barkovich A, Kjos B, Jackson Jr D, Norman D. 1988. Normal maturation of the neonatal and infant brain: MR imaging at 1.5 T. Radiology. 166(1):173-180.

Barnea-Goraly N, Menon V, Eckert M, Tamm L, Bammer R, Karchemskiy A, Dant CC, Reiss AL. 2005. White matter development during childhood and adolescence: a cross-sectional diffusion tensor imaging study. Cerebral cortex. 15(12):1848-1854.

Barron DJ, Atkins S, Edmundson C, Fewtrell D. 2014. Accelerometer derived load according to playing position in competitive youth soccer. International Journal of Performance Analysis in Sport. 14(3):734-743.

Bates D, Mächler M, Bolker B, Walker S. 2014. Fitting linear mixed-effects models using lme4. arXiv preprint arXiv:14065823.

Bates NA, Nesbitt RJ, Shearn JT, Myer GD, Hewett TE. 2015. Relative strain in the anterior cruciate ligament and medial collateral ligament during simulated jump landing and sidestep cutting tasks: implications for injury risk. The American journal of sports medicine. 43(9):2259-2269.

Bates NA, Schilaty ND, Nagelli CV, Krych AJ, Hewett TE. 2019. Multiplanar loading of the knee and its influence on anterior cruciate ligament and medial collateral ligament strain during simulated landings and noncontact tears. The American journal of sports medicine. 47(8):1844-1853.

Bayat A, Pomplun M, Tran DA. 2014. A study on human activity recognition using accelerometer data from smartphones. Procedia Computer Science. 34:450-457.

Bech K, Tygstrup I, Nerup J. 1969. The involution of the foetal adrenal cortex: a light microscopic study. Acta Pathologica Microbiologica Scandinavica. 76(3):391-400.

Belgorosky A, Baquedano M, Iacute, Sonia A, Guercio G, Rivarola MA. 2008. Adrenarche: Postnatal Adrenal Zonation and Hormonal and Metabolic Regulation. Hormone Research. 70(5):257-267.

Belkacemi L, Nelson DM, Desai M, Ross MG. 2010. Maternal undernutrition influences placental-fetal development. Biology of reproduction. 83(3):325-331.

Benyi E, Sävendahl L. 2017. The physiology of childhood growth: hormonal regulation. Hormone research in paediatrics. 88(1):6-14.

Bergeron MF, Mountjoy M, Armstrong N, Chia M, Côté J, Emery CA, Faigenbaum A, Hall G, Kriemler S, Léglise M. 2015. International Olympic Committee consensus statement on youth athletic development. British journal of sports medicine. 49(13):843-851.

Bimm J. 2018. Historical Studies in the Societal Impact of Spaceflight ed. by Steven J. Dick. Technology and Culture. 59(1):183-185.

Binkley JM, Stratford PW, Lott SA, Riddle DL. 1999. The Lower Extremity Functional Scale (LEFS): Scale Development, Measurement Properties, and Clinical Application. Physical Therapy.

Bird AL, Grant CC, Bandara DK, Mohal J, Atatoa-Carr PE, Wise MR, Inskip H, Miyahara M, Morton SM. 2017. Maternal health in pregnancy and associations with adverse birth outcomes: Evidence from Growing Up in New Zealand. Aust N Z J Obstet Gynaecol. 57(1):16-24.

Bisi M, Stagni R. 2016. Complexity of human gait pattern at different ages assessed using multiscale entropy: from development to decline. Gait & posture. 47:37-42.

Bizovska L, Svoboda Z, Vuillerme N, Janura M. 2017. Multiscale and Shannon entropies during gait as fall risk predictors—A prospective study. Gait & posture. 52:5-10.

Blimkie C, Lefevre J, Beunen GP, Renson R, Dequeker J, Van Damme P. 1993. Fractures, physical activity, and growth velocity in adolescent Belgian boys. Medicine and science in sports and exercise. 25(7):801-808.

Boddy KJ, Marsh JA, Caravan A, Lindley KE, Scheffey JO, O'Connell ME. 2019. Exploring wearable sensors as an alternative to marker-based motion capture in the pitching delivery. PeerJ. 7:e6365.

Boden BP, Griffin LY, Garrett Jr WE. 2000. Etiology and prevention of noncontact ACL injury. The Physician and sportsmedicine. 28(4):53-60.

Boey H, Aeles J, Schütte K, Vanwanseele B. 2017. The effect of three surface conditions, speed and running experience on vertical acceleration of the tibia during running. Sports biomechanics. 16(2):166-176.

Bogin B. 1999. Evolutionary perspective on human growth. Annual Review of Anthropology.109-153.

Bonnet S, Heliot R. 2007. A magnetometer-based approach for studying human movements. IEEE Transactions on Biomedical Engineering. 54(7):1353-1355.

Boonstra MC, Van Der Slikke RM, Keijsers NL, Van Lummel RC, de Waal Malefijt MC, Verdonschot N. 2006. The accuracy of measuring the kinematics of rising from a chair with accelerometers and gyroscopes. Journal of Biomechanics. 39(2):354-358.

Bosl W, Tierney A, Tager-Flusberg H, Nelson C. 2011. EEG complexity as a biomarker for autism spectrum disorder risk. BMC medicine. 9(1):1-16.

Bourdon PC, Cardinale M, Murray A, Gastin P, Kellmann M, Varley MC, Gabbett TJ, Coutts AJ, Burgess DJ, Gregson W. 2017. Monitoring athlete training loads: consensus statement. International journal of sports physiology and performance. 12(s2):S2-161-S162-170.

Bowen L, Gross AS, Gimpel M, Li F-X. 2017. Accumulated workloads and the acute: chronic workload ratio relate to injury risk in elite youth football players. British journal of sports medicine. 51(5):452-459.

Bravi A, Longtin A, Seely AJ. 2011. Review and classification of variability analysis techniques with clinical applications. Biomedical engineering online. 10:1-27.

Brayne L, Barnes A, Heller B, Wheat J. 2018. Using a wireless consumer accelerometer to measure tibial acceleration during running: agreement with a skin-mounted sensor. Sports Engineering. 21(4):487-491.

Brennan JH, Mitra B, Synnot A, McKenzie J, Willmott C, McIntosh AS, Maller JJ, Rosenfeld JV. 2017. Accelerometers for the assessment of concussion in male athletes: a systematic review and meta-analysis. Sports medicine. 47(3):469-478.

Brown P, Beek T, Carr C, O'Brien H, Cupido E, Oddy T, Horbury T. 2012. Magnetoresistive magnetometer for space science applications. Measurement Science and Technology. 23(2):025902.

Brown VA. 2021. An introduction to linear mixed-effects modeling in R. Advances in Methods and Practices in Psychological Science. 4(1):2515245920960351.

Bukhari SAR, Saleem MM, Khan US, Hamza A, Iqbal J, Shakoor RI. 2020. Microfabrication process-driven design, FEM analysis and system modeling of 3-DoF drive mode and 2-DoF sense mode thermally stable non-resonant MEMS gyroscope. Micromachines. 11(9):862.

Busa MA, Jones SL, Hamill J, van Emmerik RE. 2016. Multiscale entropy identifies differences in complexity in postural control in women with multiple sclerosis. Gait & posture. 45:7-11.

Busa MA, van Emmerik RE. 2016. Multiscale entropy: A tool for understanding the complexity of postural control. Journal of Sport and Health Science. 5(1):44-51.

Butler RJ, Hamill J, Davis I. 2007. Effect of footwear on high and low arched runners' mechanics during a prolonged run. Gait & posture. 26(2):219-225.

Cabarkapa DV, Cabarkapa D, Philipp NM, Fry AC. 2023. Impact of the Anatomical Accelerometer Placement on Vertical Jump Performance Characteristics. Sports. 11(4):92.

Camomilla V, Bergamini E, Fantozzi S, Vannozzi G. 2018. Trends supporting the in-field use of wearable inertial sensors for sport performance evaluation: A systematic review. Sensors. 18(3):873.

Campbell BC. 2011. Adrenarche and middle childhood. Human Nature. 22(3):327-349.

Cappozzo A, Catani F, Leardini A, Benedetti M, Della Croce U. 1996. Position and orientation in space of bones during movement: experimental artefacts. Clinical biomechanics. 11(2):90-100.

Castellano J, Navarro V, Fernandez-Fernandez R, Castano J, Malagon M, Aguilar E, Dieguez C, Magni P, Pinilla L, Tena-Sempere M. 2006. Ontogeny and mechanisms of action for the stimulatory effect of kisspeptin on gonadotropin-releasing hormone system of the rat. Molecular and cellular endocrinology. 257:75-83.

How the threshold "r" influences approximate entropy analysis of heart-rate variability. 2008 Computers in Cardiology; 2008: IEEE.

Castillo D, Raya-González J, Manuel Clemente F, Yanci J. 2020a. The influence of offside rule and pitch sizes on the youth soccer players' small-sided games external loads. Research in Sports Medicine. 28(3):324-338.

Castillo D, Raya-González J, Manuel Clemente F, Yanci J. 2020b. The influence of youth soccer players' sprint performance on the different sided games' external load using GPS devices. Research in Sports Medicine. 28(2):194-205.

Cavanaugh JT, Guskiewicz KM, Giuliani C, Marshall S, Mercer VS, Stergiou N. 2006. Recovery of postural control after cerebral concussion: new insights using approximate entropy. Journal of athletic training. 41(3):305.

Cech DJ. 2011. Functional movement development across the life span. Elsevier Health Sciences.

Chang H, Xue L, Qin W, Yuan G, Yuan W. 2008. An integrated MEMS gyroscope array with higher accuracy output. Sensors. 8(4):2886-2899.

Chen C-H, Huang P-W, Tang S-C, Shieh J-S, Lai D-M, Wu A-Y, Jeng J-S. 2015. Complexity of heart rate variability can predict stroke-in-evolution in acute ischemic stroke patients. Scientific reports. 5(1):1-5.

Comparison of the use of approximate entropy and sample entropy: applications to neural respiratory signal. 2005 IEEE Engineering in Medicine and Biology 27th Annual Conference; 2006: IEEE.

Chon KH, Scully CG, Lu S. 2009. Approximate entropy for all signals. IEEE engineering in medicine and biology magazine. 28(6):18-23.

Chong S, Rui S, Jie L, Xiaoming Z, Jun T, Yunbo S, Jun L, Huiliang C. 2016. Temperature drift modeling of MEMS gyroscope based on genetic-Elman neural network. Mechanical Systems and Signal Processing. 72:897-905.

Christensen R. 2002. Plane answers to complex questions. Vol. 35. Springer. 1).

Chumanov ES, Heiderscheit BC, Thelen DG. 2007. The effect of speed and influence of individual muscles on hamstring mechanics during the swing phase of sprinting. Journal of biomechanics. 40(16):3555-3562.

mChumanov ES, Schache AG, Heiderscheit BC, Thelen DG. 2012. Hamstrings are most susceptible to injury during the late swing phase of sprinting. BMJ publishing group ltd and British association of sport and exercise medicine. p. 90-90.

Clark RA, Bartold S, Bryant AL. 2010. Tibial acceleration variability during consecutive gait cycles is influenced by the menstrual cycle. Clinical Biomechanics. 25(6):557-562.

Cohen J, Cohen P, West SG, Aiken LS. 2013. Applied multiple regression/correlation analysis for the behavioral sciences. Routledge.

Comstock RD, Pierpoint LA. 2020. National high school sports-related injury surveillance study 2018-2019.

Cooper C, Dennison EM, Leufkens HG, Bishop N, van Staa TP. 2004. Epidemiology of childhood fractures in Britain: a study using the general practice research database. Journal of Bone and Mineral Research. 19(12):1976-1981.

Costa M, Goldberger AL, Peng C-K. 2005. Multiscale entropy analysis of biological signals. Physical review E. 71(2):021906.

Costa M, Goldberger AL, Peng CK. 2002. Multiscale Entropy Analysis of Complex Physiologic Time Series. Physical Review Letters. 89(6).

Costa M, Peng C-K, Goldberger AL, Hausdorff JM. 2003. Multiscale entropy analysis of human gait dynamics. Physica A: Statistical Mechanics and its applications. 330(1-2):53-60.

Courtiol J, Perdikis D, Petkoski S, Müller V, Huys R, Sleimen-Malkoun R, Jirsa VK. 2016. The multiscale entropy: Guidelines for use and interpretation in brain signal analysis. Journal of neuroscience methods. 273:175-190.

Coventry E, O'Connor KM, Hart BA, Earl JE, Ebersole KT. 2006. The effect of lower extremity fatigue on shock attenuation during single-leg landing. Clinical Biomechanics. 21(10):1090-1097.

Crowell HP, Milner CE, Hamill J, Davis IS. 2010. Reducing impact loading during running with the use of real-time visual feedback. journal of orthopaedic & sports physical therapy. 40(4):206-213.

Cummins C, Orr R, O'Connor H, West C. 2013. Global positioning systems (GPS) and microtechnology sensors in team sports: a systematic review. Sports medicine. 43:1025-1042.

Cumps E, Verhagen E, Annemans L, Meeusen R. 2008. Injury rate and socioeconomic costs resulting from sports injuries in Flanders: data derived from sports insurance statistics 2003. British journal of sports medicine. 42(9):767-772.

Dalen T, Jørgen I, Gertjan E, Havard HG, Ulrik W. 2016. Player load, acceleration, and deceleration during forty-five competitive matches of elite soccer. The Journal of Strength & Conditioning Research. 30(2):351-359.

Daniels J, Oldridge N, Nagle F, White B. 1978. Differences and changes in VO2 among young runners 10 to 18 years of age. Medicine and science in sports. 10(3):200-203.

Day BL, Fitzpatrick RC. 2005. The vestibular system. Current biology. 15(15):R583-R586.

de Dios-Álvarez V, Suárez-Iglesias D, Bouzas-Rico S, Alkain P, González-Conde A, Ayan-Perez C. 2023. Relationships between RPE-derived internal training load parameters and GPS-based external training load variables in elite young soccer players. Research in Sports Medicine. 31(1):58-73.

de Leeuw A-W, van der Zwaard S, van Baar R, Knobbe A. 2022. Personalized machine learning approach to injury monitoring in elite volleyball players. European journal of sport science. 22(4):511-520.

de Lucena GL, dos Santos Gomes C, Guerra RO. 2011. Prevalence and associated factors of Osgood-Schlatter syndrome in a population-based sample of Brazilian adolescents. The American journal of sports medicine. 39(2):415-420.

de Moraes JFVN, Batista PLO, da Silva MAFM, Pinto EF, Siqueira LP, Almeida CMM, Magalhaes FPR, dos Santos FD, Brandao JTS, de Carvalho Lima EV. 2018. Aerobic and Anaerobic Capacity of Male Students According to Age and Pubertal Stage. Journal of Exercise Physiology Online. 21(2):84-90.

De Vries W, Veeger H, Baten C, Van Der Helm F. 2009. Magnetic distortion in motion labs, implications for validating inertial magnetic sensors. Gait & posture. 29(4):535-541.

Deighan M, De Ste Croix M, Grant C, Armstrong N. 2006. Measurement of maximal muscle cross-sectional area of the elbow extensors and flexors in children, teenagers and adults. Journal of sports sciences. 24(05):543-546.

Dekaban AS, Sadowsky D. 1978. Changes in brain weights during the span of human life: relation of brain weights to body heights and body weights. Annals of Neurology: Official Journal of the American Neurological Association and the Child Neurology Society. 4(4):345-356.

Del Giudice M. 2009. Sex, attachment, and the development of reproductive strategies. Behavioral and Brain Sciences. 32(1):1-21.

Delignières D, Marmelat V. 2012. Fractal fluctuations and complexity: current debates and future challenges. Critical Reviews™ in Biomedical Engineering. 40(6).

dePeretti E, Forest M. 1976. Unconjugated dehydroepiandrosterone plasma levels in normal subjects from birth to adolescence in human: the use of a sensitive radioimmunoassay. The Journal of Clinical Endocrinology & Metabolism. 43(5):982-991.

Deprez D, Valente-dos-Santos J, e Silva MC, Lenoir M, Philippaerts RM, Vaeyens R. 2014. Modeling developmental changes in the yo-yo intermittent recovery test level 1 in elite pubertal soccer players. International journal of sports physiology and performance. 9(6):1006-1012.

Deprez DN, Fransen J, Lenoir M, Philippaerts RM, Vaeyens R. 2015. A retrospective study on anthropometrical, physical fitness, and motor coordination characteristics that influence dropout, contract status, and first-team playing time in high-level soccer players aged eight to eighteen years. The Journal of Strength & Conditioning Research. 29(6):1692-1704.

Di Rienzo M. 1998. Methodology and clinical applications of blood pressure and heart rate analysis. Vol. 60. IOS Press.

DiCesare CA, Montalvo A, Foss KDB, Thomas SM, Hewett TE, Jayanthi NA, Myer GD. 2019. Sport specialization and coordination differences in multisport adolescent female basketball, soccer, and volleyball athletes. Journal of athletic training. 54(10):1105-1114.

DiFiori JP. 2010. Evaluation of overuse injuries in children and adolescents. Current sports medicine reports. 9(6):372-378.

DiFiori JP, Benjamin HJ, Brenner JS, Gregory A, Jayanthi N, Landry GL, Luke A. 2014. Overuse injuries and burnout in youth sports: a position statement from the American Medical Society for Sports Medicine. British journal of sports medicine. 48(4):287-288.

Drew MK, Finch CF. 2016. The relationship between training load and injury, illness and soreness: a systematic and literature review. Sports medicine. 46:861-883.

Eggers TM, Massard TI, Clothier PJ, Lovell R. 2018. Measuring vertical stiffness in sport with accelerometers: Exercise caution! The Journal of Strength & Conditioning Research. 32(7):1919-1922.

Evain-Brion D. 1994. Hormonal regulation of fetal growth. Hormone Research in Paediatrics. 42(4-5):207-214.

Fan B, Li Q, Liu T. 2017. How magnetic disturbance influences the attitude and heading in magnetic and inertial sensor-based orientation estimation. Sensors. 18(1):76.

Ferretti A, Puddu G, Mariani PP, Neri M. 1984. Jumper's knee: an epidemiological study of volleyball players. The physician and sportsmedicine. 12(10):97-106.

Finch C. 2011. The long term impact of overuse in injuries on life-long participation in sport and health status. Sport Participation-Health Benefits, Injuries and Pyschological Effects. Nova Science Publishers; p. 85-104.

Finch CF. 1997. An overview of some definitional issues for sports injury surveillance. Sports medicine. 24(3):157-163.

Fleury Y, Van Melle G, Woringer V, Gaillard RC, Portmann L. 2001. Sex-dependent variations and timing of thyroid growth during puberty. The Journal of Clinical Endocrinology & Metabolism. 86(2):750-754.

Flood MW, Grimm B. 2021. EntropyHub: An open-source toolkit for entropic time series analysis. Plos one. 16(11):e0259448.

Fonseca ST, Souza TR, Verhagen E, Van Emmerik R, Bittencourt NFN, Mendonça LDM, Andrade AGP, Resende RA, Ocarino JM. 2020. Sports Injury Forecasting and Complexity: A Synergetic Approach. Sports Medicine. 50(10):1757-1770.

Ford KR, Shapiro R, Myer GD, Van Den Bogert AJ, Hewett TE. 2010. Longitudinal sex differences during landing in knee abduction in young athletes. Medicine and science in sports and exercise. 42(10):1923.

Forner-Cordero A, Mateu-Arce M, Forner-Cordero I, Alcántara E, Moreno J, Pons JL. 2008. Study of the motion artefacts of skin-mounted inertial sensors under different attachment conditions. Physiological measurement. 29(4):N21.

Fortenberry B, Gorchetchnikov A, Grossberg S. 2012. Learned integration of visual, vestibular, and motor cues in multiple brain regions computes head direction during visually guided navigation. Hippocampus. 22(12):2219-2237.

Forwood MR, Bailey DA, Beck TJ, Mirwald RL, Baxter-Jones AD, Uusi-Rasi K. 2004. Sexual dimorphism of the femoral neck during the adolescent growth spurt: a structural analysis. Bone. 35(4):973-981.

Fox JL, Stanton R, Scanlan AT. 2018. A comparison of training and competition demands in semiprofessional male basketball players. Research quarterly for exercise and sport. 89(1):103-111.

Friel NA, Chu CR. 2013. The role of ACL injury in the development of posttraumatic knee osteoarthritis. Clinics in sports medicine. 32(1):1-12.

Fukunaga Y, Takai Y, Yoshimoto T, Fujita E, Yamamoto M, Kanehisa H. 2014. Effect of maturation on muscle quality of the lower limb muscles in adolescent boys. Journal of Physiological Anthropology. 33(1):1-6.

Fuller J, Liu L-J, Murphy M, Mann R. 1997. A comparison of lower-extremity skeletal kinematics measured using skin-and pin-mounted markers. Human movement science. 16(2-3):219-242.

Gabbett TJ. 2004. Reductions in pre-season training loads reduce training injury rates in rugby league players. British journal of sports medicine. 38(6):743-749.

Gabbett TJ. 2010. The development and application of an injury prediction model for noncontact, soft-tissue injuries in elite collision sport athletes. The Journal of Strength & Conditioning Research. 24(10):2593-2603.

Gabbett TJ. 2016. The training—injury prevention paradox: should athletes be training smarter and harder? British journal of sports medicine. 50(5):273-280.

Gallo TF, Cormack SJ, Gabbett TJ, Lorenzen CH. 2016. Pre-training perceived wellness impacts training output in Australian football players. Journal of sports sciences. 34(15):1445-1451.

García-Pérez JA, Pérez-Soriano P, Llana Belloch S, Lucas-Cuevas ÁG, Sánchez-Zuriaga D. 2014. Effects of treadmill running and fatigue on impact acceleration in distance running. Sports Biomechanics. 13(3):259-266.

Gates P, Discenzo FM, Kim JH, Lemke Z, Meggitt J, Ridgel AL. 2022. Analysis of Movement Entropy during Community Dance Programs for People with Parkinson's Disease and

Older Adults: A Cohort Study. International journal of environmental research and public health. 19(2):655.

Gatev V, Stamatova L, Angelova B. 1977. Contraction time in skeletal muscles of normal children. Electromyogr Clin Neurophysiol.

Gauss CF. 1832. The intensity of the earth's magnetic force reduced to absolute measurement. Royal Scientific Society. 8(3).

Gauss CF. 1877. Erdmagnetismus und Magnetometer. Werke. Springer; p. 315-344.

Georgoulis AD, Moraiti C, Ristanis S, Stergiou N. 2006. A novel approach to measure variability in the anterior cruciate ligament deficient knee during walking: the use of the approximate entropy in orthopaedics. Journal of clinical monitoring and computing. 20:11-18.

Gianotti SM, Marshall SW, Hume PA, Bunt L. 2009. Incidence of anterior cruciate ligament injury and other knee ligament injuries: a national population-based study. Journal of science and medicine in sport. 12(6):622-627.

Gicquel C, Le Bouc Y. 2006. Hormonal regulation of fetal growth. Hormone Research in Paediatrics. 65(Suppl. 3):28-33.

Gisslèn K, Gyulai C, Söderman K, Alfredson H. 2005. High prevalence of jumper's knee and sonographic changes in Swedish elite junior volleyball players compared to matched controls. British journal of sports medicine. 39(5):298-301.

Gow BJ, Peng C-K, Wayne PM, Ahn AC. 2015. Multiscale entropy analysis of center-of-pressure dynamics in human postural control: methodological considerations. Entropy. 17(12):7926-7947.

Gracia-Tabuenca Z, Moreno MB, Barrios FA, Alcauter S. 2021. Development of the brain functional connectome follows puberty-dependent nonlinear trajectories. Neuroimage. 229:117769.

Granados A, Gebremariam A, Lee JM. 2015. Relationship between timing of peak height velocity and pubertal staging in boys and girls. Journal of clinical research in pediatric endocrinology. 7(3):235.

Greaves RF, Wudy SA, Badoer E, Zacharin M, Hirst JJ, Quinn T, Walker DW. 2019. A tale of two steroids: the importance of the androgens DHEA and DHEAS for early neurodevelopment. The Journal of steroid biochemistry and molecular biology. 188:77-85.

Greenslade Jr TB. 1985. Atwood's machine. The Physics Teacher. 23(1):24-28.

Silicon monolithic micromechanical gyroscope. TRANSDUCERS'91: 1991 International Conference on Solid-State Sensors and Actuators Digest of Technical Papers; 1991: IEEE.

Grube M, Hagen P, Jedlitschky G. 2018. Neurosteroid transport in the brain: role of ABC and SLC transporters. Frontiers in pharmacology. 9:354.

Gruber AH, Busa MA, Gorton III GE, Van Emmerik RE, Masso PD, Hamill J. 2011. Time-to-contact and multiscale entropy identify differences in postural control in adolescent idiopathic scoliosis. Gait & Posture. 34(1):13-18.

Gruber AH, McDonnell J, Davis IV JJ, Vollmar JE, Harezlak J, Paquette MR. 2021. Monitoring gait complexity as an indicator for running-related injury risk in collegiate cross-country runners: a proof-of-concept study. Frontiers in sports and active living. 3:111.

Haddad M, Stylianides G, Djaoui L, Dellal A, Chamari K. 2017. Session-RPE method for training load monitoring: validity, ecological usefulness, and influencing factors. Frontiers in neuroscience. 11:612.

Hamill J, Palmer C, Van Emmerik RE. 2012. Coordinative variability and overuse injury. Sports Medicine, Arthroscopy, Rehabilitation, Therapy & Technology. 4(1):1-9.

Hamstra-Wright KL, Swanik CB, Sitler MR, Swanik KA, Ferber R, Ridenour M, Huxel KC. 2006. Gender comparisons of dynamic restraint and motor skill in children. Clinical Journal of Sport Medicine. 16(1):56-62.

Han S, Wang J. 2011. A novel method to integrate IMU and magnetometers in attitude and heading reference systems. The Journal of Navigation. 64(4):727-738.

Hartwig TB, Naughton G, Searl J. 2011. Motion analyses of adolescent rugby union players: a comparison of training and game demands. The Journal of Strength & Conditioning Research. 25(4):966-972.

The rise in adrenal androgen biosynthesis: adrenarche. Seminars in reproductive medicine; 2004: Copyright© 2004 by Thieme Medical Publishers, Inc., 333 Seventh Avenue, New ….

Hayano J, Yamasaki F, Sakata S, Okada A, Mukai S, Fujinami T. 1997. Spectral characteristics of ventricular response to atrial fibrillation. American Journal of Physiology-Heart and Circulatory Physiology. 273(6):H2811-H2816.

Herzog MM, Kerr ZY, Marshall SW, Wikstrom EA. 2019. Epidemiology of ankle sprains and chronic ankle instability. Journal of athletic training. 54(6):603-610.

Hewett TE, Myer GD, Ford KR, Heidt Jr RS, Colosimo AJ, McLean SG, Van den Bogert AJ, Paterno MV, Succop P. 2005. Biomechanical measures of neuromuscular control and valgus loading of the knee predict anterior cruciate ligament injury risk in female athletes: a prospective study. The American journal of sports medicine. 33(4):492-501.

Hewett TE, Myer GD, Ford KR, Slauterbeck JR. 2006. Preparticipation physical examination using a box drop vertical jump test in young athletes: the effects of puberty and sex. Clinical Journal of Sport Medicine. 16(4):298-304.

Hill Y, Den Hartigh RJ, Meijer RR, De Jonge P, Van Yperen NW. 2018. Resilience in sports from a dynamical perspective. Sport, Exercise, and Performance Psychology. 7(4):333.

Hinson J. 1990. Paracrine control of adrenocortical function: a new role for the medulla? Journal of Endocrinology. 124(1):7-9.

Holden JP, Orsini JA, Siegel KL, Kepple TM, Gerber LH, Stanhope SJ. 1997. Surface movement errors in shank kinematics and knee kinetics during gait. Gait & Posture. 5(3):217-227.

Howcroft J, Kofman J, Lemaire ED, McIlroy WE. 2016. Analysis of dual-task elderly gait in fallers and non-fallers using wearable sensors. Journal of biomechanics. 49(7):992-1001.

Huffman DA. 1952. A method for the construction of minimum-redundancy codes. Proceedings of the IRE. 40(9):1098-1101.

Ibáñez L, DiMartino-Nardi J, Potau N, Saenger P. 2000. Premature adrenarche—normal variant or forerunner of adult disease? Endocrine reviews. 21(6):671-696.

Iivonen S, Sääkslahti A, Laukkanen A. 2016. A review of studies using the Körperkoordinationstest für Kinder (KTK). European Journal of Adapted Physical Activity. 8.

Izzo R, Seccia R, Giovannelli M, Cejudo A, Varde'i HC. 2022. Symmetry and performance index evaluation in a youth football group using the latest generation IMU. Journal of Physical Education and Sport. 22(3):782-789.

Jaspers A, Kuyvenhoven JP, Staes F, Frencken WG, Helsen WF, Brink MS. 2018. Examination of the external and internal load indicators' association with overuse injuries in professional soccer players. Journal of science and medicine in sport. 21(6):579-585.

Jiang S, Chen X, Gu J, Shen X. 2014. Friction moment analysis of space gyroscope bearing with ribbon cage under ultra-low oscillatory motion. Chinese Journal of Aeronautics. 27(5):1301-1311.

Joeris A, Lutz N, Blumenthal A, Slongo T, Audigé L. 2017. The AO Pediatric Comprehensive Classification of Long Bone Fractures (PCCF) Part II: Location and morphology of 548 lower extremity fractures in children and adolescents. Acta Orthopaedica. 88(2):129-132.

Johnson CD, Outerleys J, Jamison ST, Tenforde AS, Ruder M, Davis IS. 2020. Comparison of Tibial Shock during Treadmill and Real-World Running. Medicine and science in sports and exercise. 52(7):1557-1562.

Jones CM, Griffiths PC, Mellalieu SD. 2017. Training load and fatigue marker associations with injury and illness: a systematic review of longitudinal studies. Sports medicine. 47:943-974.

Kamm K, Thelen E, Jensen JL. 1990. A dynamical systems approach to motor development. Physical therapy. 70(12):763-775.

Kanehisa H, Ikegawa S, Tsunoda N, Fukunaga T. 1994. Strength and cross-sectional area of knee extensor muscles in children. European journal of applied physiology and occupational physiology. 68(5):402-405.

Kappy MS, Allen DB, Geffner ME. 2005. Principles and practice of pediatric endocrinology. Charles C Thomas Publisher.

Karlberg J. 1989. On the construction of the infancy-childhood-puberty growth standard. Acta Paediatrica. 78:26-37.

Understanding ageing effects by approximate entropy analysis of gait variability. 2007 29th Annual International Conference of the IEEE Engineering in Medicine and Biology Society; 2007: IEEE.

Kary JM. 2010. Diagnosis and management of quadriceps strains and contusions. Current reviews in musculoskeletal medicine. 3(1):26-31.

Kelly A, Winer KK, Kalkwarf H, Oberfield SE, Lappe J, Gilsanz V, Zemel BS. 2014. Age-based reference ranges for annual height velocity in US children. The Journal of Clinical Endocrinology & Metabolism. 99(6):2104-2112.

Kempton T, Sirotic AC, Coutts AJ. 2015. An integrated analysis of match-related fatigue in professional rugby league. Journal of Sports Sciences. 33(1):39-47.

Kiernan D, Hawkins DA, Manoukian MA, McKallip M, Oelsner L, Caskey CF, Coolbaugh CL. 2018. Accelerometer-based prediction of running injury in National Collegiate Athletic Association track athletes. Journal of biomechanics. 73:201-209.

Kim W, Voloshin A, Johnson S, Simkin A. 1993. Measurement of the impulsive bone motion by skin-mounted accelerometers.

Knickmeyer RC, Gouttard S, Kang C, Evans D, Wilber K, Smith JK, Hamer RM, Lin W, Gerig G, Gilmore JH. 2008. A structural MRI study of human brain development from birth to 2 years. Journal of neuroscience. 28(47):12176-12182.

Kraemer WJ, Fry AC, Frykman PN, Conroy B, Hoffman J. 1989. Resistance training and youth. Pediatric Exercise Science. 1(4):336-350.

Krahenbuhl GS, Skinner JS, Kohrt WM. 1985. Developmental aspects of maximal aerobic power in children. Exercise and sport sciences reviews. 13(1):503-538.

Kucera KL, Marshall SW, Kirkendall DT, Marchak P, Garrett WE. 2005. Injury history as a risk factor for incident injury in youth soccer. British journal of sports medicine. 39(7):462-462.

Kujala UM, Kvist M, Heinonen O. 1985. Osgood-Schlatter's disease in adolescent athletes: Retrospective study of incidence and duration. The American journal of sports medicine. 13(4):236-241.

Lafortune MA, Henning E, Valiant GA. 1995. Tibial shock measured with bone and skin mounted transducers. Journal of biomechanics. 28(8):989-993.

Lake DE, Richman JS, Griffin MP, Moorman JR. 2002. Sample entropy analysis of neonatal heart rate variability. American Journal of Physiology-Regulatory, Integrative and Comparative Physiology.

mLambert RH, Kenneth S. 1952. Navigation instrument. Google Patents.

Lamoth CJ, Ainsworth E, Polomski W, Houdijk H. 2010. Variability and stability analysis of walking of transfemoral amputees. Medical engineering & physics. 32(9):1009-1014.

Langendam L, van der Linden CMN, Clemente FM. 2017. Difference in training load and technical actions during small-sided games in junior and senior soccer players. Human Movement Special Issues. 2017(5):146-156.

Lauretani F, Bandinelli S, Griswold ME, Maggio M, Semba R, Guralnik JM, Ferrucci L. 2008. Longitudinal changes in BMD and bone geometry in a population-based study. Journal of Bone and Mineral research. 23(3):400-408.

Lee I, Yoon GH, Park J, Seok S, Chun K, Lee K-I. 2005. Development and analysis of the vertical capacitive accelerometer. Sensors and Actuators A: Physical. 119(1):8-18.

Lemme NJ, Li NY, DeFroda SF, Kleiner J, Owens BD. 2018. Epidemiology of Achilles tendon ruptures in the United States: athletic and nonathletic injuries from 2012 to 2016. Orthopaedic journal of sports medicine. 6(11):2325967118808238.

Lindsay TR, Noakes TD, McGregor SJ. 2014. Effect of treadmill versus overground running on the structure of variability of stride timing. Percept Mot Skills. 118(2):331-346. eng.

Liu C, Liu C, Shao P, Li L, Sun X, Wang X, Liu F. 2010. Comparison of different threshold values r for approximate entropy: application to investigate the heart rate variability between heart failure and healthy control groups. Physiological Measurement. 32(2):167.

Lucas-Cuevas AG, Encarnación-Martínez A, Camacho-García A, Llana-Belloch S, Pérez-Soriano P. 2017. The location of the tibial accelerometer does influence impact acceleration parameters during running. Journal of sports sciences. 35(17):1734-1738.

Lüdecke D, Ben-Shachar MS, Patil I, Waggoner P, Makowski D. 2021. performance: An R package for assessment, comparison and testing of statistical models. Journal of Open Source Software. 6(60).

Luo H, Zhang G, Carley LR, Fedder GK. 2002. A post-CMOS micromachined lateral accelerometer. Journal of Microelectromechanical systems. 11(3):188-195.

mMacKenzie D. 1990. Inventing accuracy: a historical sociology of nuclear missile guidance. MIT Press.

Maenaka K, Fujita T, Konishi Y, Maeda M. 1996. Analysis of a highly sensitive silicon gyroscope with cantilever beam as vibrating mass. Sensors and Actuators A: Physical. 54(1-3):568-573.

Maggio M, De Vita F, Fisichella A, Colizzi E, Provenzano S, Lauretani F, Luci M, Ceresini G, Dall'Aglio E, Caffarra P. 2015. DHEA and cognitive function in the elderly. The Journal of steroid biochemistry and molecular biology. 145:281-292.

Majzoub JA, Topor LS. 2018. A new model for adrenarche: inhibition of 3β-hydroxysteroid dehydrogenase type 2 by intra-adrenal cortisol. Hormone research in paediatrics. 89(5):311-319.

Malina RM. 2004. Motor development during infancy and early childhood: Overview and suggested directions for research. International journal of sport and health science. 2:50-66.

Malina RM, Bouchard C, Bar-Or O. 2004. Growth, maturation, and physical activity. Human kinetics.

Maliszewski AF, Freedson PS. 1996. Is running economy different between adults and children? Pediatric Exercise Science. 8(4):351-360.

Malone JJ, Di Michele R, Morgans R, Burgess D, Morton JP, Drust B. 2015. Seasonal training-load quantification in elite English premier league soccer players. International journal of sports physiology and performance. 10(4):489-497.

Mamon MA, Olthof SB, Burns GT, Lepley AS, Kozloff KM, Zernicke RF. 2022. Position-Specific Physical Workload Intensities in American Collegiate Football Training. Journal of Strength and Conditioning Research. 36(2):420-426.

Marceau K, Ram N, Houts RM, Grimm KJ, Susman EJ. 2011. Individual differences in boys' and girls' timing and tempo of puberty: modeling development with nonlinear growth models. Developmental psychology. 47(5):1389.

Marynowicz J, Kikut K, Lango M, Horna D, Andrzejewski M. 2020. Relationship between the session-RPE and external measures of training load in youth soccer training. The Journal of Strength & Conditioning Research. 34(10):2800-2804.

Mathie MJ, Coster AC, Lovell NH, Celler BG. 2004. Accelerometry: providing an integrated, practical method for long-term, ambulatory monitoring of human movement. Physiological measurement. 25(2):R1.

May RM. 2019. Stability and complexity in model ecosystems. Stability and Complexity in Model Ecosystems. Princeton university press.

McCullom B, Peters OS. 1924. A new electric telemeter. Technology Papers. 17(247).

McGinnis RS, Cain SM, Davidson SP, Vitali RV, Perkins NC, McLean SG. 2016. Quantifying the effects of load carriage and fatigue under load on sacral kinematics during countermovement vertical jump with IMU-based method. Sports Engineering. 19:21-34.

McGregor SJ, Busa MA, Skufca J, Yaggie JA, Bollt EM. 2009. Control entropy identifies differential changes in complexity of walking and running gait patterns with increasing speed in highly trained runners. Chaos: An Interdisciplinary Journal of Nonlinear Science. 19(2):026109.

McGuine TA, Post EG, Hetzel SJ, Brooks MA, Trigsted S, Bell DR. 2017. A prospective study on the effect of sport specialization on lower extremity injury rates in high school athletes. The American journal of sports medicine. 45(12):2706-2712.

McLaren SJ, Macpherson TW, Coutts AJ, Hurst C, Spears IR, Weston M. 2018. The relationships between internal and external measures of training load and intensity in team sports: a meta-analysis. Sports medicine. 48:641-658.

McLean S, Neal R, Myers P, Walters M. 1999. Knee joint kinematics during the sidestep cutting maneuver: potential for injury in women. Medicine and science in sports and exercise. 31(7):959-968.

Mehta S. 2019. Relationship between workload and throwing injury in varsity baseball players. Physical Therapy in Sport. 40:66-70.

Mercer JA, Vance J, Hreljac A, Hamill J. 2002. Relationship between shock attenuation and stride length during running at different velocities. European journal of applied physiology. 87(4):403-408.

Miles HL, Gidlöf S, Nordenström A, Ong KK, Hughes IA. 2010. The role of androgens in fetal growth: observational study in two genetic models of disordered androgen signalling. Archives of Disease in Childhood-Fetal and Neonatal Edition. 95(6):F435-F438.

Miller RH, Edwards WB, Deluzio KJ. 2015. Energy expended and knee joint load accumulated when walking, running, or standing for the same amount of time. Gait & posture. 41(1):326-328.

Mills K, Baker D, Pacey V, Wollin M, Drew MK. 2017. What is the most accurate and reliable methodological approach for predicting peak height velocity in adolescents? A systematic review. Journal of Science and Medicine in Sport. 20(6):572-577.

Milner CE, Hawkins JL, Aubol KG. 2020. Tibial Acceleration during Running Is Higher in Field Testing Than Indoor Testing. Medicine and Science in Sports and Exercise. 52(6):1361-1366.

Miltko A, Milner CE, Powell DW, Paquette MR. 2022. The influence of surface and speed on biomechanical external loads obtained from wearable devices in rearfoot strike runners. Sports Biomechanics.1-15.

Mirwald RL, Baxter-Jones AD, Bailey DA, Beunen GP. 2002. An assessment of maturity from anthropometric measurements. Medicine and science in sports and exercise. 34(4):689-694.

Mitschke C, Kiesewetter P, Milani TL. 2018. The effect of the accelerometer operating range on biomechanical parameters: Stride length, velocity, and peak tibial acceleration during running. Sensors. 18(1):130.

Moe-Nilssen R, Helbostad JL. 2004. Estimation of gait cycle characteristics by trunk accelerometry. Journal of biomechanics. 37(1):121-126.

Montalvo AM, Schneider DK, Webster KE, Yut L, Galloway MT, Heidt Jr RS, Kaeding CC, Kremcheck TE, Magnussen RA, Parikh SN. 2019. Anterior cruciate ligament injury risk in sport: a systematic review and meta-analysis of injury incidence by sex and sport classification. Journal of athletic training. 54(5):472-482.

Morgan DW, Martin PE, Krahenbuhl GS. 1989. Factors affecting running economy. Sports Med. 7(5):310-330.

Muro-De-La-Herran A, Garcia-Zapirain B, Mendez-Zorrilla A. 2014. Gait analysis methods: An overview of wearable and non-wearable systems, highlighting clinical applications. Sensors. 14(2):3362-3394.

Murray A. 2017. Managing the training load in adolescent athletes. International journal of sports physiology and performance. 12(s2):S2-42-S42-49.

Murray AM, Ryu JH, Sproule J, Turner AP, Graham-Smith P, Cardinale M. 2017. A Pilot Study Using Entropy as a Noninvasive Assessment of Running. Int J Sports Physiol Perform. 12(8):1119-1122. eng.

Myer GD, Faigenbaum AD, Ford KR, Best TM, Bergeron MF, Hewett TE. 2011. When to initiate integrative neuromuscular training to reduce sports-related injuries in youth? Current sports medicine reports. 10(3):155.

Myer GD, Sugimoto D, Thomas S, Hewett TE. 2013. The influence of age on the effectiveness of neuromuscular training to reduce anterior cruciate ligament injury in female athletes: a meta-analysis. The American journal of sports medicine. 41(1):203-215.

Nedergaard NJ, Robinson MA, Eusterwiemann E, Drust B, Lisboa PJ, Vanrenterghem J. 2017. The relationship between whole-body external loading and body-worn accelerometry

during team-sport movements. International journal of sports physiology and performance. 12(1):18-26.

Negahban H, Salavati M, Mazaheri M, Sanjari MA, Hadian MR, Parnianpour M. 2010. Non-linear dynamical features of center of pressure extracted by recurrence quantification analysis in people with unilateral anterior cruciate ligament injury. Gait & Posture. 31(4):450-455.

NFHS. 2019. High school athletics participation survey 2018-2019. [accessed 2022 June 29]. https://www.nfhs.org/media/1020412/2018-19_participation_survey.pdf.

Nicholson AD, Liu RW, Sanders JO, Cooperman DR. 2015. Relationship of calcaneal and iliac apophyseal ossification to peak height velocity timing in children. JBJS. 97(2):147-154.

Nilsson O, Marino R, De Luca F, Phillip M, Baron J. 2005. Endocrine regulation of the growth plate. Hormone research in paediatrics. 64(4):157-165.

Nobari H, Gonçalves LG, Aquino R, Clemente FM, Rezaei M, Carlos-Vivas J, Pérez-Gómez J, Pueo B, Ardigò LP. 2022. Wearable Inertial Measurement Unit to Measure External Load: A Full-Season Study in Professional Soccer Players. Applied Sciences. 12(3):1140.

Nobari H, Sögüt M, Oliveira R, Perez-Gomez J, Suzuki K, Zouhal H. 2021. Wearable inertial measurement unit to accelerometer-based training monotony and strain during a soccer season: A within-group study for starters and non-starters. International Journal of Environmental Research and Public Health. 18(15):8007.

Norris M, Anderson R, Kenny IC. 2014. Method analysis of accelerometers and gyroscopes in running gait: A systematic review. Proceedings of the Institution of Mechanical Engineers, Part P: Journal of Sports Engineering and Technology. 228(1):3-15.

Noyes FR, Barber Westin SD. 2012. Anterior cruciate ligament injury prevention training in female athletes: a systematic review of injury reduction and results of athletic performance tests. Sports health. 4(1):36-46.

Olsen SJ, Fleisig GS, Dun S, Loftice J, Andrews JR. 2006. Risk factors for shoulder and elbow injuries in adolescent baseball pitchers. The American journal of sports medicine. 34(6):905-912.

Omidvarnia A, Mesbah M, Pedersen M, Jackson G. 2018. Range Entropy: A Bridge between Signal Complexity and Self-Similarity. Entropy. 20(12):962.

Ondrak KS, Morgan DW. 2007. Physical activity, calcium intake and bone health in children and adolescents. Sports medicine. 37(7):587-600.

Palmert MR, Hayden DL, Mansfield MJ, Crigler JF, Crowley WF, Chandler DW, Boepple PA. 2001. The Longitudinal Study of Adrenal Maturation during Gonadal Suppression: Evidence That Adrenarche Is a Gradual Process. The Journal of Clinical Endocrinology & Metabolism. 86(9):4536-4542.

Papaiakovou G, Giannakos A, Michailidis C, Patikas D, Bassa E, Kalopisis V, Anthrakidis N, Kotzamanidis C. 2009. The effect of chronological age and gender on the development of sprint performance during childhood and puberty. The Journal of Strength & Conditioning Research. 23(9):2568-2573.

Parshad RD, McGregor SJ, Busa MA, Skufca JD, Bollt E. 2012. A statistical approach to the use of control entropy identifies differences in constraints of gait in highly trained versus untrained runners. Mathematical Biosciences & Engineering. 9(1):123.

Passaro VM, Cuccovillo A, Vaiani L, De Carlo M, Campanella CE. 2017. Gyroscope technology and applications: A review in the industrial perspective. Sensors. 17(10):2284.

Peiper A. 1963. Cerebral function in infancy and childhood. Plenum Publishing Corporation.

Perroni F, Pintus A, Frandino M, Guidetti L, Baldari C. 2018. Relationship among repeated sprint ability, chronological age, and puberty in young soccer players. The Journal of Strength & Conditioning Research. 32(2):364-371.

Phibbs PJ, Jones B, Roe G, Read D, Darrall-Jones J, Weakley J, Rock A, Till K. 2018. The organised chaos of English adolescent rugby union: Influence of weekly match frequency on the variability of match and training loads. European journal of sport science. 18(3):341-348.

Pincus S. 1995. Approximate entropy (ApEn) as a complexity measure. Chaos: An Interdisciplinary Journal of Nonlinear Science. 5(1):110-117.

Pincus SM. 1991. Approximate entropy as a measure of system complexity. Proceedings of the National Academy of Sciences. 88(6):2297-2301.

Pincus SM, Goldberger AL. 1994. Physiological time-series analysis: what does regularity quantify? American Journal of Physiology-Heart and Circulatory Physiology. 266(4):H1643-H1656.

Pincus SM, Huang W-M. 1992. Approximate entropy: statistical properties and applications. Communications in Statistics-Theory and Methods. 21(11):3061-3077.

Pino-Ortega J, Gómez-Carmona CD, Nakamura FY, Rojas-Valverde D. 2022. Setting kinematic parameters that explain youth basketball behavior: Influence of relative age effect according to playing position. Journal of Strength and Conditioning Research. 36(3):820-826.

Pitcher CA, Elliott CM, Williams SA, Licari MK, Kuenzel A, Shipman PJ, Valentine JP, Reid SL. 2012. Childhood muscle morphology and strength: alterations over six months of growth. Muscle & nerve. 46(3):360-366.

Pol R, Hristovski R, Medina D, Balague N. 2019. From microscopic to macroscopic sports injuries. Applying the complex dynamic systems approach to sports medicine: a narrative review. British journal of sports medicine. 53(19):1214-1220.

Powell JW, Barber-Foss KD. 1999. Injury patterns in selected high school sports: a review of the 1995-1997 seasons. Journal of athletic training. 34(3):277.

Prader A. 1984. Biomedical and Endocrinological Aspects of Normal Growth and Development. Springer US; p. 1-22.

Preatoni E, Bergamini E, Fantozzi S, Giraud L, Orejel Bustos A, Vannozzi G, Coamomilla V. 2022. The Use of Wearable Sensors for Preventing, Assessing, and Informing Recovery from Sport-Related Musculoskeletal Injuries: A Systematic Scoping Review. sensors. 22(9):3225.

Quatman CE, Ford KR, Myer GD, Hewett TE. 2006. Maturation leads to gender differences in landing force and vertical jump performance: a longitudinal study. The American journal of sports medicine. 34(5):806-813.

Quirino J, Santos TRT, Okai-Nóbrega LA, de Araújo PA, Carvalho R, Ocarino JdM, Souza TR, Fonseca ST. 2021. Runners with a history of injury have greater lower limb movement regularity than runners without a history of injury. Sports Biomechanics.1-13.

Radelet MA, Lephart SM, Rubinstein EN, Myers JB. 2002. Survey of the injury rate for children in community sports. Pediatrics. 110(3):e28-e28.

Rago V, Brito J, Figueiredo P, Costa J, Barreira D, Krustrup P, Rebelo A. 2020. Methods to collect and interpret external training load using microtechnology incorporating GPS in professional football: a systematic review. Research in Sports Medicine. 28(3):437-458.

Ramponi DR, Baker C. 2019. Sever's disease (calcaneal Apophysitis). Advanced emergency nursing journal. 41(1):10-14.

Ramsden E. 2011. Hall-effect sensors: theory and application. Elsevier.

Rauch F, Bailey DA, Baxter-Jones A, Mirwald R, Faulkner R. 2004. The ‘muscle-bone unit’during the pubertal growth spurt. Bone. 34(5):771-775.

Reardon LE, Leen-Feldner EW, Hayward C. 2009. A critical review of the empirical literature on the relation between anxiety and puberty. Clinical psychology review. 29(1):1-23.

Reed ES. 1982. An outline of a theory of action systems. Journal of motor behavior. 14(2):98-134.

Remer T, Boye KR, Hartmann MF, Wudy SA. 2005. Urinary Markers of Adrenarche: Reference Values in Healthy Subjects, Aged 3–18 Years. The Journal of Clinical Endocrinology & Metabolism. 90(4):2015-2021.

Renström P, Johnson RJ. 1985. Overuse injuries in sports. Sports Medicine. 2(5):316-333.

Richman JS, Moorman JR. 2000. Physiological time-series analysis using approximate entropy and sample entropy. American Journal of Physiology-Heart and Circulatory Physiology. 278(6):H2039-H2049.

Rickles D, Hawe P, Shiell A. 2007. A simple guide to chaos and complexity. Journal of Epidemiology & Community Health. 61(11):933-937.

Riva F, Toebes M, Pijnappels M, Stagni R, Van Dieën J. 2013. Estimating fall risk with inertial sensors using gait stability measures that do not require step detection. Gait & posture. 38(2):170-174.

Robot Navigator Guides Jet Pilots. 1954. Popular Mechanics. New York City, NY: Hearst Communications, Inc.

Rogers J, Costello M, Harkins T, Hamaoui M. 2011. Effective use of magnetometer feedback for smart projectile applications. Navigation. 58(3):203-219.

Rojas-Valverde D, Sánchez-Ureña B, Pino-Ortega J, Gómez-Carmona C, Gutiérrez-Vargas R, Timón R, Olcina G. 2019. External workload indicators of muscle and kidney mechanical injury in endurance trail running. International Journal of Environmental Research and Public Health. 16(20):3909.

Rommers N, Mostaert M, Goossens L, Vaeyens R, Witvrouw E, Lenoir M, D'Hondt E. 2019. Age and maturity related differences in motor coordination among male elite youth soccer players. Journal of sports sciences. 37(2):196-203.

Roos KG, Marshall SW, Kerr ZY, Golightly YM, Kucera KL, Myers JB, Rosamond WD, Comstock RD. 2015. Epidemiology of overuse injuries in collegiate and high school athletics in the United States. The American journal of sports medicine. 43(7):1790-1797.

Rowland TW, Varzeas MR, Walsh CA. 1991. Aerobic responses to walking training in sedentary adolescents. Journal of Adolescent Health. 12(1):30-34.

Rudroff T, Kelsey MM, Melanson EL, McQueen MB, Enoka RM. 2013. Associations between neuromuscular function and levels of physical activity differ for boys and girls during puberty. The Journal of pediatrics. 163(2):349-354.

Ruff C. 2003. Growth in bone strength, body size, and muscle size in a juvenile longitudinal sample. Bone. 33(3):317-329.

Rumpf MC, Cronin JB, Oliver JL, Hughes MG. 2013. Vertical and leg stiffness and stretch-shortening cycle changes across maturation during maximal sprint running. Human movement science. 32(4):668-676.

Ryan JL, Pracht EE, Orban BL. 2019. Inpatient and emergency department costs from sports injuries among youth aged 5–18 years. BMJ Open Sport & Exercise Medicine. 5(1):e000491.

Ryan MR, Napier C, Greenwood D, Paquette MR. 2021. Comparison of different measures to monitor week-to-week changes in training load in high school runners. International Journal of Sports Science & Coaching. 16(2):370-379.

Saggese G, Baroncelli GI, Bertelloni S. 2002. Puberty and bone development. Best practice & research Clinical endocrinology & metabolism. 16(1):53-64.

Salter J, Black J, Mallett J, Barrett S, Towlson C, Hughes JD, De St Croix M. 2022. Does biologically categorised training alter the perceived exertion and neuromuscular movement profile of academy soccer players compared to traditional age-group categorisation? European Journal of Sport Science.1-10.

Sampson JA, Murray A, Williams S, Halseth T, Hanisch J, Golden G, Fullagar H. 2018. Injury risk-workload associations in NCAA American college football. Journal of science and medicine in sport. 21(12):1215-1220.

Sandrey MA, Chang Y-J, McCrory JL. 2019. The effect of fatigue on leg muscle activation and tibial acceleration during a jumping task. Journal of Sport Rehabilitation. 29(8):1093-1099.

Sañudo B, Sánchez-Hernández J, Bernardo-Filho M, Abdi E, Taiar R, Núñez J. 2019. Integrative neuromuscular training in young athletes, injury prevention, and performance optimization: A systematic review. Applied Sciences. 9(18):3839.

Savelsbergh G, Davids K, Van der Kamp J, Bennett SJ. 2013. Development of movement coordination in children: applications in the field of ergonomics, health sciences and sport. Routledge.

Schmidt RA. 1975. A schema theory of discrete motor skill learning. Psychological review. 82(4):225.

Scholl TO, Chen X, Khoo CS, Lenders C. 2004. The dietary glycemic index during pregnancy: influence on infant birth weight, fetal growth, and biomarkers of carbohydrate metabolism. Am J Epidemiol. 159(5):467-474.

Schoner G. 1995. Recent developments and problems in human movement science and their conceptual implications. Ecological Psychology. 7(4):291-314.

Schroeder AN, Comstock RD, Collins CL, Everhart J, Flanigan D, Best TM. 2015. Epidemiology of overuse injuries among high-school athletes in the United States. The Journal of pediatrics. 166(3):600-606.

Schütte KH, Sackey S, Venter R, Vanwanseele B. 2018. Energy cost of running instability evaluated with wearable trunk accelerometry. J Appl Physiol (1985). 124(2):462-472. eng.

Schütte KH, Seerden S, Venter R, Vanwanseele B. 2018. Influence of outdoor running fatigue and medial tibial stress syndrome on accelerometer-based loading and stability. Gait & posture. 59:222-228.

Schverer M, Lanfumey L, Baulieu E-E, Froger N, Villey I. 2018. Neurosteroids: non-genomic pathways in neuroplasticity and involvement in neurological diseases. Pharmacology & Therapeutics. 191:190-206.

Schwartz MH, Trost JP, Wervey RA. 2004. Measurement and management of errors in quantitative gait data. Gait & posture. 20(2):196-203.

Seefeldt V, Haubenstricker J. 1982. Patterns, phases, or stages: An analytical model for the study of developmental movement. The development of movement control and coordination. 309:318.

Seger JY, Thorstensson A. 2000. Muscle strength and electromyogram in boys and girls followed through puberty. European journal of applied physiology. 81(1):54-61.

SFIA. 2020. Sports & Fitness Industry Association U.S. trends in team sports report, 2019. [accessed 2022 June 29]. https://sfia.org/.

Shannon CE. 1948. A mathematical theory of communication. The Bell system technical journal. 27(3):379-423.

Shannon CE. 1949. Communication in the presence of noise. Proceedings of the IRE. 37(1):10-21.

Shea K, Pfeiffer R, Wang J, Curtin M, Apel P. 2004. Anterior cruciate ligament injury in pediatric and adolescent soccer players: an analysis of insurance data. J Pediatr Orthop. 24(6):623-628.

Shea KG, Grimm NL, Ewing CK, Aoki SK. 2011. Youth sports anterior cruciate ligament and knee injury epidemiology: who is getting injured? In what sports? When? Clinics in sports medicine. 30(4):691-706.

Sheerin KR, Reid D, Besier TF. 2019. The measurement of tibial acceleration in runners—A review of the factors that can affect tibial acceleration during running and evidence-based guidelines for its use. Gait & Posture. 67:12-24.

Sheu Y, Chen L-H, Hedegaard H. 2016. Sports-and Recreation-related Injury Episodes in the United States, 2011-2014. National health statistics reports.(99):1-12.

Shields BM, Knight BA, Hill A, Hattersley AT, Vaidya B. 2011. Fetal thyroid hormone level at birth is associated with fetal growth. The Journal of Clinical Endocrinology & Metabolism. 96(6):E934-E938.

Simons C, Bradshaw EJ. 2016. Do accelerometers mounted on the back provide a good estimate of impact loads in jumping and landing tasks? Sports biomechanics. 15(1):76-88.

Slaughter PR, Adamczyk PG. 2020. Tracking quantitative characteristics of cutting maneuvers with wearable movement sensors during competitive women's ultimate frisbee games. Sensors. 20(22):6508.

Smith N, Jeffers F, Freeman J. 1991. A high-sensitivity magnetoresistive magnetometer. Journal of applied physics. 69(8):5082-5084.

Snook L, Paulson L-A, Roy D, Phillips L, Beaulieu C. 2005. Diffusion tensor imaging of neurodevelopment in children and young adults. Neuroimage. 26(4):1164-1173.

Soangra R, Lockhart TE. 2013. Comparison of intra individual physiological sway complexity from force plate and inertial measurement unit - biomed 2013. Biomed Sci Instrum. 49:180-186. eng.

Soangra R, Moon S, Rezvanian S, Lockhart TE. 2017. Lower extremity muscle fatigue influences nonlinear variability in trunk accelerations. Biomed Sci Instrum. 53:47-54. eng.

50 years of the bonded resistance strain gage–an American retrospective. 1988): History of strain gages, brittle coatings, strain gauge loadcells, Preprints of a Round table of IMEKO TC3 and TC15 at the IMEKO XI Word Congress in Houston, Texas; 1988.

Stein PK. 1996. The early strain gage accelerometers: The inventors and their times. The Shock and Vibration Bulletin.

Stergiou N, Decker LM. 2011. Human movement variability, nonlinear dynamics, and pathology: is there a connection? Human movement science. 30(5):869-888.

Stergiou N, Harbourne RT, Cavanaugh JT. 2006. Optimal movement variability: a new theoretical perspective for neurologic physical therapy. Journal of Neurologic Physical Therapy. 30(3):120-129.

Stracciolini A, Casciano R, Friedman HL, Meehan III WP, Micheli LJ. 2015. A closer look at overuse injuries in the pediatric athlete. Clinical Journal of Sport Medicine. 25(1):30-35.

Stracciolini A, Casciano R, Levey Friedman H, Stein CJ, Meehan WP, 3rd, Micheli LJ. 2014. Pediatric sports injuries: a comparison of males versus females. Am J Sports Med. 42(4):965-972.

Suzuki T, Sasano H, Takeyama J, Kaneko C, Freije WA, Carr BR, Rainey WE. 2000. Developmental changes in steroidogenic enzymes in human postnatal adrenal cortex: immunohistochemical studies. Clinical endocrinology. 53(6):739-747.

Tarantino D, Palermi S, Sirico F, Corrado B. 2020. Achilles tendon rupture: mechanisms of injury, principles of rehabilitation and return to play. Journal of functional morphology and kinesiology. 5(4):95.

Tau GZ, Peterson BS. 2010. Normal development of brain circuits. Neuropsychopharmacology. 35(1):147-168.

Taylor DC, Dalton JR JD, Seaber AV, Garrett JR WE. 1993. Experimental muscle strain injury: early functional and structural deficits and the increased risk for reinjury. The American journal of sports medicine. 21(2):190-194.

Thelen E. 1995. Motor development: A new synthesis. American psychologist. 50(2):79.

Thelen E, Ulrich BD, Wolff PH. 1991. Hidden skills: A dynamic systems analysis of treadmill stepping during the first year. Monographs of the society for research in child development.i-103.

Tirabassi J, Brou L, Khodaee M, Lefort R, Fields SK, Comstock RD. 2016. Epidemiology of high school sports-related injuries resulting in medical disqualification: 2005-2006 through 2013-2014 academic years. The American journal of sports medicine. 44(11):2925-2932.

Tochigi Y, Segal NA, Vaseenon T, Brown TD. 2012. Entropy analysis of tri-axial leg acceleration signal waveforms for measurement of decrease of physiological variability in human gait. Journal of Orthopaedic Research. 30(6):897-904.

Tonson A, Ratel S, Le Fur Y, Cozzone P, Bendahan D. 2008. Effect of maturation on the relationship between muscle size and force production. Medicine and science in sports and exercise. 40(5):918-925.

Topor LS, Asai M, Dunn J, Majzoub JA. 2011. Cortisol stimulates secretion of dehydroepiandrosterone in human adrenocortical cells through inhibition of 3βHSD2. The Journal of Clinical Endocrinology & Metabolism. 96(1):E31-E39.

Trecroci A, Cavaggioni L, Caccia R, Alberti G. 2015. Jump rope training: Balance and motor coordination in preadolescent soccer players. Journal of sports science & medicine. 14(4):792.

Tsutsui T, Iizuka S, Sakamaki W, Maemichi T, Torii S. 2022. Growth until Peak Height Velocity Occurs Rapidly in Early Maturing Adolescent Boys. Children. 9(10):1570.

Tu C, D'Odorico P, Suweis S. 2021. Dimensionality reduction of complex dynamical systems. Iscience. 24(1):1-13.

Tumanski S. 2001. Thin film magnetoresistive sensors.

Tursz A, Crost M. 1986. Sports-related injuries in children: A study of their characteristics, frequency, and severity, with comparison to other types of accidental injuries. Am J Sports Med. 14(4):294-299.

Udofa A, Ryan L, Clark K, Weyand P. 2017. Ground Reaction Forces During Competitive Track Events: A Motion Based Assessment Method. ISBS Proceedings Archive. 35(1):120.

Valasek AE, Young JA, Huang L, Singichetti B, Yang J. 2019. Age and sex differences in overuse injuries presenting to pediatric sports medicine clinics. Clinical Pediatrics. 58(7):770-777.

Valovich McLeod TC, Decoster LC, Loud KJ, Micheli LJ, Parker JT, Sandrey MA, White C. 2011. National Athletic Trainers' Association position statement: prevention of pediatric overuse injuries. Journal of athletic training. 46(2):206-220.

Van der Kruk E, Reijne MM. 2018. Accuracy of human motion capture systems for sport applications; state-of-the-art review. European journal of sport science. 18(6):806-819.

Van der Sluis A, Elferink-Gemser M, Brink M, Visscher C. 2015. Importance of peak height velocity timing in terms of injuries in talented soccer players. International journal of sports medicine.327-332.

Van der Sluis A, Elferink-Gemser M, Coelho-e-Silva M, Nijboer J, Brink M, Visscher C. 2013. Sport injuries aligned to peak height velocity in talented pubertal soccer players. International journal of sports medicine.351-355.

Van Hees VT, Gorzelniak L, Dean León EC, Eder M, Pias M, Taherian S, Ekelund U, Renström F, Franks PW, Horsch A. 2013. Separating movement and gravity components in an acceleration signal and implications for the assessment of human daily physical activity. PloS one. 8(4):e61691.

Van Praagh E, Doré E. 2002. Short-term muscle power during growth and maturation. Sports medicine. 32(11):701-728.

Van Praagh E, Fellmann N, Bedu M, Falgairette G, Coudert J. 1990. Gender Difference in the Relationship of Anaerobic Power Output to Body Composition in Children. Pediatric Exercise Science. 2(4).

Vandorpe B, Vandendriessche J, Lefèvre J, Pion J, Vaeyens R, Matthys S, Philippaerts R, Lenoir M. 2011. The Körperkoordinationstest für kinder: Reference values and suitability for 6–12-year-old children in Flanders. Scandinavian journal of medicine & science in sports. 21(3):378-388.

Venturelli M, Bishop D, Pettene L. 2008. Sprint training in preadolescent soccer players. International Journal of Sports Physiology and Performance. 3(4):558-562.

Viru A, Loko J, Harro M, Volver A, Laaneots L, Viru M. 1999. Critical periods in the development of performance capacity during childhood and adolescence. European Journal of Physical Education. 4(1):75-119.

Walter PL. 1997. The history of the accelerometer. Sound and vibration. 31(3):16-23.

Wang L-i, Lin D-c, Huang C. 2004. Age effect on jumping techniques and lower limb stiffness during vertical jump. Research in Sports Medicine. 12(3):209-219.

Warden SJ, Brukner P. 2003. Patellar tendinopathy. Clinics in sports medicine. 22(4):743-759.

Weedon MN, Frayling TM, Shields B, Knight B, Turner T, Metcalf BS, Voss L, Wilkin TJ, McCarthy A, Ben-Shlomo Y. 2005. Genetic regulation of birth weight and fasting glucose by a common polymorphism in the islet cell promoter of the glucokinase gene. Diabetes. 54(2):576-581.

West SW, Clubb J, Torres-Ronda L, Howells D, Leng E, Vescovi JD, Carmody S, Posthumus M, Dalen-Lorentsen T, Windt J. 2021. More than a metric: how training load is used in elite sport for athlete management. International journal of sports medicine. 42(04):300-306.

Whiting SJ, Vatanparast H, Baxter-Jones A, Faulkner RA, Mirwald R, Bailey DA. 2004. Factors that affect bone mineral accrual in the adolescent growth spurt. The Journal of nutrition. 134(3):696S-700S.

Whittle MW. 1999. Generation and attenuation of transient impulsive forces beneath the foot: a review. Gait & posture. 10(3):264-275.

WHO MGRSG. 2006. WHO Motor Development Study: windows of achievement for six gross motor development milestones. Acta paediatrica. 95:86-95.

Wilkerson GB, Gupta A, Allen JR, Keith CM, Colston MA. 2016. Utilization of practice session average inertial load to quantify college football injury risk. Journal of strength and conditioning research. 30(9):2369-2374.

Willy RW. 2018. Innovations and pitfalls in the use of wearable devices in the prevention and rehabilitation of running related injuries. Physical Therapy in Sport. 29:26-33.

Witchel SF, Topaloglu AK. 2019. Puberty: gonadarche and adrenarche. Yen and Jaffe's reproductive endocrinology.394-446. e316.

Wittmann F, Lambercy O, Gassert R. 2019. Magnetometer-based drift correction during rest in IMU arm motion tracking. Sensors. 19(6):1312.

Wood CL, Lane LC, Cheetham T. 2019. Puberty: Normal physiology (brief overview). Best practice & research Clinical endocrinology & metabolism. 33(3):101265.

Xie H, Fedder GK. 2003. Integrated microelectromechanical gyroscopes. Journal of aerospace engineering. 16(2):65-75.

Xu Q, Hou Z, Kuang Y, Miao T, Ou F, Zhuo M, Xiao D, Wu X. 2019. A tuning fork gyroscope with a polygon-shaped vibration beam. Micromachines. 10(12):813.

Yagüe PH, De La Fuente JM. 1998. Changes in height and motor performance relative to peak height velocity: A mixed-longitudinal study of Spanish boys and girls. American Journal of Human Biology: The Official Journal of the Human Biology Association. 10(5):647-660.

Yazdi N, Ayazi F, Najafi K. 1998. Micromachined inertial sensors. Proceedings of the IEEE. 86(8):1640-1659.

Yentes JM. 2018. Entropy. Nonlinear Analysis for Human Movement Variability. CRC press; p. 173-260.

Yentes JM, Hunt N, Schmid KK, Kaipust JP, McGrath D, Stergiou N. 2013. The appropriate use of approximate entropy and sample entropy with short data sets. Annals of biomedical engineering. 41(2):349-365.

Yentes JM, Raffalt PC. 2021. Entropy analysis in gait research: methodological considerations and recommendations. Annals of biomedical engineering. 49(3):979-990.

Yoon SW, Lee S, Najafi K. 2012. Vibration-induced errors in MEMS tuning fork gyroscopes. Sensors and Actuators A: Physical. 180:32-44.

Yoshimoto T, Takai Y, Fujita E, Fukunaga Y, Kintaka H, Nishizono H, Kanehisa H, Yamamoto M. 2012. Influence of the torque generating capacity of the lower extremity muscles on the running and jump performance in primary and junior high school boys. Japanese Journal of Physical Fitness and Sports Medicine. 61(1):79-88.

Yoshimoto T, Takai Y, Fukunaga Y, Fujita E, Kanehisa H, Yamamoto M. 2014. Effect of maturation on sprint and jump performances in adolescent boys. Gazz Med Ital. 173:265-272.

Yu B, Garrett WE. 2007. Mechanisms of non-contact ACL injuries. British journal of sports medicine. 41(suppl 1):i47-i51.

Yu B, McClure S, Onate J, Guskiewicz K, Kirkendall D, Garrett W. 2005. Age and gender effects on lower extremity kinematics of youth soccer players in a stop-jump task. Am J Sports Med. 33(9):1356-1364.

Yu L, Mei Q, Xiang L, Liu W, Mohamad NI, István B, Fernandez J, Gu Y. 2021. Principal component analysis of the running ground reaction forces with different speeds. Frontiers in bioengineering and biotechnology. 9:629809.

Zeng W, Glass L. 1996. Statistical properties of heartbeat intervals during atrial fibrillation. Physical Review E. 54(2):1779.

Zhou S, Glowacki J. 2018. Dehydroepiandrosterone and bone. Vitamins and Hormones. Elsevier; p. 251-271.

Ziegert J, Lewis J. 1979. The effect of soft tissue on measurements of vibrational bone motion by skin-mounted accelerometers.

Zifchock RA, Davis I, Hamill J. 2006. Kinetic asymmetry in female runners with and without retrospective tibial stress fractures. Journal of biomechanics. 39(15):2792-2797.

Appendices

Appendix A. IRB Approval Letter

THE UNIVERSITY OF
TENNESSEE
KNOXVILLE

July 22, 2022

Joshua Trueblood Weinhandl,

UTK - Coll of Education, Hlth, & Human - Kinesiology, Recreation and

Re: UTK IRB-22-07037-XP

Study Title: Acceleration Profiles of Adolescent Fútbol Players

Dear Joshua Trueblood Weinhandl:

The UTK Institutional Review Board (IRB) reviewed your application for the above referenced project. It determined that your application is eligible for expedited review under 45 CFR 46.110(b)(1), Categories 6 and 7. The IRB has reviewed these materials and determined that they do comply with proper consideration for the rights and welfare of human subjects and the regulatory requirements for the protection of human subjects.

Therefore, this letter constitutes full approval by the IRB of your application (version 1.1) as submitted, including the following documents that have been dated and stamped IRB approved:

- ChildAssent_IMU v 1.1
- InformedConsent_IMU v 1.0
- KFC-LetterOfApproval v 1.0
- ScreeningEmail_IMU v 1.0
- RecruitmentEmail_IMU v 1.0
- StudyAnnouncement v 1.0
- LEFS v 1.0
- Fitness_Activity_Questionnaire v 1.0

You are approved to enroll a maximum of 150 participants. Approval of this study will be valid from July 22, 2022.

Any revisions in the approved application consent forms, instruments, recruitment materials, etc., must be submitted to and approved by the IRB prior to implementation. In addition, you are responsible for reporting any unanticipated serious adverse events or other problems involving risks to subjects or others in the manner required by the local IRB policy.

The IRB has determined that your project does not require annual Continuing Review (renewal). Approval of this study is valid for three years. If a Study Update Form is not submitted in iMedRIS and approved by the IRB prior to 07/21/2025, the study will be automatically closed by the IRB and no further study activity will be permitted until a Study Update Form is received. Please be sure to also submit a Study Closure Request (Form 7) when all research activity, including data analysis, has been completed.

Sincerely,

Lora Beebe, Ph.D., PMHNP-BC, FAAN

Chair

Institutional Review Board | Office of Research & Engagement
1534 White Avenue Knoxville, TN 37996-1529
865-974-7697 865-974-7400 fax irb.utk.edu

BIG ORANGE. BIG IDEAS.
Flagship Campus of the University of Tennessee System

CONSENT FOR RESEARCH PARTICIPATION

Research Study Title: Acceleration profiles and sex differences among adolescent soccer players

Researcher(s): Joshua T. Weinhandl, PhD, University of Tennessee, Knoxville
Jake A. Melaro, MS, University of Tennessee, Knoxville
Joshua Lardie, MS, University of Tennessee, Knoxville

Why am I being asked to be in this research study?

We are asking your child to be in this research study because he/she is between the ages of 9 to 17 years old and is recreationally active. We are also asking your child to be in this research study because he/she is currently playing on a competitive soccer team that practices at least twice a week. Individuals who are not between the ages of 9 to 17 or have sustained a musculoskeletal injury of the lower extremity during the past 6 months will not be asked to be in this research study.

How long will I be in the research study?

If you agree for your child to be in the study, his/her participation will involve 2 study sessions lasting approximately 20 minutes each.

What will happen if I say "Yes, I want to be in this research study"?

If you agree for your child to be in this study, we will visit him/her at the Crushplex training facility on two separate occasions during scheduled practices, once at the beginning of the season and again at the end of the season.

You will fill out the informed consent and your child will be given an assent form (which will be thoroughly explained to them), as well as a fitness activity questionnaire and lower extremity functional scale form prior to the first testing session.

After these forms are completed and on the day of the first testing session, we will then place two small sensors on your child's leg directly above your ankle at the beginning of practice. He/she will then jog from one end of the turf field to the other and back at an easy pace. Following the jog and a slight break, he/she will then sprint around cones in the shape of an 'M' twice, once in both directions. Following another short break, he/she will then do a side-shuffling drill between two cones as fast as he/she can. Then, following a final short break, he/she will hop three times (3x) as far as they can on their right leg before again hopping three times (3x) on the other leg as far as they can. The testing session will then be completed. The testing session will be repeated again at the conclusion of the season at another scheduled practice.

What happens if I say "No, I do not want to be in this research study"?

Being in this study is up to you and your child. You can say no now or leave the study later. Either way, your decision(s) won't affect your standing with the club, your relationship with your coaches, or standing with the University of Tennessee, Knoxville.

What happens if I say "Yes" but change my mind later?

Even if you decide to be in the study now, you can change your mind and stop at any time. If you decide to stop before the study is completed, you can tell the PI and/or co-PI that you wantto withdraw from the study at any time. If you decide to withdraw from the study, your information will be kept de-identified and kept in a locked drawer in our Biomechanics lab on the university campus. Only study personnel will have access to any forms and data that have already been collected.

Are there any possible risks to me?

It is possible that someone could find out you were in this study or see your study information,but we believe this risk is small because of the procedures we use to protect your information. These procedures are described later in this form.

Possible risks include lower extremity injury during the study movements. These risks will be minimized. Your child will complete a required to warm up before data collection, so his/her muscles are ready to move, and provided ample opportunity to familiarize themselves with the movements to reduce risk of injury. Further, breaks will be provided in the unlikely case that they experience discomfort or pain. The movements included are movements they should be familiar with, due to their practicing at least twice a week. In the *very* unlikely case that they hurt themselves during the study visit, Knox Crush FC staff will provide appropriate first-aid and contact medical services. If you realize afterwards that they have become injured, you should seek medical assistance.

Are there any benefits to being in this research study?

We do not expect you or your child to directly benefit from being in this study. Your participation may help us to learn more about the relationship between youth athletes' physical development and the differences in complexity of their movements. We hope the knowledge gained from this study will benefit others in the future.

Who can see or use the information collected for this research study?

We will protect the confidentiality of your information by keeping all forms in a locker drawer or on a password-encrypted computer drive in the Biomechanics lab, which is locked every day. Only the investigators conducting this study will have access to your personal information. If information from this study is published or presented at scientific meetings, your name and other personal information will not be used. We will make every effort to prevent anyone who is not on the research team from knowing that you gave us information or what information came from you. Although it is unlikely, there are times when others may need to see the information we collect about you. These include people at the University of Tennessee, Knoxville who oversee research to make sure it is conducted properly.

What will happen to my information after this study is over?

We will keep your information to use for future research. Your name and other information thatcan directly identify you will be kept secure and stored separately from your research data collected as part of the study. We will not share your research data with other researchers.

Will I be paid for being in this research study?

You and your child will not be paid for being in this study.

Will it cost me anything to be in this research study?

It will not cost you anything to be in this study

What else do I need to know?

We may need to stop your and your child's participation in the study without your consent if he/she does not follow the study instructions, no longer meet the study's eligibility requirements, if his/her safety comes into question, or if the study is stopped for any reason.

The University of Tennessee does not automatically pay for medical claims or give other compensation for injuries or other problems should you realize your child is injured outside of the study visit.

Who can answer my questions about this research study?

If you have questions or concerns about this study, or have experienced a research related problem or injury, contact the researchers, Dr. Joshua Weinhandl (**jweinhan@utk.edu**, 865-974-9556), Jake Melaro (**jmelaro@vols.utk.edu**, 865-974-2091) or Joshua Lardie (**jlardie@vols.utk.edu**, 865-974-2091).

For questions or concerns about your rights or to speak with someone other than the researchteam about the study, please contact:

Institutional Review Board
The University of Tennessee, Knoxville
1534 White Avenue
Blount Hall, Room 408
Knoxville, TN 37996-1529
Phone: 865-974-7697
Email: **utkirb@utk.edu**

STATEMENT OF CONSENT

I have read this form and the research study has been explained to me. I have been given the chance to ask questions and my questions have been answered. If I have more questions, I havebeen told who to contact. By signing this document, I am agreeing to be in this study. I will receive a copy of this document after I sign it.

Name of Adult Participant	Signature of Adult Participant	Date

Researcher Signature (to be completed at time of informed consent)

I have explained the study to the participant and answered all his/her questions. I believe that he/she understands the information described in this consent form and freely consents to be inthe study.

Name of Research Team Member	Signature of Research Team Member	Date

Appendix C. Recruitment Announcement

Hello,

Your child is invited to participate in a biomechanical research study investigating how movement complexity differs among males and female soccer players at different stages of development and over the course of a season. This information will hopefully aid in preventing injury and improving performance in adolescent athletes.

We are particularly interested in recruiting males and female soccer players that practice at least twice (2x) per week. We ask that the player be between the ages of 9 and 17. We also ask that the player not have any lower back or leg injuries within the past six months prior to testing.

This study will involve placing two small sensors on your child right above their ankles before they perform several movement tasks. For task 1, the player will jog the length of a turf field and back at an easy pace; for task 2, the player will sprint twice around cones in the shape of an 'M', once in both directions and with a small break in between sprints; for task 3, following a short break the player will perform a shuffle drill between two cones as fast as they can; and finally for task 4, following a short break the player will hop three (3x) times as far as they can on both their right and left legs.

The current study will require you to come the Crushplex training facility (1501 Kirby Road, Knoxville, TN) for two sessions (once at the beginning of the season and again at the end of the season), which will last approximately 15 minutes each. If you feel your child fits the criteria for this study and are willing to let them participate, please contact the research investigators Dr. Joshua Weinhandl (jweinhan@utk.edu), Jake Melaro (jmelaro@vols.utk.edu), or Joshua Lardie (jlardie@vols.utk.edu) via email or telephone (865) 974-2091 (office number).

Thank you for your time,
Jake Melaro, MS
Graduate Assistant/PhD Candidate, Biomechanics
The University of Tennessee, Knoxville
Department of Kinesiology, Recreation, and Sports Studies

Appendix D. Study Recruitment Flyer

Male and Female Soccer Players Needed for a Biomechanics Study

Your child may be able to participate if he/she:

- Practices at least twice (2_x) per week
- Are between the age of 9 to 17 years
- No previous lower back or lower extremity injury that required surgery

The University of Tennessee Biomechanics/Sports Medicine Lab is conducting a research study to examine if there are differences in movement complexity over the course of a season.

Participants will be required to perform **two (2)** 15-minute testing sessions at the Crushplex facility (**1501 Kirby Rd, Knoxville, TN**)

- **One (1)** session at the beginning of the season
- **One (1)** session at the end of the end of the season.

Contact: Jake Melaro
jmelaro@vols.utk.edu

THE UNIVERSITY OF TENNESSEE KNOXVILLE
BIOMECHANICS

Appendix E. Lower Extremity Functional Scale Form

Lower Extremity Functional Scale

We are interested in knowing whether or not you are having any difficulty at all with the activities listed below. Please provide an honest answer for each activity.

KEY
0 - Extreme difficulty or unable to perform activity
1 - Quite a bit of difficulty
2 - Moderate difficulty
3 - A little bit of difficulty
4 - No difficulty

Today, ***do you*** or ***would you*** have any difficulty at all with:	Extreme 0	Quite a bit 1	Moderate 2	Minimal 3	None 4
1. Any of your usual work, housework or school activities	☐	☐	☐	☐	☐
2. Your usual hobbies, recreational or sporting activities	☐	☐	☐	☐	☐
3. Getting into or out of the bath	☐	☐	☐	☐	☐
4. Walking between rooms	☐	☐	☐	☐	☐
5. Putting on your shoes or socks	☐	☐	☐	☐	☐
6. Squatting	☐	☐	☐	☐	☐
7. Lifting an object, like a bag of groceries from the floor	☐	☐	☐	☐	☐
8. Performing light activities around your home	☐	☐	☐	☐	☐
9. Performing heavy activities around your home	☐	☐	☐	☐	☐
10. Getting into or out of a car	☐	☐	☐	☐	☐
11. Walking 2 blocks	☐	☐	☐	☐	☐
12. Walking a mile	☐	☐	☐	☐	☐
13. Going up or down 10 stairs (about 1 flight)	☐	☐	☐	☐	☐
14. Standing for 1 hour	☐	☐	☐	☐	☐
15. Sitting for 1 hour	☐	☐	☐	☐	☐
16. Running on even ground	☐	☐	☐	☐	☐
17. Running on uneven ground	☐	☐	☐	☐	☐
18. Making sharp turns while running fast	☐	☐	☐	☐	☐
19. Hopping	☐	☐	☐	☐	☐
20. Rolling over in bed	☐	☐	☐	☐	☐

FITNESS ACTIVITY QUESTIONNAIRE

Please describe your current participation in the following types of exercise:

1. Aerobic (aerobic classes, walking, jogging, stair climbing, hiking, cycling, etc.)
Frequency (# of days per week): _____
Duration (time spent per session): _____minutes
Intensity (difficulty level): light somewhat hard hard very hard
How long have you been participating in aerobic activity as described above?
_____Years

2. Anaerobic (weight training, sprinting, etc.)
Frequency (# of days per week): _____
Duration (time spent per session): _____minutes
Intensity (difficulty level): light somewhat hard hard very hard
How long have you been participating in anaerobic activity as described above?
_____Years

3. Organized or Recreational sports
Type of sport(s):_____
Frequency (# of days per week): _____
Duration (time spent per session): _____minutes
Intensity (difficulty level): light somewhat hard hard very hard
How long have you been participating in sports activity as described above?
_____Years

Appendix G. Study Protocol

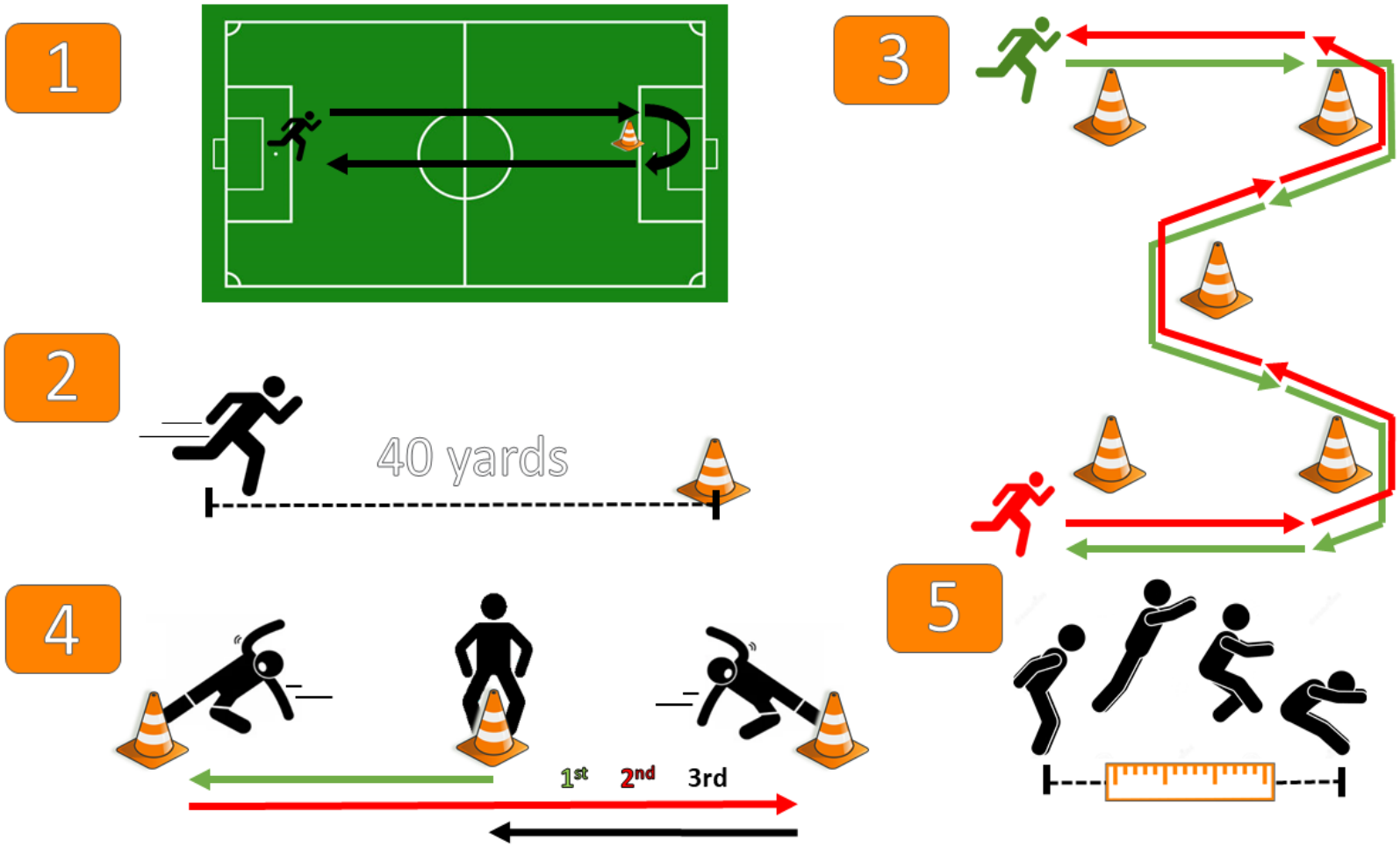

Figure 1: Experimental study protocol including (1) down and back jog, (2) 40-yd dash , (3) M-cone drill, (4) 5-10-5 drill, and (5) standing broad jump.

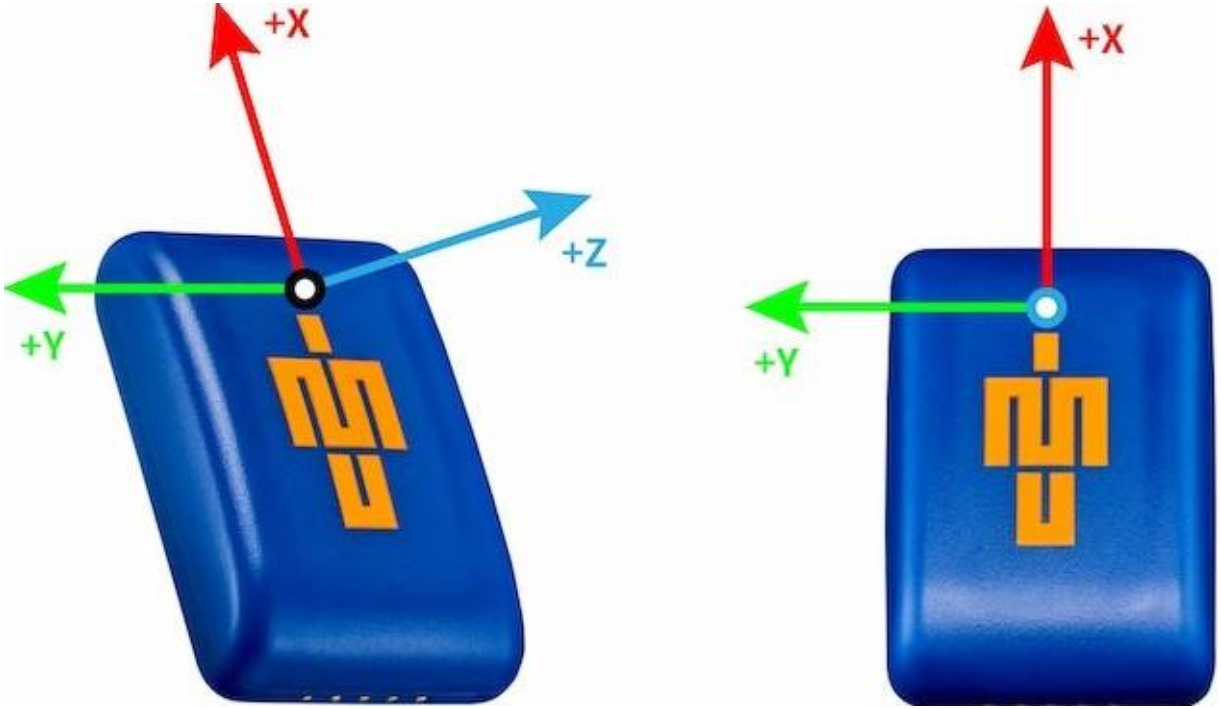

Figure 2: Vicon© Blue Trident dual-g inertial measurement unit coordinate system conventions

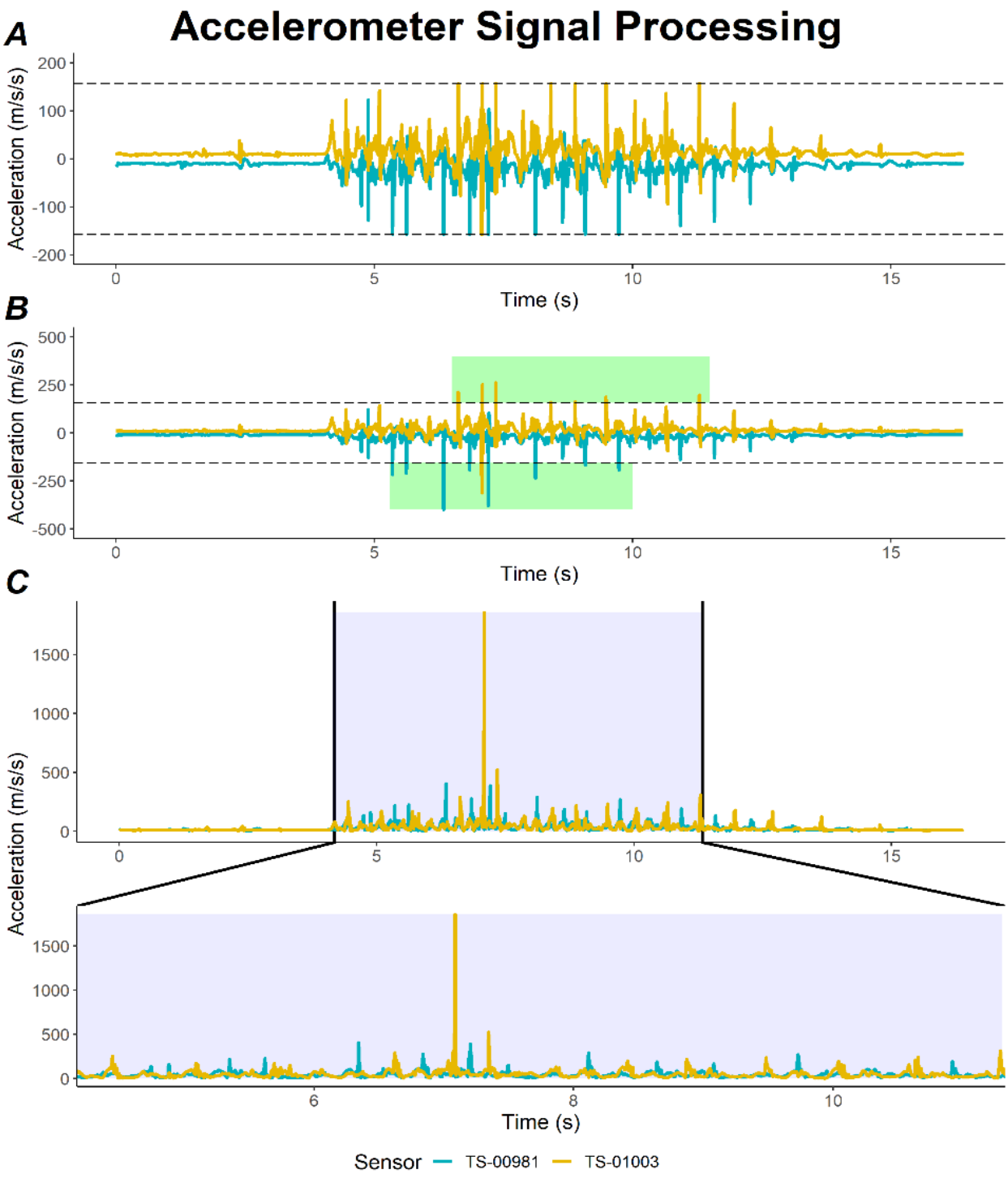

Figure 3: (A) Raw 3D acceleration components saturate low-g sensor at 16 G's. (B) Saturated data points replaced at same time points with high-g sensor data. (C) Resultant acceleration calculated from XYZ components and signal clipped following visual examination to remove extracurricular data.

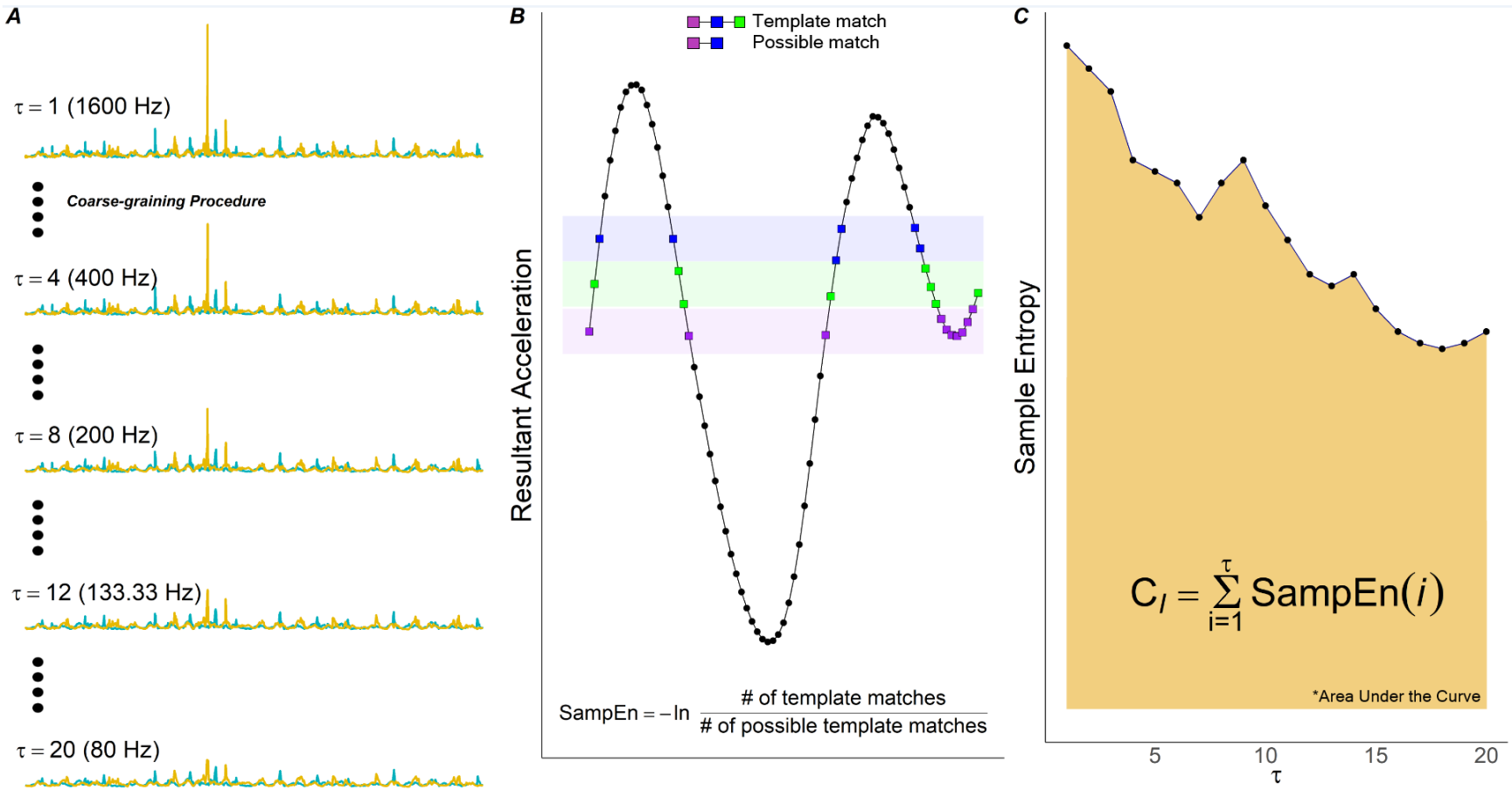

Figure 4: (A) A coarse-graining procedure will be used on the original resultant acceleration time series from τ=[1 20]. (B) Each coarse-grained time series will then be fed into a base SampEn algorithm. (C) SampEn values will be plotted across τ and the area under the curve will be calculated to determine CI.

$$[CI, Acc_P, Acc_I]_{ij} = 1 + \beta_{0j} + \varepsilon_{ij}$$

*Null Model

$$[CI, Acc_P, Acc_I]_{ij} = \beta_{0j} + \beta_1 PHV_{ij} + \varepsilon_{ij}$$

*Model 1

$$[CI, Acc_P, Acc_I]_{ij} = \beta_{0j} + \beta_1 PHV_{ij} + \beta_2 Sex_{ij} + \varepsilon_{ij}$$

*Model 2

$$[CI, Acc_P, Acc_I]_{ij} = \beta_{0j} + \beta_1 PHV_{ij} + \beta_2 Sex_{ij} + \beta_3 Session_{ij} + \varepsilon_{ij}$$

*Model 3

Compare Fits

- **AIC**
- **BIC**
- **R^2**
- **ICC**
- **RMSE**

Figure 5: Statistical workflow for linear mixed effects model comparisons showing how the model was iteratively built from the null- to the full-model (Model 3). j = *j*th subject; i = *i*th data point; β_{0j} = random intercept for the *j*th subject; *PHV* = PHV offset; *Sex* = subject sex; *Session* = testing session; β = fixed effect estimate; ε = residual error term; CI = complexity index; Acc_P = acceleration peak; Acc_I = acceleration integral; AIC = Akaike information criteria; BIC = Bayesian information criteria; R^2 = coefficient of determination; ICC = intraclass correlation coefficient; RMSE = root-mean-squared error.

Appendix L. Aggregated Complexity Results

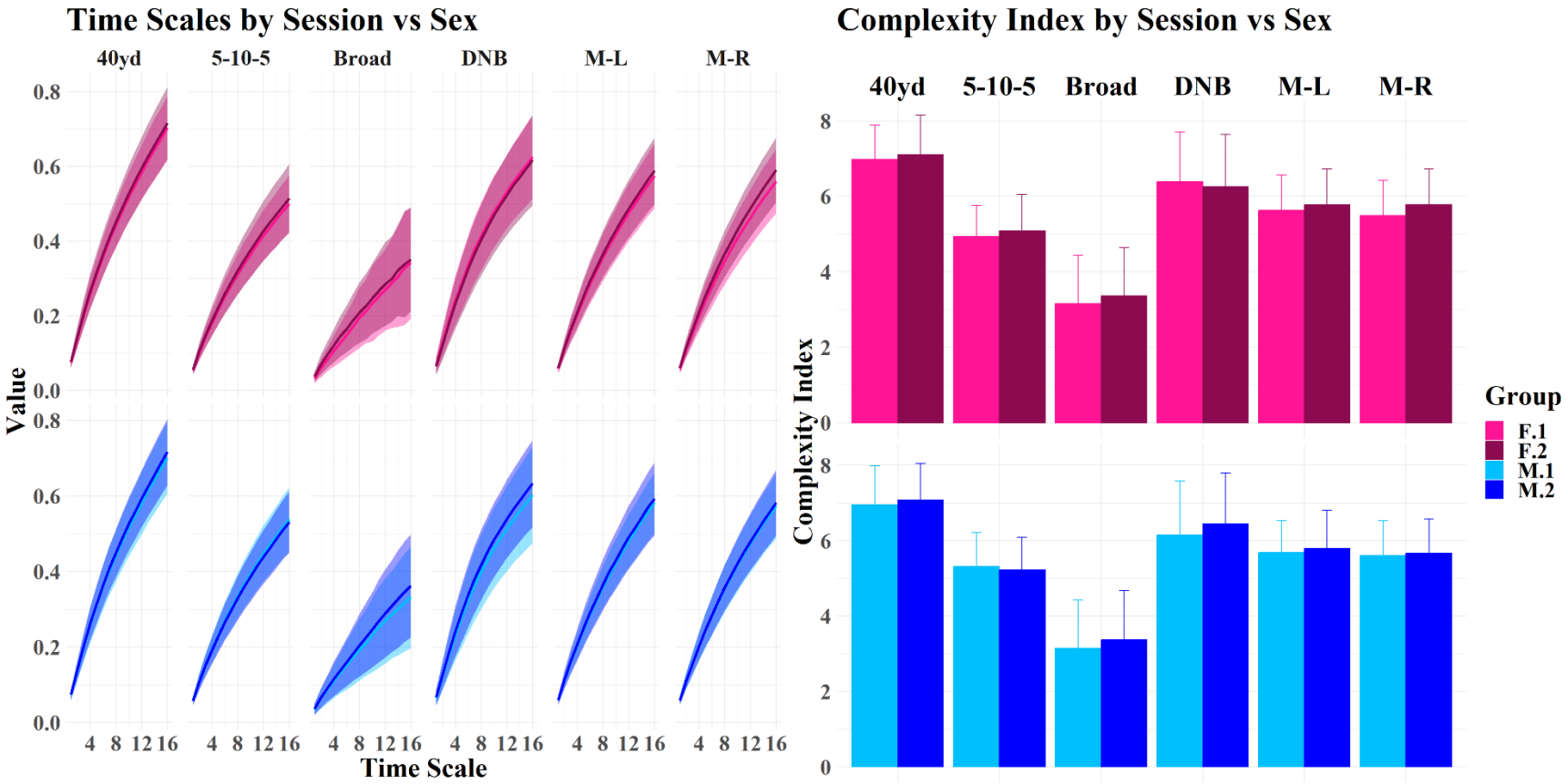

Figure 6: Multiscale entropy and complexity index results across drills. F.1 = Female Pre-season; F.2 = Female Post-season; M.1 = Male Pre-season; M.2 = Male Post-season; Both y-axes are unitless measures.

Appendix M. Aggregated Acceleration Peaks and Integral Results

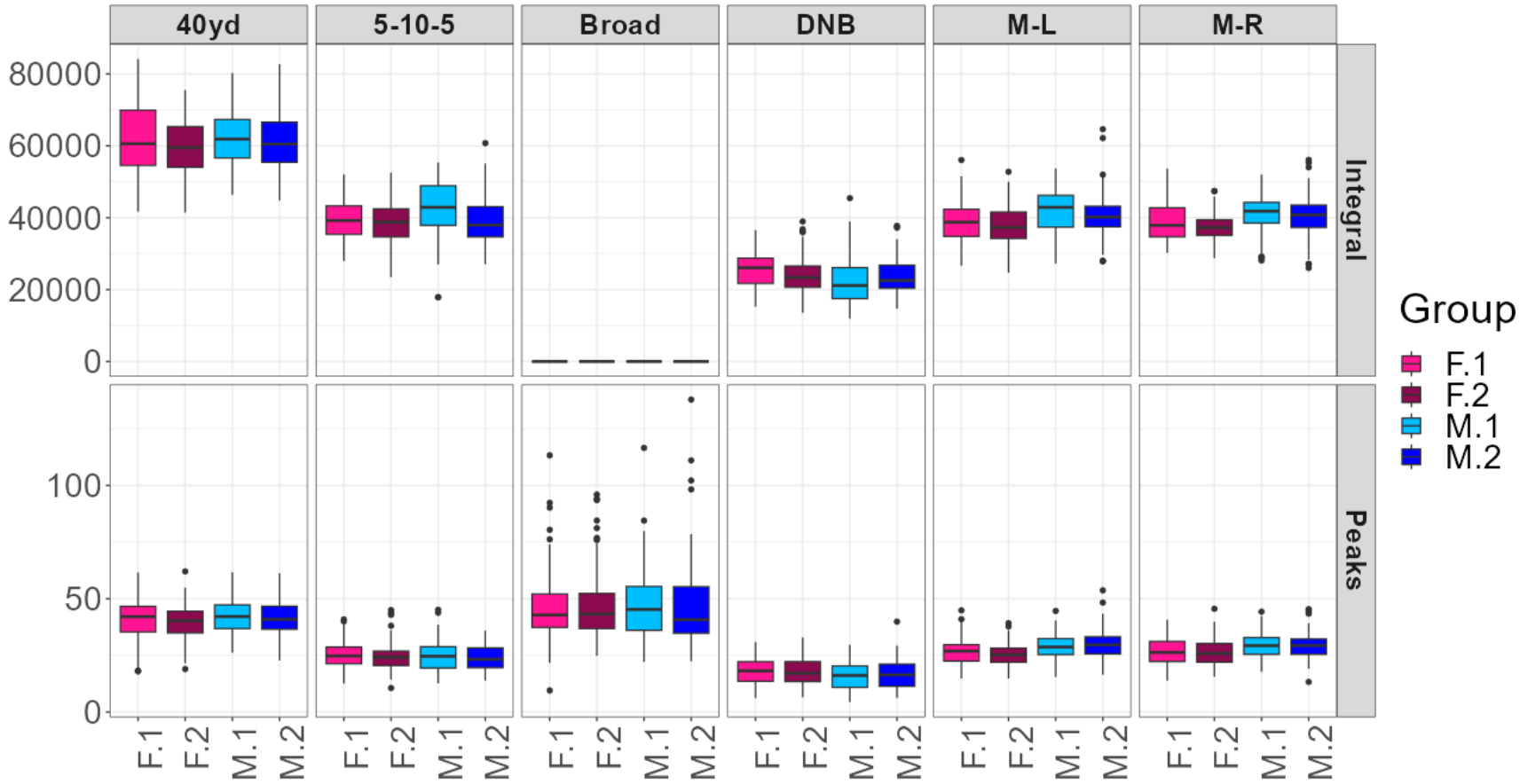

Figure 7: Acceleration peaks and integral results across drills. F.1 = Female Pre-season; F.2 = Female Post-season; M.1 = Male Pre-season; M.2 = Male Post-season; Peaks are reported in units of gravity (G's) and integrals in arbitrary units (A.U.s).

Appendix N. Individual Anthropometric and Testing Data

Table 1: Individual Anthropometric and Testing Data

			Pre-season					Post-season			
Subject	**Sex**	**Δ Days**	**Age**	**Ht (cm)**	**Mass (kg)**	**Leg (cm)**	**PHV (yrs)**	**Ht (cm)**	**Mass (kg)**	**Leg (cm)**	**PHV (yrs)**
S001	1	63	10.74	142	32.95	75	-3.49	145.5	37.73	73.5	-2.87
S002	1	63	10.89	148.5	45	75.5	-2.68	148	48.09	74.5	-2.51
S003	1	63	10.33	137.5	29.5	74.5	-4.06	137.4	29.73	68.9	-3.47
S004	1		11.05	147.5	39.32	77.5	-3				
S005	1	63	10.88	140.5	32.82	72.5	-3.34	143.9	32.45	76.4	-3.34
S006	1	63	10.49	144.5	37	74.5	-3.24	141.9	34	71.2	-3.15
S007	1	63	10.41	147	46.82	75.5	-2.98	148	46.73	77.5	-3.01
S008	1	63	10.66	149.5	43.64	76.5	-2.8	149.1	41.82	72	-2.36
S009	1	63	10.84	145.5	41.23	73	-2.8	136.6	40.55	63.5	-2.65
S010	1	63	10.98	149	36.41	78	-2.97	149.1	37	75.1	-2.6
S011	1	63	10.29	132	31.36	69	-4.02	134.4	29.73	68.2	-3.69
S012	1	63	10.42	141	32.05	75.5	-3.76	141.7	32	74.4	-3.53
S013	1	63	11.06	142	39.95	75	-3.26	142	41	71	-2.78
S014	1	63	10.54	134	27.5	69	-3.82	136	27.36	68	-3.48
S015	1	63	11.06	141.5	34.86	74	-3.29	142.2	34.09	70.2	-2.79
S016	1	63	10.18	140.5	34.32	73	-3.62	140	34.55	70.6	-3.38
S017	1	77	13.58	154.3	40.91	76.1	-1.07	158	43.82	77.5	-0.69
S018	1		13.8	170.6	54	88.6	-0.41				
S019	1		13.83	168	49.64	84.5	-0.26				
S020	1	77	13.78	155	33.82	78.6	-1.31	156	34.91	79	-1.16
S021	1	77	12.43	161.1	66.73	86.2	-1.6	161.5	68.73	81.5	-0.93
S022	1	77	12.92	164.2	50.36	81.6	-0.76	167	54	83.5	-0.54
S023	1	77	13.77	166.9	50.36	84	-0.34	168	52.27	84.5	-0.17
S024	1		13.91	171.2	56.09	89.8	-0.41				

Table 1: Continued

S025	1		13.44	167.6	49	83.9	-0.42				
S026	1	77	13.13	163.9	54.82	85.1	-1.05	165	45.64	84	-0.84
S027	1	77	13.82	172.4	52.82	85.1	0.23	172.5	54.82	86	0.24
S028	1	77	13.49	167	42.73	86.2	-0.83	169	43.91	86.5	-0.54
S029	1	77	13.38	153.2	34.09	74.3	-1.18	154.5	40.64	74	-0.82
S030	0	63	11.82	146.5	37.09	72.5	-0.59	147	37.91	72.8	-0.47
S031	0	63	12.99	158	38.82	80.6	0.53	158.1	39.64	81.1	0.61
S032	0	63	13.08	168.3	51	81.6	1.49	167	51.55	85	1.32
S033	0	63	12.52	165.2	59.73	81.3	1.08	165	64.27	80.9	1.23
S034	0	63	12.58	169.2	56.73	82.3	1.31	169.7	58	81.2	1.51
S035	0	63	13.08	176.2	77.82	85.7	2.16	176.6	78.09	86.7	2.23
S036	0		12.37	145.8	34.64	72.1	-0.4				
S037	0	63	13.12	168	64.18	84.2	1.5	166.3	66.41	83.8	1.51
S038	0		12.24	167.7	66.36	84.1	1.07				
S039	0	63	12.85	151.7	35.55	75.8	0.13	151.8	40	75.3	0.33
S040	0	63	11.43	165	52.64	82.5	0.34	165	51.91	83	0.4
S041	0		12.91	166.1	55.36	81.2	1.29				
S042	0	63	12.16	158.7	43.82	76.9	0.39	159.2	45.36	78.2	0.48
S043	0	63	13.22	163	5	80.5	0.64	163	53.27	78	1.44
S044	0	63	13.29	163.2	55.18	80.3	1.31	166	55.64	80.6	1.61
S045	0	63	13.96	163.6	56.27	82.8	1.57	163.4	58.73	83.2	1.65
S046	0	63	13.54	160.9	56.09	79.7	1.3	163	57.27	80	1.55
S047	0		14.05	152.2	44.82	74.2	1				
S048	0	63	13.75	162	49.27	82.3	1.29	162	49.64	81.9	1.4
S049	0	63	13.85	165.2	54.64	83.4	1.6	167.8	56	83.7	1.9
S050	0	63	14.12	158.2	51.27	78.2	1.4	158.5	53.09	79	1.49
S051	0	63	13.36	160.2	44	82.3	0.88	162.5	43.55	86.5	0.94

Table 1: Continued

S052	0	63	13.41	152.8	34.09	79.2	0.32	152.8	34.45	75.5	0.6
S053	0	63	13.93	160.6	53.27	76.7	1.59	153	53.36	63.6	1.72
S054	0	63	13.4	166.5	51.18	82.1	1.49	166	51.82	80.8	1.62
S055	0	63	13.25	156.6	45.27	72.6	1.02	157.4	45.82	72.6	1.18
S056	0	70	14.05	166.5	55.64	84.2	1.78	167.5	56.09	82.5	2.04
S057	0		13.2	159.4	58.64	80.4	1.02				
S058	0		12.4	155.1	43.36	80	0.1				
S059	0	70	12.51	161.2	40.82	83.7	0.4	161.7	34.27	82.7	0.48
S060	0		12.39	160	59.73	76.5	0.86				
S061	0		12.59	162.8	58.64	80.3	0.97				
S062	0	70	13.33	161	45.36	82	0.96	162.6	47.18	84.1	1.09
S063	0	70	12.61	154.1	38.64	80.1	0.05	154.6	40.09	80.3	0.18
S064	0	60	9.84	139.2	32.18	70.8	-2.07	140.1	32	70.6	-1.93
S065	0	60	10.72	143.7	36.55	72.7	-1.33	143.6	37.73	72.6	-1.22
S066	0	60	11.11	146.9	39.18	72.5	-0.87	148	40.45	74.6	-0.77
S067	0	60	10.45	148.8	43.09	75.6	-1.1	149	44.09	74.9	-0.96
S068	0	60	11.1	146.5	36.82	73	-0.97	148	39.18	74	-0.78
S069	0	60	10.27	141	32.55	67.8	-1.63	140.3	33.55	68.1	-1.58
S070	0	60	10.35	149.9	35.55	73.5	-1.18	149.4	37	71.8	-1.03
S071	0	60	10.76	154.4	41.36	76.5	-0.67	154.6	42.45	75.6	-0.51
S072	0		10.52	142.1	29.55	70	-1.6				
S073	0	60	10.84	150.1	49.73	75.8	-0.69	150	50.91	75.3	-0.57
S074	1		13.98	167	52.27	84	-0.21				
S075	1	63	13.39	156	42	78.9	-1.28	156.6	42.18	78.5	-1.1
S076	1	63	13.79	159.7	50.09	81.3	-0.85	160.9	51	81.6	-0.67
S077	1	63	13.2	160.3	44.55	82.3	-1.24	161	46	83.7	-1.24
S078	1	63	13.89	160.4	52.55	82.1	-0.79	161.4	51.73	81.4	-0.53

Table 1: Continued

S079	1	63	13.75	166.9	53.36	86.8	-0.66	168	53.36	84.5	-0.17
S080	1		14.04	149.7	46.55	72.7	-0.9				
S081	1	63	13.82	162.8	53.36	80.4	-0.32	163.8	53.18	81.4	-0.26
S082	1	63	13.99	166.4	49.55	85.8	-0.54	167.9	49.45	85.9	-0.3
S083	1	63	13.5	183.5	84.27	89.3	1.27	184.1	87.55	91.9	1.15
S084	1	63	14.07	158.1	40.73	81.4	-1.07	158.8	43.82	81.1	-0.84
S085	1	63	13.35	159.5	48.82	80.5	-0.99	159.8	48.27	79.6	-0.79
S086	1	63	13.22	158.5	43.73	78.6	-1.01	159.8	44.55	78.4	-0.76
S087	1	63	13.94	186.4	78.18	95.6	0.99	187.5	78.55	97.5	0.97
S088	1	63	13.23	176.7	64.09	90.7	-0.08	178.5	61.82	91	0.14
S089	1		13.65	179	62.64	89.1	0.57				
S090	1	63	11.5	142.5	38.36	71	-2.67	142.7	44.82	72.2	-2.61
S091	1	63	12.15	157.5	35.55	82	-2.08	158.5	43	82	-1.81
S092	1	63	11.98	142.6	32	73.3	-2.82	143.7	33.09	71.3	-2.42
S093	1	63	11.87	154.6	51.27	79.3	-1.98	155.6	50.91	78.8	-1.77
S094	1	63	11.55	149.5	37.82	75.7	-2.45	150.5	37.55	76.2	-2.35
S095	1	63	11.49	143.4	39.36	74.3	-2.91	143.5	39.64	75	-2.91
S096	1	63	11.37	161	43.64	82.1	-1.94	163	45.55	83.9	-1.84
S097	1	63	11.85	152.6	57.27	74.9	-1.63	153.5	58.55	76.5	-1.63
S098	1	63	11.92	144.5	57.27	69.8	-1.88	145	58.64	70.5	-1.82
S099	0	71	13.82	155.1	44.27	76.3	1	154.8	52	73.4	1.29
S100	0	71	13.48	157.8	50.73	76.4	1.13	159	49.18	78	1.19
S101	0	71	13.89	167.1	63.82	84.5	1.8	168.2	66.27	80.7	2.17
S102	0	71	12.89	156.5	49.64	76.8	0.69	155.5	51.73	76.8	0.72
S103	0	71	14.07	159.1	56.18	75.2	1.65	159.8	56.27	76.4	1.72
S104	0	71	14.13	162.4	52.18	81.9	1.57	163.2	52.64	80.5	1.78
S105	0		13.54	161.9	52.18	82.5	1.19				

Table 1: Continued

S106	0	71	13.95	164.8	54.91	83	1.64	166.9	56.36	83.9	1.85
S107	0	71	13.59	162.1	54.45	79.8	1.4	164.5	54.64	79.4	1.68
S108	0	71	13.58	170.8	62.09	85	1.9	171.2	62.36	83.7	2.06
S109	0	71	14.11	163.3	59	79.9	1.8	164.2	52.18	80.2	1.86
S110	0	71	14.01	151.7	40.55	72.8	0.95	154	41	73.7	1.53
S111	0	71	12.92	161	45.91	81.2	0.79	162.5	47.64	82.5	0.94
S112	0	71	12.59	151	42.27	75.3	0.09	158.7	43.64	75.5	0.74
S113	0	71	12.96	155	48.18	77.5	0.56	157.4	50.73	77.9	0.83
S114	0	71	12.79	162.8	56	80.3	1.04	164	58	81.3	1.17
S115	0	71	12.34	152.6	39.91	80.1	-0.18	159	39.36	74.5	0.61
S116	0		12.87	172	73.36	84.8	1.74				
S117	0	71	12.68	154.5	49.18	80.3	0.27	155.7	51	78.2	0.55
S118	0	71	13.06	144.2	33.18	73.2	-0.26	145	34	73.8	-0.14
S119	0		12.85	160.6	52.09	77.6	0.98				
S120	1		12.64	148.7	37.27	74.7	-1.98				
S121	1	63	13.05	162	51.09	78.7	-0.6	163.2	52.18	77.4	-0.24
S122	1	63	12.27	151	37.18	75.5	-1.98	151.4	37.18	74.6	-1.79
S123	1	63	12.89	150.3	41.82	76.8	-1.88	152.5	42.36	73.8	-1.23
S124	1	63	12.87	154.8	39.82	78.7	-1.64	146.4	34.55	70	-1.59
S125	1	63	11.68	148.5	38.09	73.5	-2.26	149.5	38.27	76	-2.37
S126	1	63	12.77	159.5	38.09	82.5	-1.63	161.9	39	81.4	-1.16
S127	1	63	13.17	167	62.82	84.6	-0.51	169.1	64.82	86.1	-0.36
S128	1	63	12.81	162.4	53	84.2	-1.27	157.5	55.55	77	-0.89
S129	1	63	13.02	162.7	51.18	81.8	-0.89	164.6	52.27	79.6	-0.35
S130	1	63	12.58	151.5	49.45	75.7	-1.64	152.5	50.82	75.8	-1.47

Sex = 0/Female, 1/Male; Δ days = days between testing sessions; Age in years; Ht = standing height; Leg = leg length; PHV = offset from PHV (years)

Appendix O. Individual Performance Data

Table 2: Individual Performance Data

		Pre-season					Post-season				
Subject	**Sex**	**40yd**	**5-10-5**	**Broad**	**M-L**	**M-R**	**40yd**	**5-10-5**	**Broad**	**M-L**	**M-R**
S001	1	6.5	7.35	175	6.42	6.09	7.24	7.16	156	6.64	6.7
S002	1	6.95	7.34	165	6.66	7.7	7.34	7.56	164	6.53	6.65
S003	1	6.75	8.28	180	6.54	6.16	6.34	7.45	180	5.98	6.19
S004	1	8.06	10.19	135	7.64	8.09					
S005	1	6.78	8.9	116	6.65	7.23	6.75	6.87	140	6.05	6.5
S006	1	6.88	7.83	175	6.37	6.38	6.34	7.92	156	6.38	6.64
S007	1	6.81	8.9	127	7.09	6.55	7.91	6.98	137	6.58	6.45
S008	1	6.24	7.05	170	6.4	6.81	6.43	6.87	210	5.9	6.19
S009	1	6.3	6.85	162	6.29	6.42	6.71	6.75	172	5.94	6.24
S010	1	6.19	6.72	162	5.93	6.01	6.54	6.99	195	5.99	5.84
S011	1	6.2	7.01	162	6.65	6.1	6.54	6.83	168	5.89	6.77
S012	1	6.87	8.72	173	6.26	6.42	6.73	7.14	180	5.69	5.79
S013	1	7.45	8.69	132	6.7	6.54	7.6	7.96	175	6.54	6.37
S014	1	7.02	8.21	155	6.47	6.36	6.95	8.61	175	6.4	6.36
S015	1	7.28	7.04	140	5.96	6.05	6.77	6.55	135	5.92	5.84
S016	1	6.81	7.7	140	6.48	6.07	6.9	6.57	187	5.9	5.93
S017	1	7.14	6.97	186	6.39	6.28	7.26	7.17	187	6.85	6.35
S018	1	5.96	6.56	227	6.08	6.2					
S019	1	6.79	6.01	186	5.72	5.99					
S020	1	6.95	6.57	170	5.94	6.31	7.19	7.29	190	6.23	6.56
S021	1	7.02	6.52	200	6.24	6.01	7.5	7.42	187	6.68	6.7
S022	1	6.37	7.33	185	5.63	5.38	6.67	6.7	198	5.93	5.92

Table 2: Continued

S023	1	6.18	6.06	185	6.01	6.03	6.15	6.35	210	5.74	5.82
S024	1	6.14	6.05	185	6.17	6.17					
S025	1	6.39	5.82	226	5.77	5.66					
S026	1	7.04	6.47	170	6.27	6.51	7.08	7.16	192	6.41	7.25
S027	1	5.77	5.87	245	6.06	6.06	5.86	6.01	240	5.84	5.94
S028	1	6.84	6.04	215	5.72	5.61	6.42	6.44	230	5.86	5.74
S029	1	6.17	5.93	226	5.62	5.8	6.47	6.4	215	5.7	5.71
S030	0	6.61	6.27	205	6.26	5.91	6.6	6.22	185	5.95	5.85
S031	0	5.92	5.95	205	5.75	5.67	5.87	5.94	210	5.48	5.51
S032	0	5.71	5.89	223	5.82	5.77	5.68	6.24	210	5.76	5.6
S033	0	6	6.26	223	5.95	5.86	5.79	6.05	202	6.07	5.97
S034	0	5.88	6.14	223	6.23	6.32	6.41	6.9	220	6.19	6.01
S035	0	6.91	7.26	210	6.51	5.83	6.87	7.98	192	5.96	6.03
S036	0	6.76	6.52	210	6.24	6.55					
S037	0	6.26	6.18	193	5.92	5.82	6.26	6.71	190	5.73	5.78
S038	0	7.23	6.46	193	6.66	6.76					
S039	0	5.93	6.57	190	5.68	5.71	6.09	6.61	193	5.43	5.43
S040	0	6.46	6.29	180	6	6.09	6.49	7.14	200	6.46	6.01
S041	0	6.71	7.17	198	6.18	6.51					
S042	0	6.62	6.17	188	6.28	6.67	6.8	6.59	190	6.19	6.48
S043	0	6.06	6.2	220	5.81	5.78	6.11	6.75	225	5.5	5.19
S044	0	5.94	5.99	190	5.84	5.95	6.01	6.23	205	5.65	5.91
S045	0	6.16	6.45	206	5.87	6	6.32	6.78	230	5.88	5.99
S046	0	6.19	6.36	196	5.57	5.89	6.3	6.76	208	5.44	5.32
S047	0	6.25	6.28	175	6.52	6.25					

Table 2: Continued

S048	0	5.7	6.41	191	6.28	6.23	5.73	6.24	190	5.74	5.62
S049	0	6.52	6.04	197	5.97	6.01	6.32	7.22	208	5.92	5.74
S050	0	5.91	6.05	210	6.07	6.11	6.03	6.45	208	5.49	5.54
S051	0	6.49	7.19	229	6.02	6.21	6.64	6.97	251	5.99	5.89
S052	0	6.36	6.46	216	6.23	5.93	6.58	7.47	190	5.98	5.86
S053	0	6.25	6.6	160	5.91	5.62	6.17	6.7	190	5.49	5.23
S054	0	5.91	6.13	206	5.9	5.94	6.25	6.77	208	5.68	5.55
S055	0	6.29	6.17	200	6.04	5.81	6.25	6.23	230	5.89	5.91
S056	0	6.65	7.81	172	6.05	6.2	6.87	6.65	208	5.83	5.85
S057	0	7.06	7.76	157	6.04	6.26					
S058	0	6.28	7.01	165	6.29	5.6					
S059	0	6.21	6.88	176	5.75	5.86	6.4	6.79	210	5.87	5.94
S060	0	6.67	7.11	166	6.11	6.28					
S061	0	7.38	7.56	165	6.46	6.54					
S062	0	6.23	7.3	185	5.89	6.13	6.5	6.7	225	6.17	5.81
S063	0	7.06	7.04	175	6.35	6.42	6.78	6.83	219	5.36	5.37
S064	0	7.65	8.38	148	6.74	6.86	8.14	7.82	170	6.28	6.54
S065	0	6.83	8.01	192	6.07	6.08	7.22	6.14	214	6	5.85
S066	0	6.87	7.8	183	6.17	5.89	6.94	7.27	170	5.78	5.92
S067	0	7	7.4	183	6.41	6.61	7.05	6.85	174	6.31	6.18
S068	0	6.32	6.98	160	5.49	5.56	6.51	6.3	190	5.72	5.34
S069	0	6.52	6.2	198	5.32	5.44	6.7	5.61	206	5.46	5.62
S070	0	7.71	7.6	177	6.52	6.3	7.94	6.8	165	6.24	6.9
S071	0	6.73	6.79	198	6.23	6.09	6.52	6.32	215	5.96	6.04
S072	0	7.47	7.23	150	6.29	5.6					

Table 2: Continued

S073	0	6.84	7.07	200	6.2	5.8	6.71	6.85	200	6.13	6.16
S074	1	5.69	6.56	233	5.79	5.67					
S075	1	5.92	6.99	184	5.64	5.41	6.57	5.75	230	5.45	5.56
S076	1	5.28	6.07	243	5.22	5.49	5.74	5.39	245	5.05	5.09
S077	1	6.12	6.62	190	5.86	5.96	6.43	6.03	180	5.72	6.19
S078	1	6.08	6.49	213	6.19	6.15	6.19	6.32	205	5.73	5.86
S079	1	5.4	6.61	240	5.2	5.47	5.49	5.34	244	5.15	5.17
S080	1	5.48	6.26	240	5.44	5.38					
S081	1	5.56	7	244	5.44	5.56	5.71	5.52	230	5.11	5.09
S082	1	5.63	6.42	225	5.52	5.32	5.76	5.52	240	5.34	5.44
S083	1	5.34	6.27	250	5.48	5.26	5.68	5.69	227	4.82	4.97
S084	1	6.24	7.12	212	5.45	6	6.46	5.9	220	5.76	5.75
S085	1	6.04	6.26	230	5.53	5.54	6.53	6.07	204	5.65	5.8
S086	1	6.07	6.66	220	5.95	5.49	6.2	5.87	235	5.54	5.47
S087	1	5.89	6.53	225	5.51	5.37	5.91	6.06	240	5.25	5.58
S088	1	5.63	6.64	236	5.92	5.43	5.61	5.81	243	5.1	4.99
S089	1	5.14	6.3	223	5.46	5.58					
S090	1	6.58	6.55	170	5.88	5.86	6.91	6.49	185	6.02	5.99
S091	1	6.17	6.43	205	5.59	5.67	6.07	6.76	220	5.93	5.74
S092	1	6.29	6.8	220	5.86	5.88	6.46	6.92	215	5.99	5.95
S093	1	6.13	6.43	205	5.87	5.93	6.4	6	220	5.94	5.99
S094	1	5.93	6.52	205	5.85	5.82	6.3	6.42	208	5.77	5.63
S095	1	6.66	6.64	190	5.3	6.02	6.58	6.6	185	5.83	5.87
S096	1	6.31	6.2	223	4.98	6.16	6.33	5.91	210	5.5	5.79

Table 2: Continued

S097	1	6.62	6.87	230	5.88	5.99	6.77	7.33	218	5.94	5.81
S098	1	7.26	7.27	182	6.34	6.68	7.52	7.36	155	6.68	6.55
S099	0	6.29	6.33	205	5.08	5.19	6.15	6.46	221	5.16	5.26
S100	0	6.05	6.68	185	5.26	5.39	6.16	6.8	246	5.67	5.34
S101	0	6.38	7.44	210	5.32	5.56	6.56	7.37	228	5.57	5.97
S102	0	6	5.93	205	5.2	5.39	5.92	6.09	220	5.54	5.51
S103	0	6.06	6.8	187	5.26	5.27	6.21	6.21	229	5.25	5.33
S104	0	6.03	6.37	210	4.99	5.69	6.19	6.37	208	5.26	5.34
S105	0	6	6.56	230	5	5.43					
S106	0	5.99	6.55	229	4.88	5.31	6.3	6.38	230	5.14	5.21
S107	0	5.97	6.79	210	4.8	5.08	5.97	6.37	221	5.35	5.17
S108	0	6.08	6.53	237	5.35	5.34	5.85	6.07	193	5.19	5.4
S109	0	5.79	6.33	215	5.22	4.89	5.91	6.33	230	5.23	5.64
S110	0	6.34	6.75	170	5.73	5.77	6.33	7.08	183	5.91	5.7
S111	0	6.19	7	193	5.93	6	6.35	6.96	220	5.58	6.05
S112	0	6.33	6.83	234	5.65	5.3	6.25	6.92	230	5.63	5.57
S113	0	6.58	6.62	234	5.4	5.61	6.71	6.21	253	5.2	5.06
S114	0	5.95	6.45	233	5.22	5.27	6.12	6.42	221	5.58	5.34
S115	0	6.76	6.98	194	5.45	5.59	6.61	6.49	220	5.3	5.6
S116	0	6.32	6.91	172	5.76	5.7					
S117	0	6.3	6.56	175	5.58	5.65	6.3	6.43	226	4.87	5.14
S118	0	6.78	7.78	156	5.87	5.79	6.86	7.44	193	5.96	5.68
S119	0	6.26	7.28	198	5.37	5.62					
S120	1	6.21	6.2	210	5.89	5.69					

Table 2: Continued

S121	1	5.81	6.01	247	5.55	5.54	6.04	5.97	250	5.43	5.58
S122	1	5.68	5.89	204	5.34	5.55	6.06	5.87	218	5.46	5.29
S123	1	6.65	7.21	164	6	6.15	6.8	7.29	180	5.97	5.97
S124	1	6.27	6.79	215	5.68	5.82	6.37	6.92	200	5.67	5.61
S125	1	6.43	6.11	204	5.84	5.74	6.37	6.59	188	5.68	5.55
S126	1	6.46	6.59	206	5.64	5.74	6.6	6.89	185	5.85	5.62
S127	1	6.03	6.55	211	6.1	6.02	6.13	6.47	200	5.81	6.01
S128	1	7.26	7.64	178	6.39	6.43	7.41	7.35	185	6.31	6.4
S129	1	5.82	6.32	231	6.18	5.92	6.1	6.05	243	4.99	5.23
S130	1	6.72	7.2	185	6.26	6.05	6.88	7.33	188	6.19	6.25

Sex = 0/Female, 1/Male; 40yd = 40 yard dash (sec); 5-10-5 = 5-10-5 shuffle drill (sec); Broad = broad jump (cm); M-L, M-R = M-drill to left and right, respectively (sec)

Appendix P. Participant PHV Breakdown

Table 3: Participant PHV breakdown by sex.

	Female (n=52)	**Male (n=55)**
Pre-puberty (<-1.5 years PHV)	n = 2 (2%)	n = 31 (29%)
Pre-PHV (-1.5 to -0.5 years PHV)	n = 8 (7%)	n = 19 (18%)
Circa-PHV (-0.5 to 0.5 years PHV)	n = 10 (9%)	n = 4 (4%)
Post-PHV (0.5 to 1.5 years PHV)	n = 21 (20%)	n = 1 (1%)
Post-pubertal (>1.5 years PHV)	n = 11 (10%)	n = 0 (0%)

n = number of participants in PHV category; % = percentage of participants relative to total study sample size rounded to nearest integer. Cutoffs previously used by Van der Sluis et al. (2013; 2015)

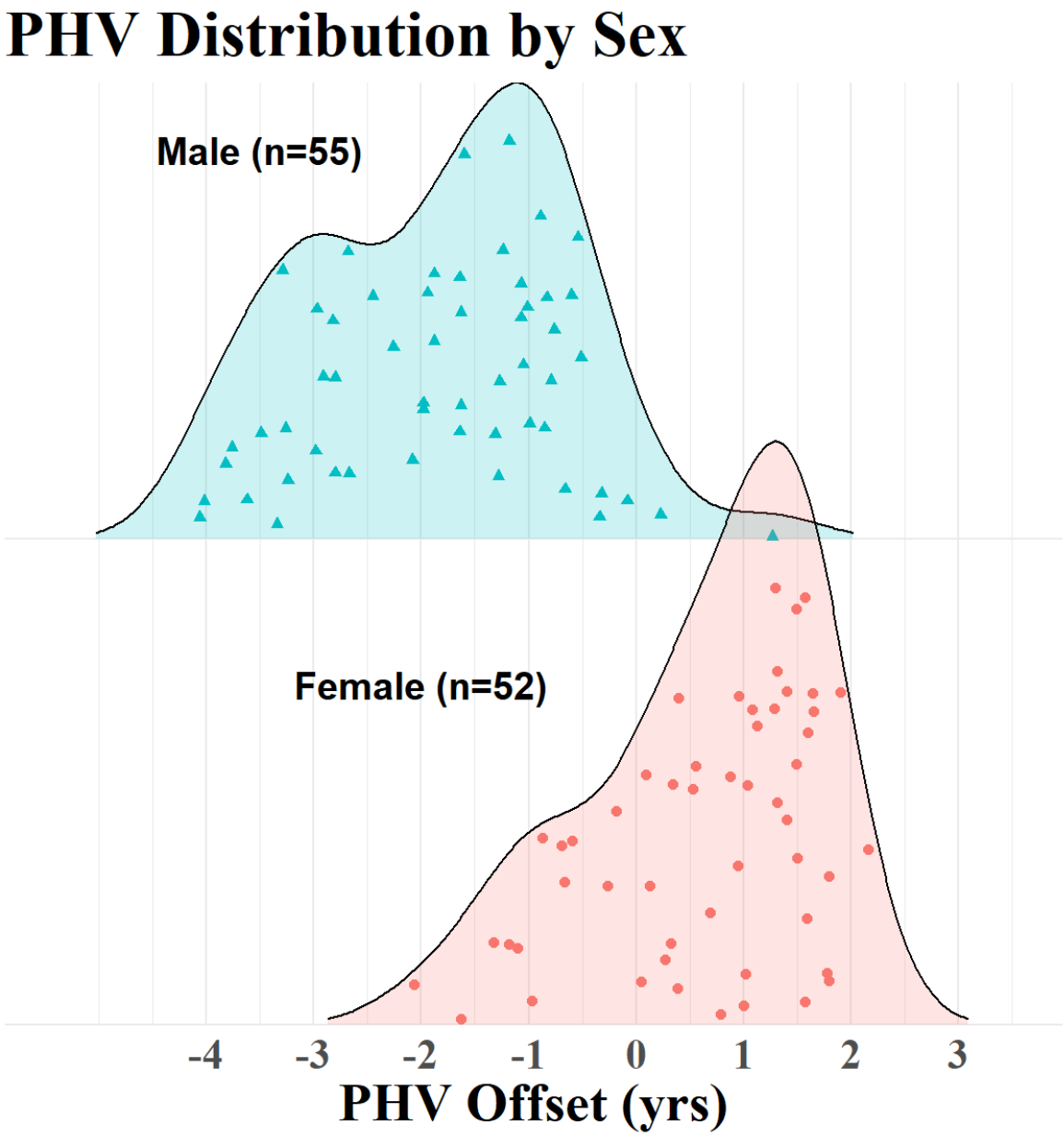

Figure 8: PHV distribution for male (blue) and female (pink) participants.

Appendix Q. Entropy Parameterization and Comparisons

Introduction

While the blueprint outlining the cause for many overuse sports injuries has not yet been elucidated, many researchers have sought to characterize the different parameters that precede them so that future injuries can be forecast and potentially circumvented. Modelling the complex systems and elements producing these injuries is a difficult task. More sensitive and specific injury forecast models requiring the identification of "… factors that would prevent the state of the system from desired to undesired state shifts as a result of perturbations" (Tu et al. 2021, p.1). Many non-linear systems analyses aiming to prevent injury operate via holistic interpretation of the system's resilience and behavior both in the long-term and within attractor states.

The resilience of a complex system is operationally defined as its ability to maintain its operational status in the presence of perturbations, whereby the duration of the system response to the perturbation is inversely proportional to the resiliency of the system (Arnoldi et al. 2016; May 2019). Attractor states are defined as a system's convergence towards or divergence from a set of states, and in this biomechanical context an example could be the coordination patterns between joints used to navigate the demands imposed by the system (Hill et al. 2018). Injuries are the undesirable attractor to which the system is moved towards by specific biomechanical perturbations (excessive tissue loading during dynamic movements, initial joint contact angles, lack of tissue recovery, joint coordination, etc.). Previous biomechanics investigations have quantified complexity differences within human movement and trends delineating variation between groups (e.g., pathological and non-pathological) in measured biological signals via entropy analyses (Costa et al. 2002; Costa et al. 2003; Bisi and Stagni 2016).

The overall system complexity cannot be fully described from entropy analysis of a signal on a single time scale of an individual subsystem's behavior. The inexorable link between elements of the subsystems create an "infinite entanglement" between their interactions and subsequent states (Delignières and Marmelat 2012). However, Yentes (2018) has stated that information about the underlying complex system can still be gleaned from entropy analyses of the temporal structure of the variability within a signal representative of a subsystem. It is critical, though, that certain assumptions are met and parameters appropriately-tuned prior to the deployment of any entropy analysis (Yentes and Raffalt 2021). Therefore, the primary purpose of this investigation is to compare different combinations of entropy analyses and their parameters on lower-leg acceleration time-series collected during various dynamic movements.

Methods

Participants

Participants were recruited via word of mouth, fliers, social media, and emails. 10 healthy, recreationally active young adults participated in this pilot study. Inclusion criteria includes the following: no history of lower extremity surgical repair, no lower extremity injuries within the past six months, and no lower extremity pain on the day of testing.

Experimental Procedures

All experimental testing (Figure 9) took place on an outdoor, synthetic turf field following a brief dynamic warm-up. Participants were fitted with two small inertial measurement units (IMUs) on their distal-medial tibias just superior to the medial malleolus and data collections began with an "easy pace" jog lengthwise down the field and back. Then, participants completed an M-drill once in both directions in which they changed directions rapidly while sprinting around a series of cones. Next, participants completed a 5-10-5 shuffle drill where they

began by straddling a central cone and then laterally shuffling between cones placed 5 meters from the middle cone. Finally, participants performed a triple hop for distance on the right and then left leg, signifying the completion of their testing session.

Instrumentation

IMUs containing a high-g accelerometer (1600 Hz; Vicon Blue Trident, Vicon Motion Systems Ltd, Oxford, UK) were used to measure 3D linear accelerations at the distal tibia during testing. These data were imported into Python v3.10.4 (Python Software Foundation, Beaverton, OR, USA) for processing and analysis and R 4.2.1 (R Foundation for Statistical Computing, Vienna, AUST) for visualization.

Data Reduction & Analysis

Raw tri-axial accelerometry data was imported from the IMU sensors to calculate the resultant linear accelerations for input to subsequent entropy analyses. The EntropyHub open-source toolkit (Flood and Grimm 2021) has functions native to Python that were used to analyze the acceleration time series for each experimental task (jog, M-cone drill, 5-10-5 shuffle drill, and triple hop for distance). For each time series, we calculated the: a) Approximate, b) Sample, and c) Multiscale entropy of the signal while varying the parameters associated with each analysis. These values are unitless and used to convey the "complexity" of the signal in terms of regularity and predictability (McGregor et al. 2009; Parshad et al. 2012).

Approximate entropy (ApEn) (Pincus SM 1991) was created to quantify the rate of regularity in a time data series:

$$\text{ApEn}\ (m, r, N) = \lim_{N \to \infty} [\phi^m(r) - \phi^{m+1}(r)]$$

whereby *m* is the embedding template dimension, *r* is the resolution threshold, and *N* is the length of your time-series vector. The ApEn algorithm divides the series into vector

templates of length *m* for comparison. Blocks are considered possible matches if the difference between all the corresponding block elements is ≤ *r*. Once that condition is met, if the subsequent point difference is also ≤ *r* then the blocks are a match and conditional probabilities calculated (template matches divided by possible matches).

Sample entropy (SampEn) (Richman and Moorman 2000) was developed to address the regularity bias present from self-counting template matches in ApEn and sensitivity to smaller time series:

$$\text{SampEn}\ (m, r, N) = -ln\left(\frac{A}{B}\right)$$

whereby *B* and *A* are defined as the total number of template matches of length *m* and total number of forward matches of length *m+1*, respectively:

$$A = \left\{\frac{[(N-m-1)(N-m)]}{2}\right\} A^m(r),\ \ B = \left\{\frac{[(N-m-1)(N-m)]}{2}\right\} B^m(r)$$

Multiscale entropy (MSE) (Costa et al. 2002) was introduced to address the inconsistencies that the traditional ApEn and SampEn algorithms exhibited between random noise and physiologically complex signals. Some pathologies (i.e., cardiac arrythmias) have statistical properties associated with uncorrelated noise because of the erratic fluctuations in the original signal (Zeng and Glass 1996; Hayano et al. 1997; Di Rienzo 1998). MSE accounts for these complex temporal fluctuations by working across temporal scales via coarse-graining the original time series:

$$y_j^{(\tau)} = \frac{1}{\tau} \sum_{i=(j-1)\tau+1}^{j\tau} x_i, \qquad 1 \leqslant j \leqslant N/\tau$$

before employing another entropy algorithm (typically SampEn) on the coarse-grained time series.

A grid search was used to compare different ApEn and SampEn combinations of m = [0, 1, …, 4] and r = [0.01, 0.05, 0.1, 0.015, 0.2, 0.25] times the standard deviation of the time series. These ranges were chosen based on previous entropy analyses of biological signals (Pincus SM and Huang 1992; Pincus SM and Goldberger 1994; Yentes et al. 2013). MSE employs a 3rd parameter, τ, which signifies the number of time scales computed during the coarse-graining procedure prior to the execution of whichever base entropy analysis the user prefers, ApEn or the more common SampEn. The area under the curve of the ApEn or SampEn values plotted across time scales, known as the complexity index (C_I), is defined as:

$$\mathrm{C}_I = \sum_{i=1}^{\tau} \mathrm{SampEn}(i)$$

whereby we need only sum the entropy values (in this case, SampEn values) across the time scales of interest.

Chon et al. (2009) developed equations to estimate maximum values for r by fitting multiple nonlinear least squares to Monte-Carlo simulations and normalizing r to the short-term (sd_1) and long-term (sd_2) variability of the signal based on the embedding dimension m:

$$m = 2: \hat{r}_{max} = \left(-0.036 + 0.26\sqrt{\mathrm{sd}_1/\mathrm{sd}_2}\right)/\sqrt[4]{N/1{,}000}$$
$$m = 3: \hat{r}_{max} = \left(-0.08 + 0.46\sqrt{\mathrm{sd}_1/\mathrm{sd}_2}\right)/\sqrt[4]{N/1{,}000}$$
$$m = 4: \hat{r}_{max} = \left(-0.12 + 0.62\sqrt{\mathrm{sd}_1/\mathrm{sd}_2}\right)/\sqrt[4]{N/1{,}000}$$
$$m = 5: \hat{r}_{max} = \left(-0.16 + 0.78\sqrt{\mathrm{sd}_1/\mathrm{sd}_2}\right)/\sqrt[4]{N/1{,}000}$$
$$\mathrm{m} = 6: \hat{r}_{max} = \left(-0.19 + 0.91\sqrt{\mathrm{sd}_1/\mathrm{sd}_2}\right)/\sqrt[4]{N/1{,}000}$$
$$m = 7: \hat{r}_{max} = \left(-0.2 + 1.0\sqrt{\mathrm{sd}_1/\mathrm{sd}_2}\right)/\sqrt[4]{N/1{,}000}$$

Where for a sequence $x(n) = \{x(1), x(2), \ldots, x(N)\}$:

$$sd_1 = \{x(2) - x(1), x(3) - x(4), \ldots, x(N) - x(N-1)\}$$

and sd_2 is simply the standard deviation of $x(n)$. We calculated this maximum threshold value, henceforth referred to as r_{Chon}, across drills and subjects to determine its variability between trials.

Results

ApEn and SampEn results (Figure 10) were stable and comparable across combinations of embedding dimensions m and threshold tolerances r for all dynamic drills. Entropy values following a MSE using SampEn ($m, r, \tau=20$) and a coarse-graining procedure were also similar across conditions (Figure 11). Non-parametric Kruskal-Wallis tests run individually for each drill indicated that mean rank order C_I was statistically different across time scales τ = [1, 4, 8, 12, 16, 20], $H(5)$ = [57.9 – 63.04], $p < 0.001$ (Table 4; Figure 12). C_I pairwise comparisons were computed via Bonferroni-corrected Dunn's tests (Table 4; Figure 13). Finally, the r_{Chon} values calculated for each MSE analysis ranged from ~ 0.025 – 0.09 * SD (Table 4).

Discussion

Approximate vs Sample Entropy

The purpose of this investigation was to compare ApEn and SampEn results using accelerometer signals collected during dynamic movements. Both showed stability and similar trends for all drill conditions across all combinations of m and r. SampEn, however, has some advantages over ApEn.

SampEn was developed by Richman and Moorman (2000) in response to the regularity bias present in the ApEn algorithm stemming from double-counting the template vector against itself to preserve finite logarithms. This bias can be as high as 20-30% if the number of template matches remains low and can be exacerbated by smaller dataset lengths N (Pincus SM and Huang 1992). Further, the ApEn bias towards regularity can actually 'flip-flop' as a function of

the signal-to-noise ratio present in the time series and the sensitivity of the algorithm to *m* and *r* parameter modifications (Pincus S 1995). Considering previous reports in the literature and the stability of both algorithms in Figure 10**,** we have decided that SampEn is the appropriate base entropy for our experimental data.

Parameters m *and* r

The *m* and *r* parameters should, above all, allow us to characterize true features of the signal by optimizing the accuracy of our base entropy (SampEn) at each time scale of a MSE analysis (Gow et al. 2015). By choosing smaller values for *m* and *r*, we can increase the number of matches *m* and *m*+1 and, consequently, our confidence in the entropy estimates. However, the SampEn conditional property ($\frac{A}{B}$) approaches 1 as *r* increases, reducing the discriminatory power of our analysis across different signals. This suggests that our *r* threshold should be large enough to be robust to signal noise yet small enough to produce *m* and *m*+1. Our calculated r_{Chon} = [0.02 – 0.05] * SD across drills were smaller than the standard *r* = 0.2 * SD, though Liu et al. *(2010)* has shown that the empirical results derived by Chon et al. (2009) may not always be a good approximation of the maximum *r* threshold for a given signal. Therefore, we piloted a combination of *r* = [0.01 – 0.25] * SD. Based on the stability of both the ApEn and SampEn measures across values of *m* (Figure 10), we believe that the smaller r_{Chon} values calculated for our accelerometer data would be unduly influenced by noise present in the signal. Further, template length *m* selection dictates where information content is assessed during the SampEn analysis. Autoregressive models (Lake et al. 2002), mutual information and false nearest neighbor methods (Chen X et al. 2006) have been employed to empirically determine optimal *m* selection. The coarse-graining process and multiple time scales used in MSE analysis predominantly negates the influence of *m* on entropy estimate stability, though. Choosing *m* then

becomes a product of the data being analyzed as we are limited by signal length, *N*. The accelerometer signals vary from N ≈ 3,000 – 12,000, which recommendations set forth by Pincus (1991; 1992; 1994; 1995) states an *m* of 2-3 would be appropriate. Considering that a smaller *m* will increase our confidence in the entropy estimates and *r* should be large enough to withstand the influence of signal noise, we have decided that $m = 2$ and $r = [0.1 – 0.2]*SD$ would be appropriate for our SampEn base entropy analysis.

Multiscale Entropy and parameter τ

The creation of MSE by Costa et al. (2002) gave researchers the ability to estimate the order and randomness of biological signals across temporal scales and allows for the indexing of non-linear deterministic correlations that conventional power spectral density analyses cannot provide (Courtiol et al. 2016). The multifaceted network of bodily systems each exhibit non-linear behavior across time scales (Reed 1982), and, per Shannon (1949), the father of information theory, simply measuring the entropy at a single time scale cannot reflect the dynamics of the entire system. A cascading effect likely occurs from perturbations to the subsystems of an overall system and MSE allows for us to observe how the system integrates these interactions at higher temporal scales (Busa and van Emmerik 2016). Finally, previous studies have shown that calculating the C_I at each time scale gives researchers the ability to potentially discriminate between populations based on the evolution of their observed entropy values at different time scales performing certain tasks (Gruber et al. 2011; Chen C-H et al. 2015; Bisi and Stagni 2016; Busa et al. 2016). This suggests that MSE may be a potential screening tool for determining those at risk of injury. As seen in Table 4 & Figure 12, subject rank-order changes by complexity indices from lower to higher time scales. Considering the sample population of our pilot data, we would expect based on the literature that these

differences in rank order and C_I magnitude would be amplified between more 'heterogenous' or pathological groups.

Conclusions

When computing the entropy of accelerometer data collected during dynamic tasks for the purpose of discriminating between different populations, we recommend that researchers use MSE with a coarse-graining procedure followed by base SampEn algorithm analysis. Parameter values $m = 2$ and $r = 0.1\text{-}0.2 * SD$ should be used to reduce the influence of noise on entropy results while providing enough tolerance for matching vectors without biasing towards regularity. A grid search using combinations of these parameters should be used, though, to establish validity. C_I values should be reported so that entropy comparisons across time scales can be made which better reflect overall system differences.

Table 4: Kruskal-Wallis test, rChon values, and Dunn's test pairwise comparison results

Drill	***n***	***dof***	***H***	r_{Chon}
5-10-5	60	5	61.84	0.048 ± .01
DNB	60	5	92.31	0.032 ± .01
M-Drill	60	5	63.04	0.054 ± .02
THL	60	5	58.17	0.035 ± .03
THR	60	5	57.93	0.029 ± .03

Drill	τ = 1	τ = 4	τ = 8	τ = 12	τ = 16	τ = 20
5-10-5	0.07 ± .02 [a,b,c]	0.56 ± .13 [b,d]	1.72 ± .38 [c]	3.35 ± .71	5.33 ± 1.11	7.61 ± 1.56
DNB	0.06 ± .01 [a,b,c]	0.48 ± .09 [b,c]	1.52 ± .30 [c]	2.98 ± .56	4.79 ± .86	6.90 ± 1.19
M-Drill	0.06 ± .03 [a,b,c]	0.54 ± .10 [b,c]	1.78 ± .27 [c]	3.53 ± .49	5.63 ± .71	7.98 ± 0.96
THL	0.03 ± .01 [a,b,c]	0.28 ± .08 [a,b,c]	0.87 ± .29 [c]	1.68 ± .60	2.68 ± 1.00	3.82 ± 1.46
THR	0.03 ± .01 [a,b,c]	0.26 ± .11 [b,c]	0.80 ± .36 [c]	1.54 ± .69	2.41 ± 1.08	3.42 ± 1.55

The following symbols denote significant rank-order differences between C_l these time scales: a: τ=12, b: τ=16, c : τ=20

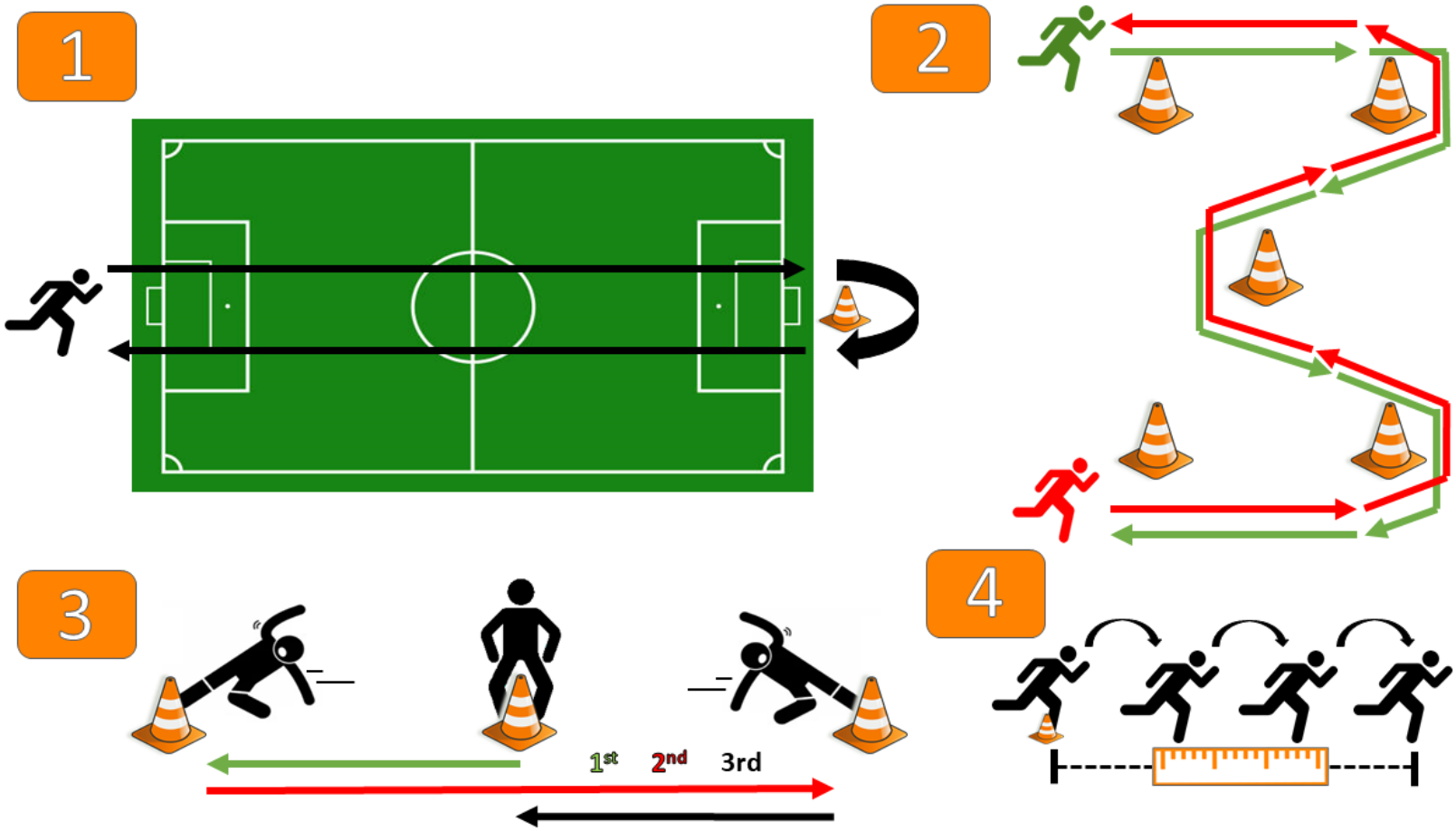

Figure 9: Pilot drill protocol for entropy parameterization. (1) down and back jog, (2) M-cone drill, (3) 5-10-5 drill, and (4) triple hop for distance.

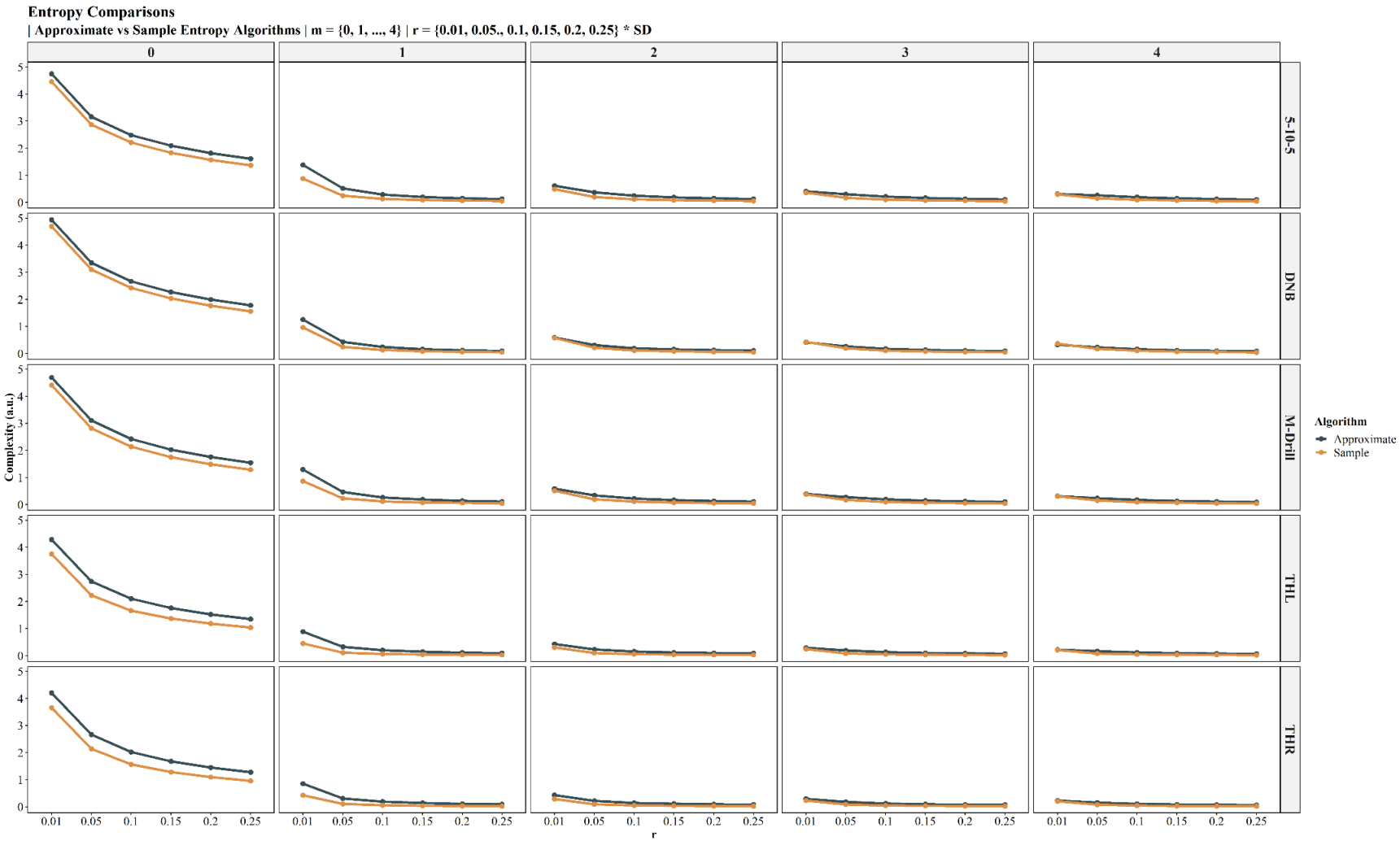

Figure 10: Approximate (blue) and sample (orange) entropy comparisons across embedding dimensions *m*, threshold tolerances *r**SD, and drills.

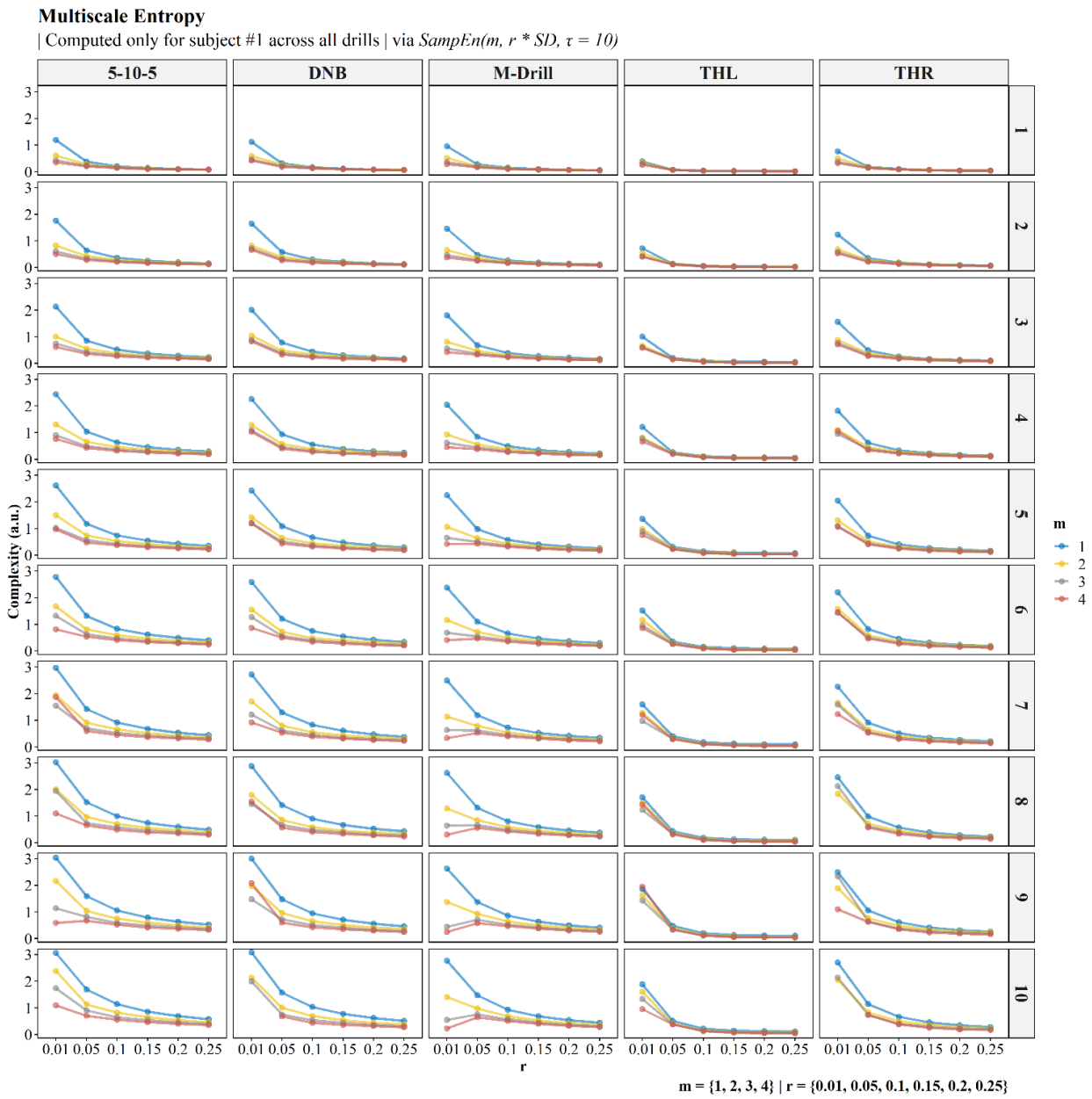

Figure 11: Multiscale Entropy comparisons using coarse-graining procedure and SampEn(m, r, τ=20) base entropy across time scales for each drill for Subject #1.

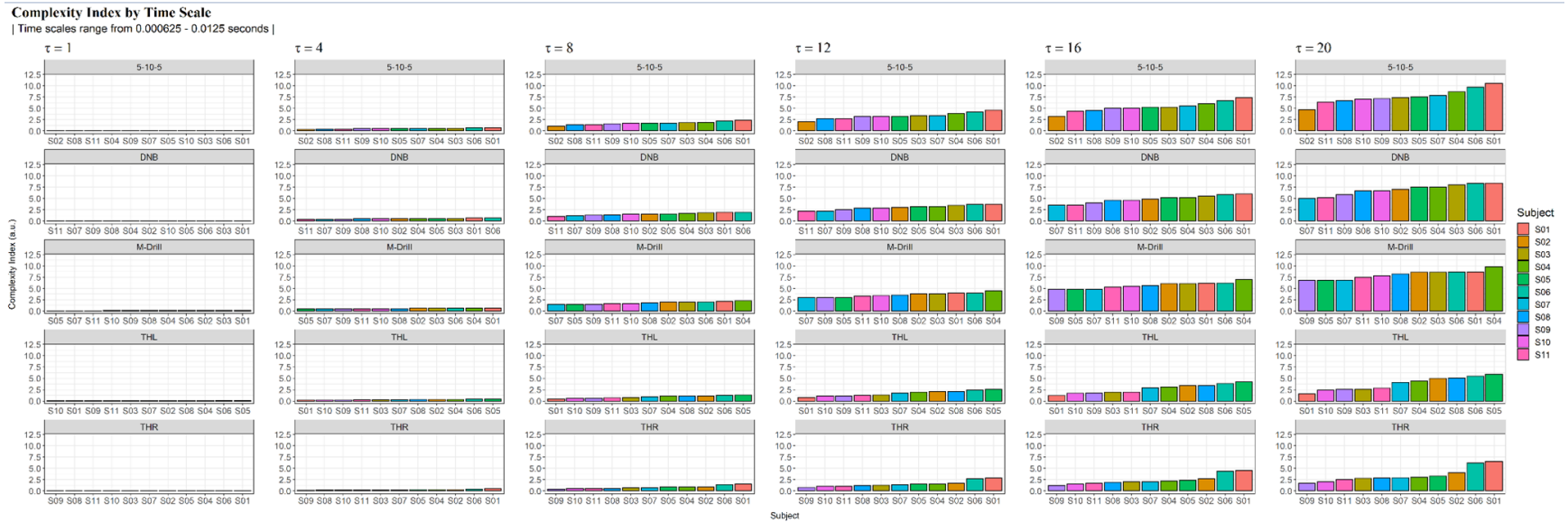

Figure 12: Complexity Index (CI) values across time scales and drills. CI bars are color-coded to subjects.

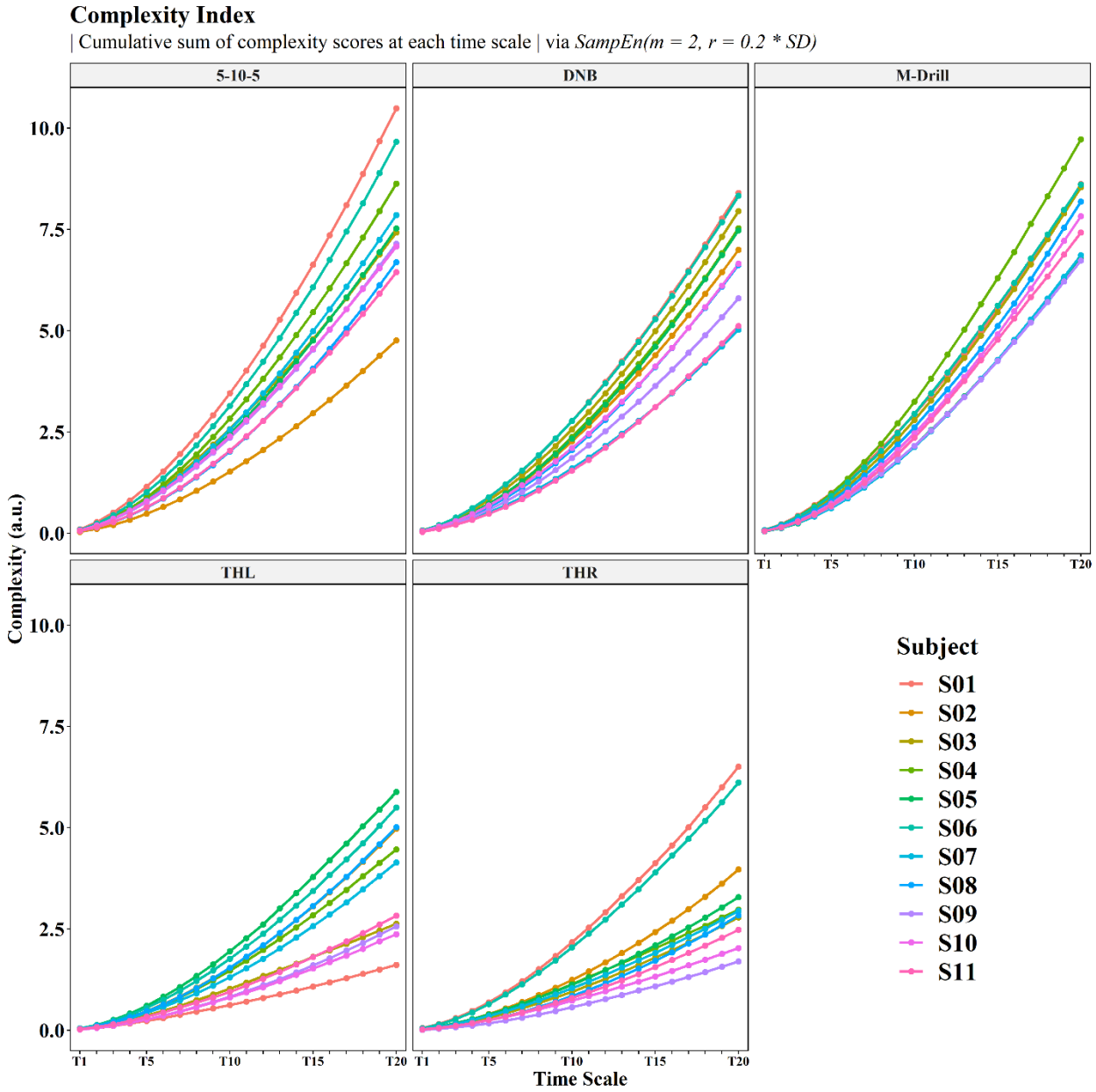

Figure 13: Complexity Index (CI) values across drills and time scales for all subjects where SampEn(m = 2, r = 0.2 * SD).

Appendix R. Surface Effects on Current Study Dependent Variables

Tables and Figures

Table 5: Complexity Index (CI) values by across surfaces and sex.

	Female		Male	
Drill	**Grass (n=13)**	**Turf (n=40)**	**Grass (n=25)**	**Turf (n=31)**
40yd	6.73 (0.74)	7.15 (1.02)	7.05 (0.86)	6.99 (1.09)
5-10-5	5.13 (0.94)	4.97 (0.88)	7.05 (0.86)	5.3 (0.86)
Broad	3.13 (1.32)	3.31 (1.27)	3.41 (1.31)	3.13 (1.28)
DNB	6.75 (1.34)	6.2 (1.34)	6.3 (1.21)	6.3 (1.54)
M-L	5.61 (0.83)	5.74 (0.98)	5.79 (0.94)	5.69 (0.93)
M-R	5.54 (0.81)	5.68 (0.98)	5.69 (0.87)	5.59 (0.96)

Means ± (Standard Deviations); CI reported in A.U.s

Table 6: Acceleration peaks across surfaces and sex.

	Female		Male	
Drill	**Grass (n=13)**	**Turf (n=40)**	**Grass (n=25)**	**Turf (n=31)**
40yd	35.5 (9.29)	42.47 (7.53)	41.64 (7.03)	42.23 (7.85)
5-10-5	22.87 (5.89)	25.43 (5.89)	23.41 (5.74)	25.06 (6.3)
Broad	45.18 (13.5)	46.59 (15.85)	49.62 (20.05)	44.45 (13.62)
DNB	19.03 (7.22)	17.49 (5.59)	19.59 (6.06)	13.54 (4.99)
M-L	24 (4.83)	26.7 (5.66)	28.86 (4.96)	29.64 (6.31)
M-R	24.47 (5.31)	27.32 (5.9)	28.89 (4.85)	29.89 (5.68)

Means ± (Standard Deviations); peaks reported in units of gravity

Table 7: Acceleration integrals across surfaces and sex.

	Female		Male	
Drill	**Grass (n=13)**	**Turf (n=40)**	**Grass (n=25)**	**Turf (n=31)**
40yd	54228.07 (5894.43)	62800.64 (8587.59)	64211.09 (7484.93)	58989.76 (7362.36)
5-10-5	39556.9 (6606.19)	38810 (5157.1)	42970 (6695.48)	39042.42 (6718.02)
Broad				
DNB	27651.81 (5861.5)	23812.71 (4138.82)	26330.57 (5643.56)	20045.83 (3672.21)
M-L	36774.53 (3691.59)	39035.84 (5776.88)	42883.77 (6012.09)	39537.73 (5469.28)
M-R	37581.72 (4224.32)	38258.75 (5110.47)	43067.69 (5035.41)	38784.17 (5220.22)

Means ± (Standard Deviations); integrals reported in A.U.s

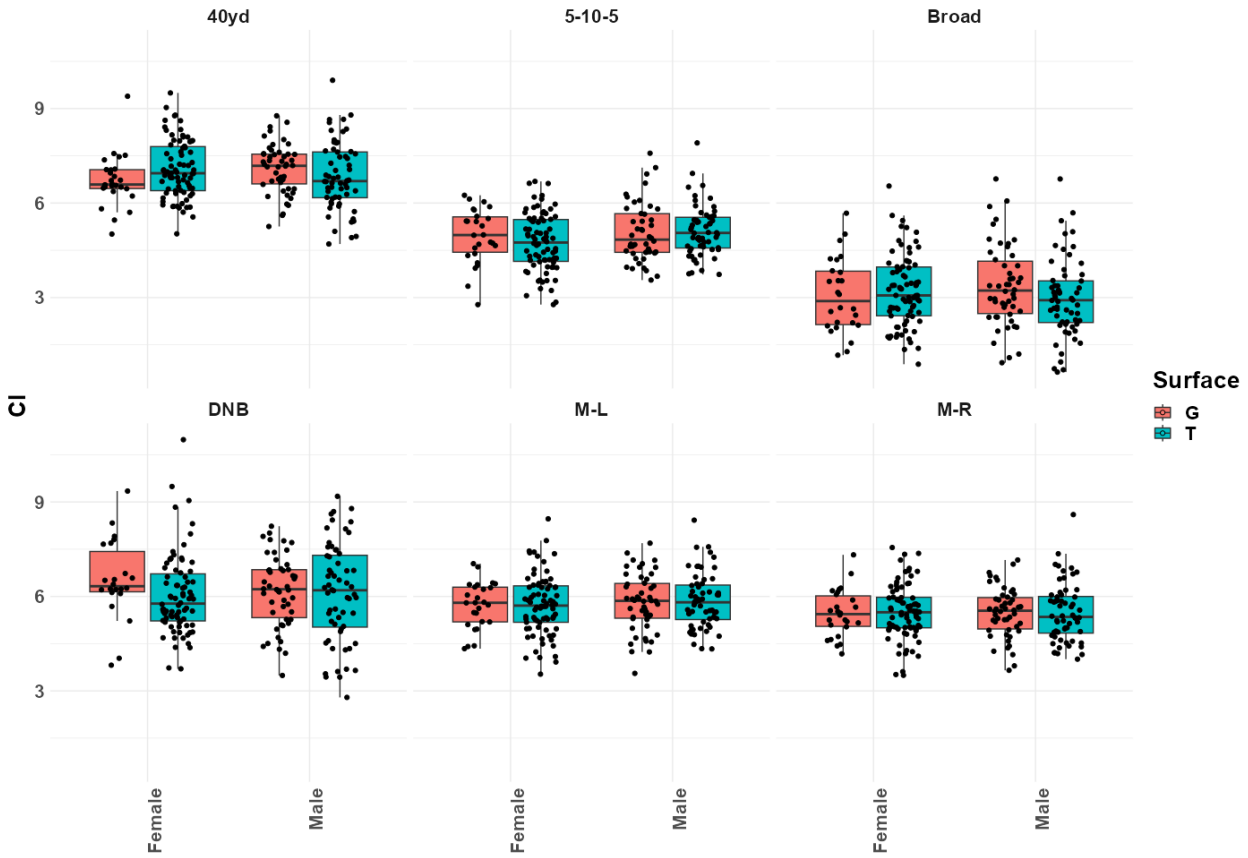

Figure 14: Complexity Index (CI) boxplots by drill and sex; CI units in A.U.s; G = Grass; T = Turf

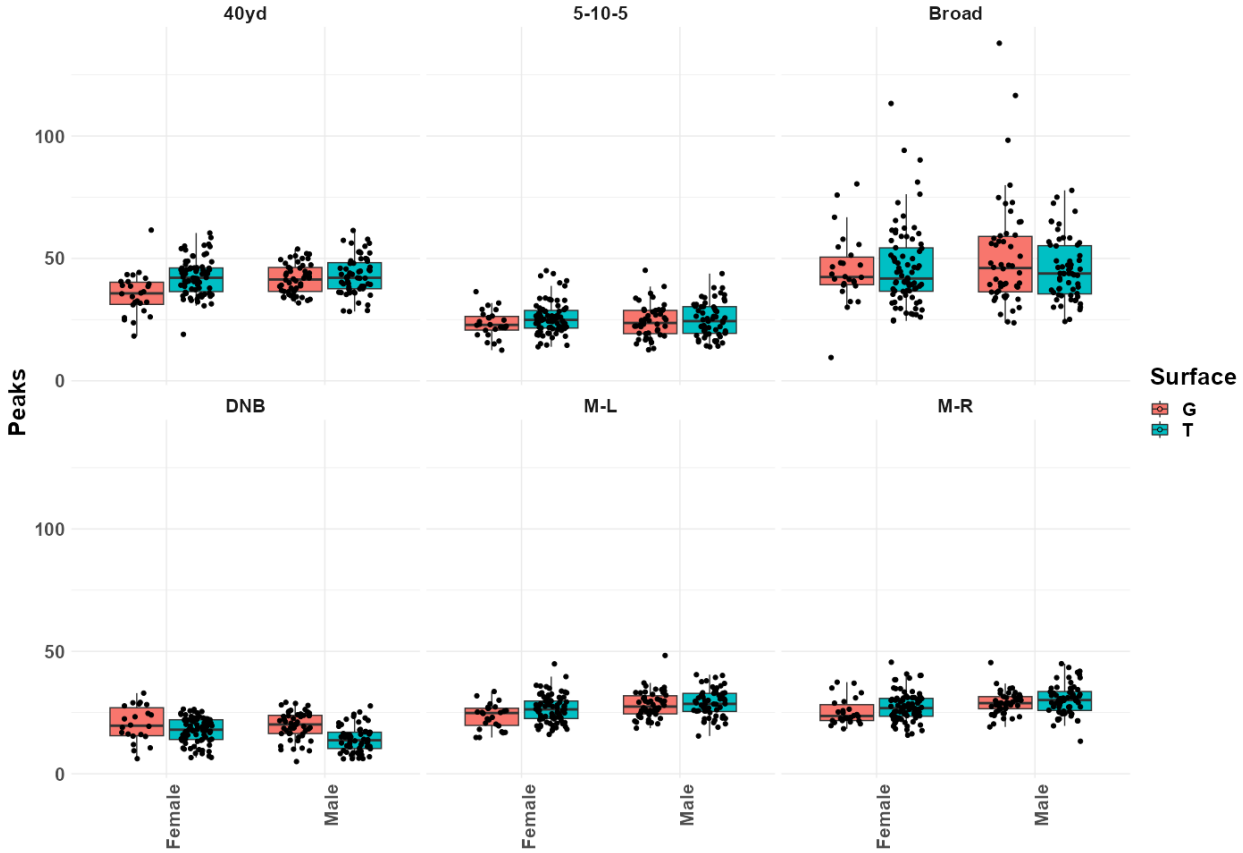

Figure 15: Acceleration peaks boxplots by drill and sex; G = Grass; T = Turf

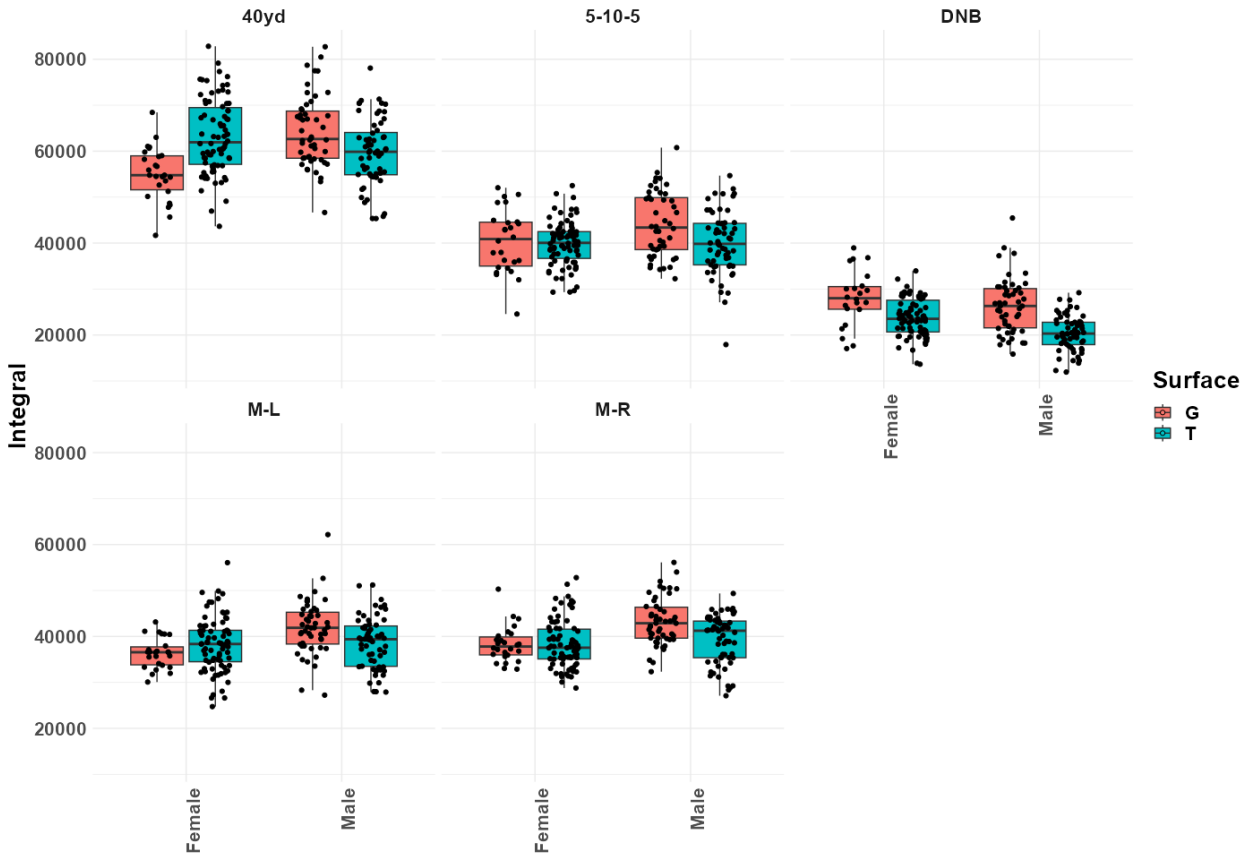

Figure 16: Acceleration integrals boxplots by drill and sex; integral units in A.U.s; G = Grass; T = Turf

Appendix S. Pilot Study Surface Effects on Acceleration Metrics

The purpose of this pilot study was to determine if acceleration impacts differed between turfgrass surfaces during a dynamic movement (right M-drill). Synthetic turfgrass is intended to mimic the properties of a natural surface. We hypothesize that there will be no significant difference between the synthetic surface and the natural surfaces.

Methods

23 young healthy adult participants (13 males; 1.73 ± 0.11 m; 70.2 ± 12.4 kg) performed an M-drill that simulates lower-extremity movements commonly executed in many training and competition settings. Each participant performed the M-drill so that the initial cut was performed off of the right foot. The task was performed on three different surfaces: a synthetic turf and two types of turfgrass (cold- and warm-season). The synthetic turf surface (SYN) was a third-generation synthetic turf with a crumb rubber infill and a foam-based shock pad underneath. The other two natural surfaces were cold- (Kentucky Bluegrass – KBG) and warm-season (Bermuda – BER) turfgrasses. A 3-axis linear inertial measurement unit (IMU) (1600 Hz; IMeasureU Blue Trident, Vicon Motion Systems Ltd., Oxford, UK) was fixed to the mediodistal tibia superior to the medial malleolus of the right ankle. All trials were performed once in athletic footwear without cleats provided by the subjects following brief instruction. The peak resultant tibial acceleration and the integral of the resultant acceleration over the duration of the drill were calculated. Separate one-way analysis of variances (ANOVAs) were conducted to compare the effect of SYN, KBG, and BER on peak tibial accelerations and tibial acceleration integrals ($\alpha = .05$).

Results and Discussion

No significant surface effect between the three turfgrasses for peak tibial accelerations [$F(2, 68) = 1.883$, $p = 0.160$] or tibial acceleration integrals [$F(2, 68) = 0.76$, $p = .472$] were found (Table

8; Figure 17). Our hypothesis of no significant difference on impact attenuation between the SYN, KBG, and BER was supported. The belief that impacts obtained via tibial-mounted accelerometer do not differ between synthetic turf and natural grass surfaces during a dynamic movement agrees with our findings.

Table 8: Acceleration peaks and integrals for M-drill on different turfgrasses.

	Synthetic Turf	**Kentucky Bluegrass**	**Bermuda Turfgrass**
Peak Acceleration	312.0±112.3	382.1±129.5	337.6±132.9
Acceleration Integral	257.0±38.6	272.7±49.2	267.4±45.2

Means ± (standard deviations); peak accelerations in m/s/s; acceleration integrals in arbitrary units (A.U.s)

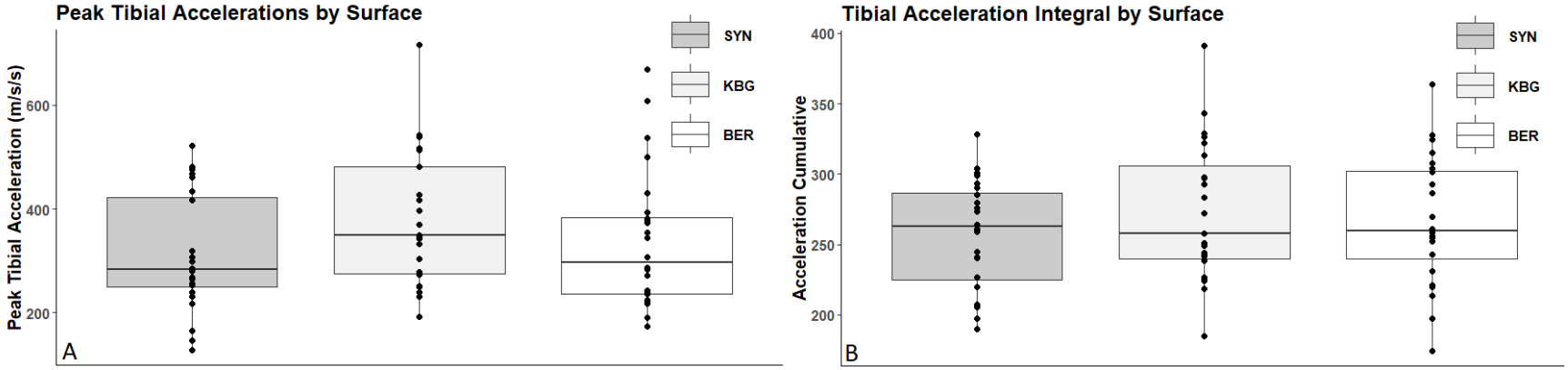

Figure 17: A) Peak resultant acceleration and B) acceleration integral by surface for synthetic (SYN), Kentucky bluegrass (KBG), and Bermuda turfgrass (BER)

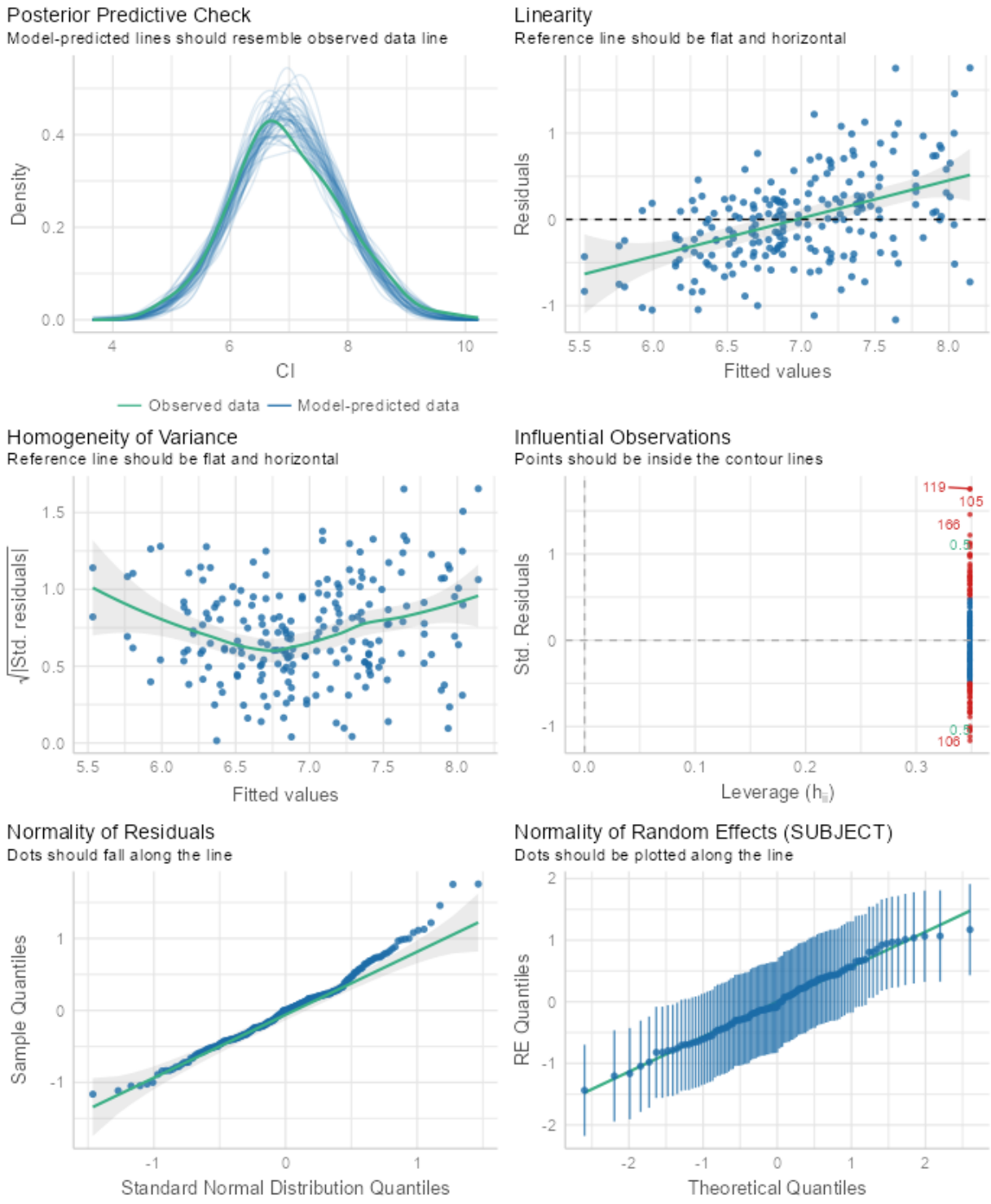

Figure 18: Null model Complexity Index (CI) LMER assumption tests for 40yd

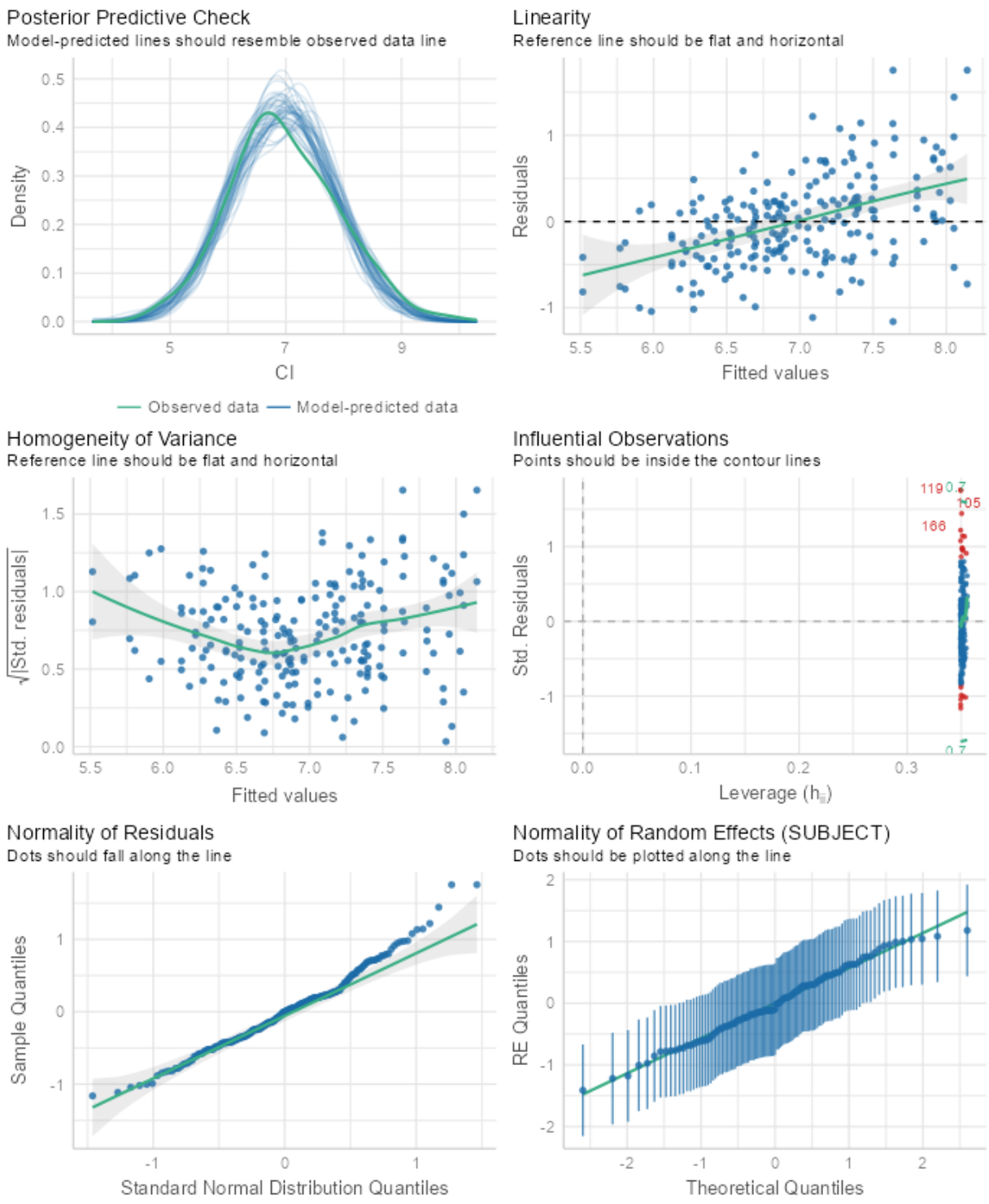

Figure 19: Model 1 Complexity Index (CI) LMER assumption tests for 40yd

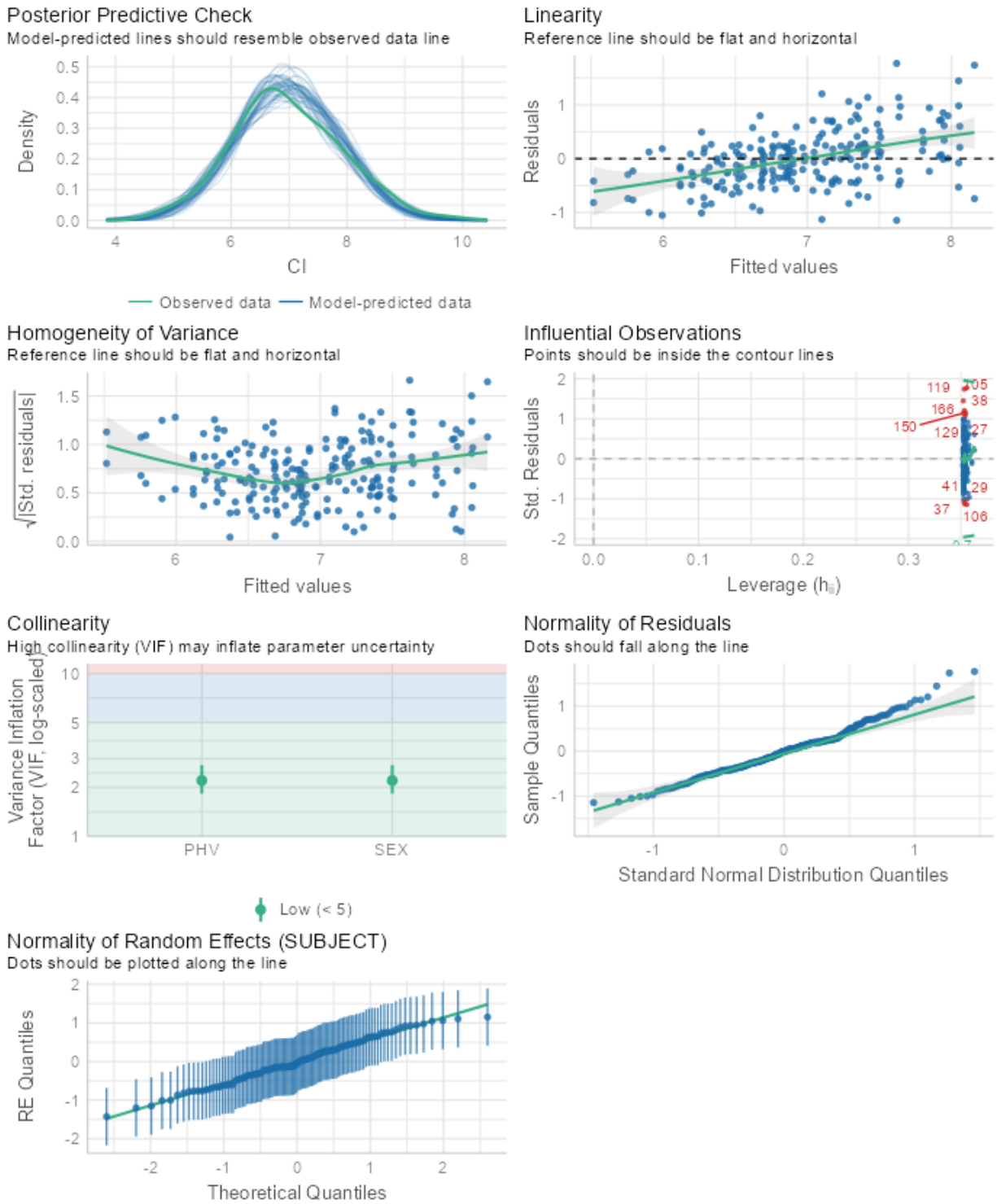

Figure 20: Model 2 Complexity Index (CI) LMER assumption tests for 40yd

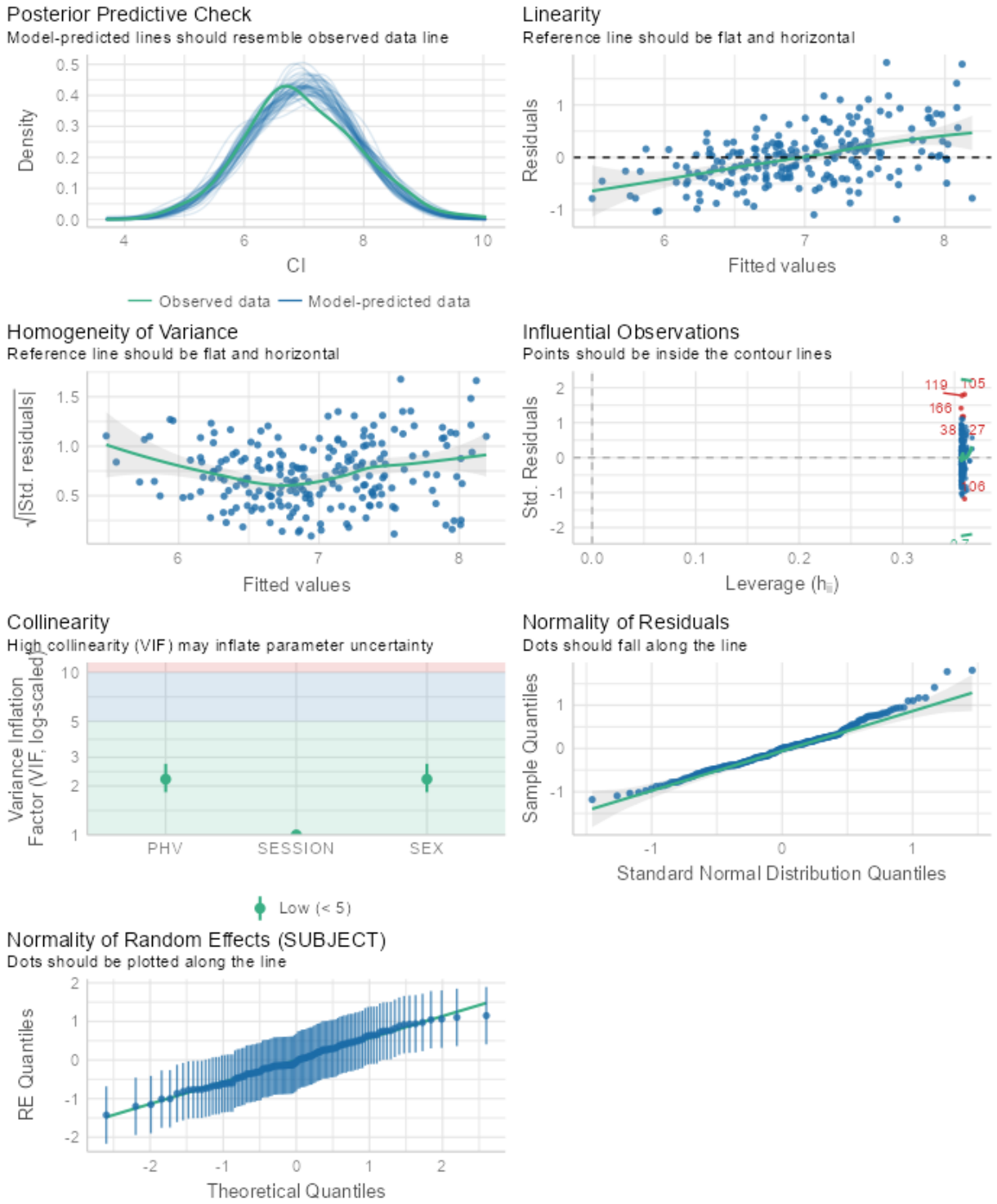

Figure 21: Model 3 Complexity Index (CI) LMER assumption tests for 40yd

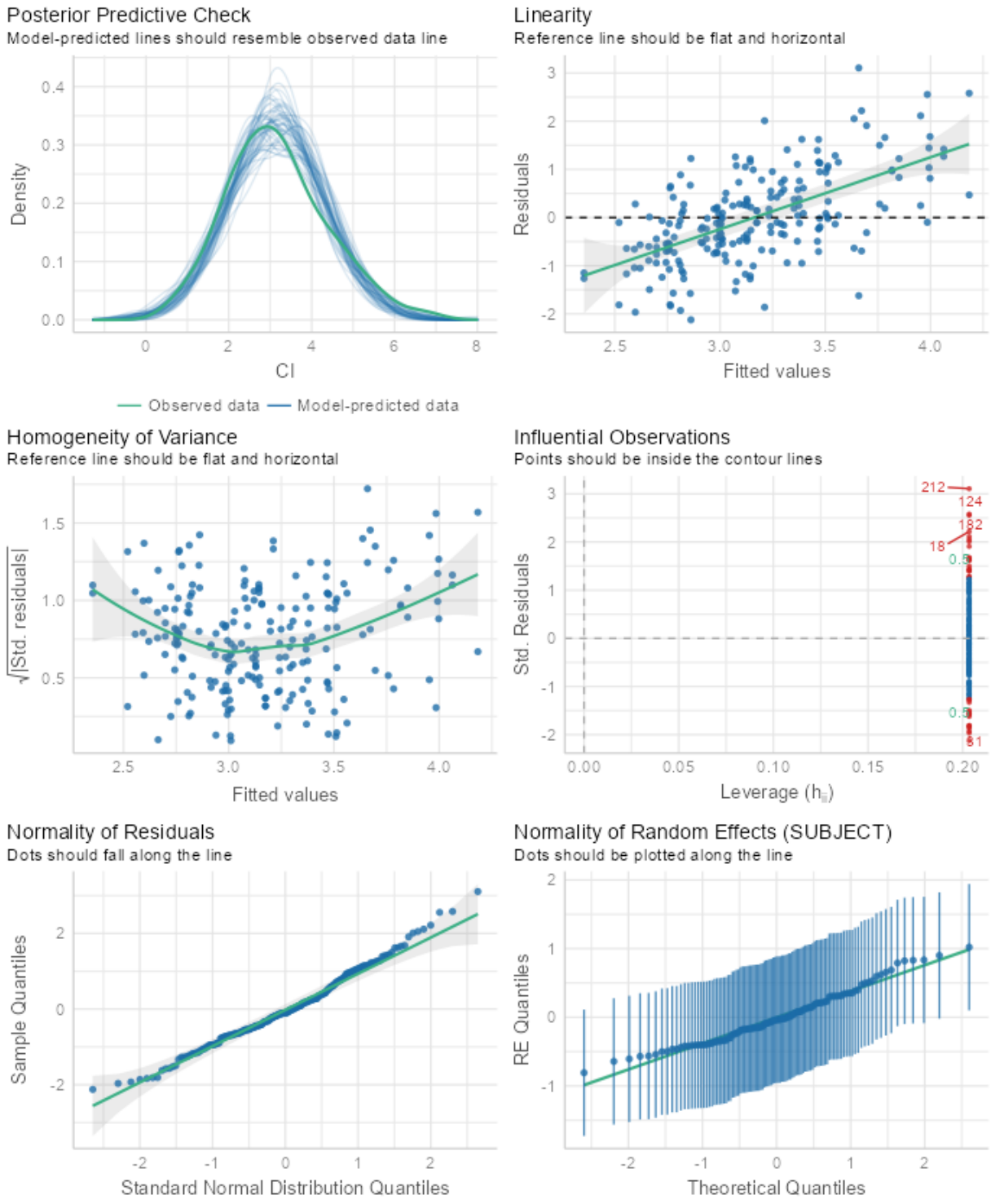

Figure 22: Null Model Complexity Index (CI) LMER sssumption tests for Broad

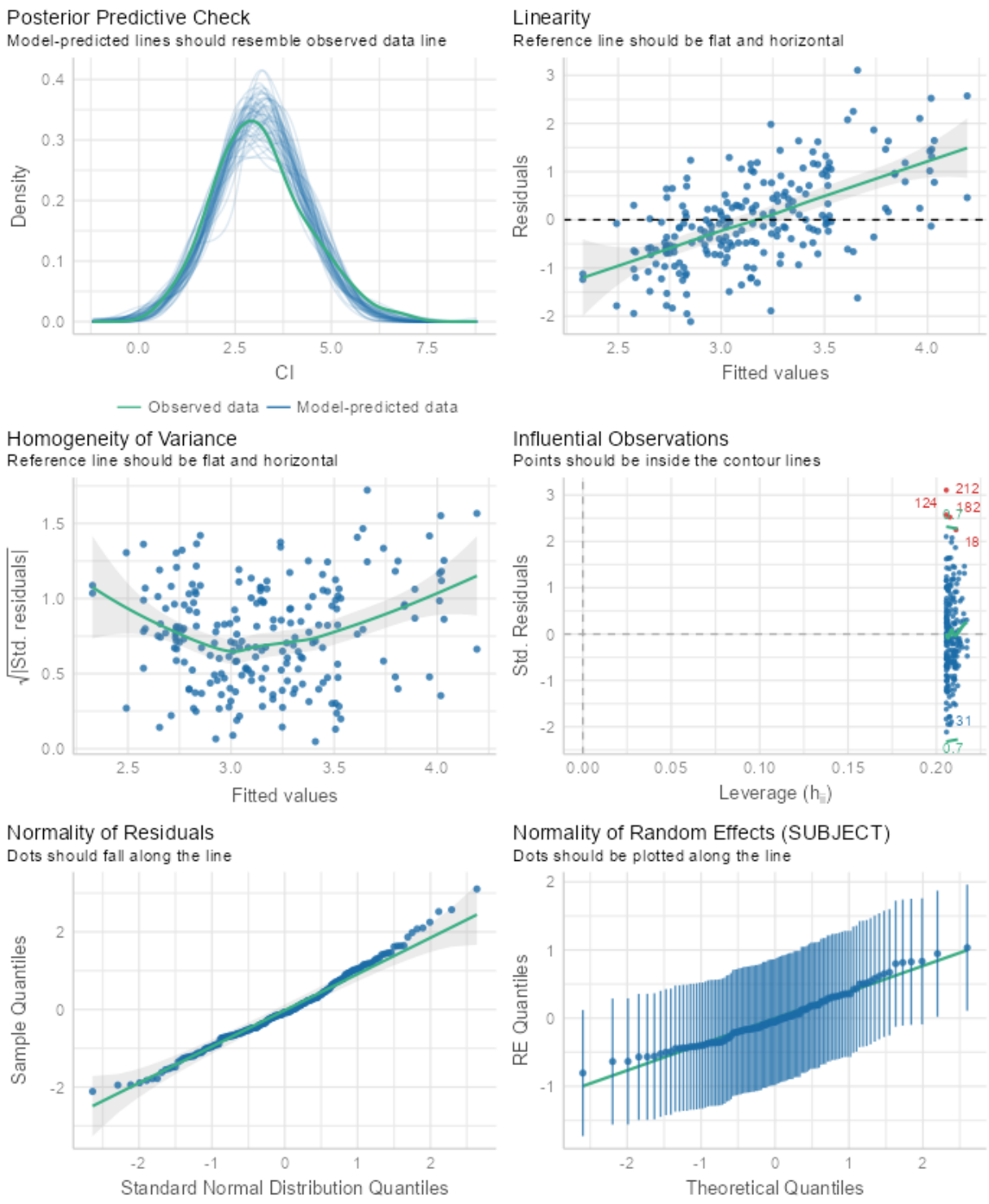

Figure 23: Model 1 Complexity Index (CI) LMER assumption tests for Broad

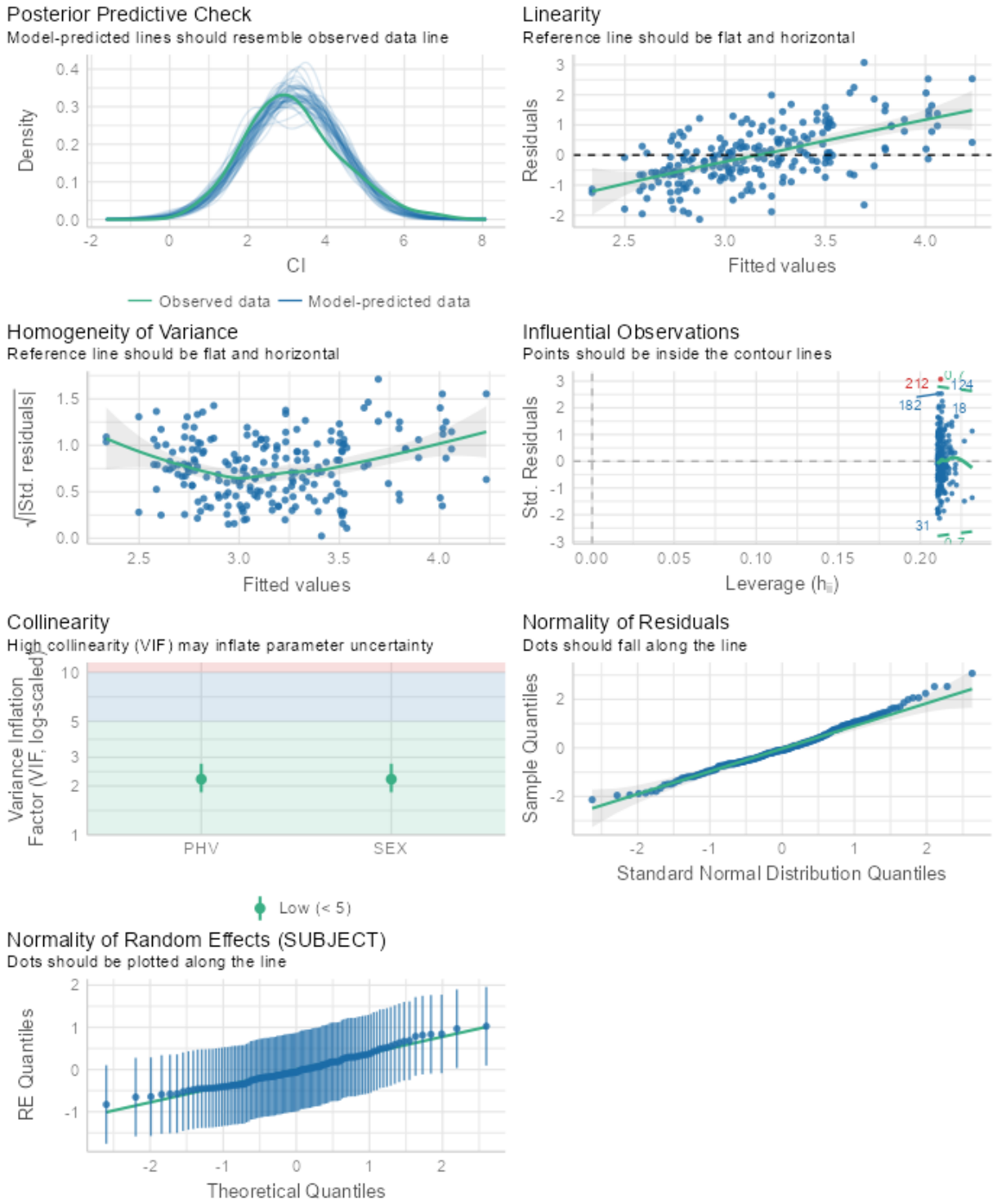

Figure 24: Model 2 Complexity Index (CI) LMER assumption tests for Broad

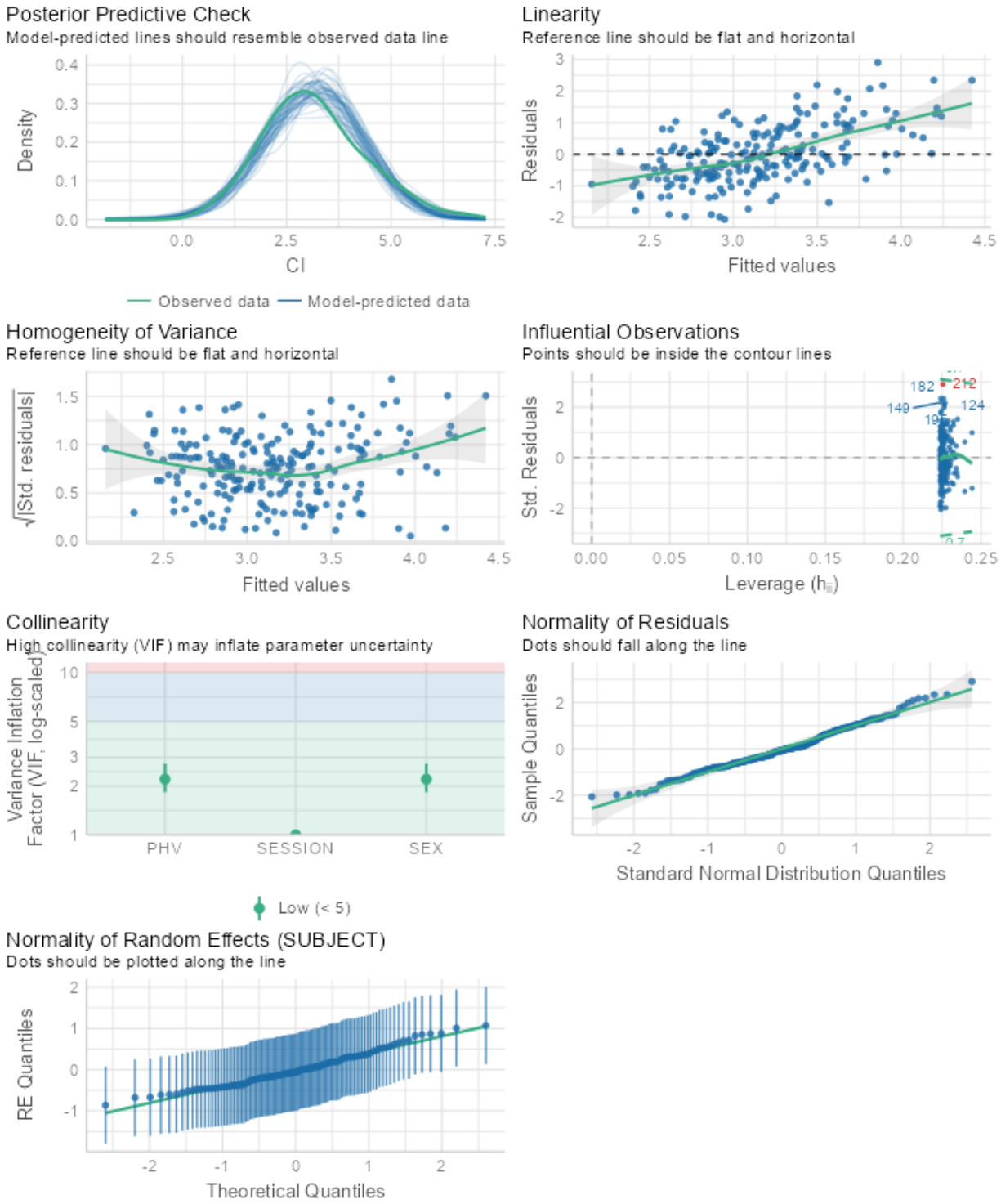

Figure 25: Model 3 Complexity Index (CI) LMER assumption tests for Broad

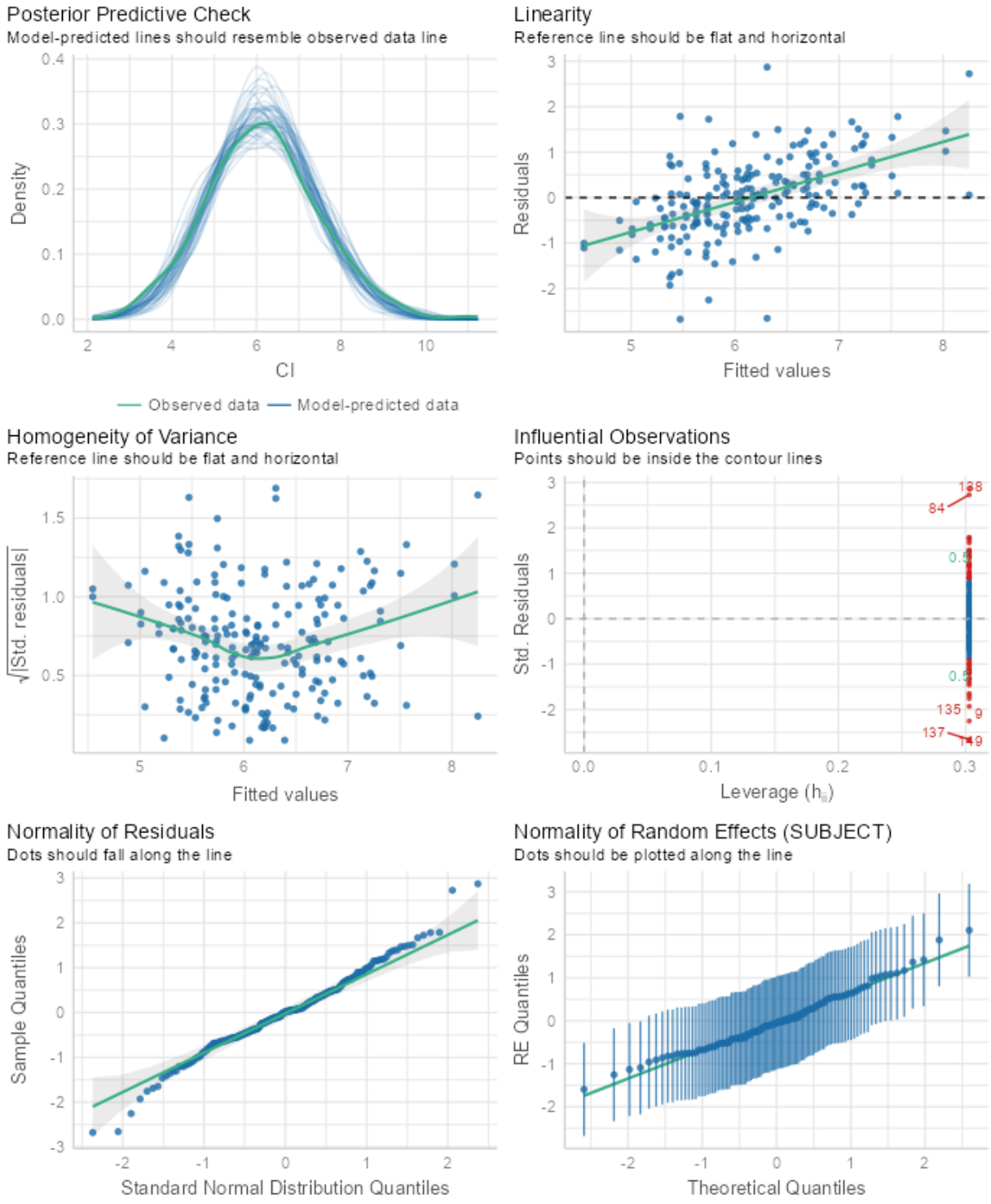

Figure 26: Null model Complexity Index (CI) LMER assumption tests for DNB

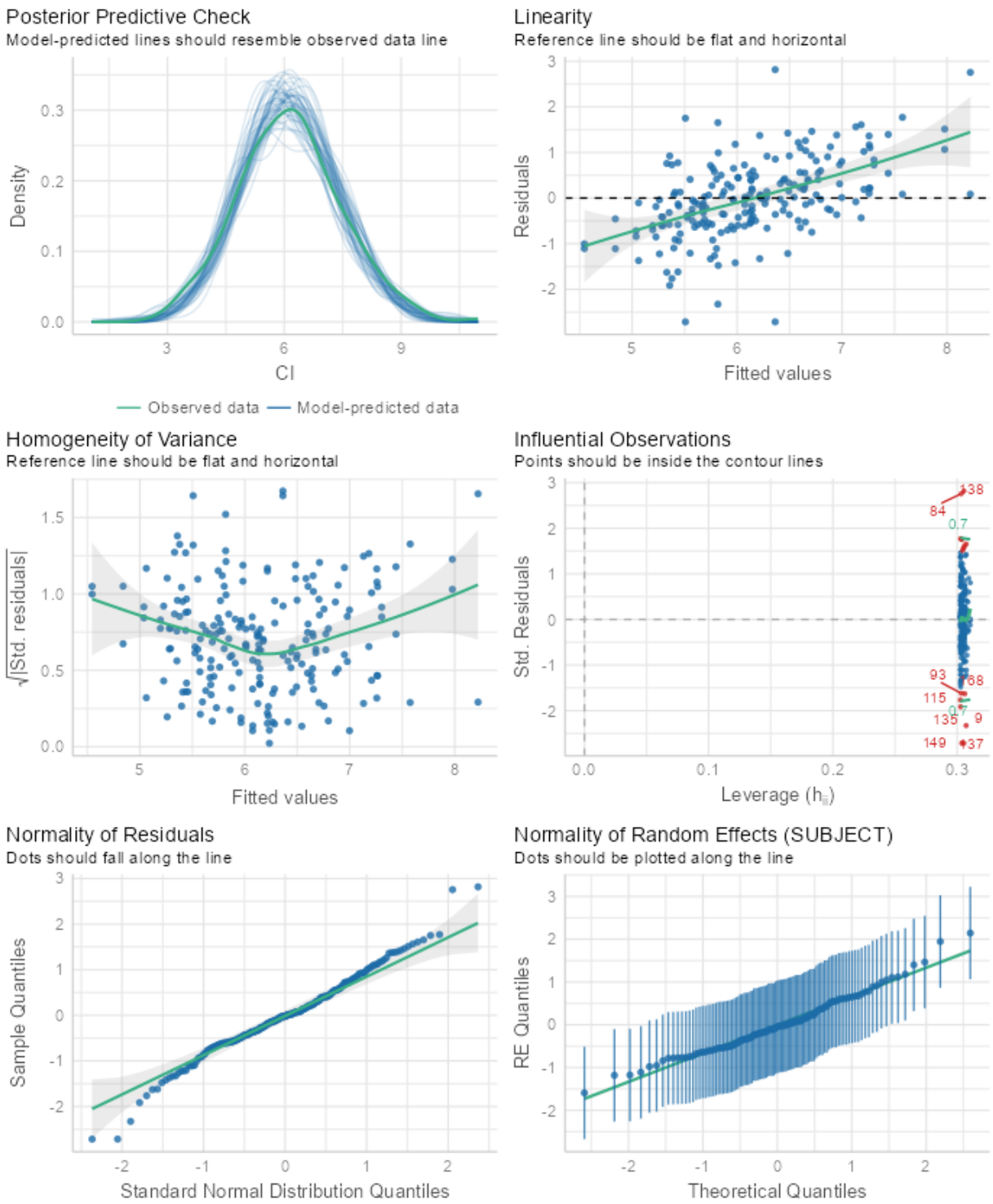

Figure 27: Model 1 Complexity Index (CI) LMER assumption tests for DNB

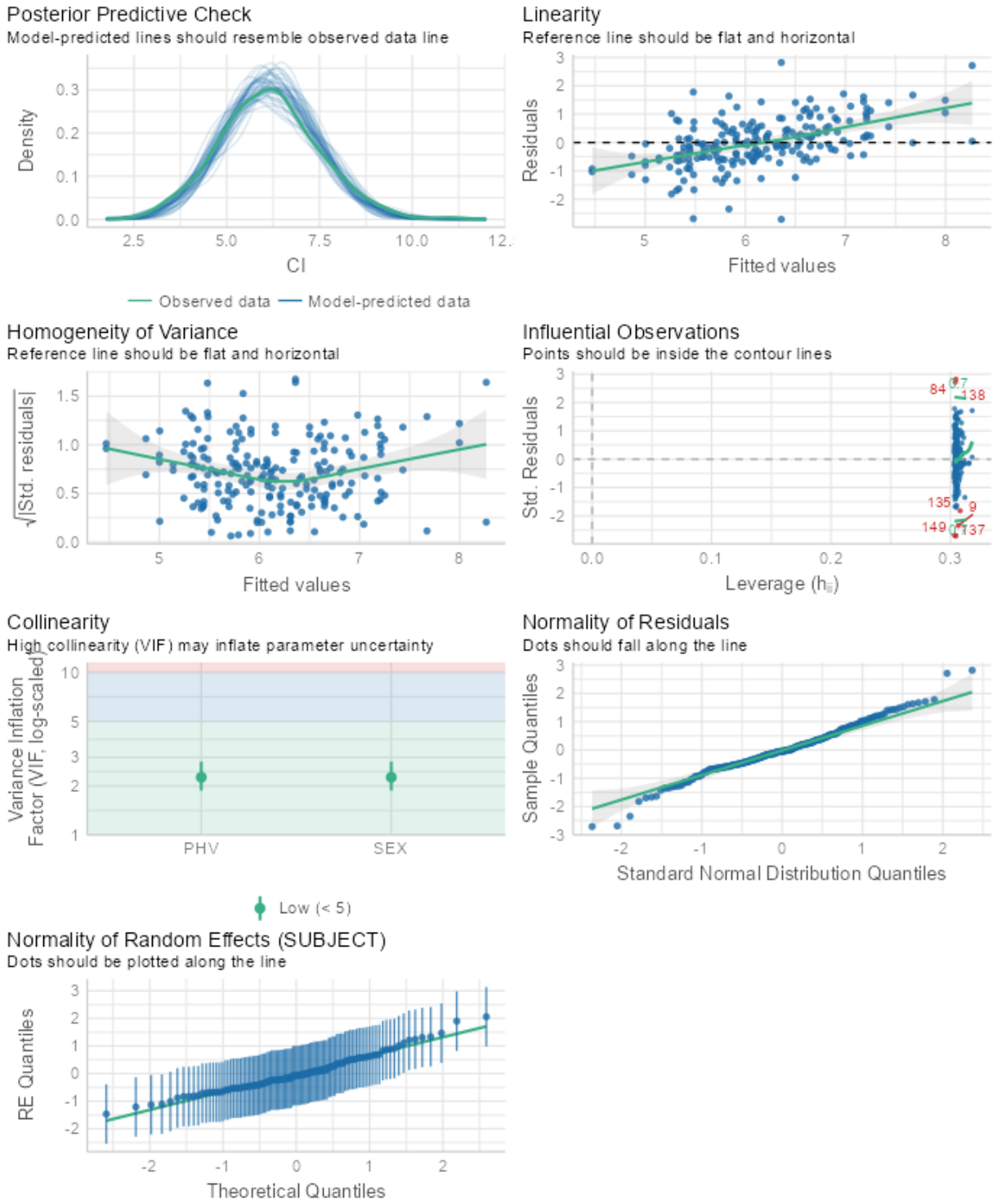

Figure 28: Model 2 Complexity Index (CI) LMER assumption tests for DNB

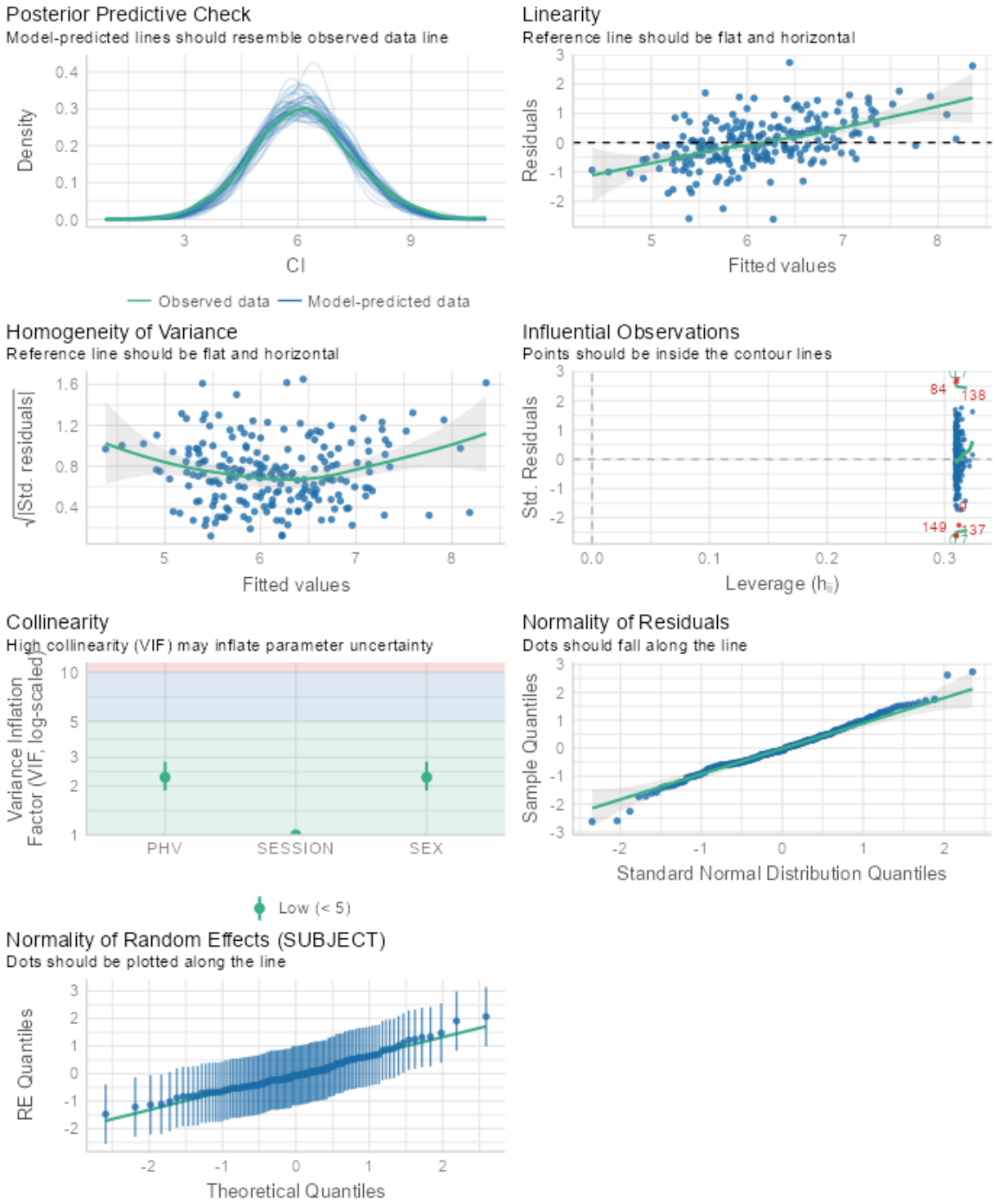

Figure 29: Model 3 Complexity Index (CI) LMER assumption tests for DNB

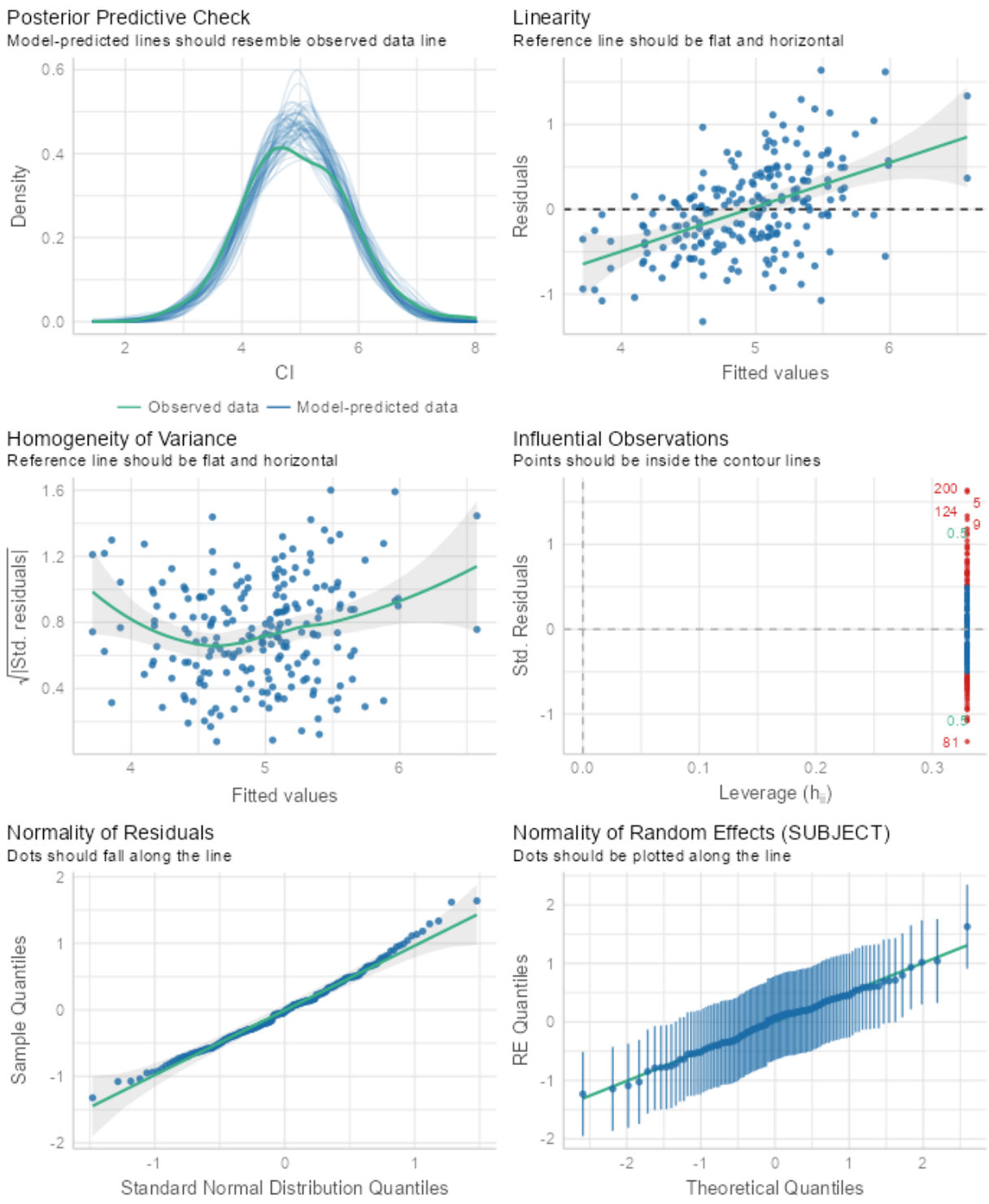

Figure 30: Null model Complexity Index (CI) LMER assumption tests for 5-10-5 shuffle drill

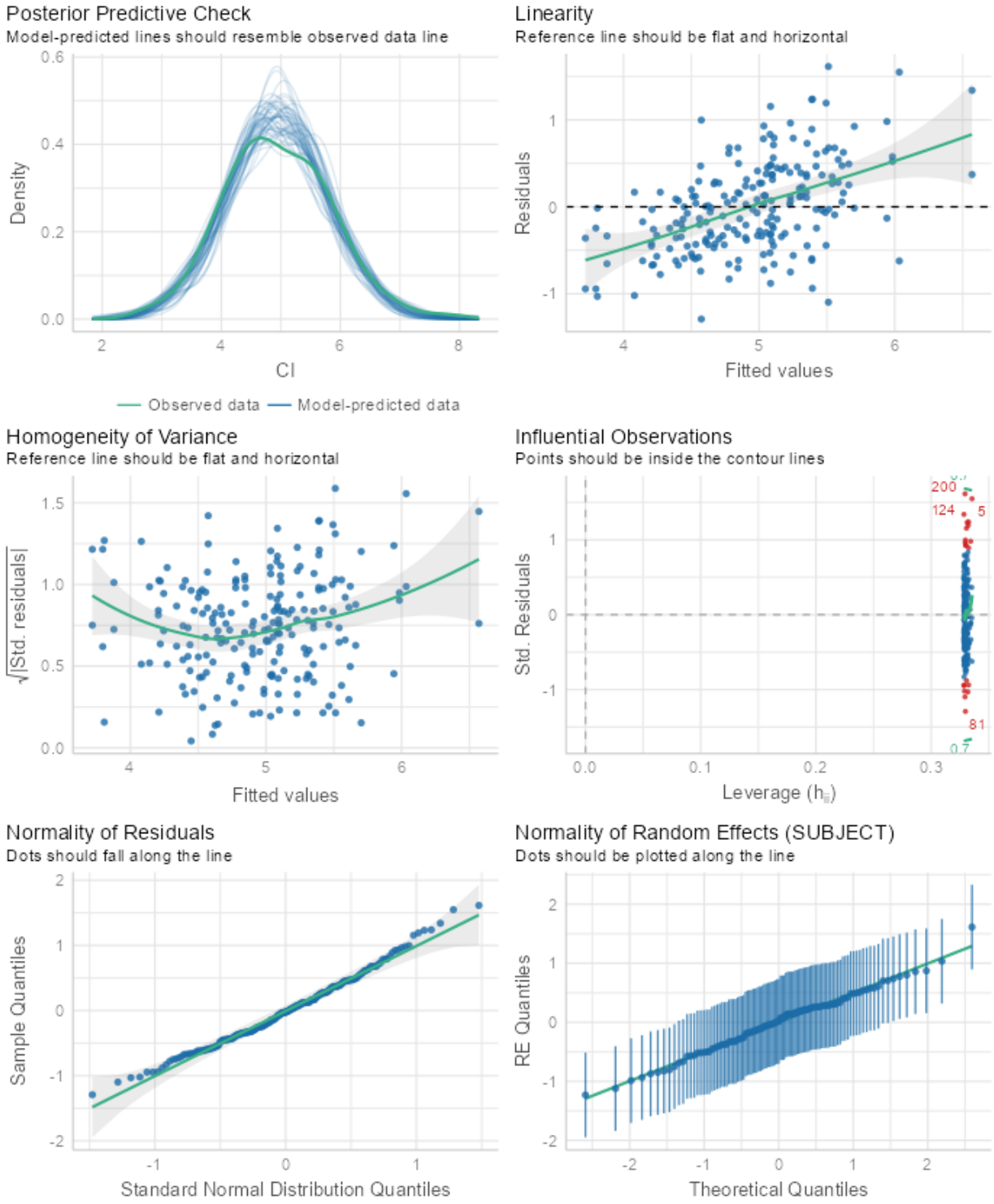

Figure 31: Model 1 Complexity Index (CI) LMER assumption tests for 5-10-5 shuffle drill

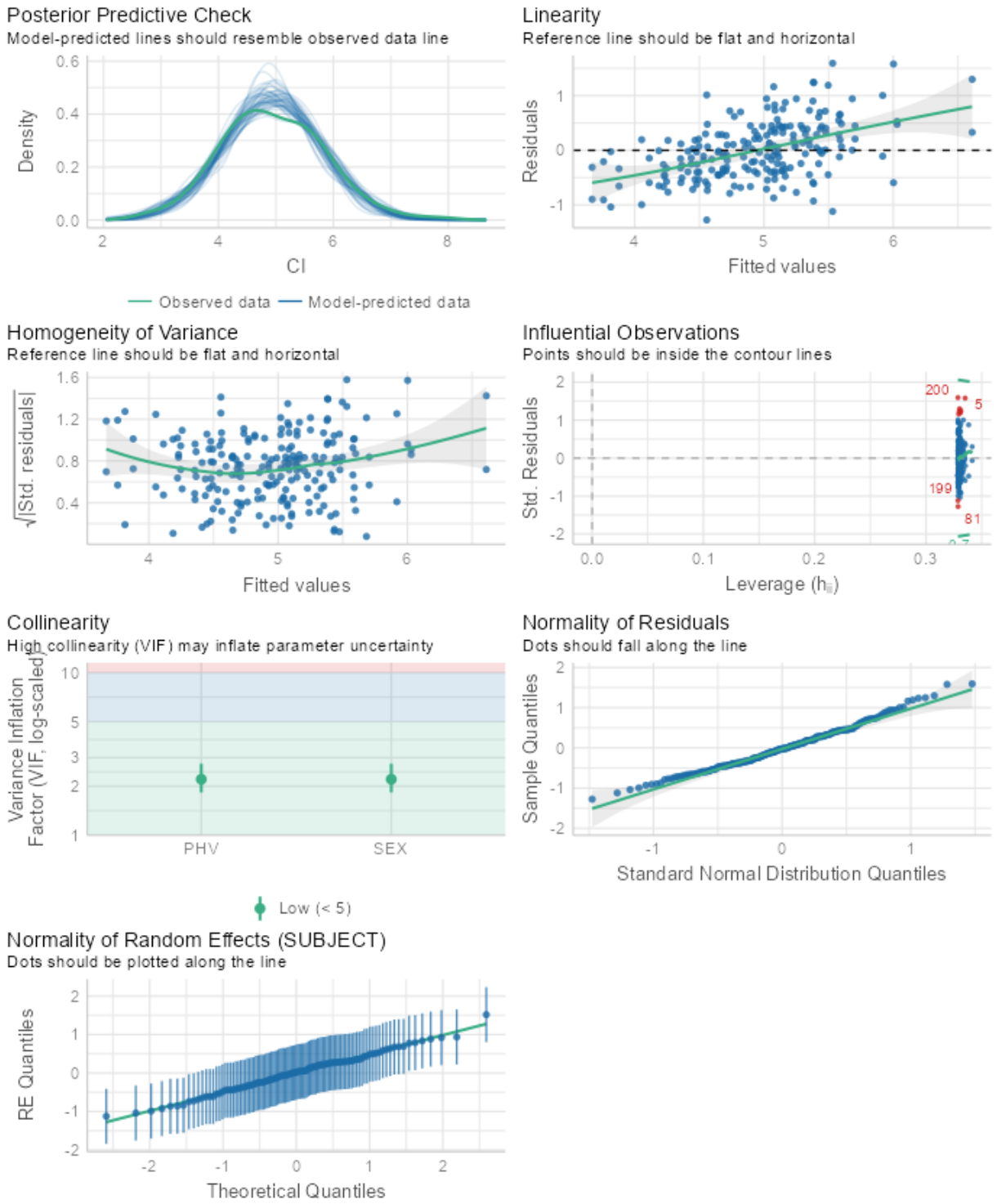

Figure 32: Model 2 Complexity Index (CI) LMER assumption tests for 5-10-5 shuffle drill

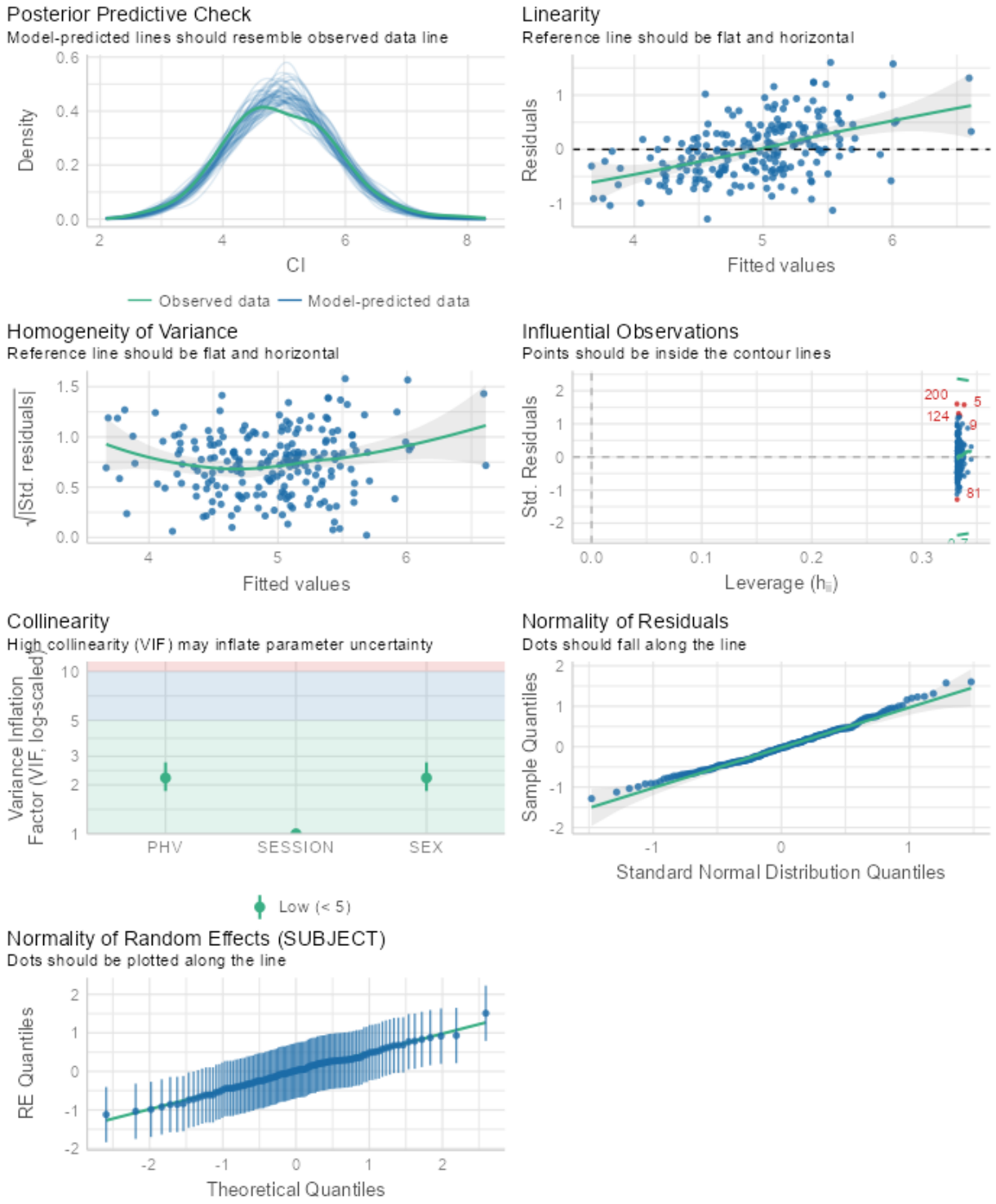

Figure 33: Model 3 Complexity Index (CI) LMER assumption tests for 5-10-5 shuffle drill

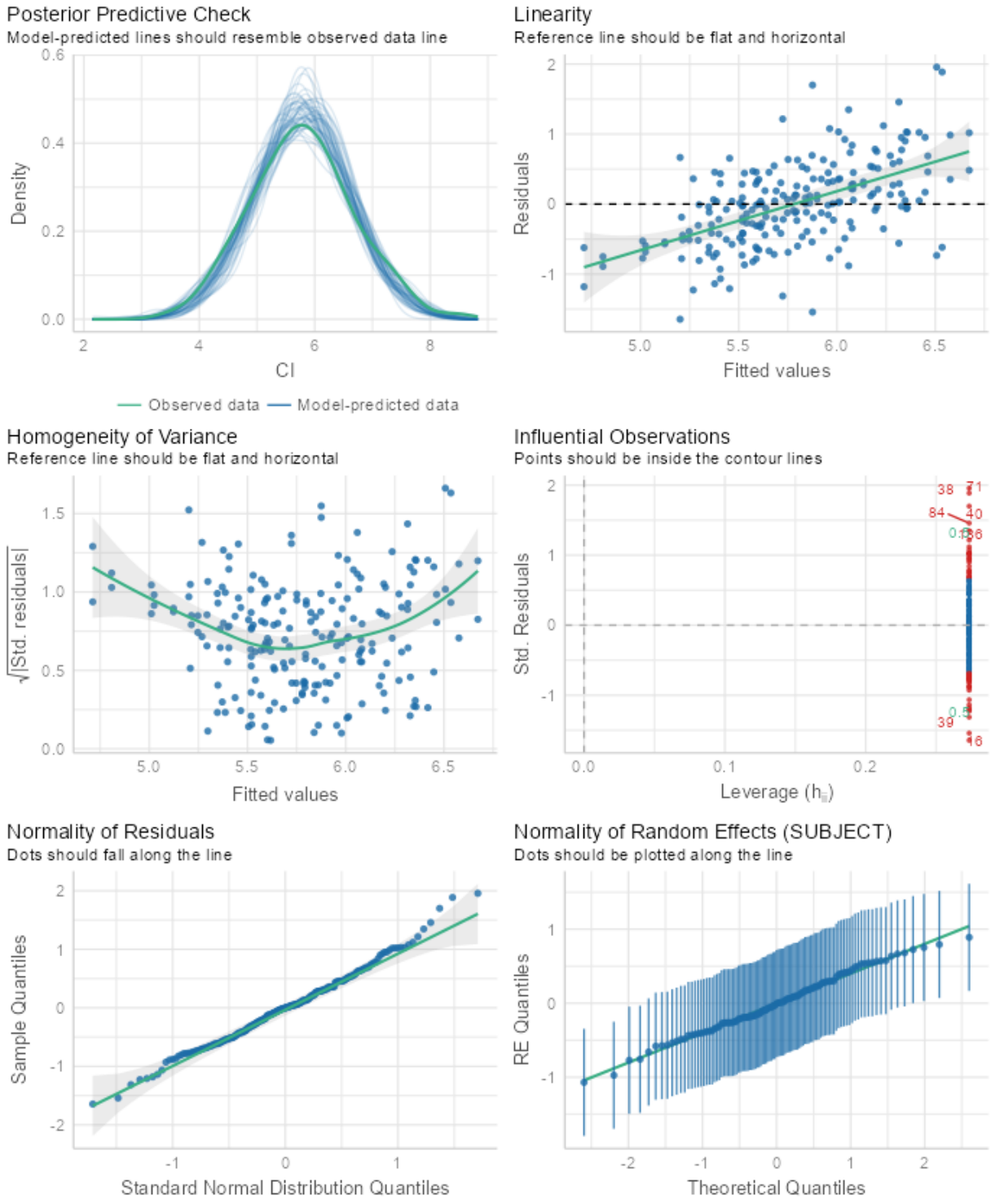

Figure 34: Null model Complexity Index (CI) LMER assumption tests for M-L

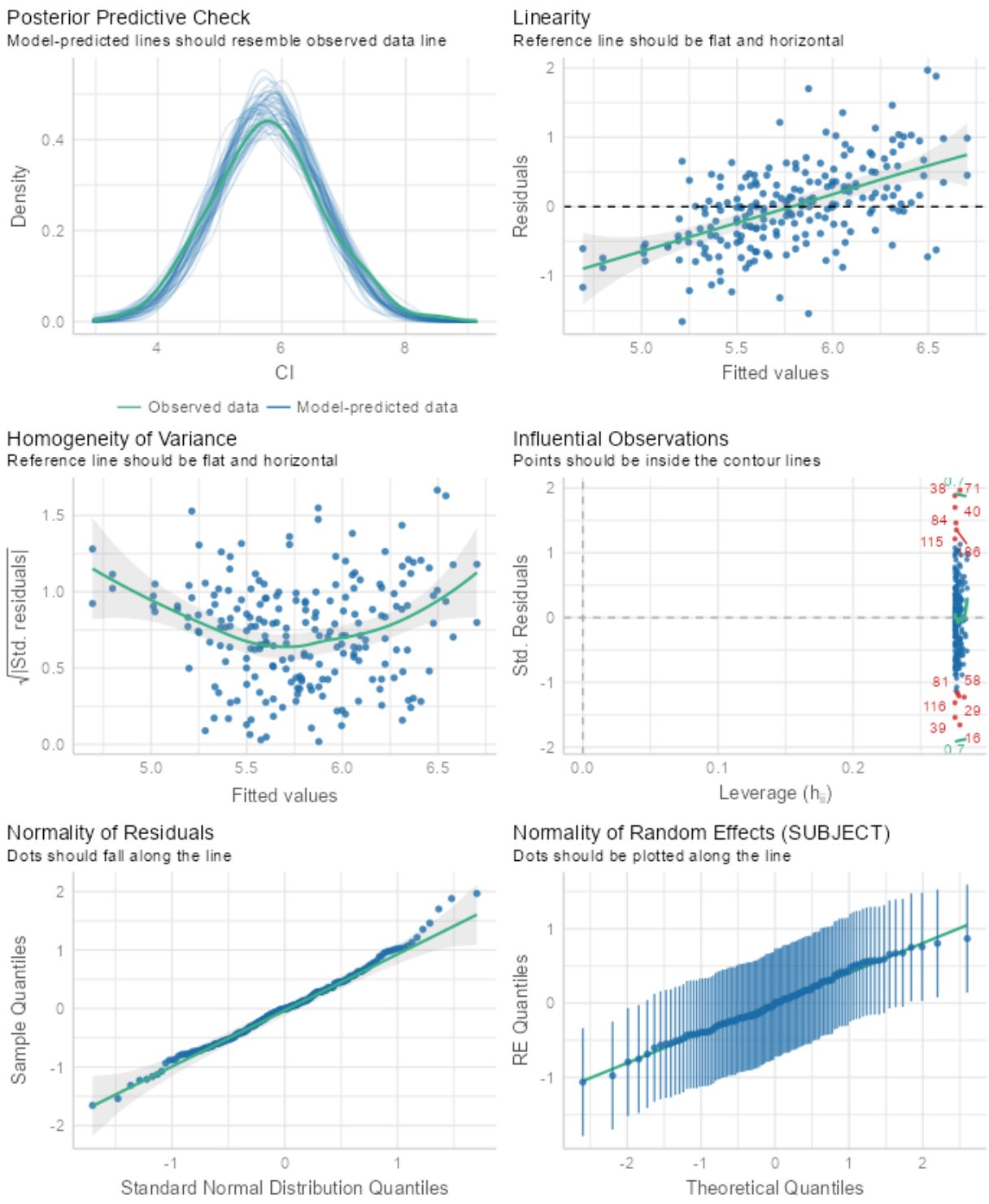

Figure 35: Model 1 Complexity Index (CI) LMER assumption tests for M-L

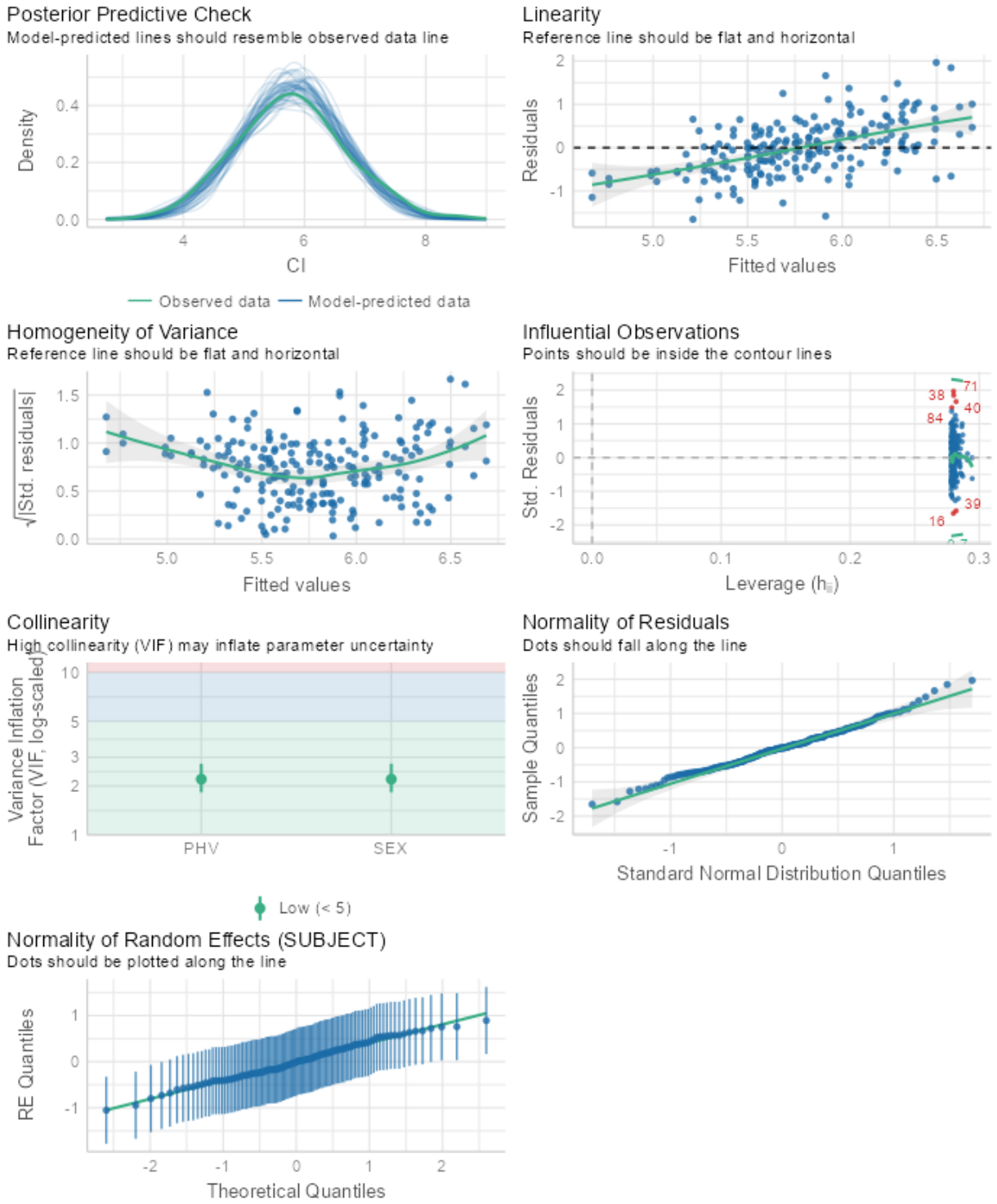

Figure 36: Model 2 Complexity Index (CI) LMER assumption tests for M-L

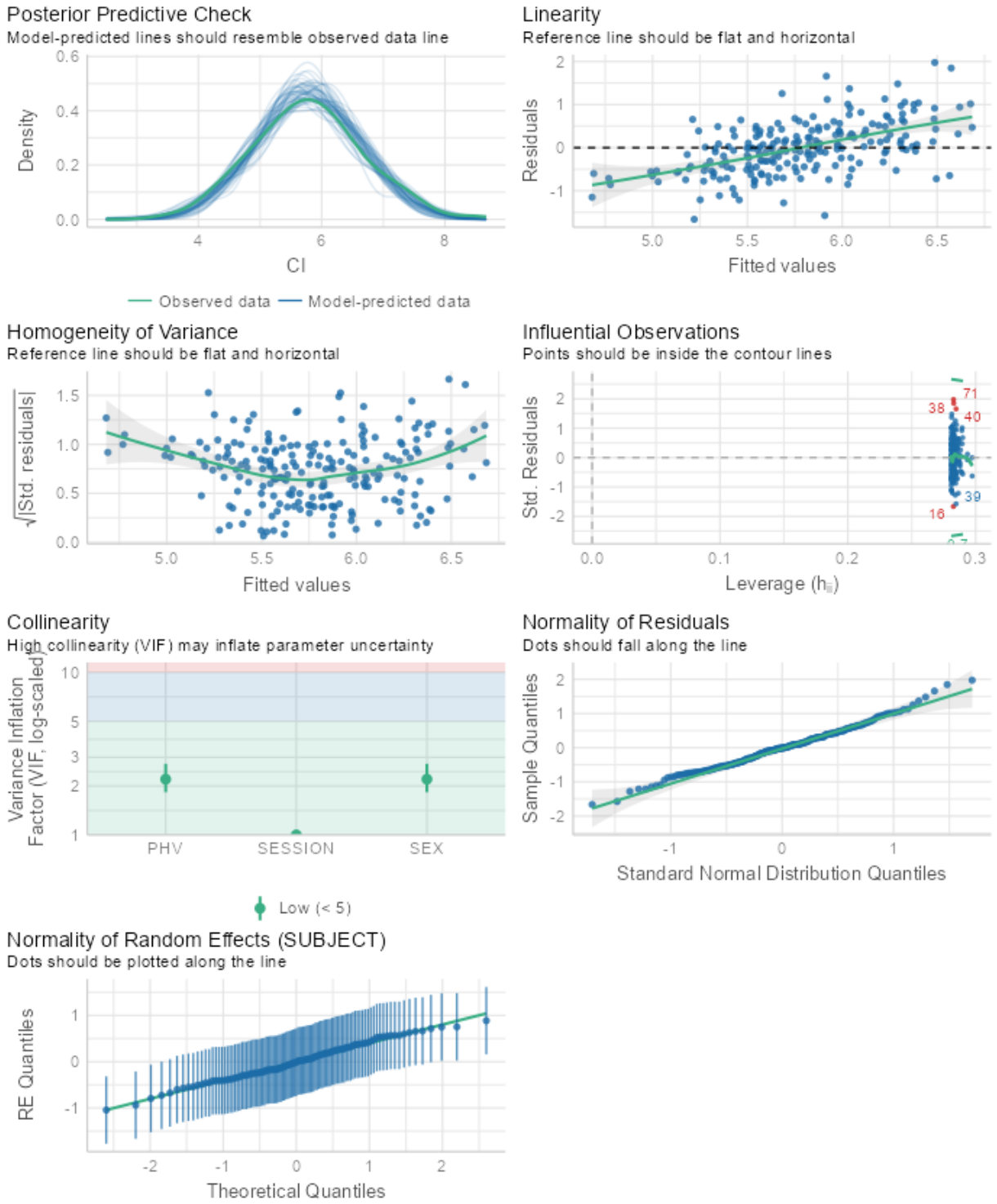

Figure 37: Model 3 Complexity Index (CI) LMER assumption tests for M-L

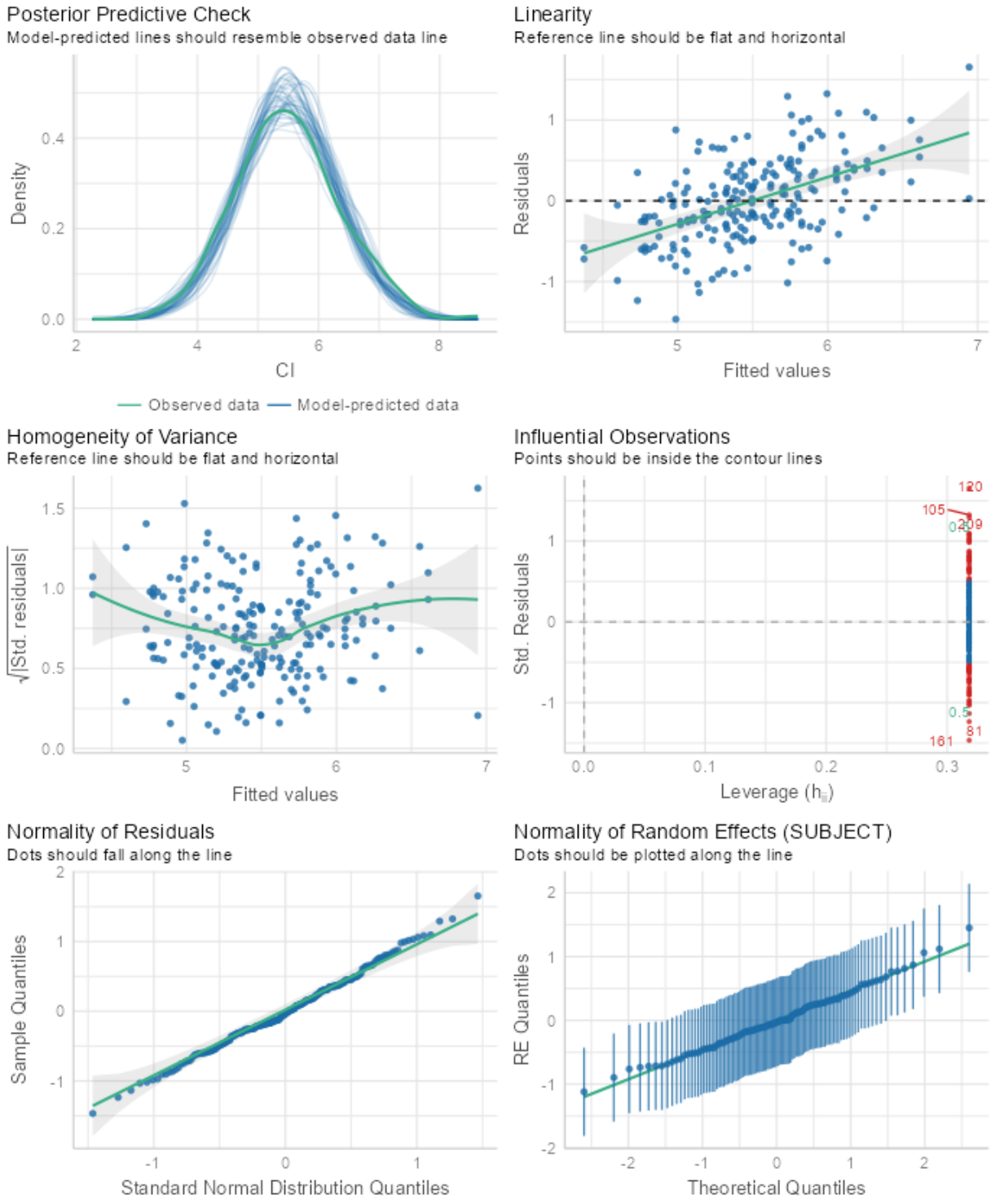

Figure 38: Null model complexity index (CI) LMER assumption tests for M-R

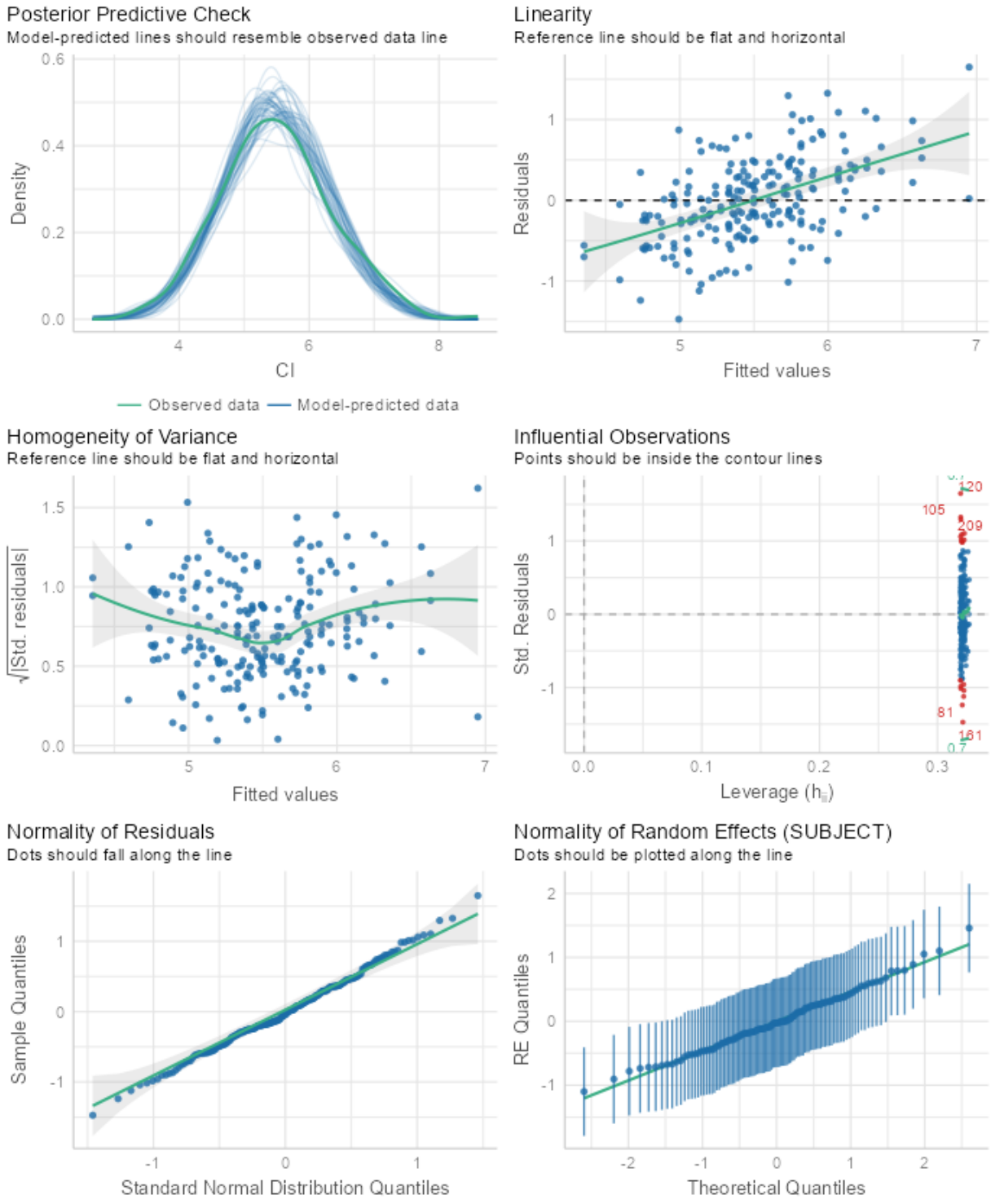

Figure 39: Model 1 Complexity Index (CI) LMER assumption tests for M-R

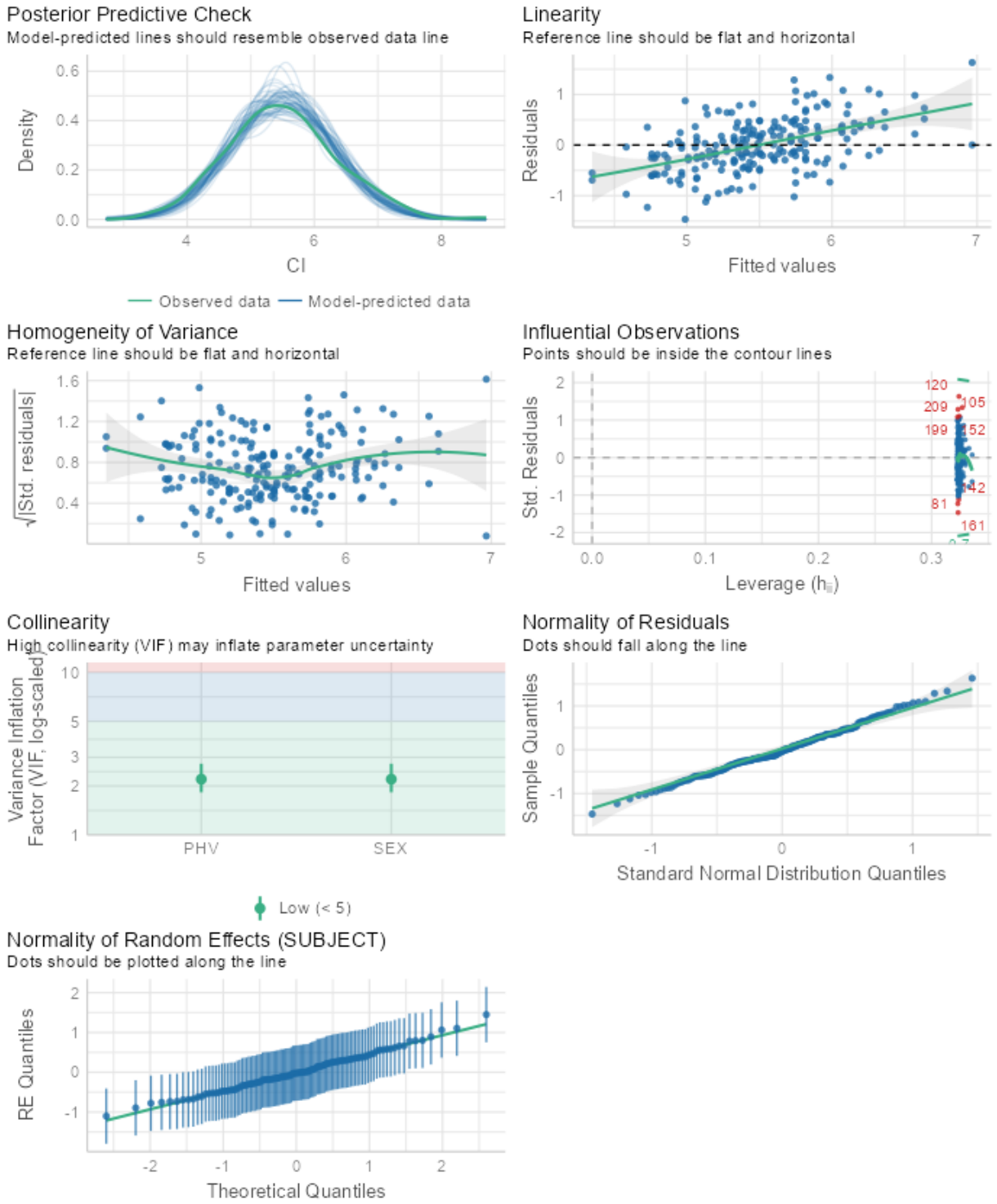

Figure 40: Model 2 Complexity Index (CI) LMER assumption tests for M-R

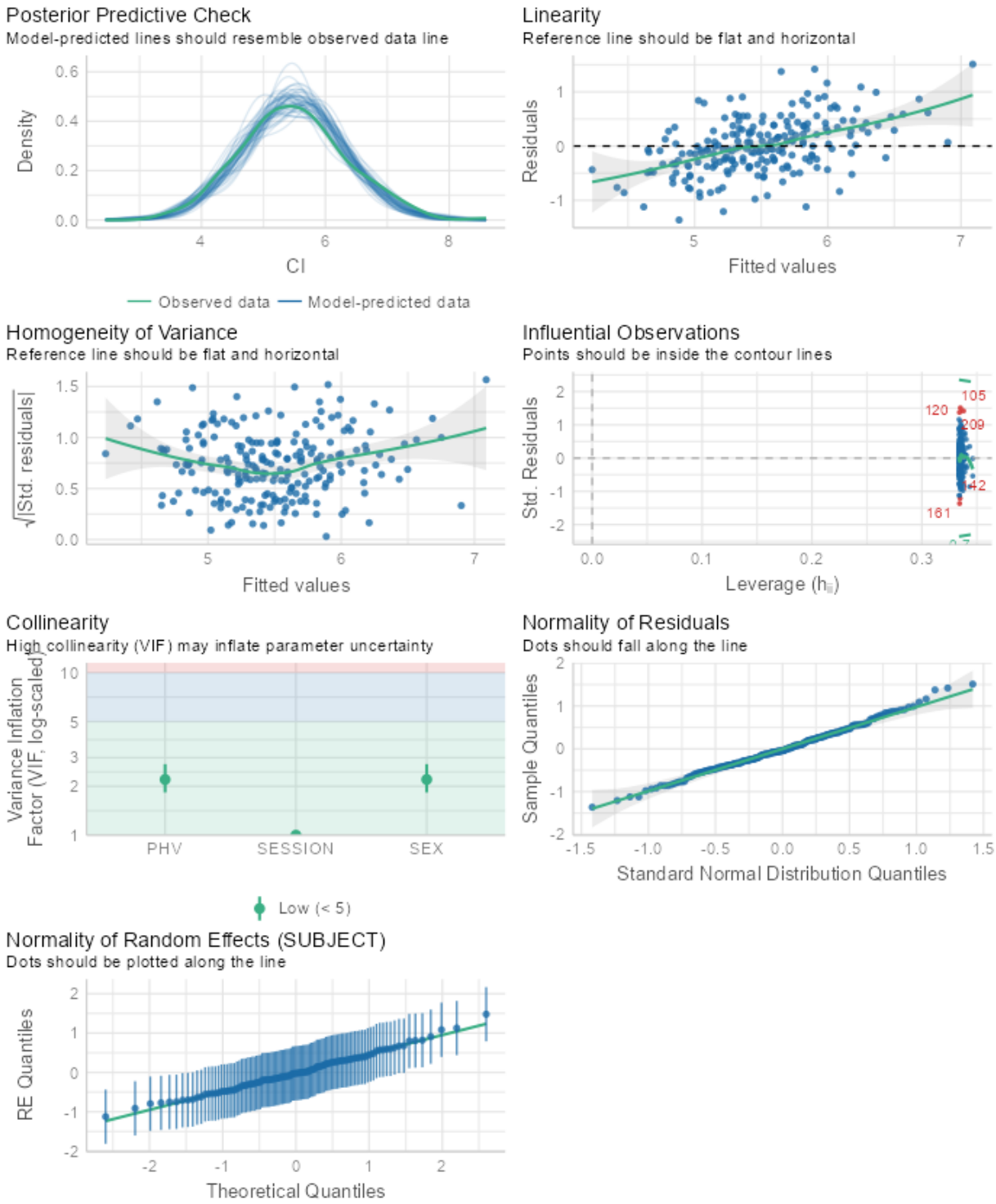

Figure 41: Model 3 Complexity Index (CI) LMER assumption tests for M-R

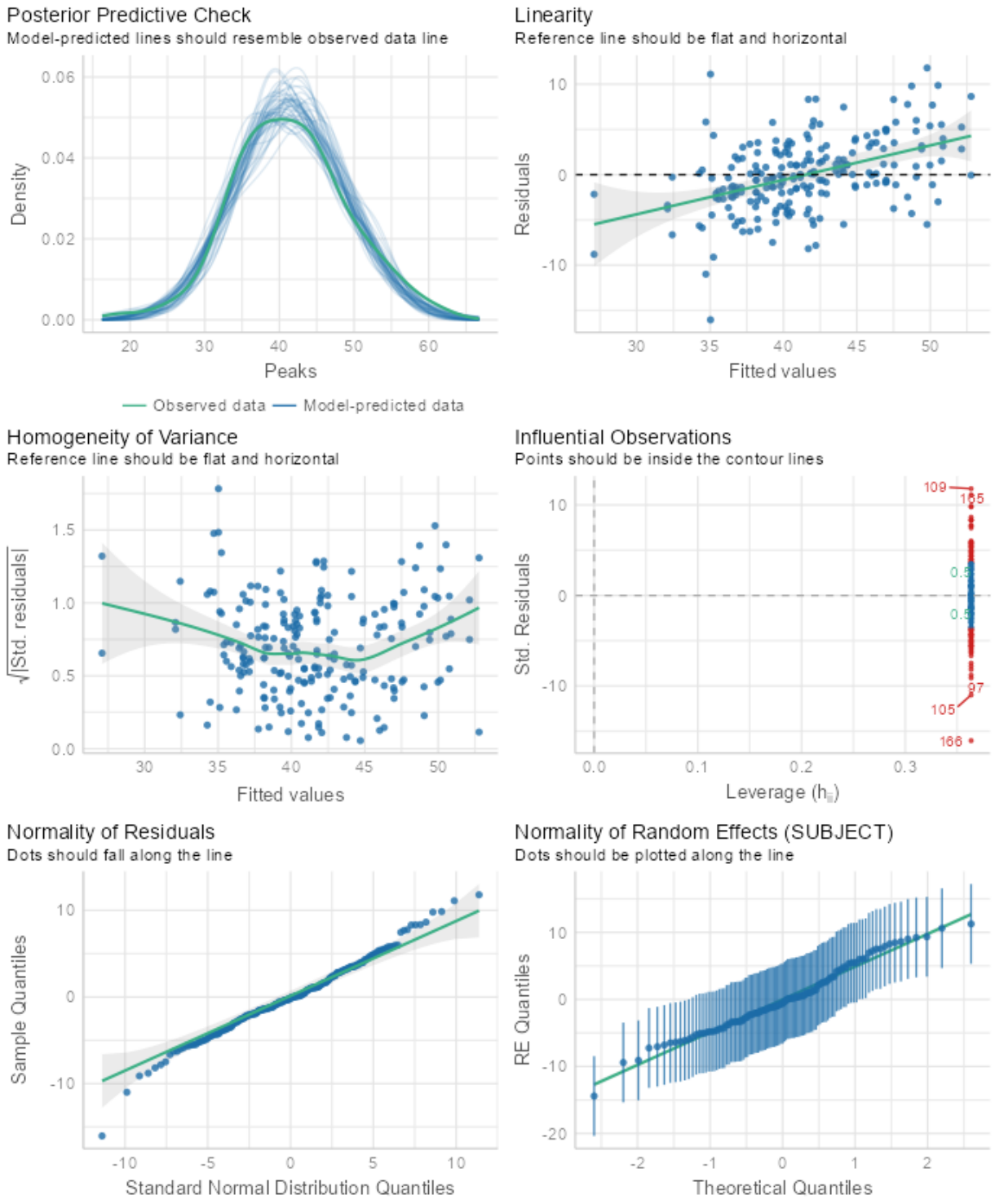

Figure 42: Null model acceleration peaks LMER model assumption tests for 40yd

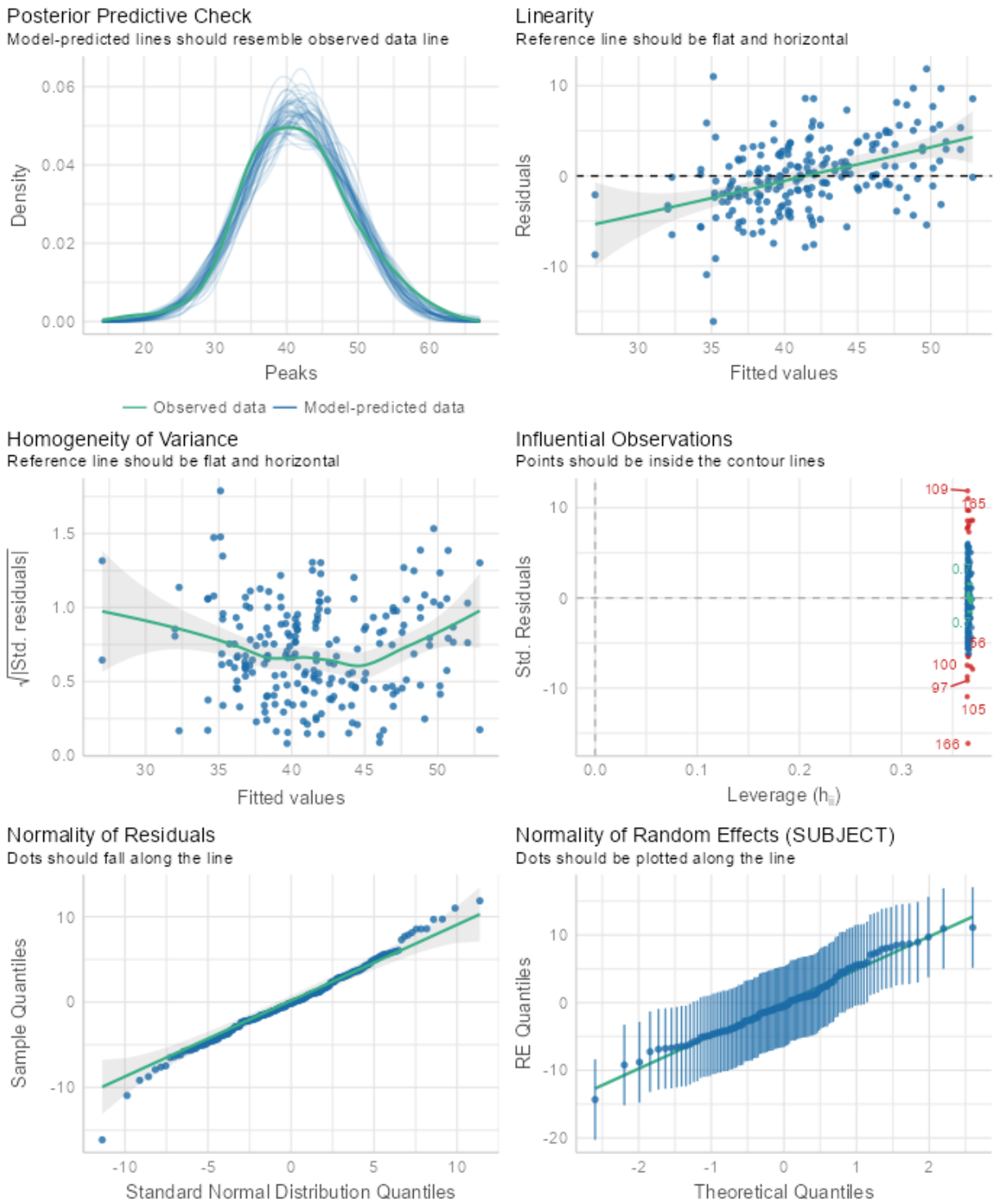

Figure 43: Model 1 acceleration peaks LMER model assumption tests for 40yd

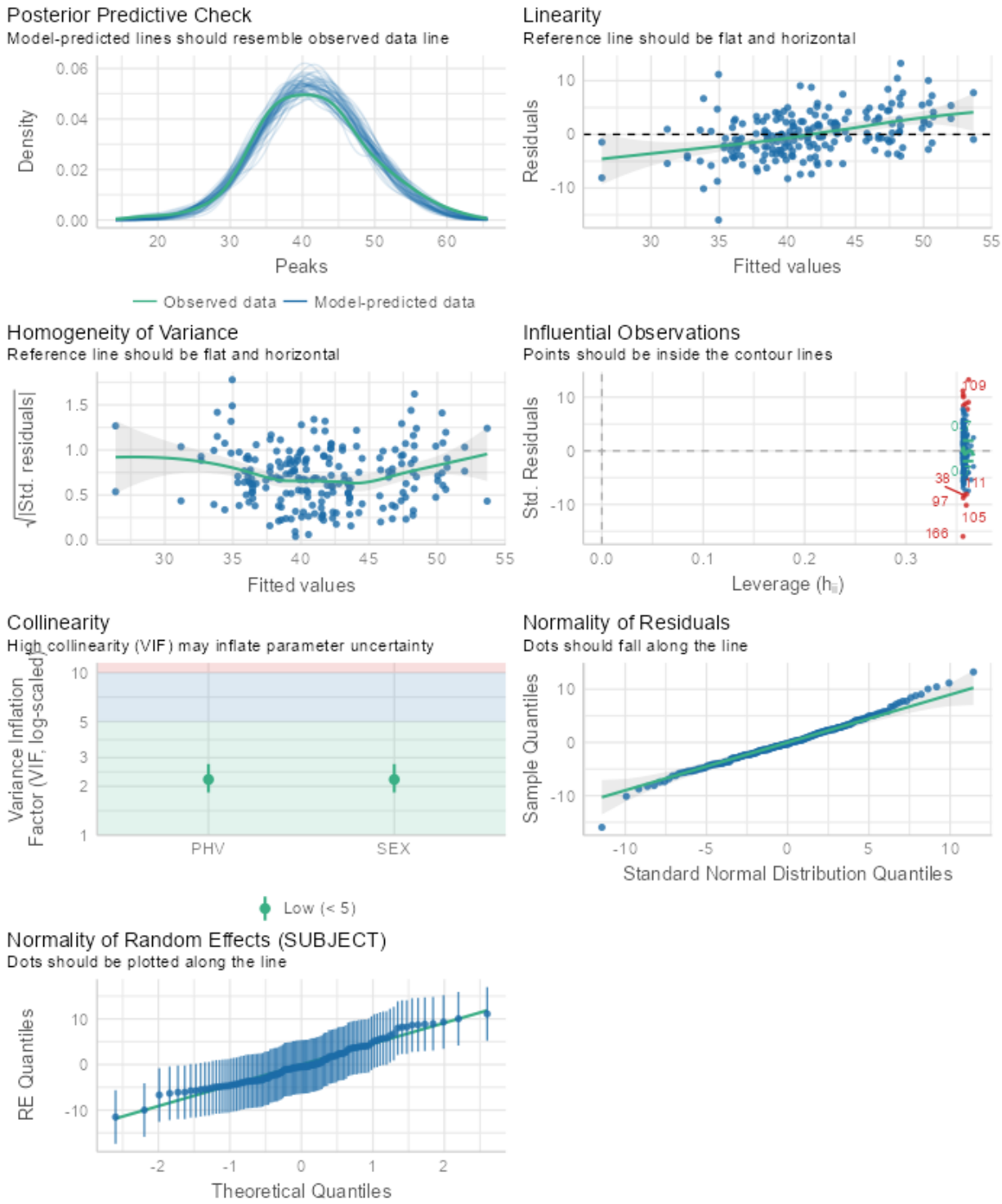

Figure 44: Model 2 acceleration peaks LMER model assumption tests for 40yd

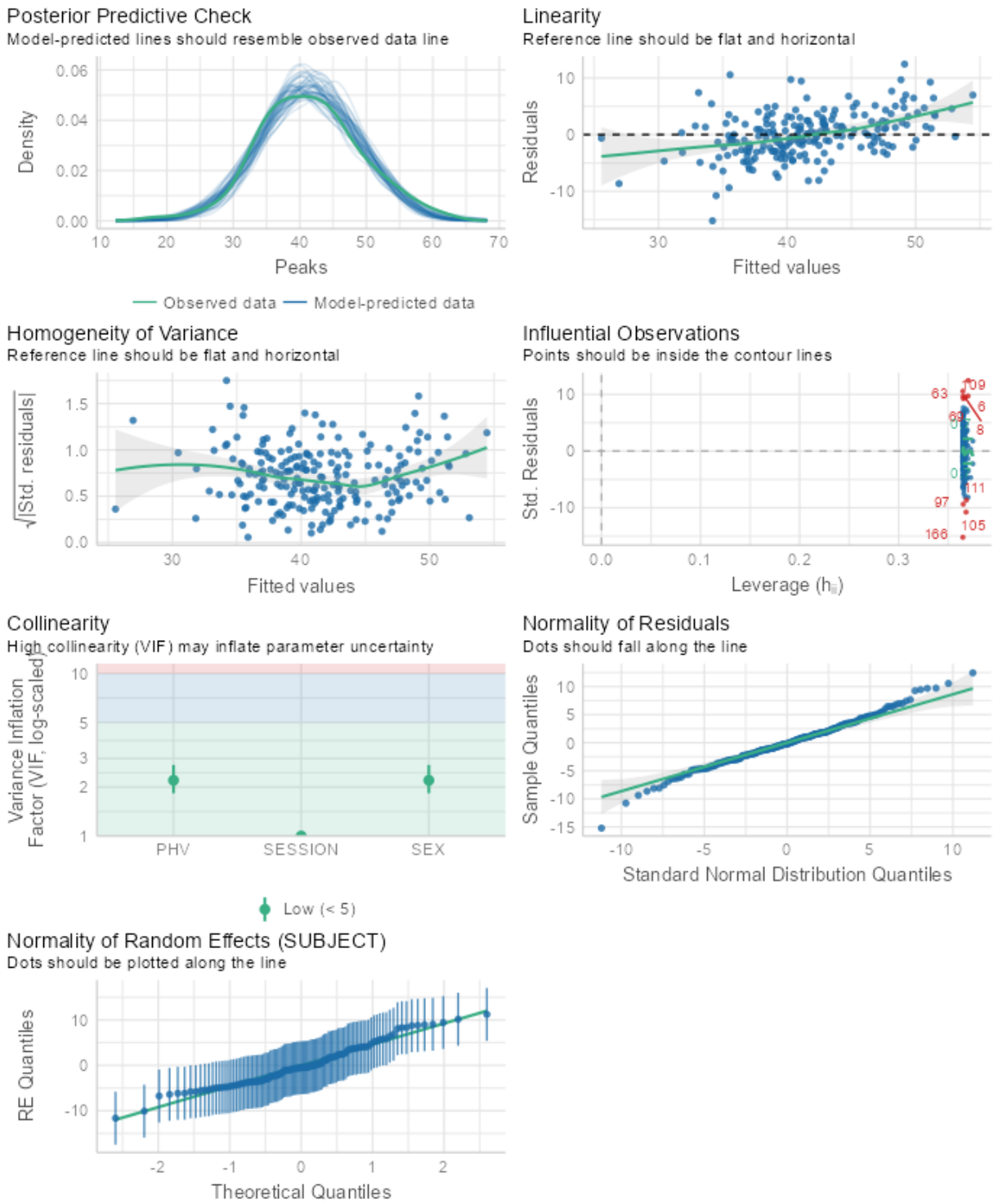

Figure 45: Model 3 acceleration peaks LMER model assumption tests for 40yd

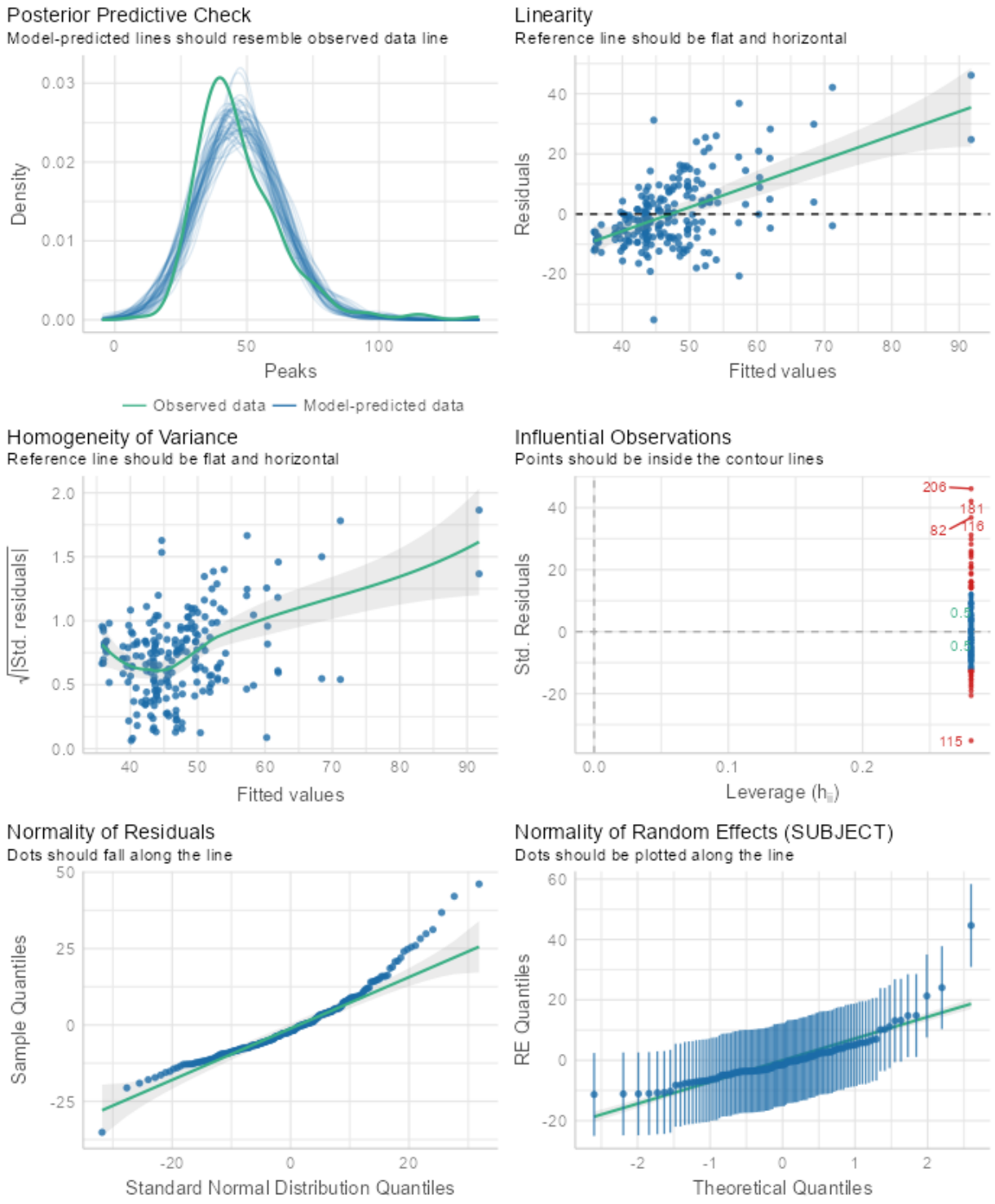

Figure 46: Null model acceleration peaks LMER model assumption tests for Broad

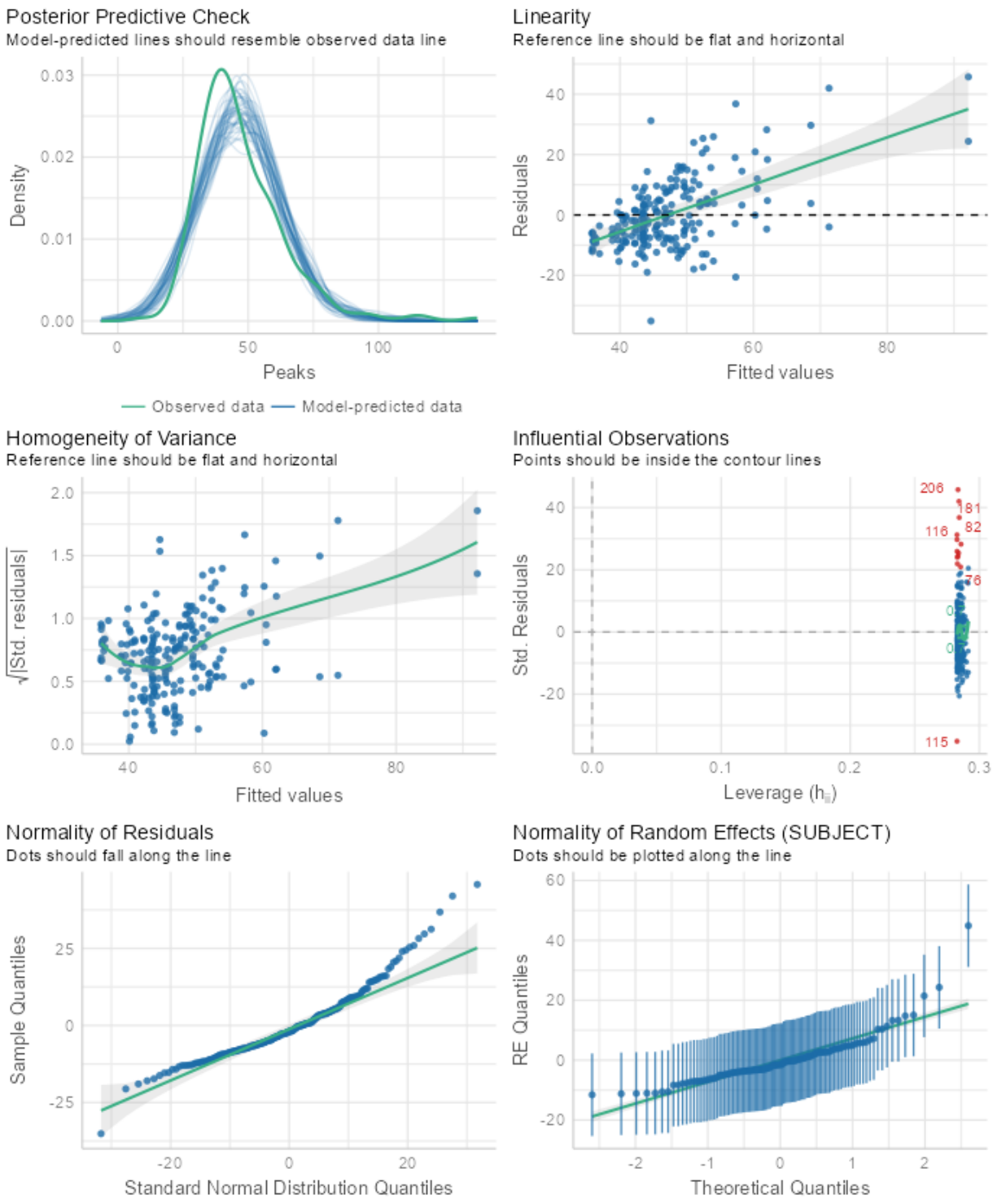

Figure 47: Model 1 acceleration peaks LMER model assumption tests for Broad

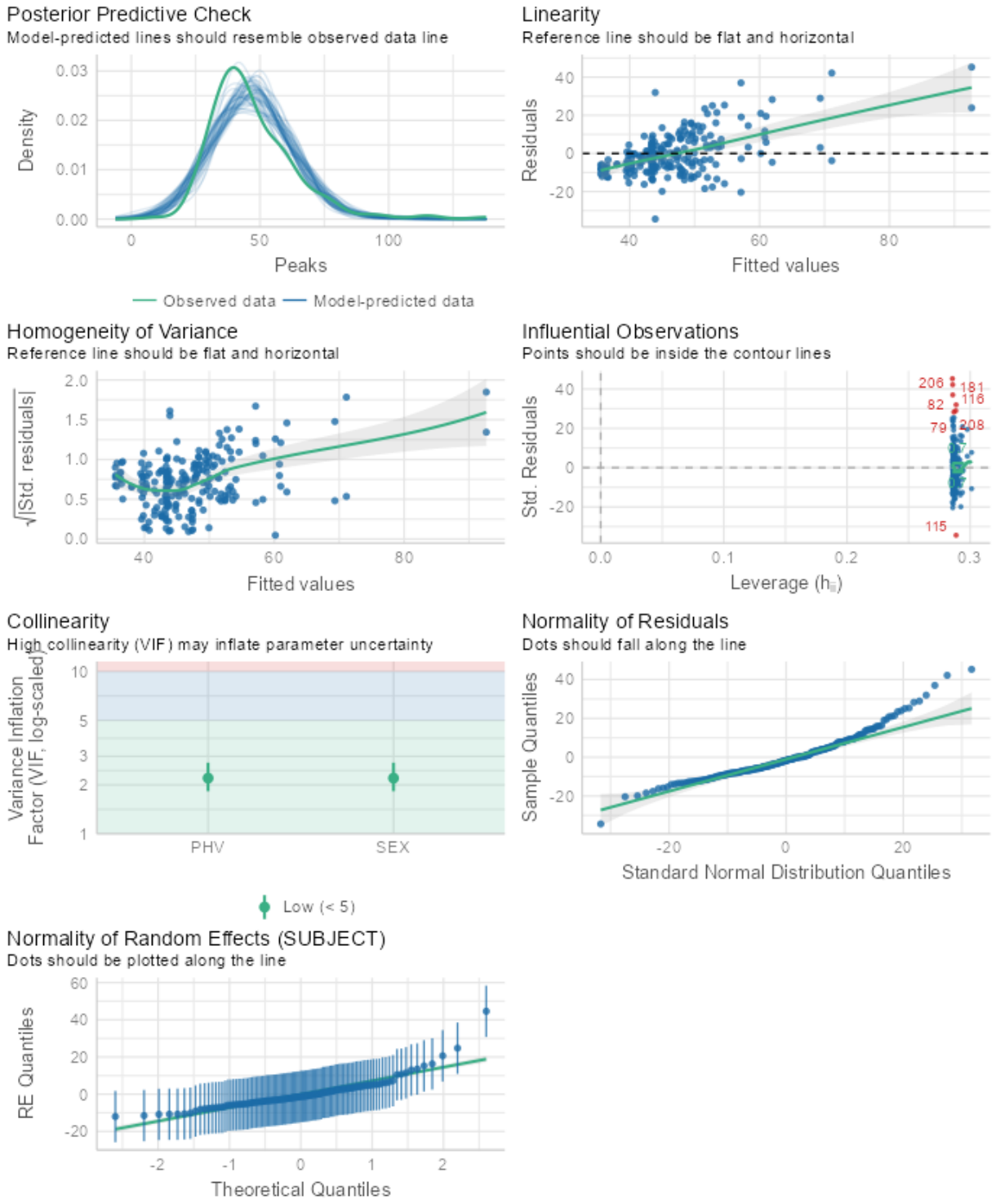

Figure 48: Model 2 acceleration peaks LMER model assumption tests for Broad

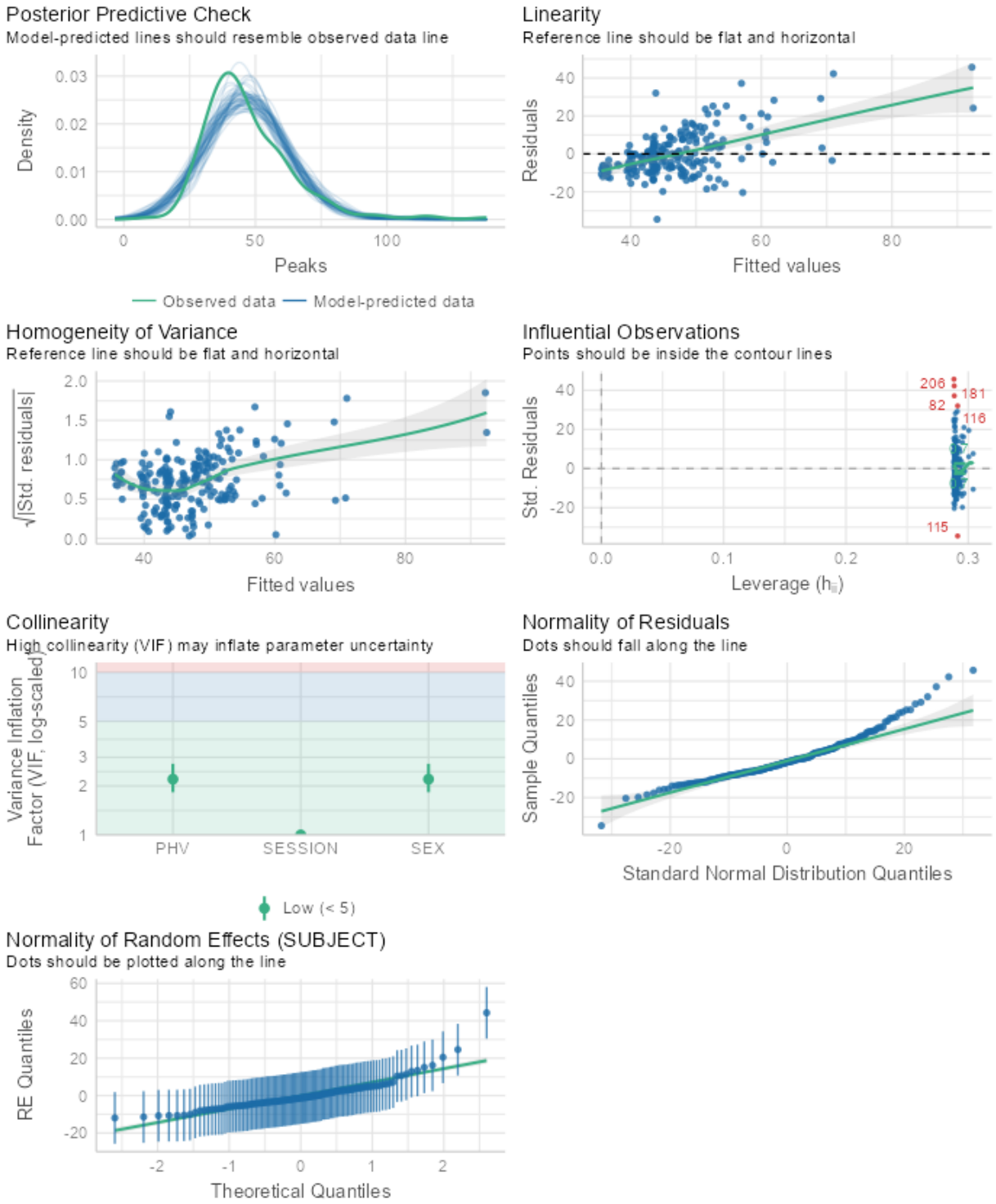

Figure 49: Model 3 acceleration peaks LMER model assumption tests for Broad

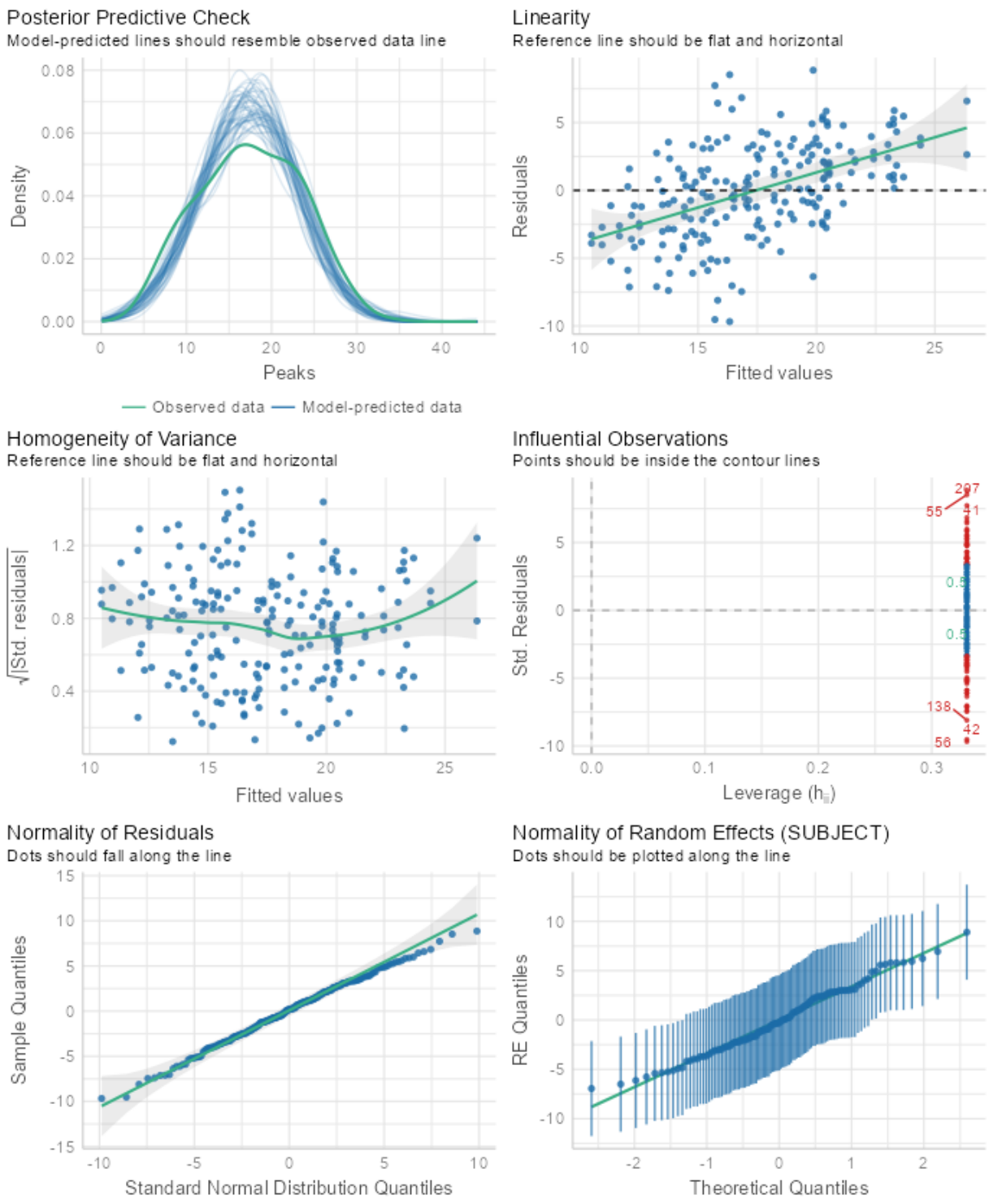

Figure 50: Null model acceleration peaks LMER model assumption tests for DNB

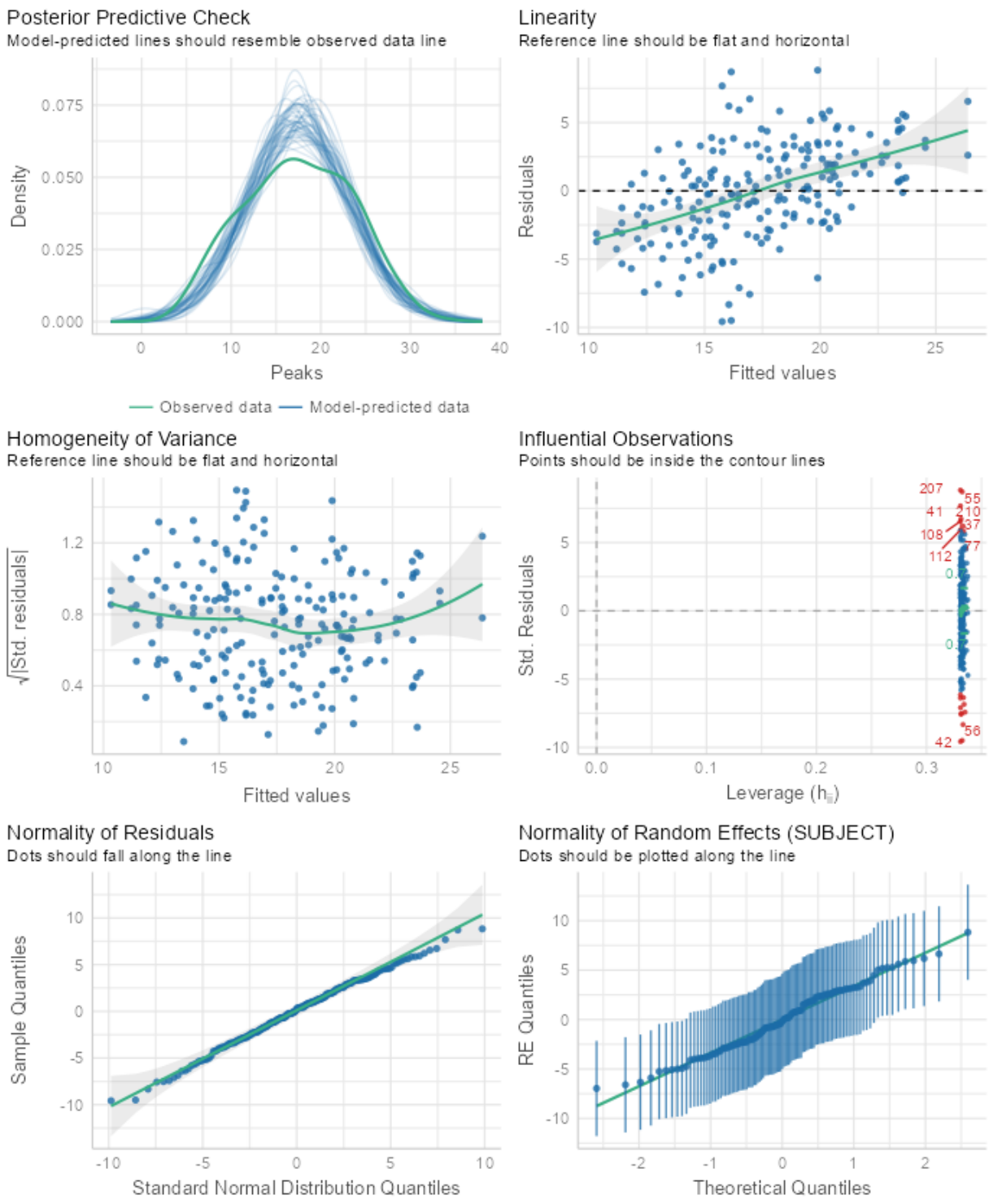

Figure 51: Model 1 acceleration peaks LMER model assumption tests for DNB

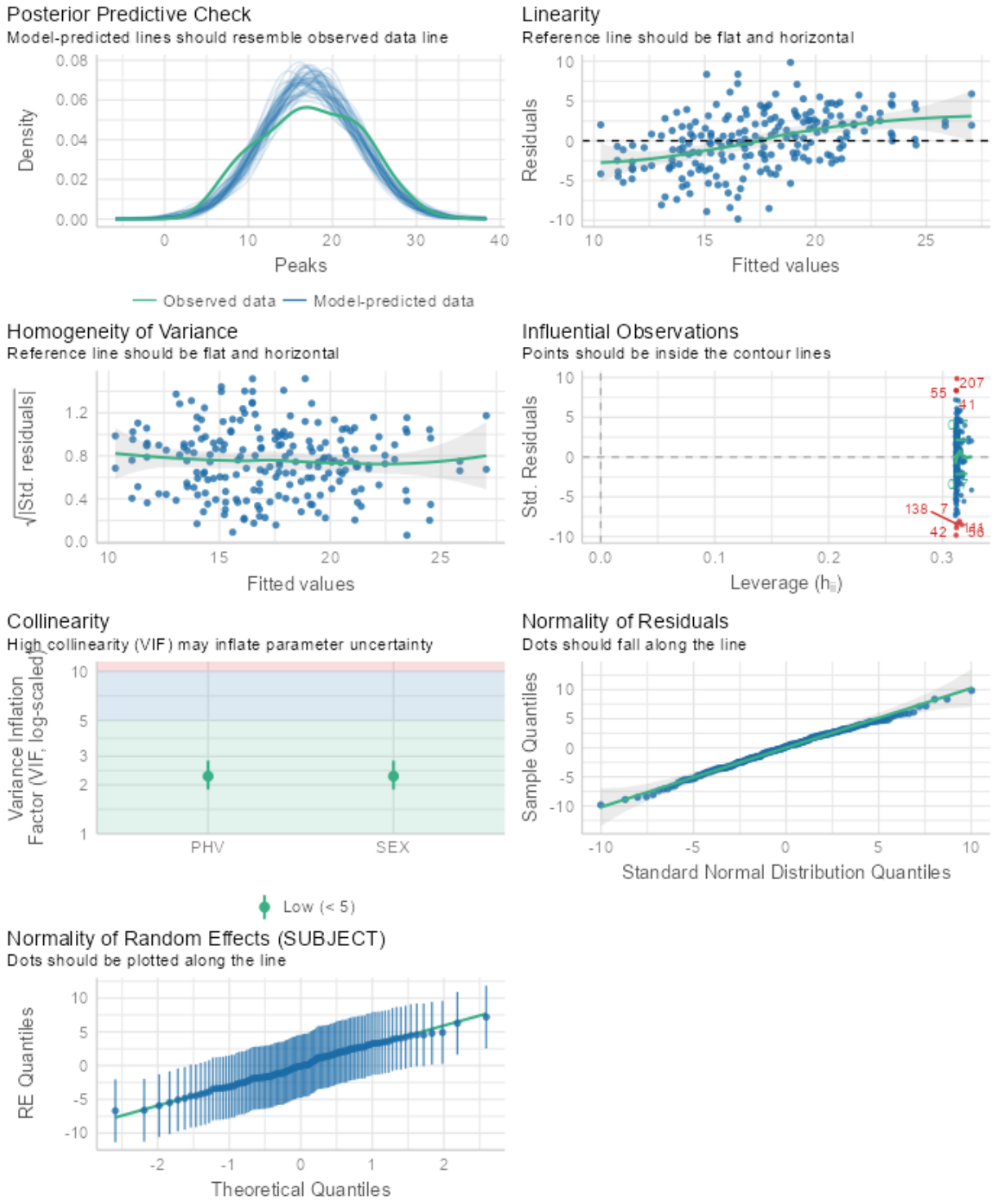

Figure 52: Model 2 acceleration peaks LMER model assumption tests for DNB

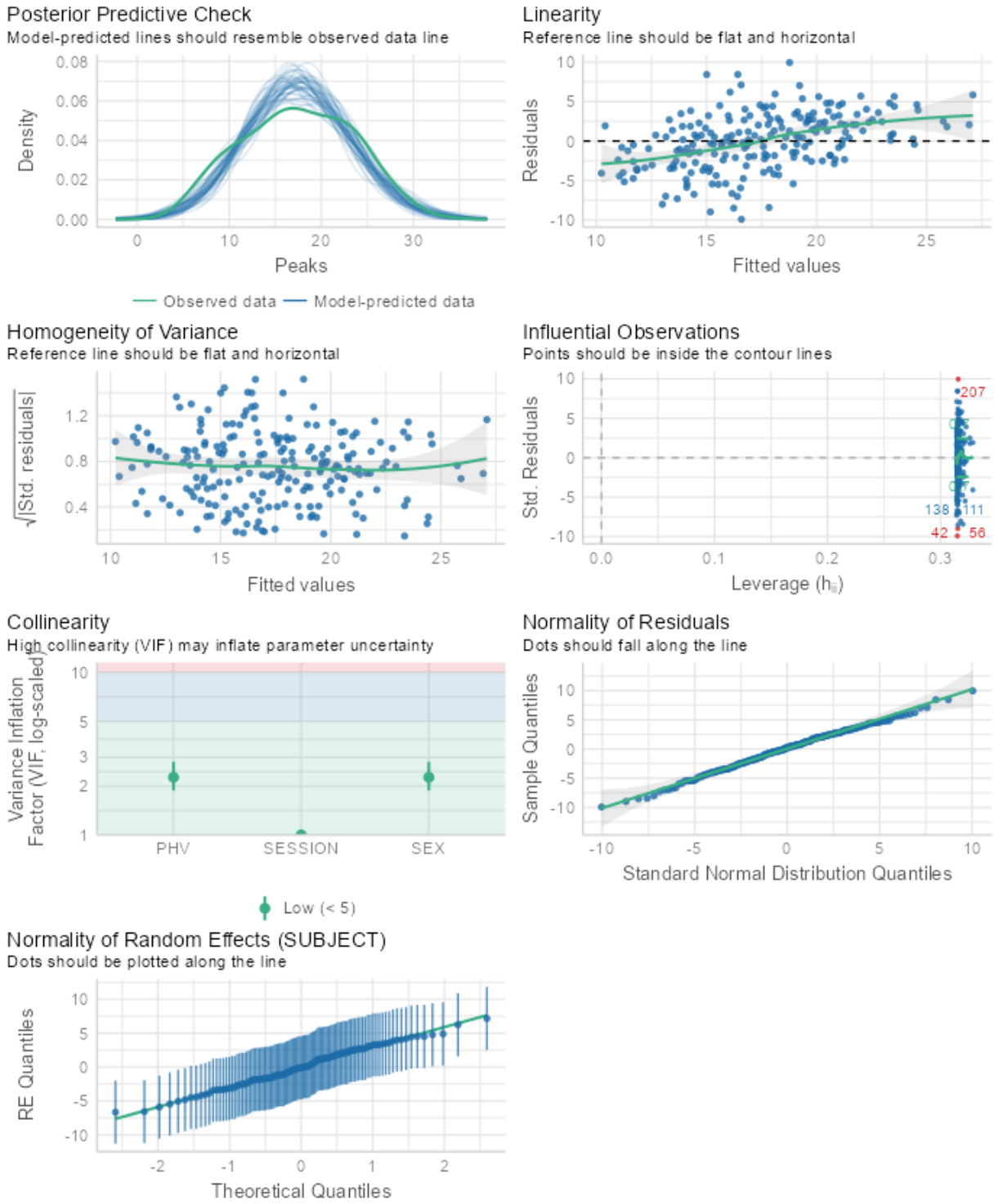

Figure 53: Model 3 acceleration peaks LMER model assumption tests for DNB

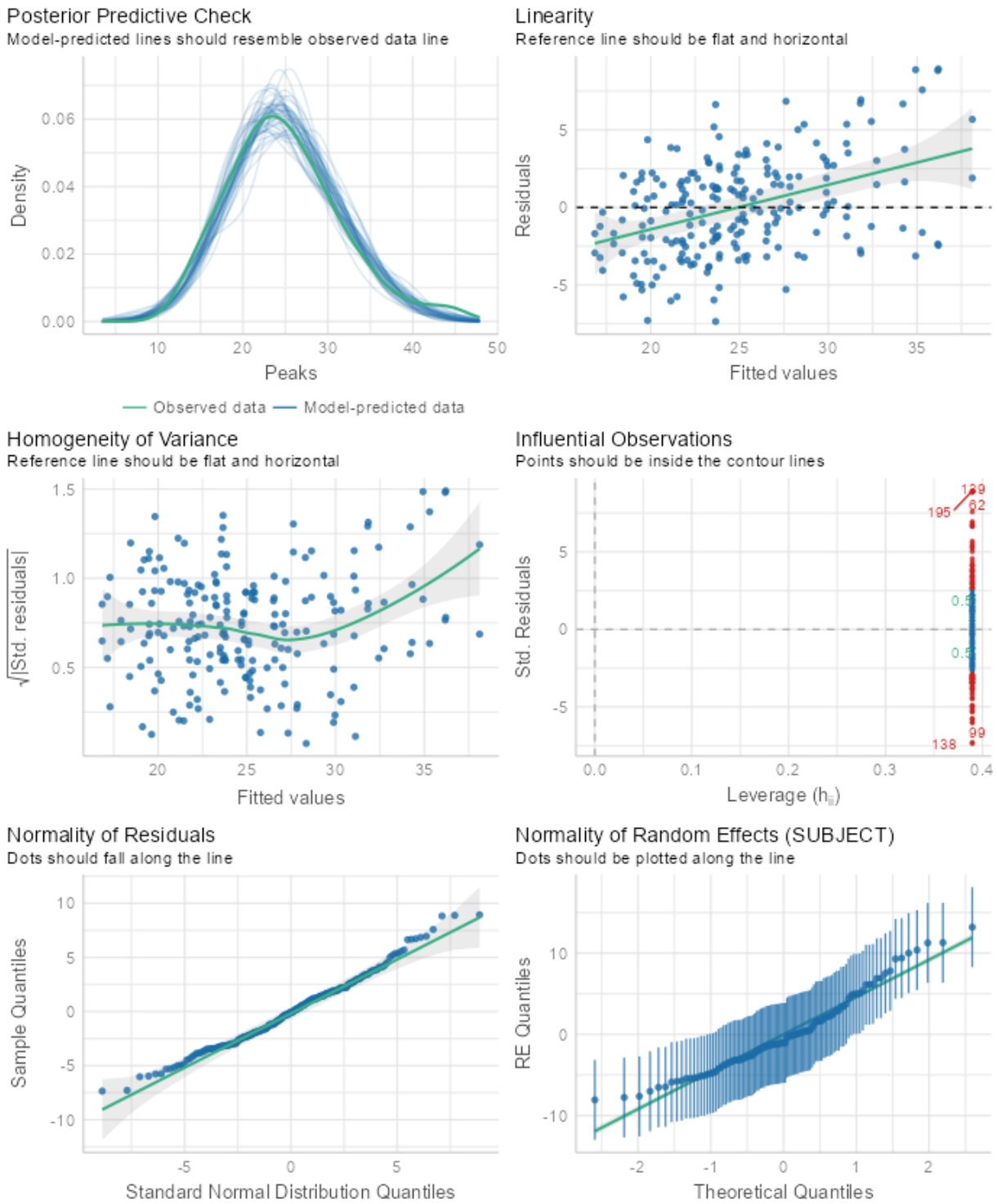

Figure 54: Null model acceleration peaks LMER model assumption tests for 5-10-5 shuffle drill

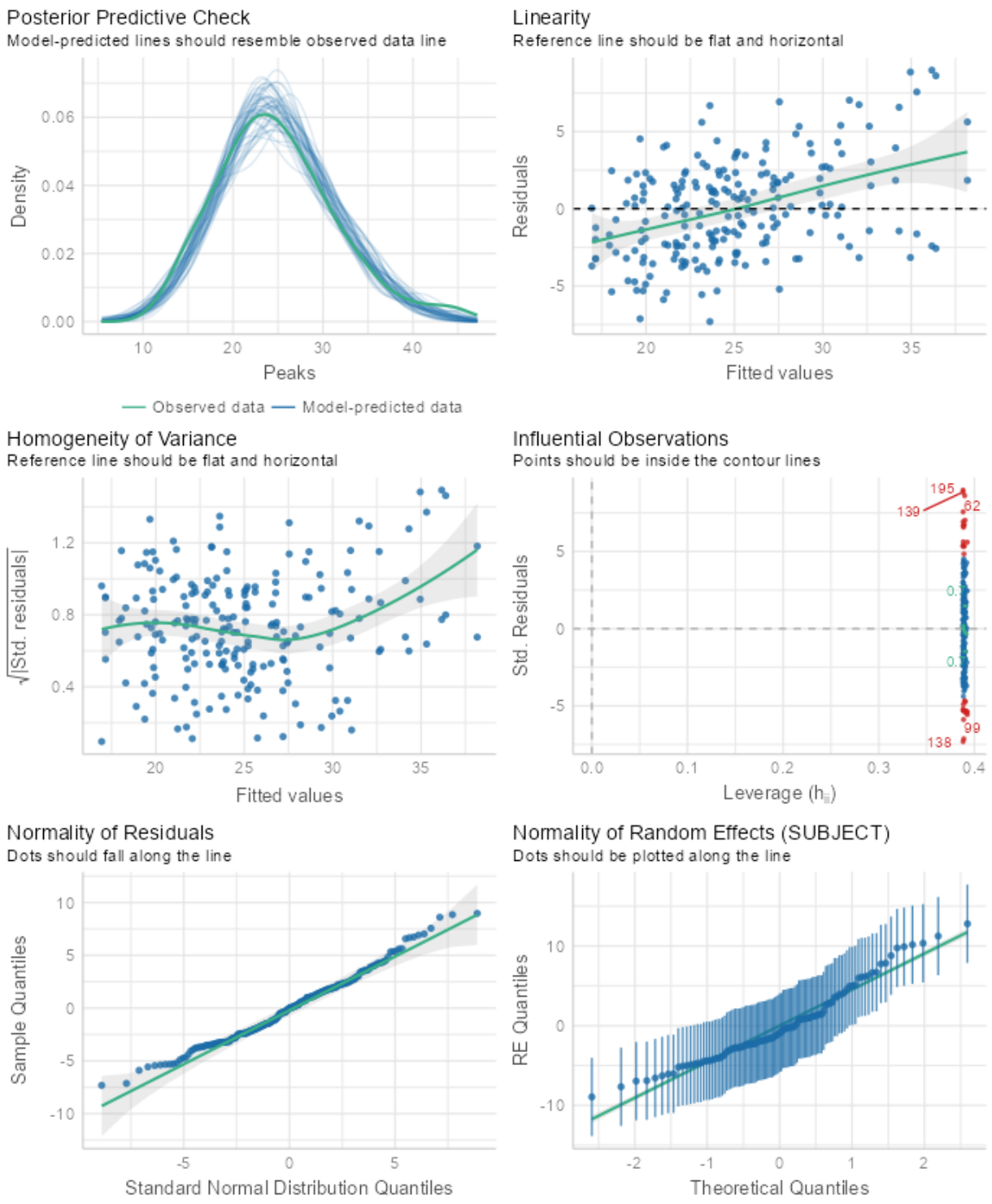

Figure 55: Model 1 acceleration peaks LMER model assumption tests for 5-10-5 shuffle drill

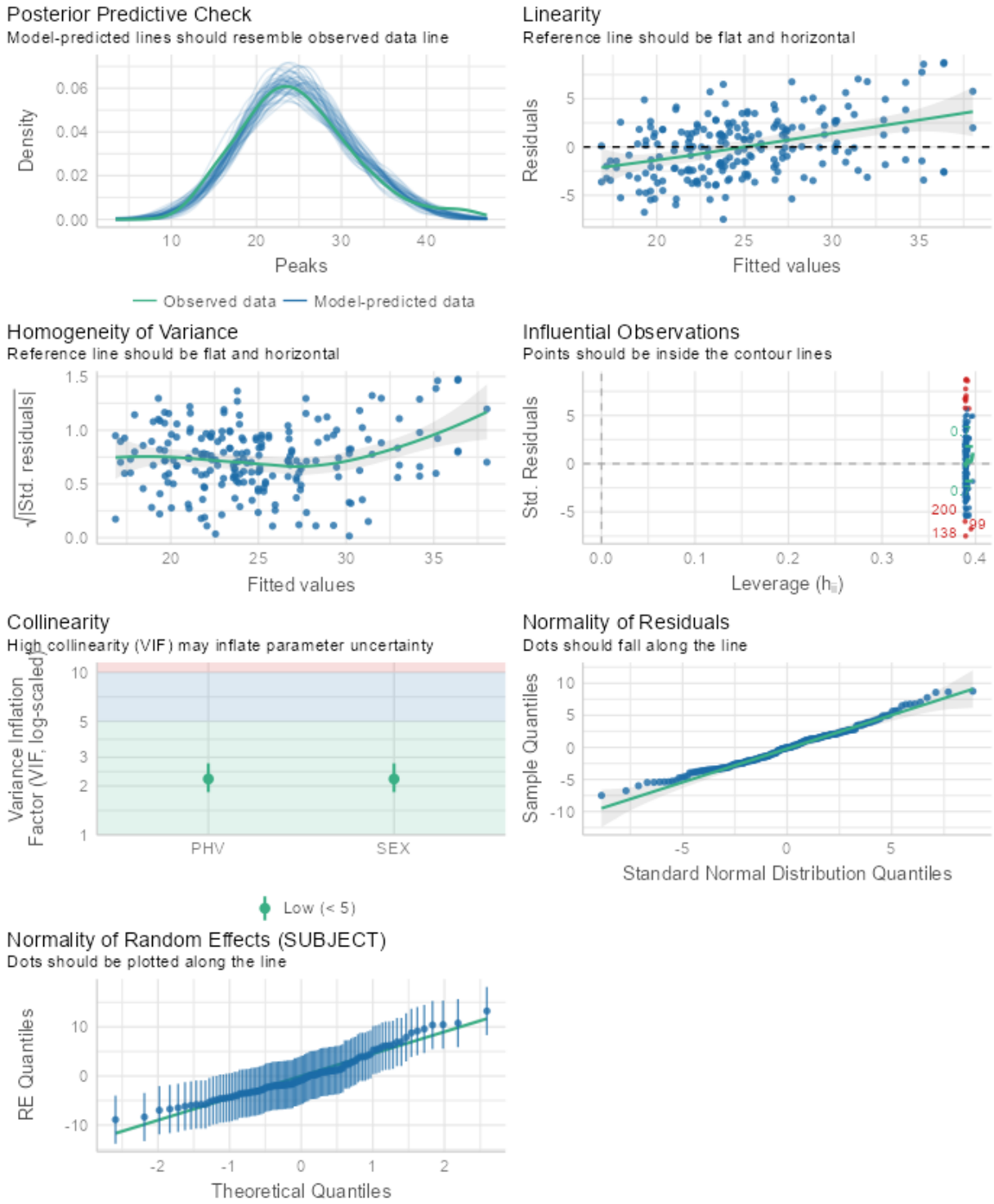

Figure 56: Model 2 acceleration peaks LMER model assumption tests for 5-10-5 shuffle drill

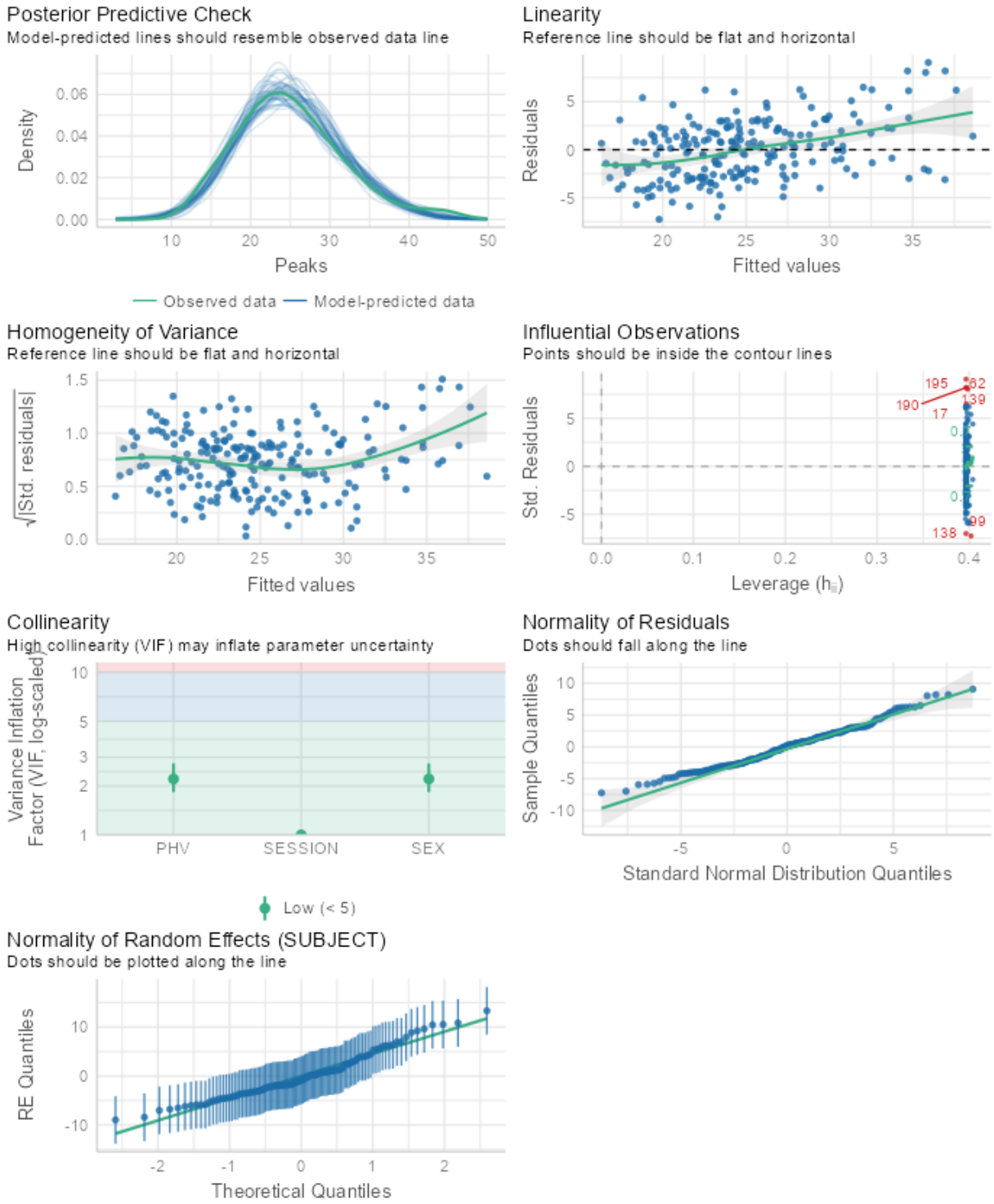

Figure 57: Model 3 acceleration peaks LMER model assumption tests for 5-10-5 shuffle drill

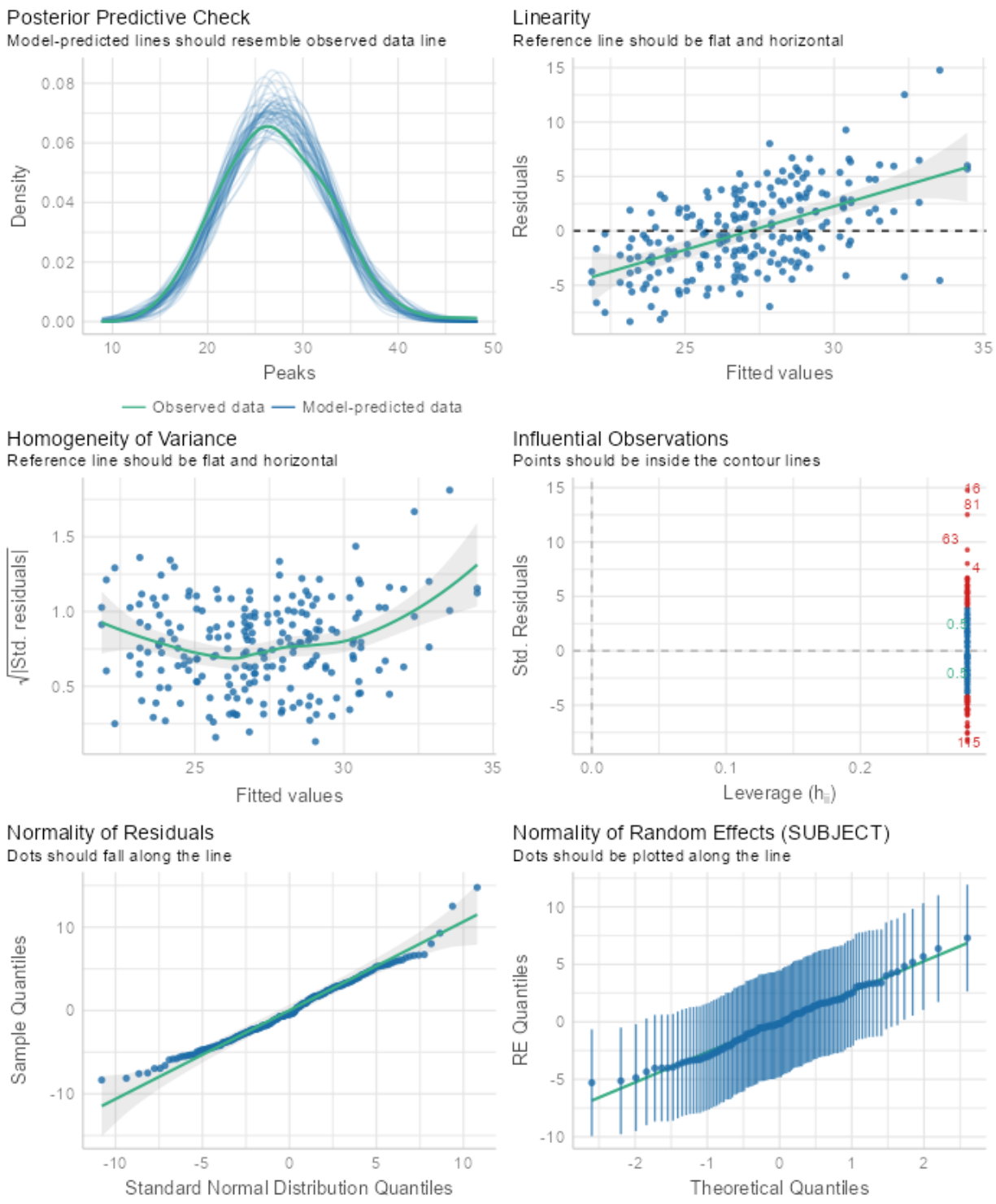

Figure 58: Null model acceleration peaks LMER model assumption tests for M-L

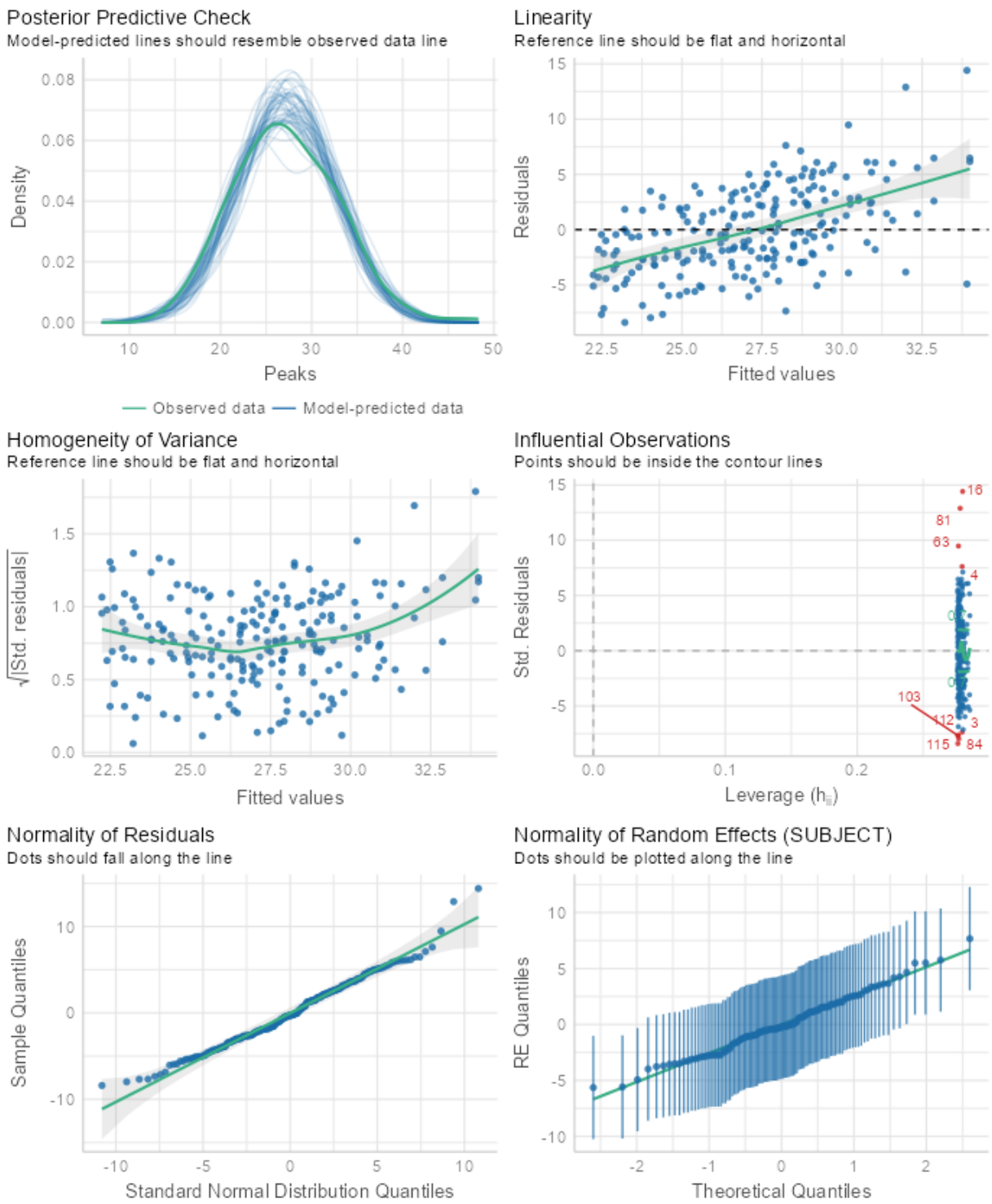

Figure 59: Model 1 acceleration peaks LMER model assumption tests for M-L

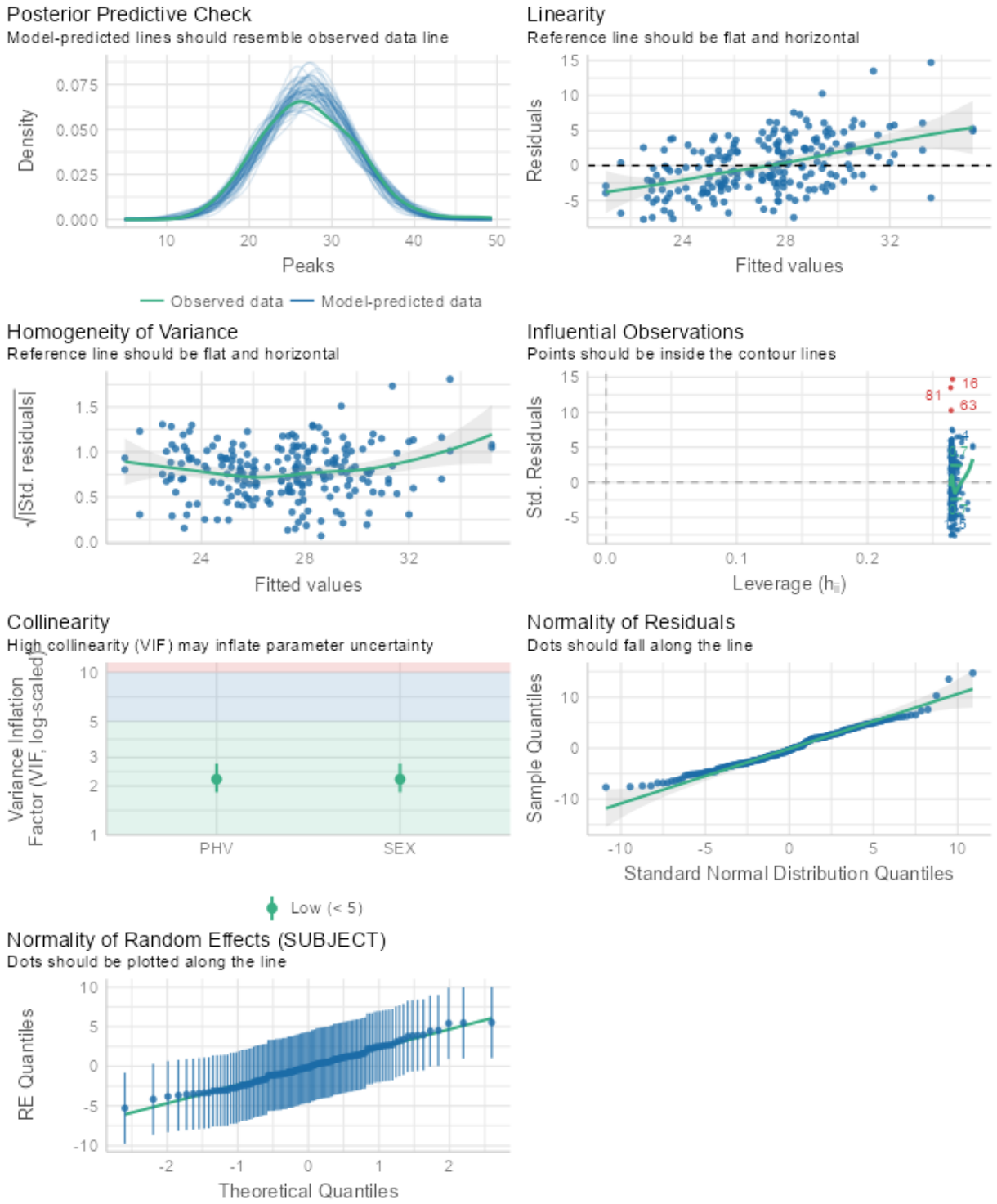

Figure 60: Model 2 acceleration peaks LMER model assumption tests for M-L

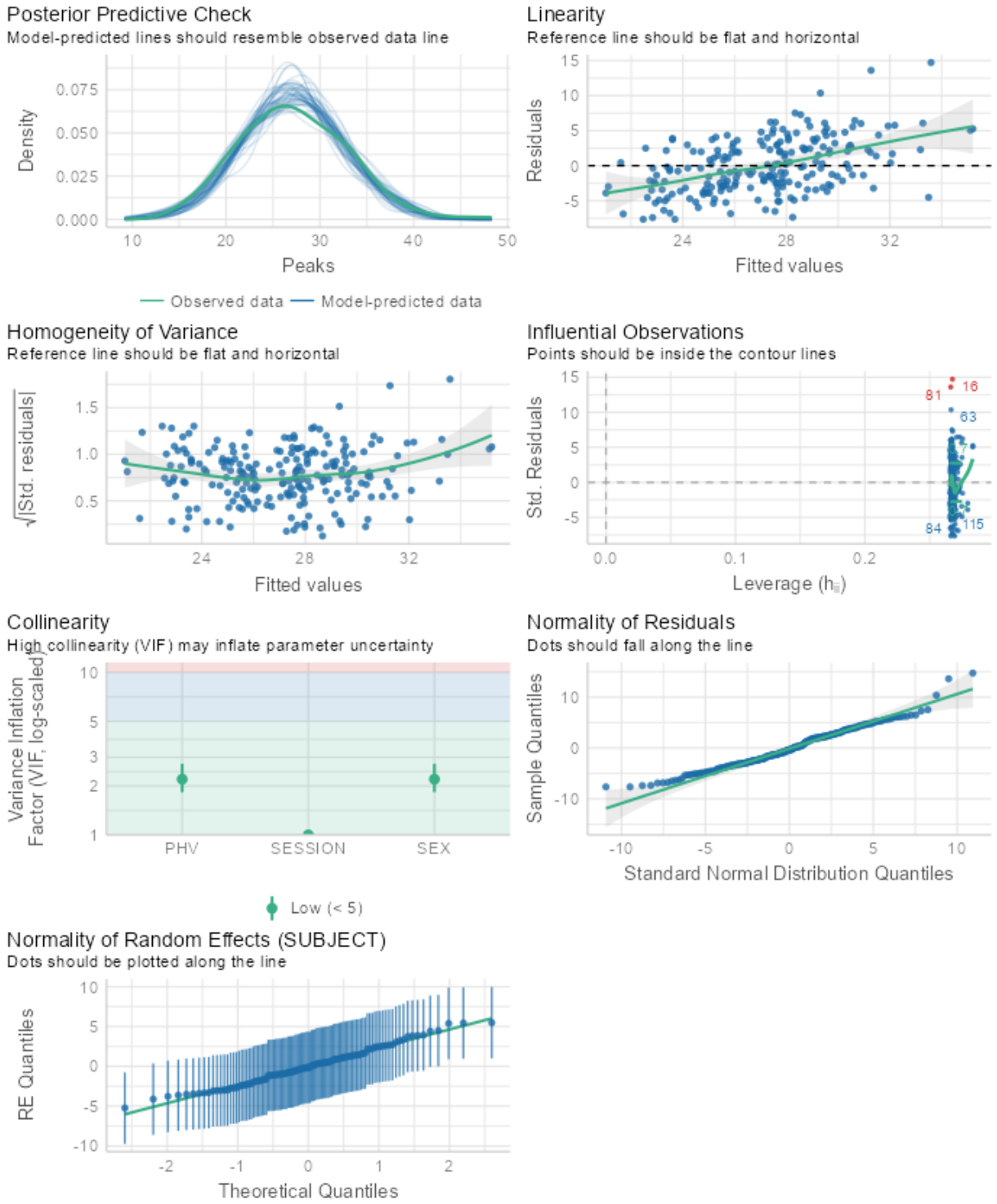

Figure 61: Model 3 acceleration peaks LMER model assumption tests for M-L

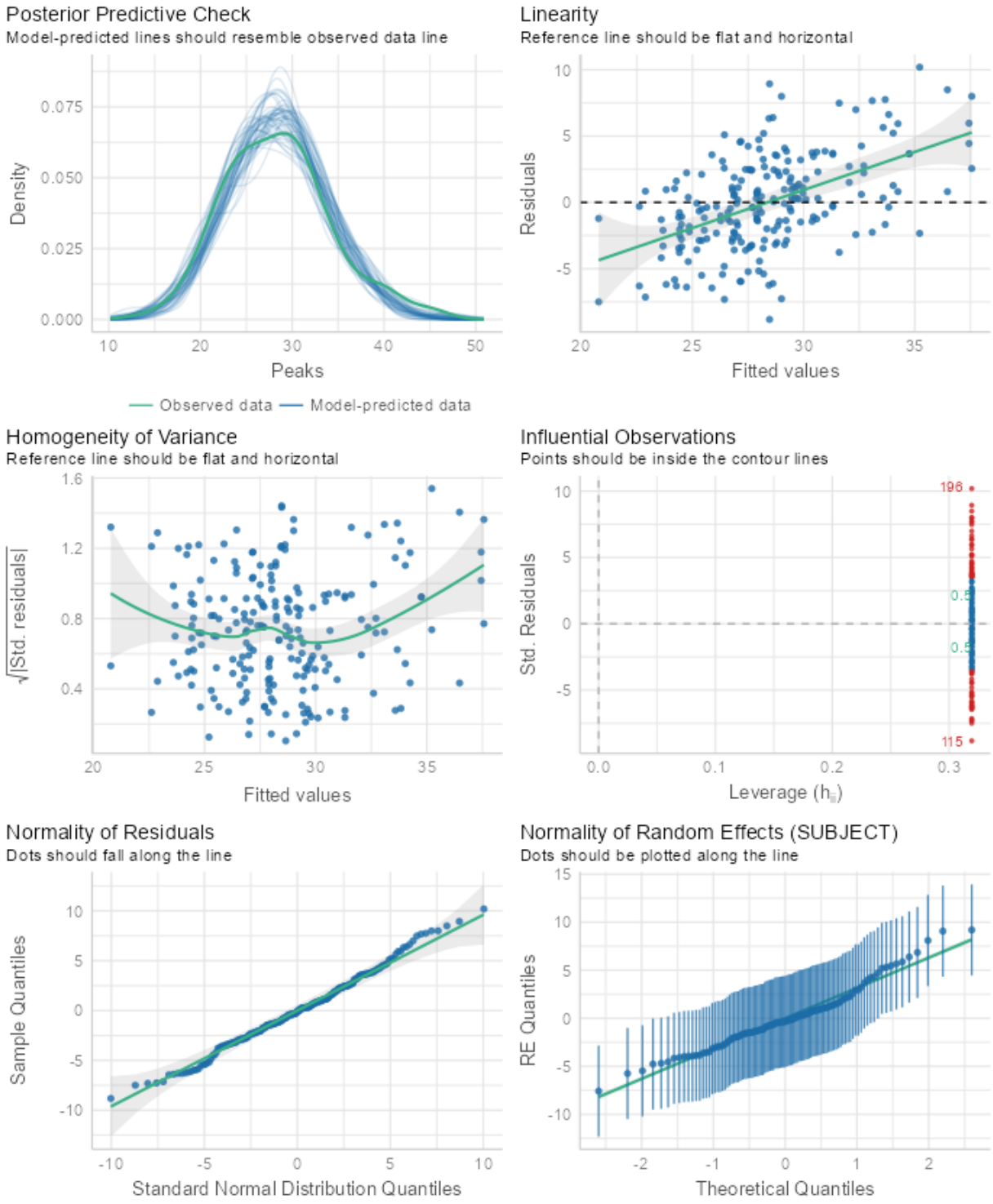

Figure 62: Null model acceleration peaks LMER model assumption tests for M-R

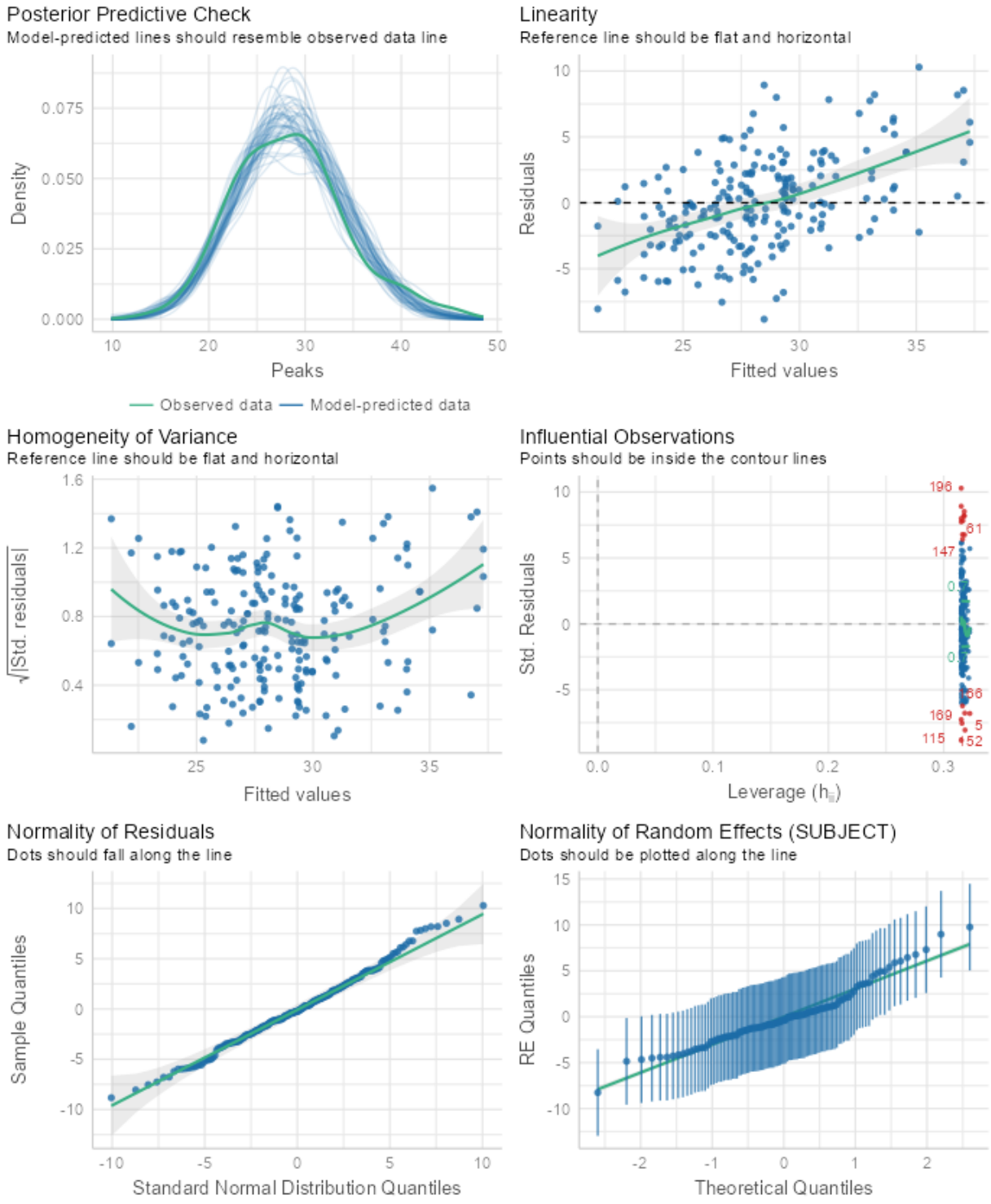

Figure 63: Model 1 acceleration peaks LMER model assumption tests for M-R

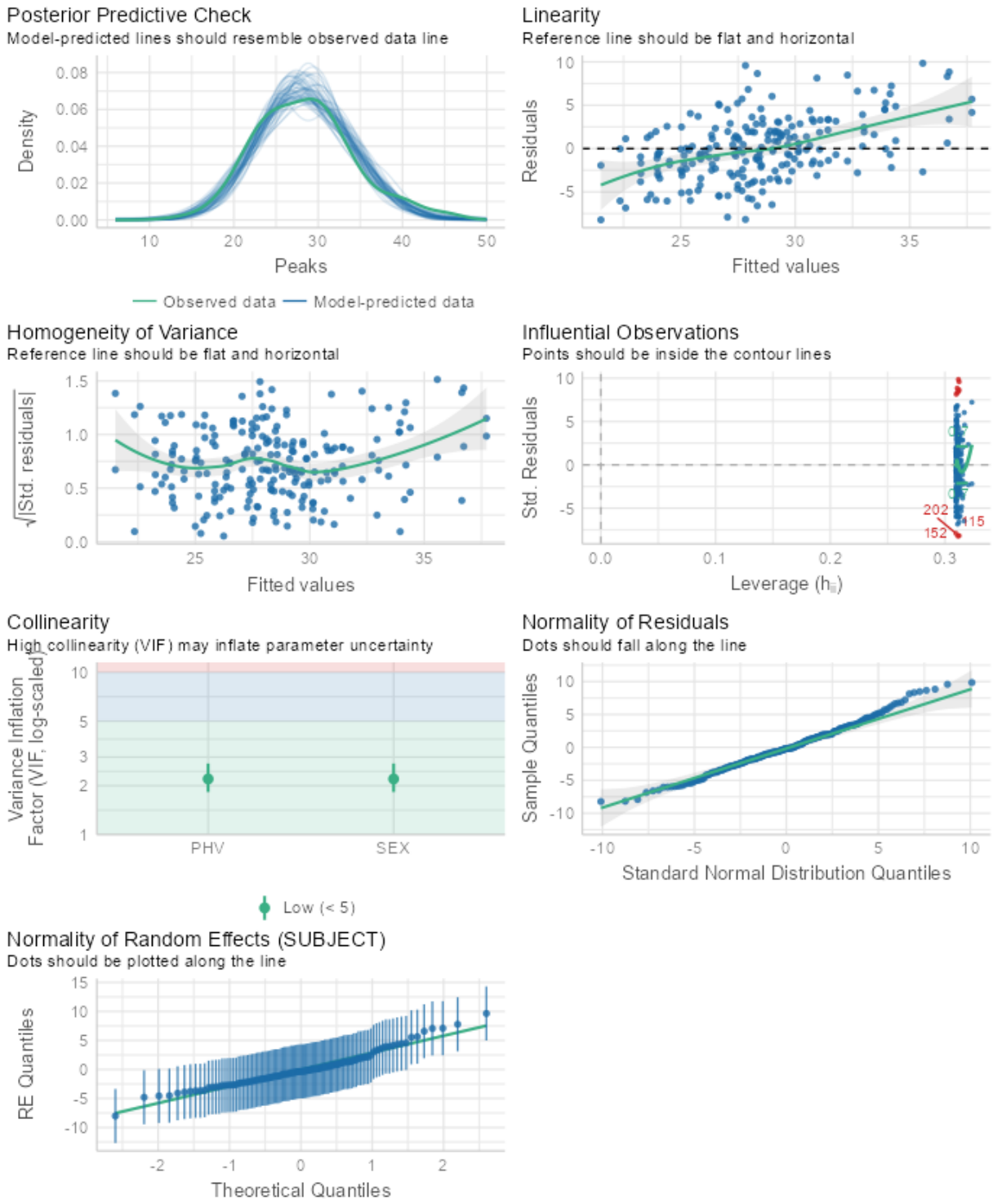

Figure 64: Model 2 acceleration peaks LMER model assumption tests for M-R

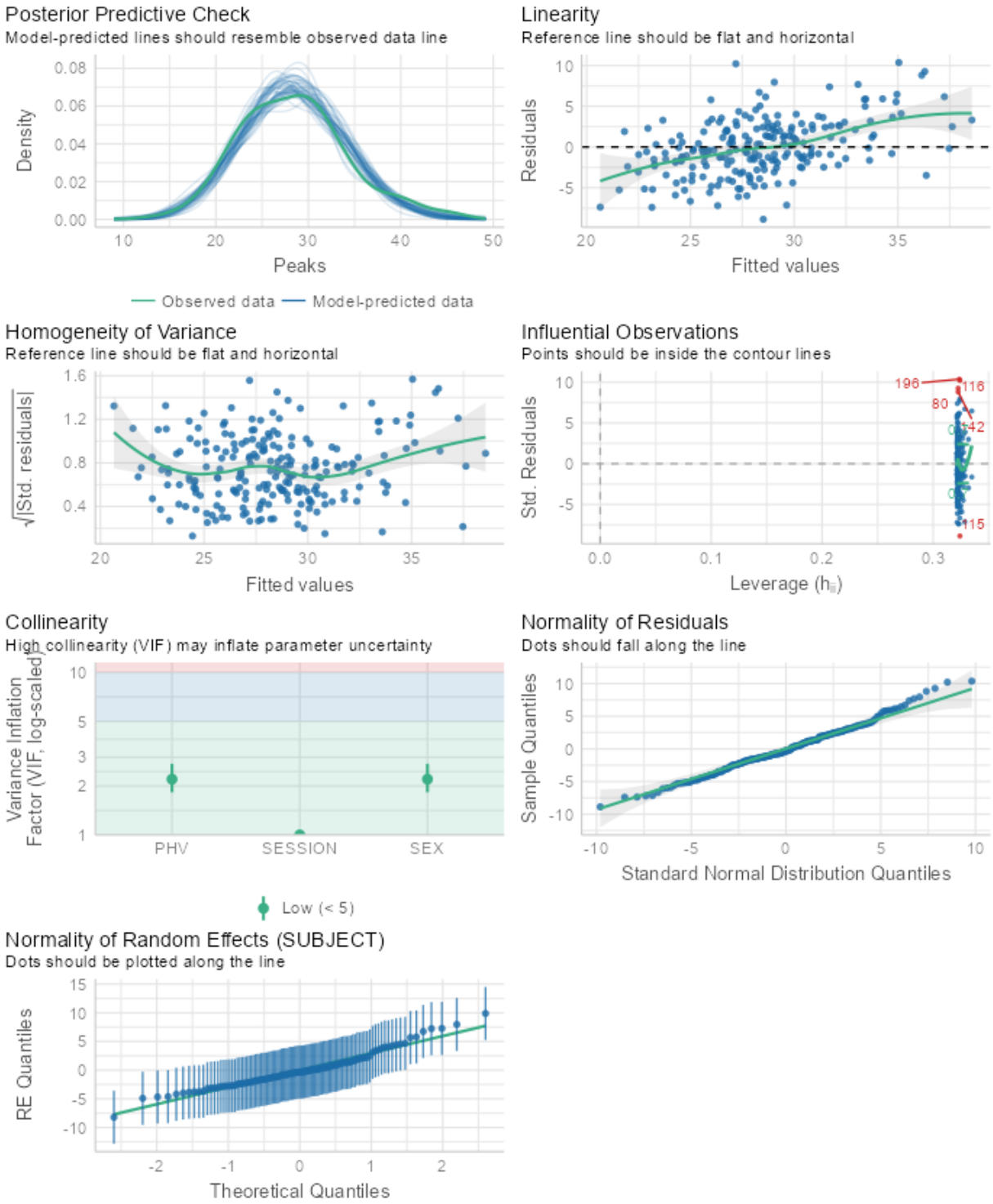

Figure 65: Model 3 acceleration peaks LMER model assumption tests for M-R

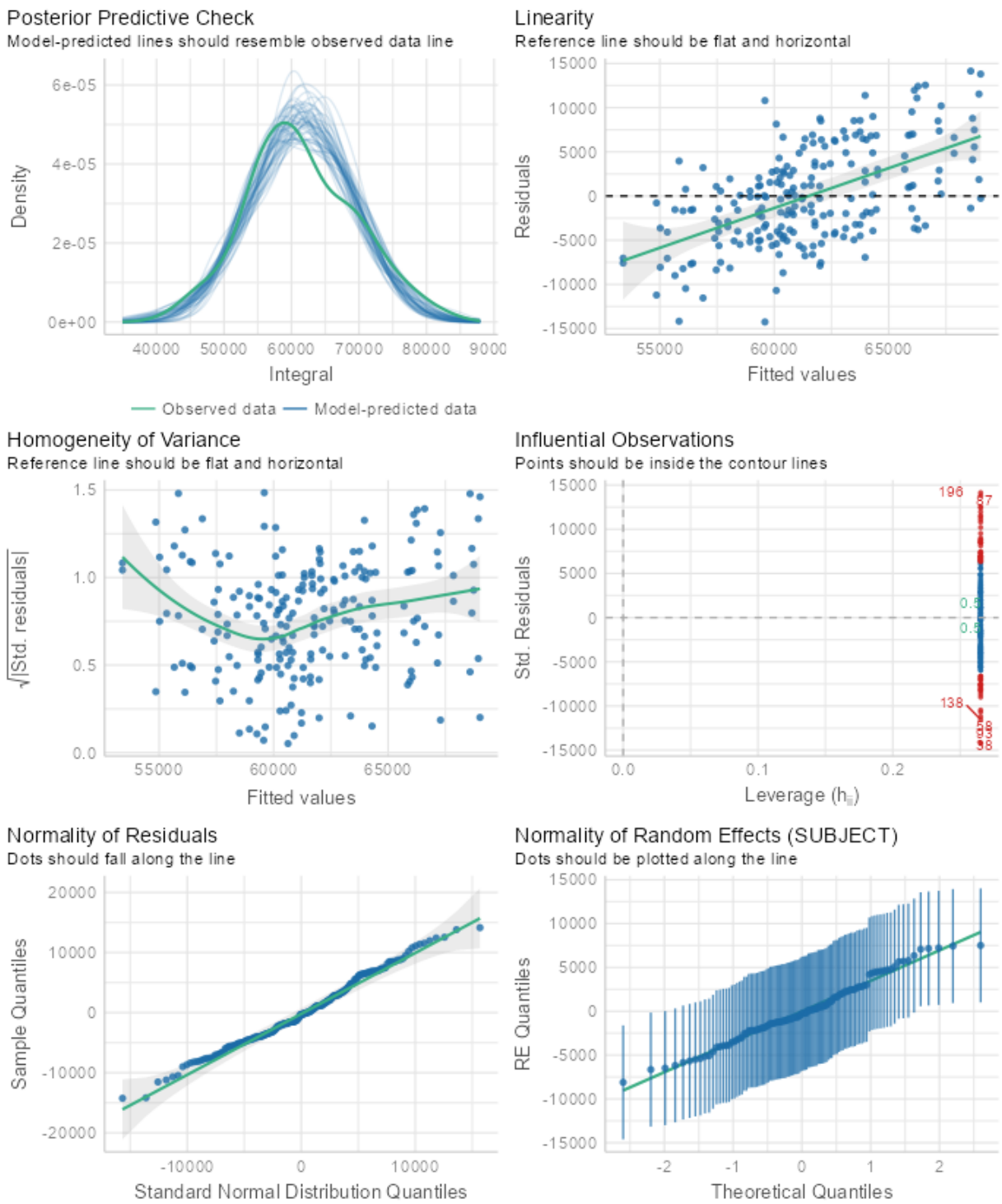

Figure 66: Null model acceleration integrals LMER model assumption tests for 40yd

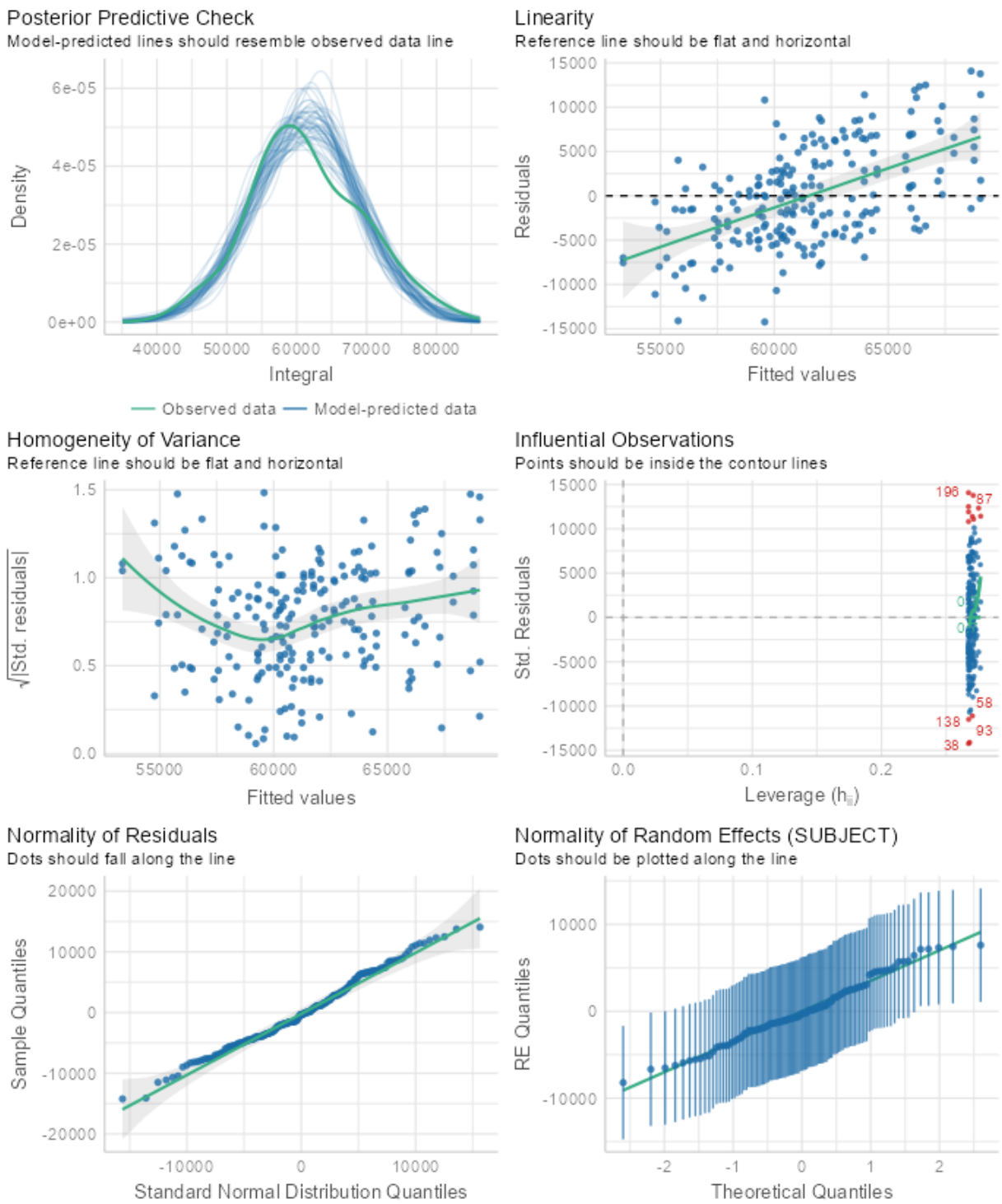

Figure 67: Model 1 acceleration integrals LMER model assumption tests for 40yd

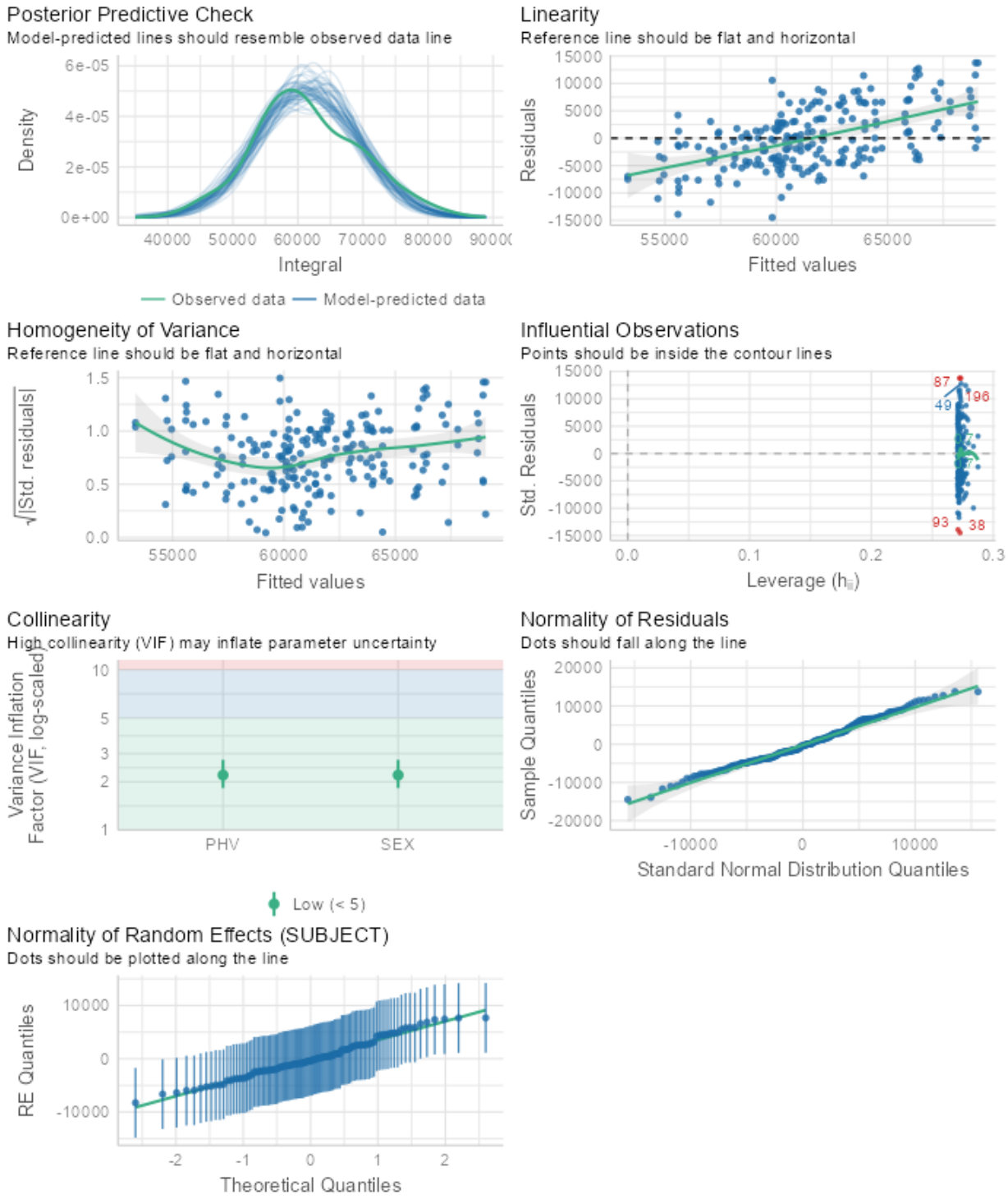

Figure 68: Model 2 acceleration integrals LMER model assumption tests for 40yd

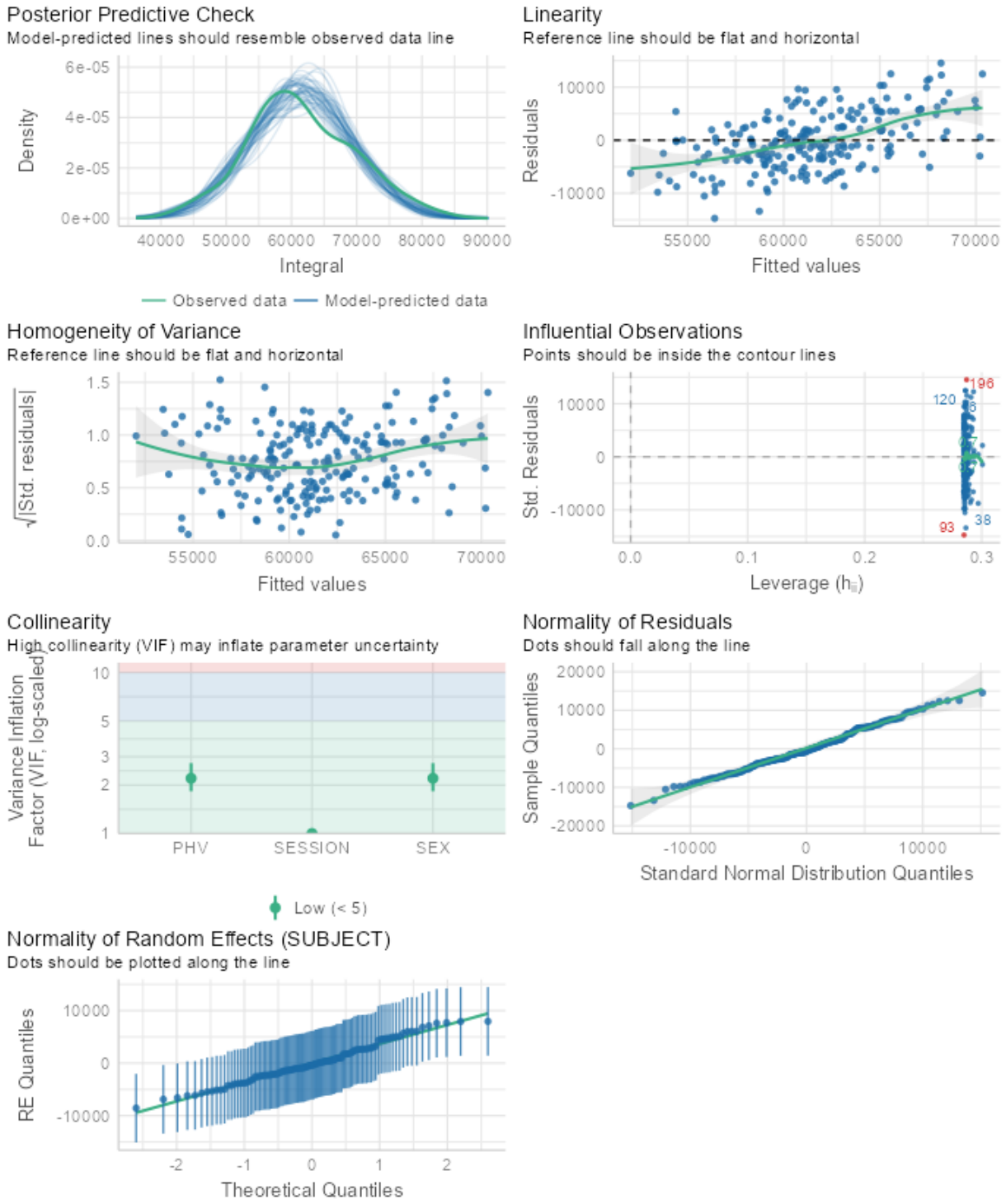

Figure 69: Model 3 acceleration integrals LMER model assumption tests for 40yd

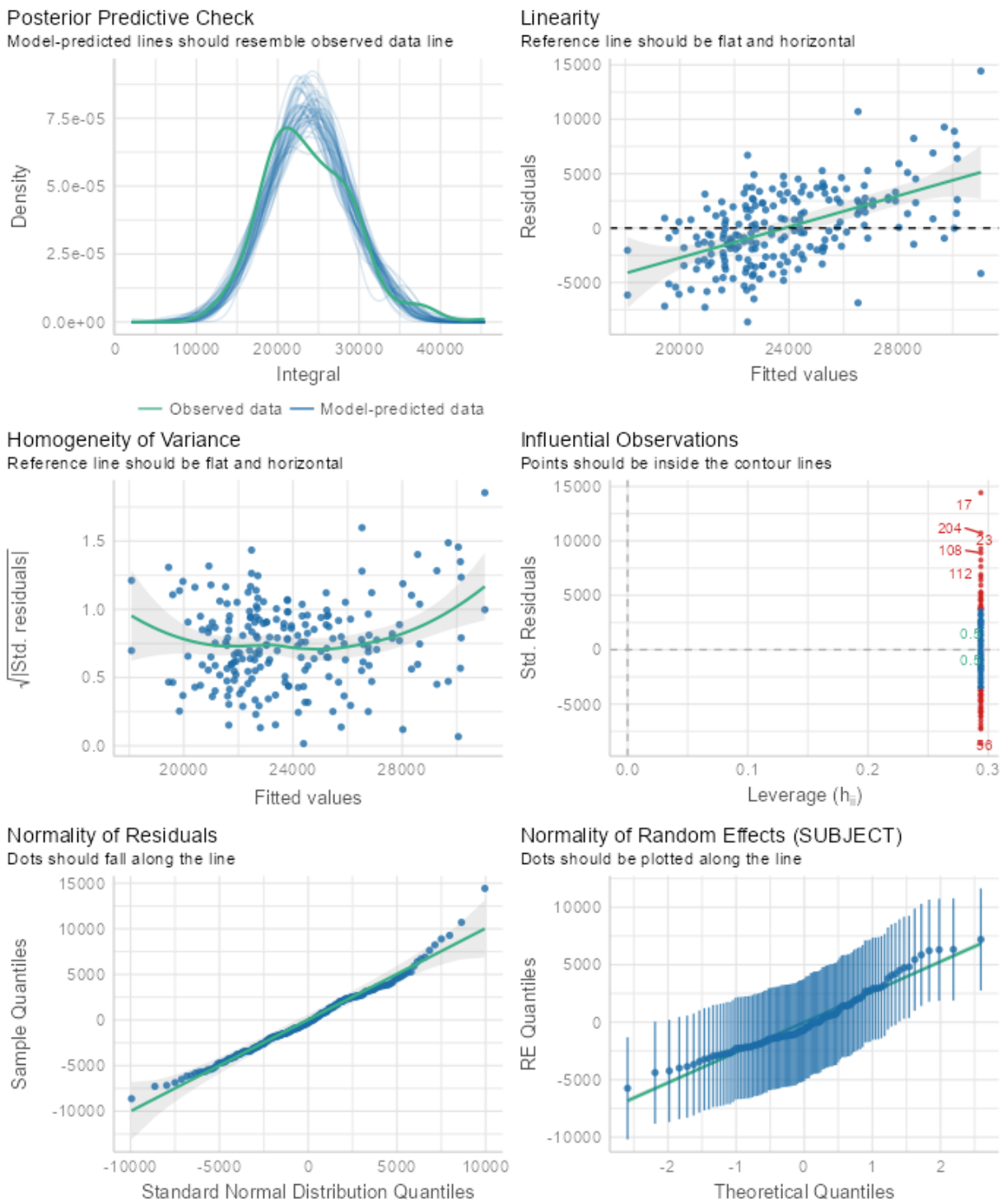

Figure 70: Null model acceleration integrals LMER model assumption tests for DNB

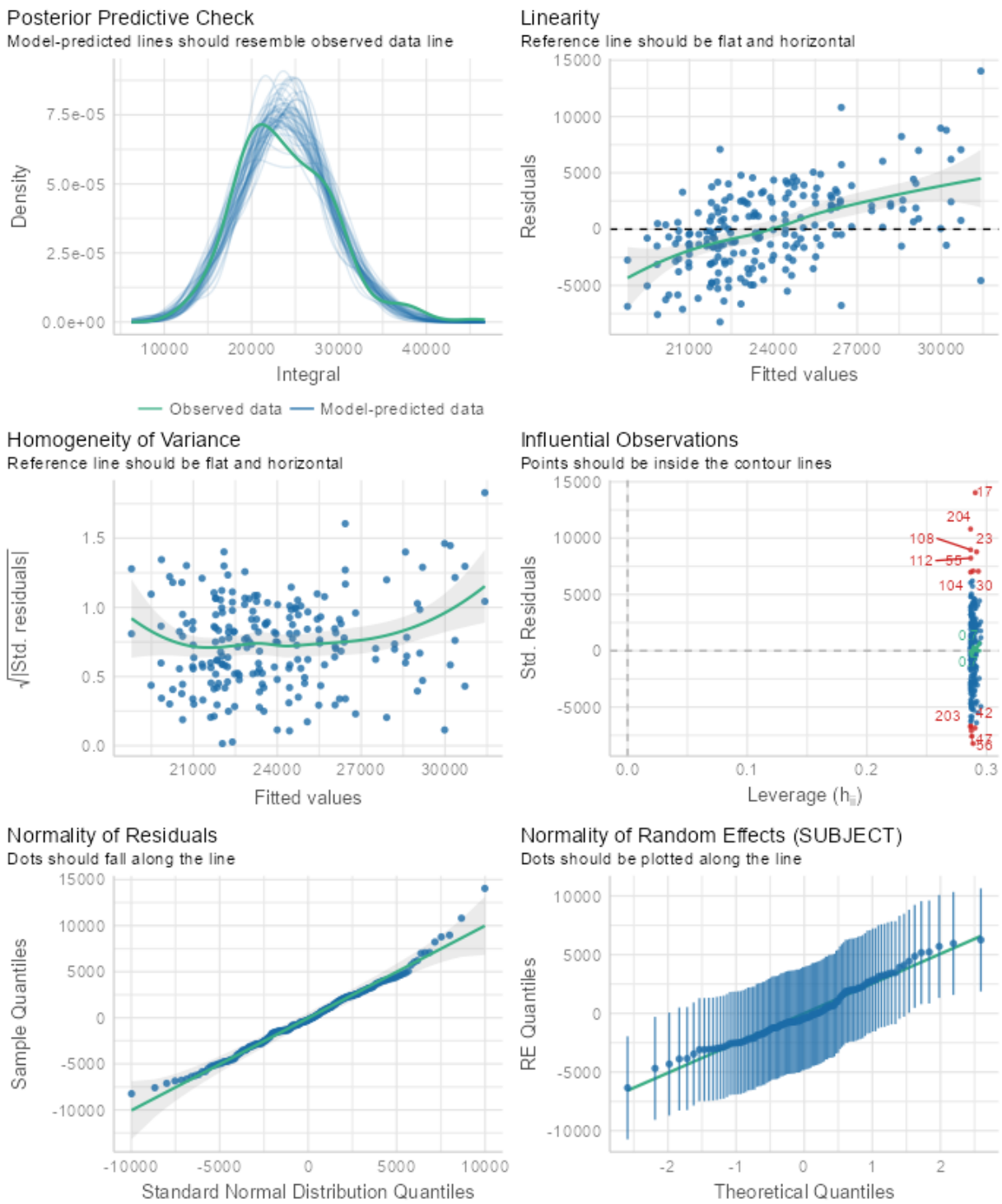

Figure 71: Model 1 acceleration integrals LMER model assumption tests for DNB

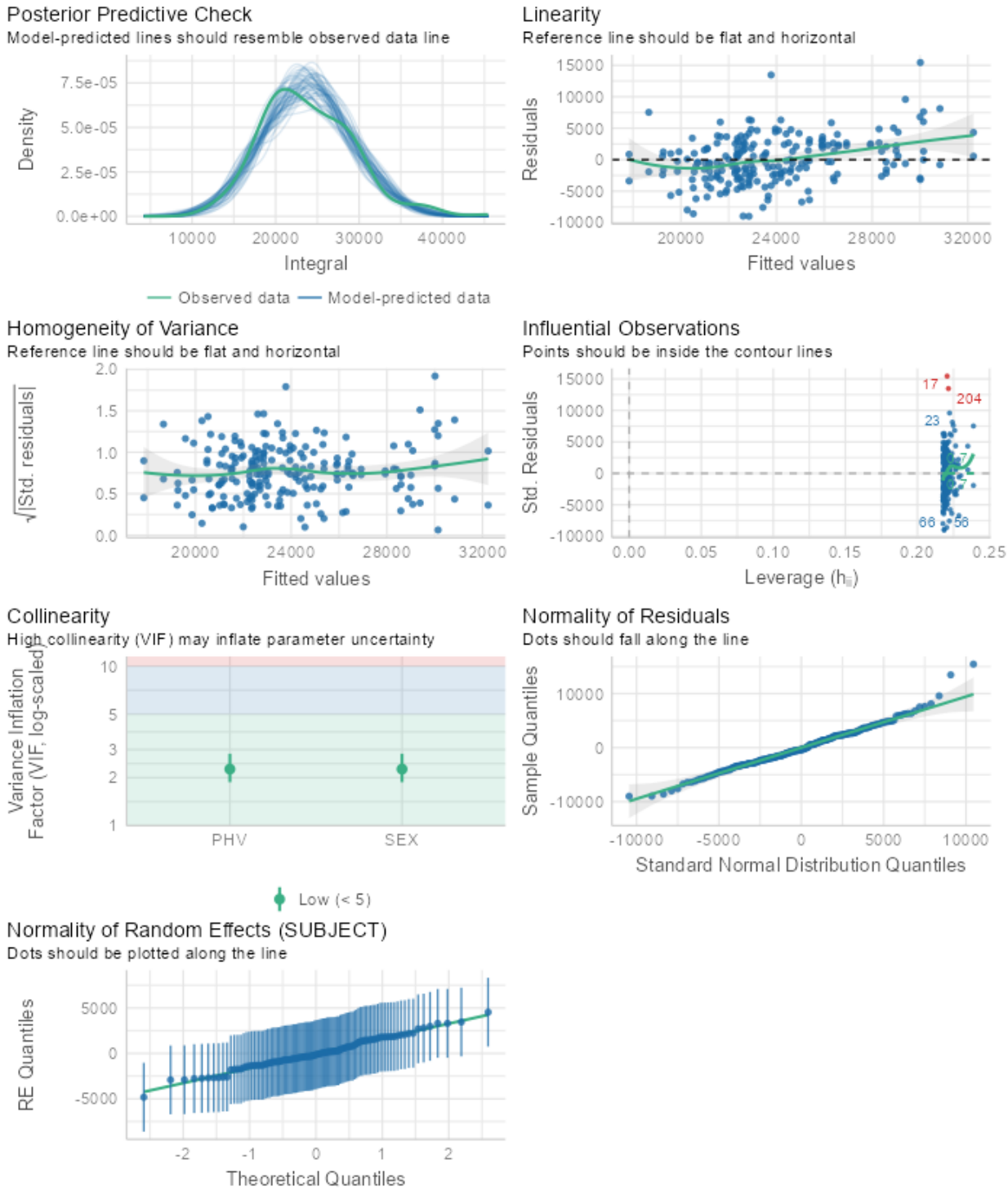

Figure 72: Model 2 acceleration integrals LMER model assumption tests for DNB

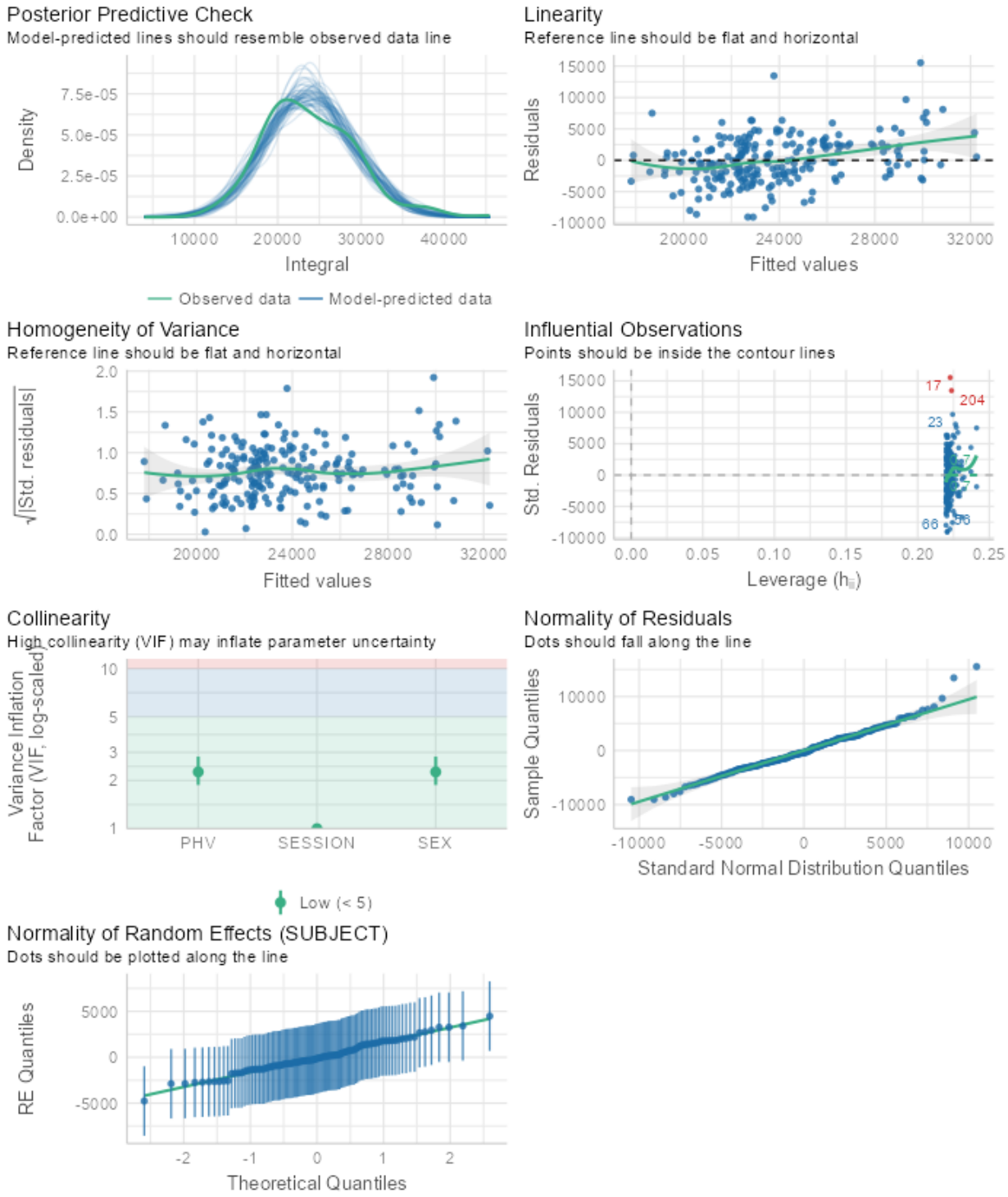

Figure 73: Model 3 acceleration integrals LMER model assumption tests for DNB

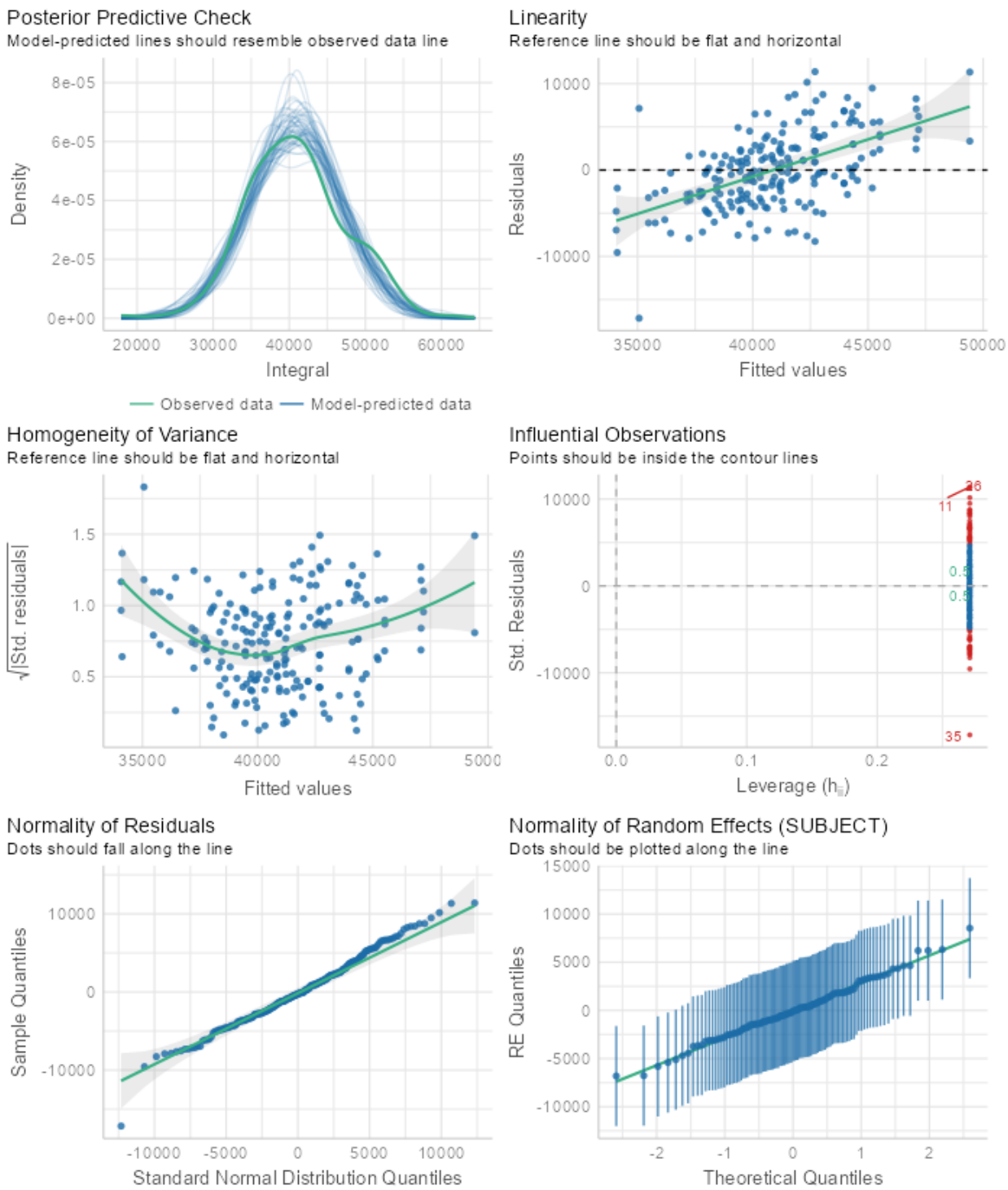

Figure 74: Null model acceleration integrals LMER model assumption tests for 5-10-5 shuffle drill

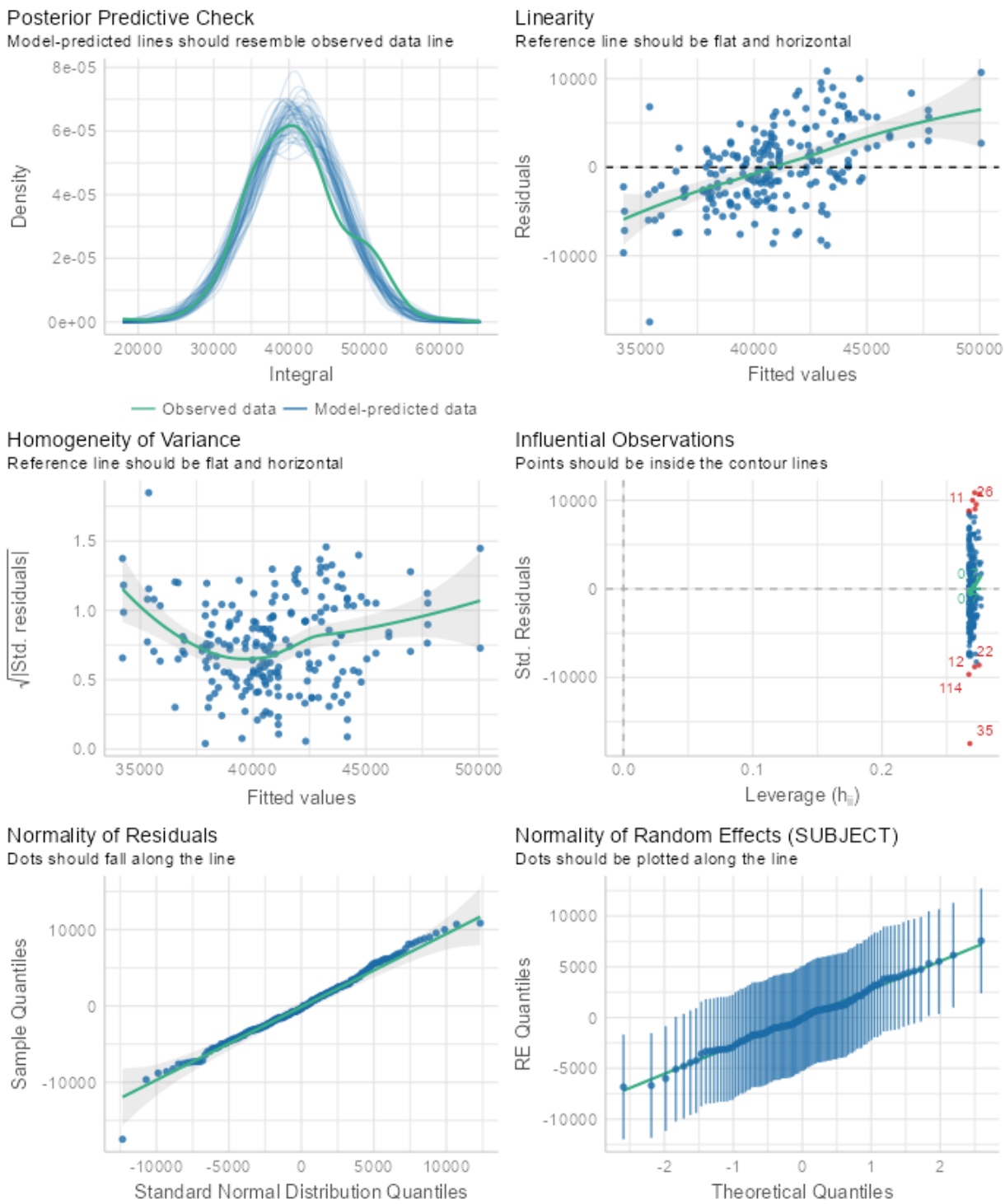

Figure 75: Model 1 acceleration integrals LMER model assumption tests for 5-10-5 shuffle drill

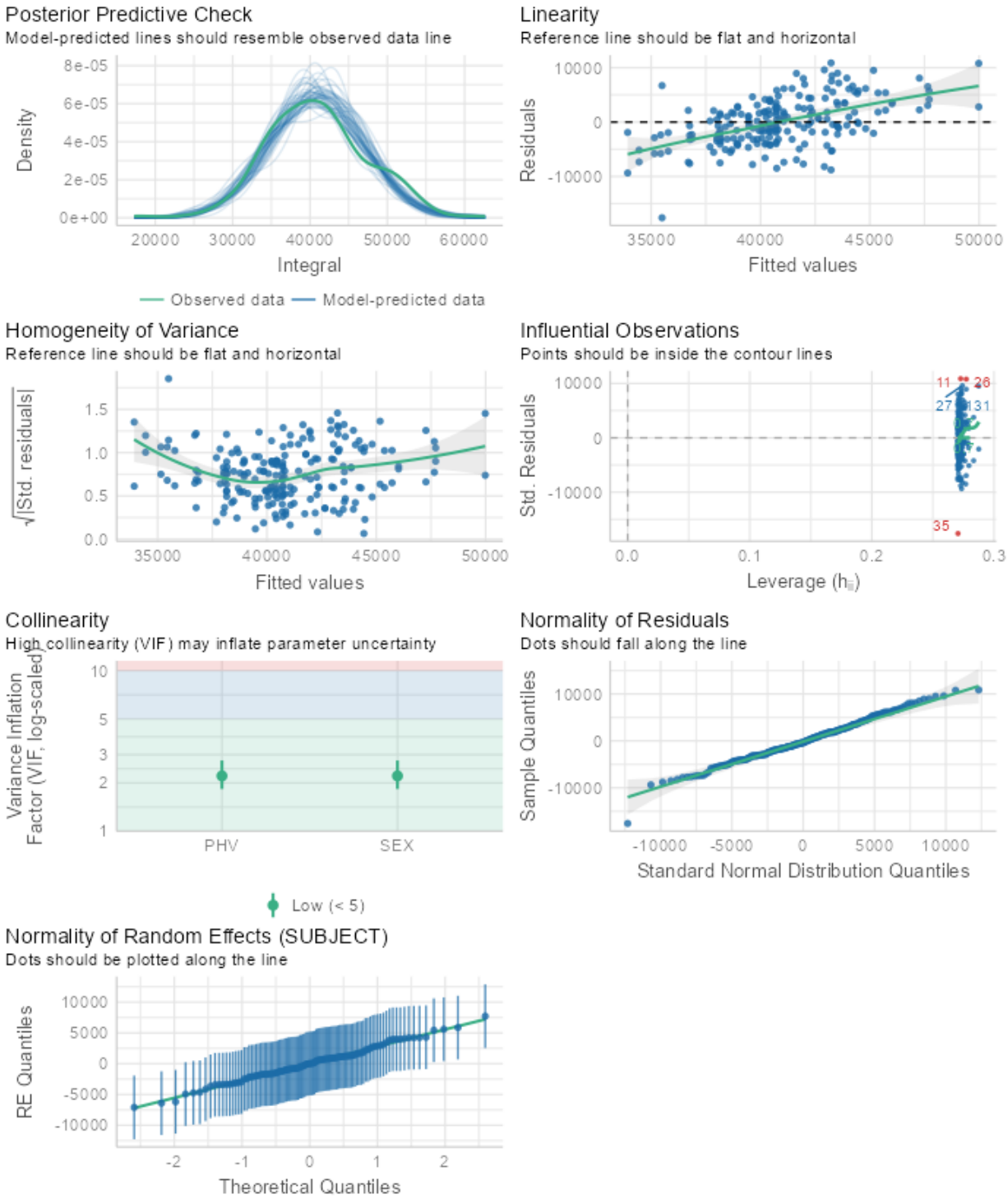

Figure 76: Model 2 acceleration integrals LMER model assumption tests for 5-10-5 shuffle drill

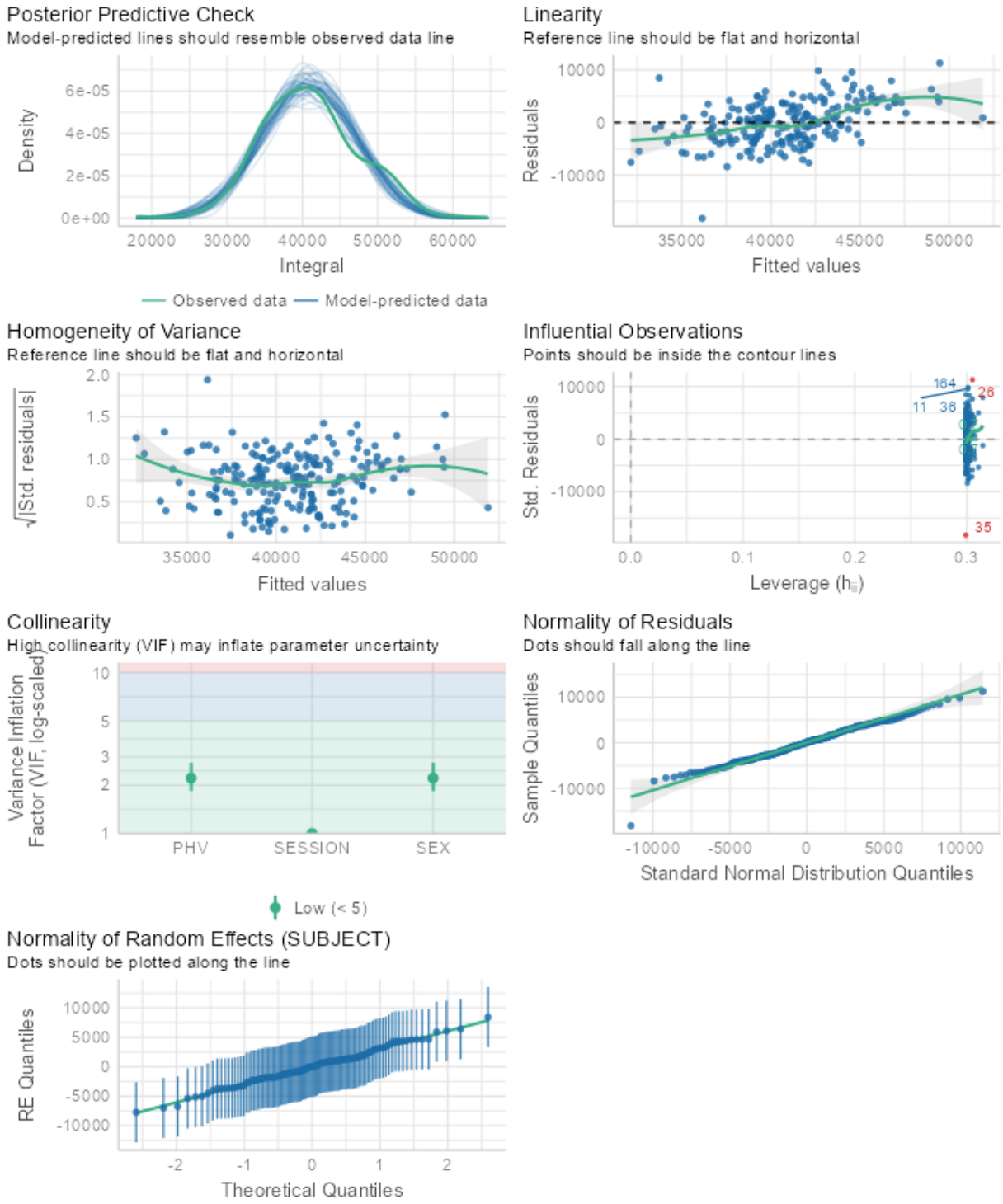

Figure 77: Model 3 acceleration integrals LMER model assumption tests for 5-10-5 shuffle drill

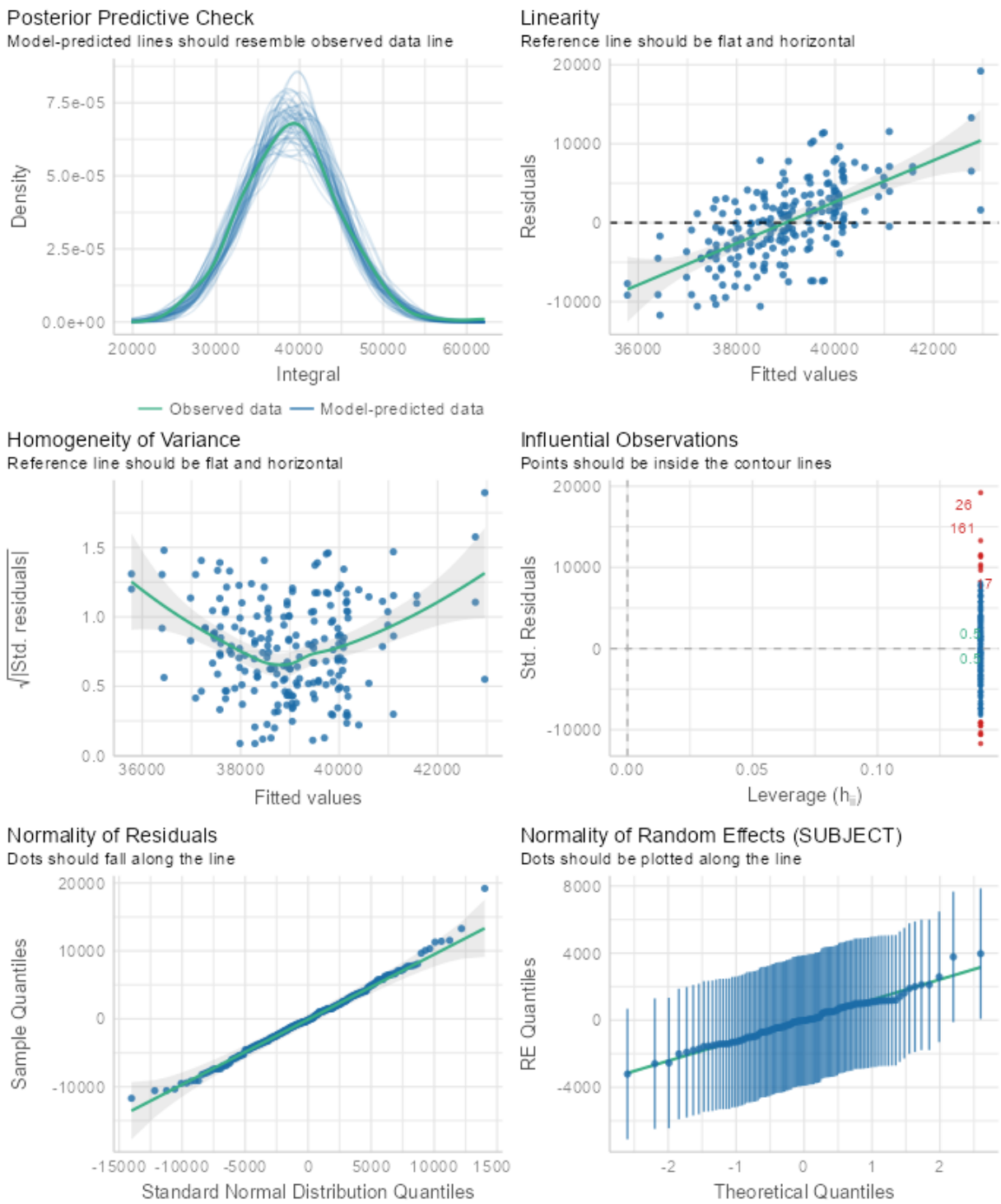

Figure 78: Null model acceleration integrals LMER model assumption tests for M-L

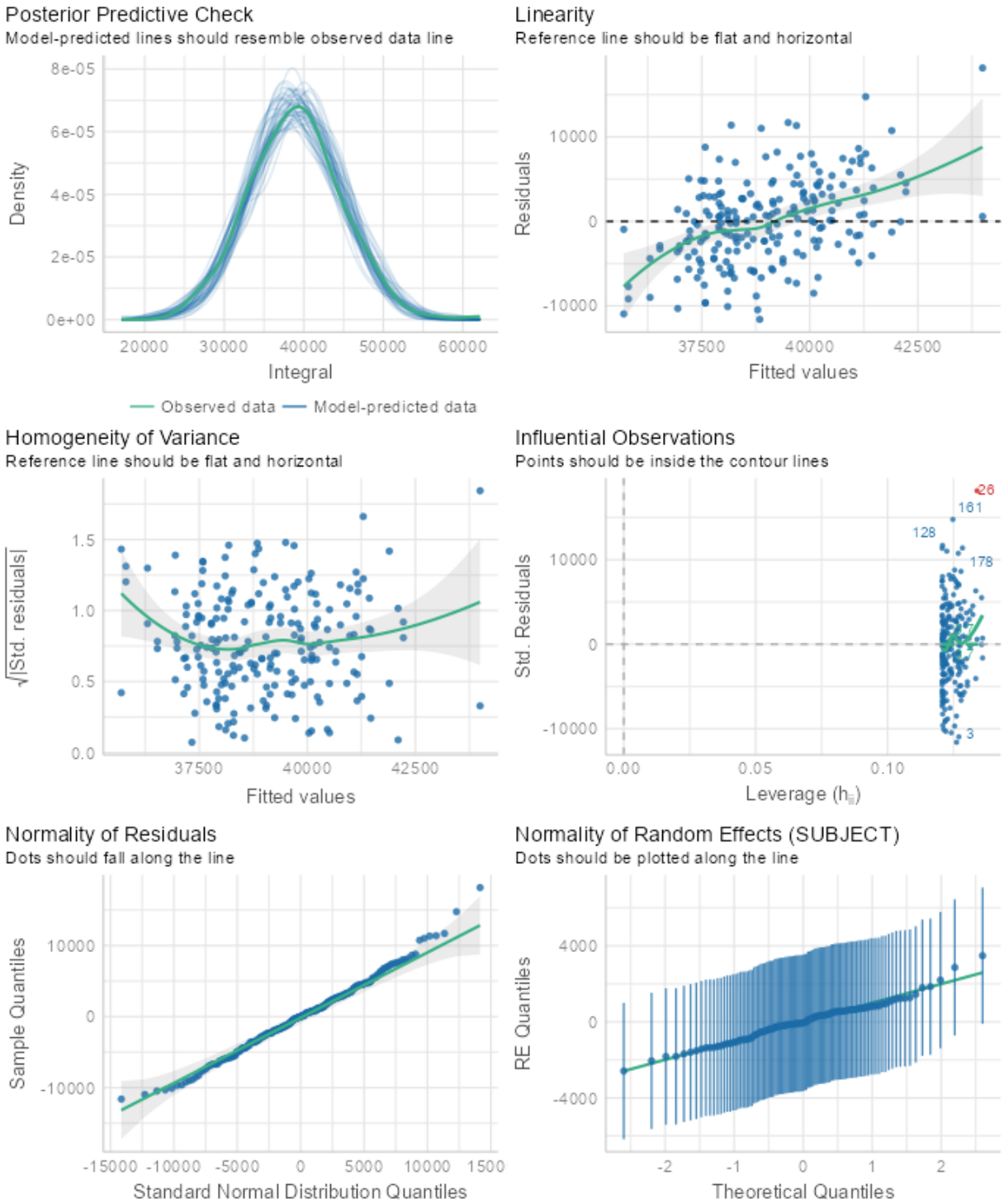

Figure 79: Model 1 acceleration integrals LMER model assumption tests for M-L

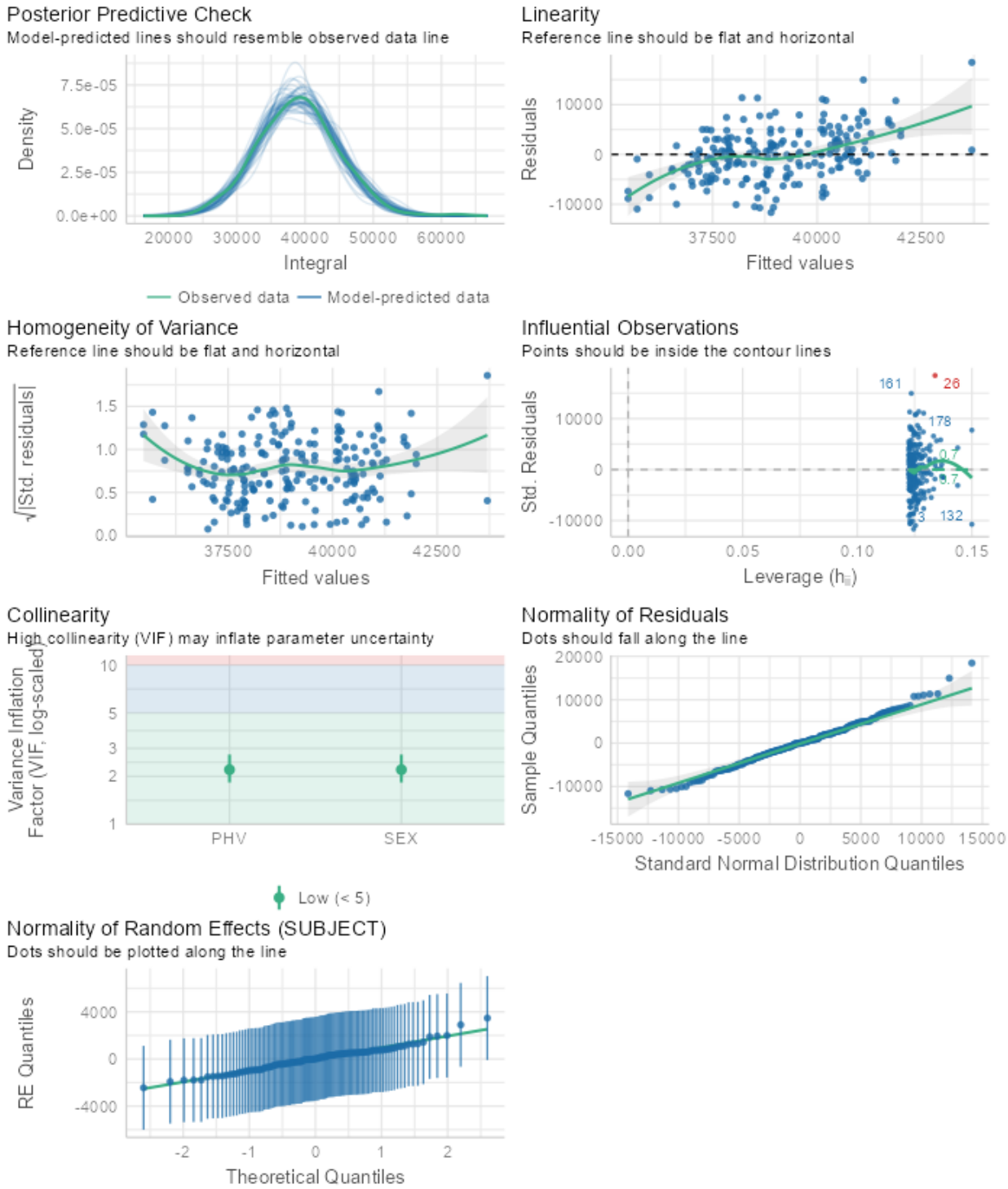

Figure 80: Model 2 acceleration integrals LMER model assumption tests for M-L

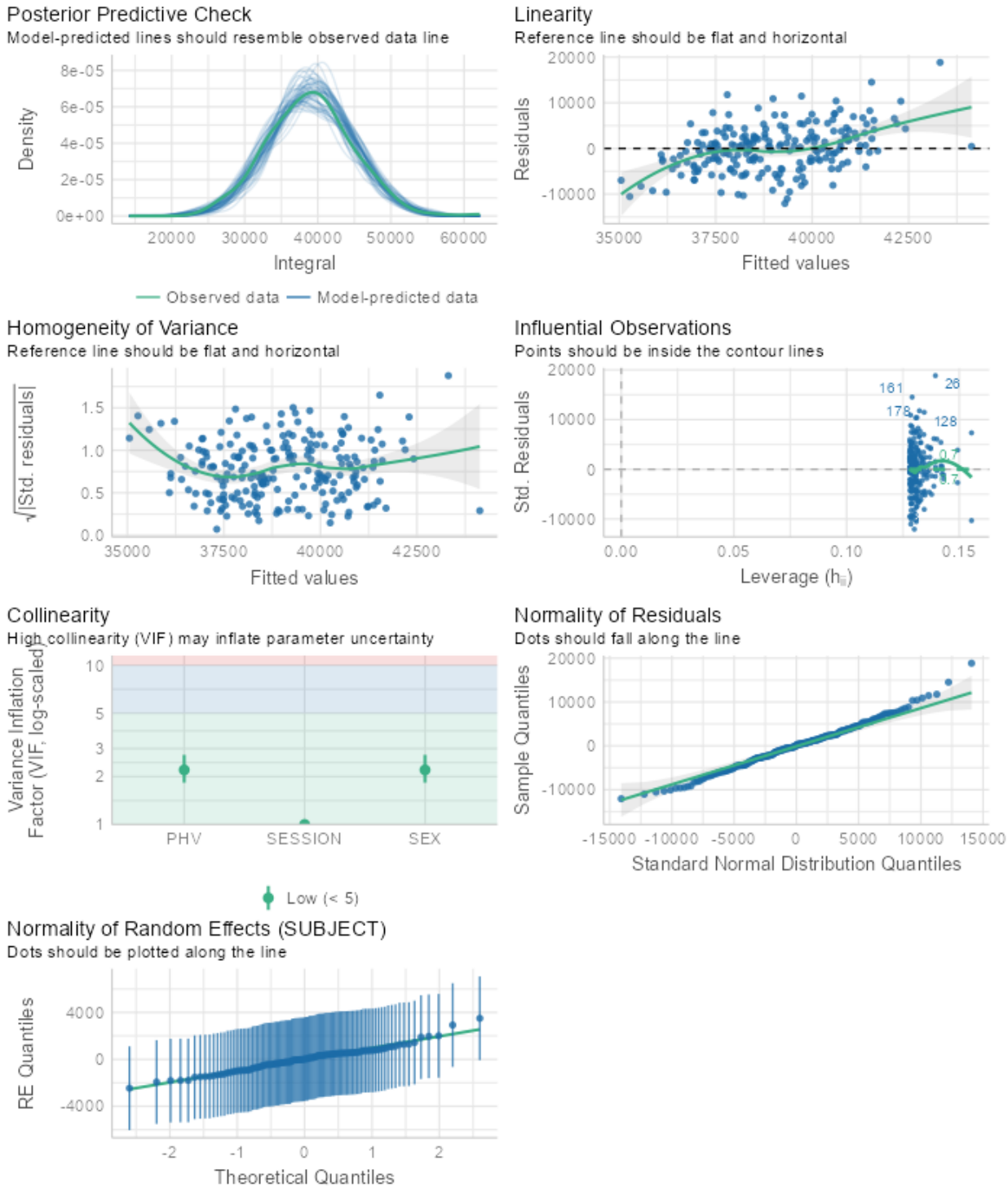

Figure 81: Model 3 acceleration integrals LMER model assumption tests for M-L

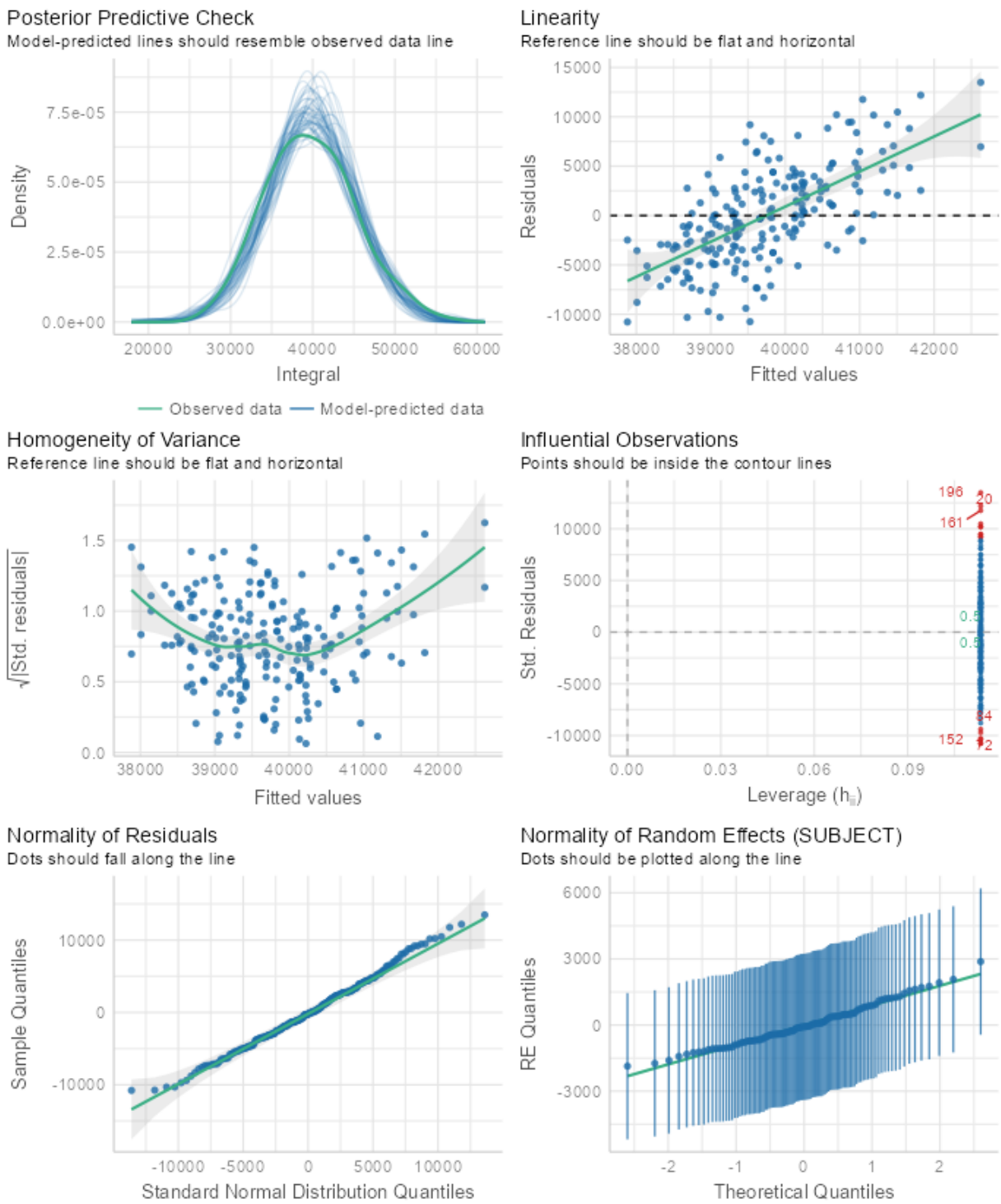

Figure 82: Null model acceleration integrals LMER model assumption tests for M-R

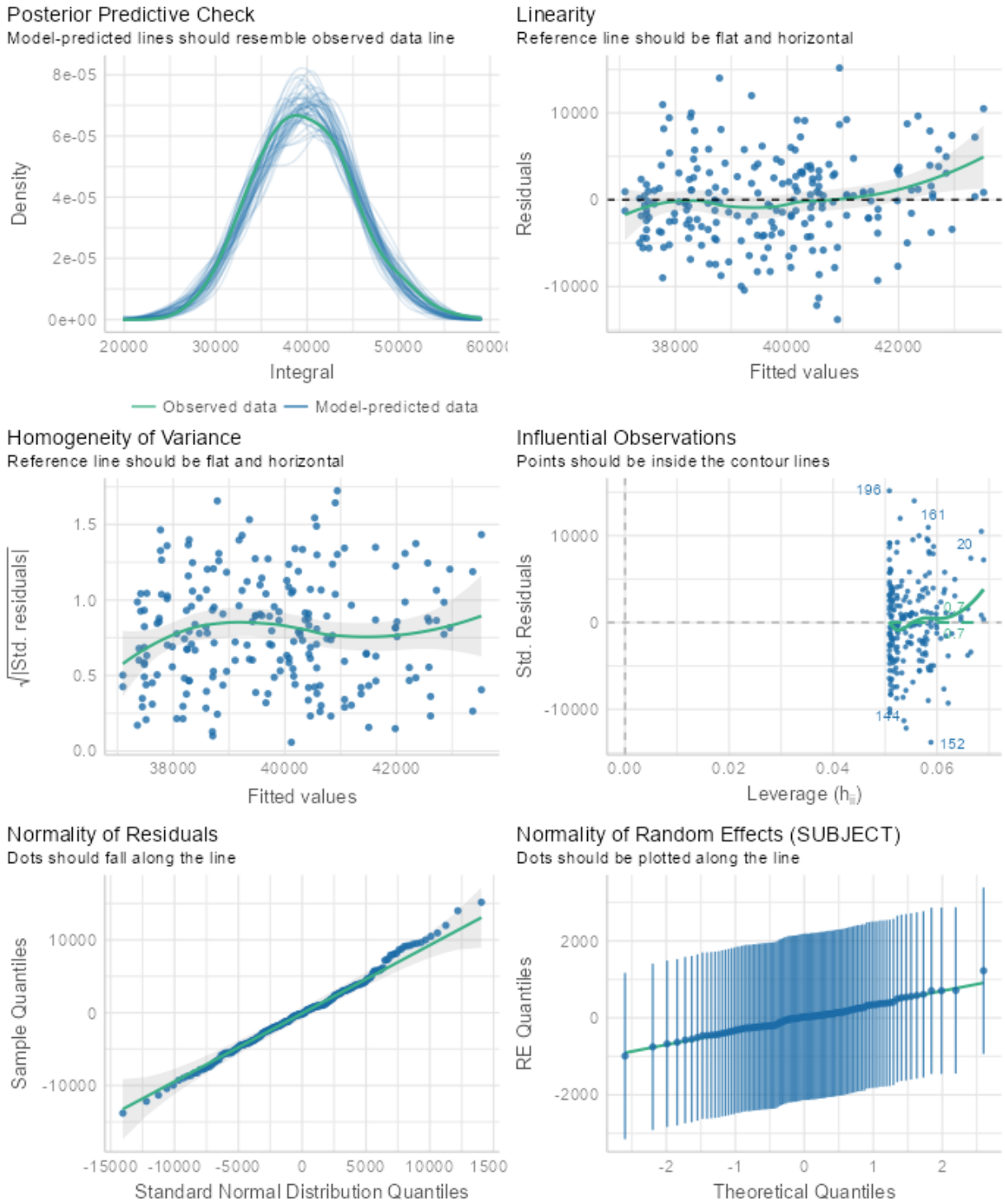

Figure 83: Model 1 acceleration integrals LMER model assumption tests for M-R

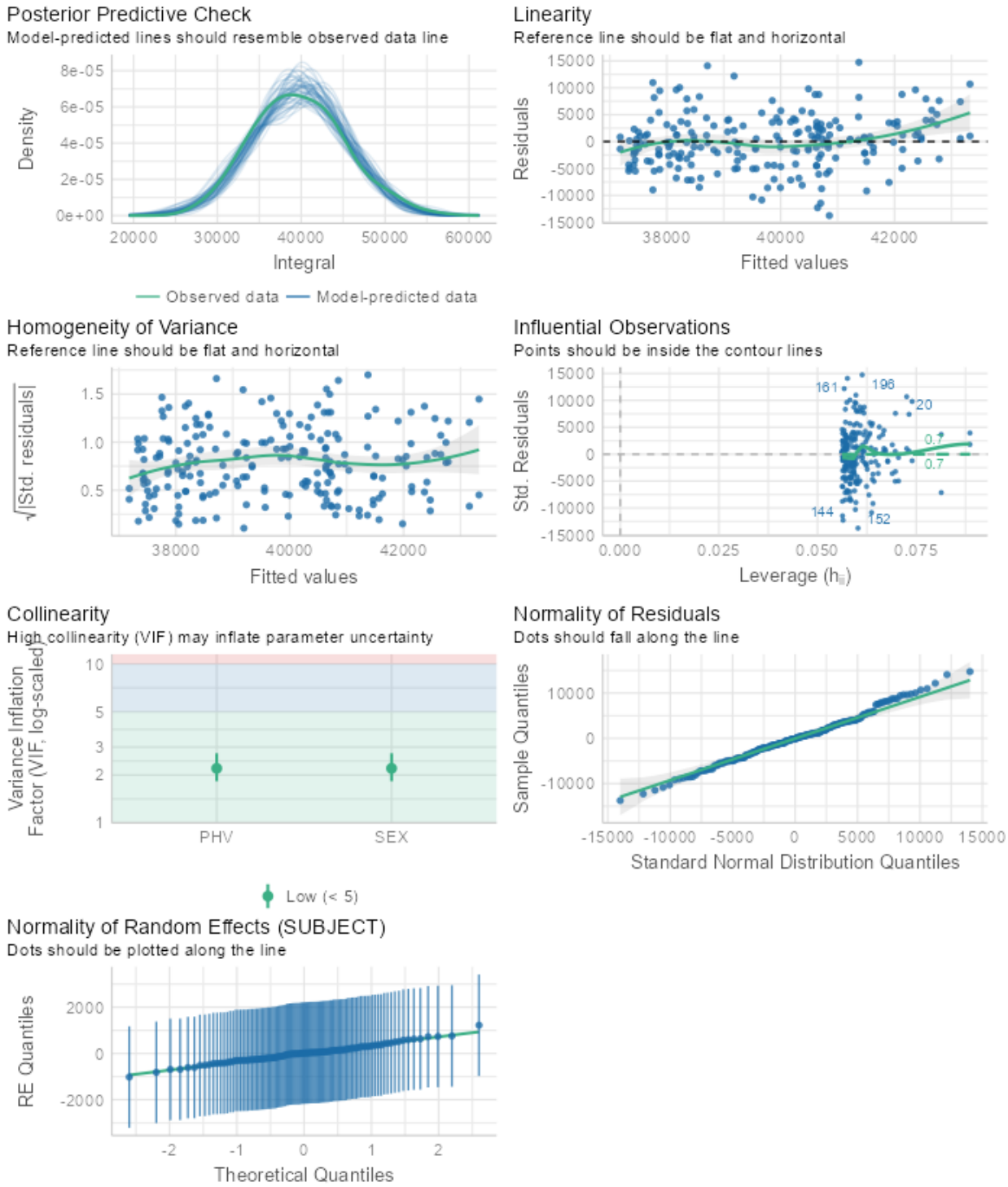

Figure 84: Model 2 acceleration integrals LMER model assumption tests for M-R

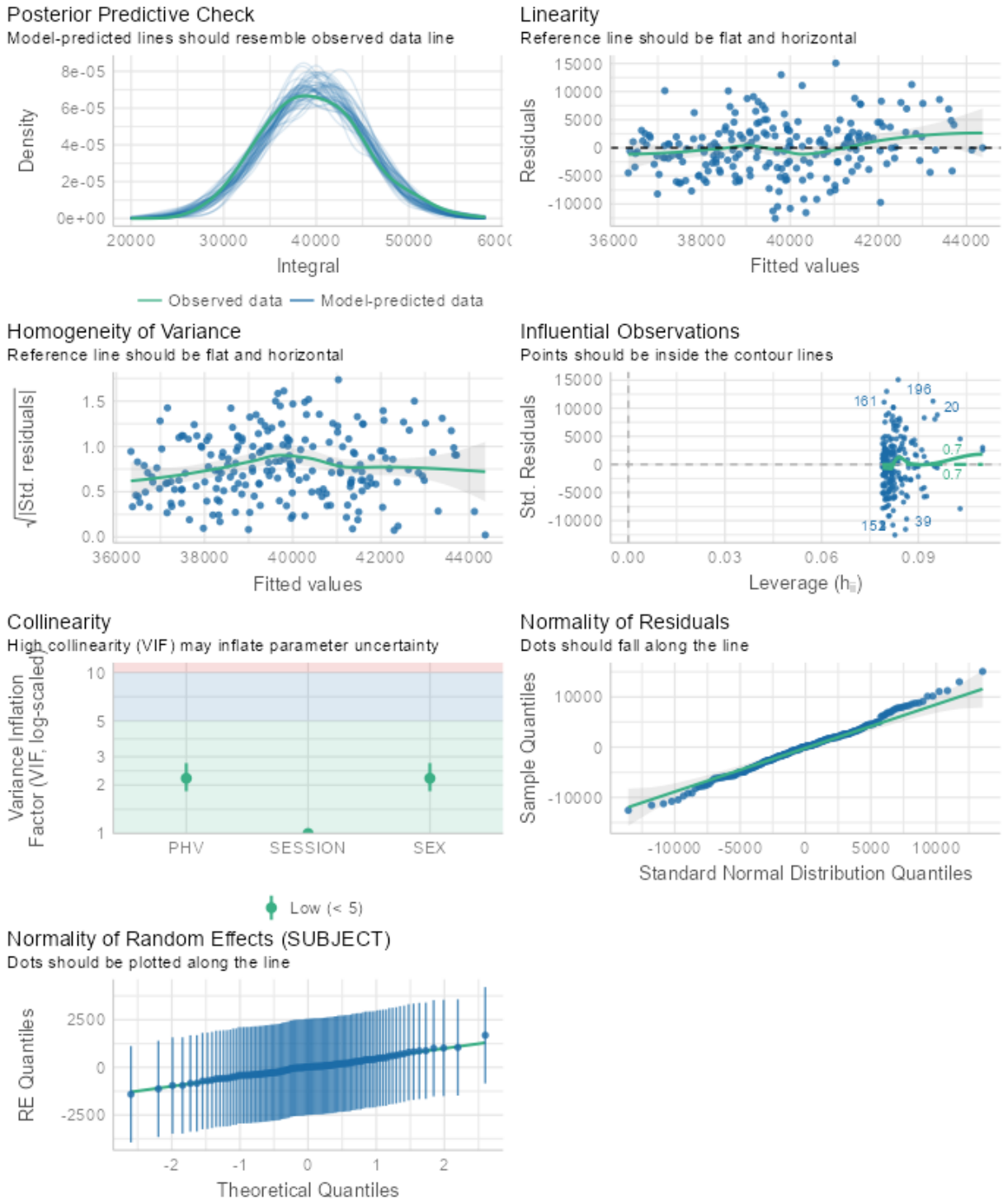

Figure 85: Model 3 acceleration integrals LMER model assumption tests for M-R

Appendix U. Karlberg ICP model of growth

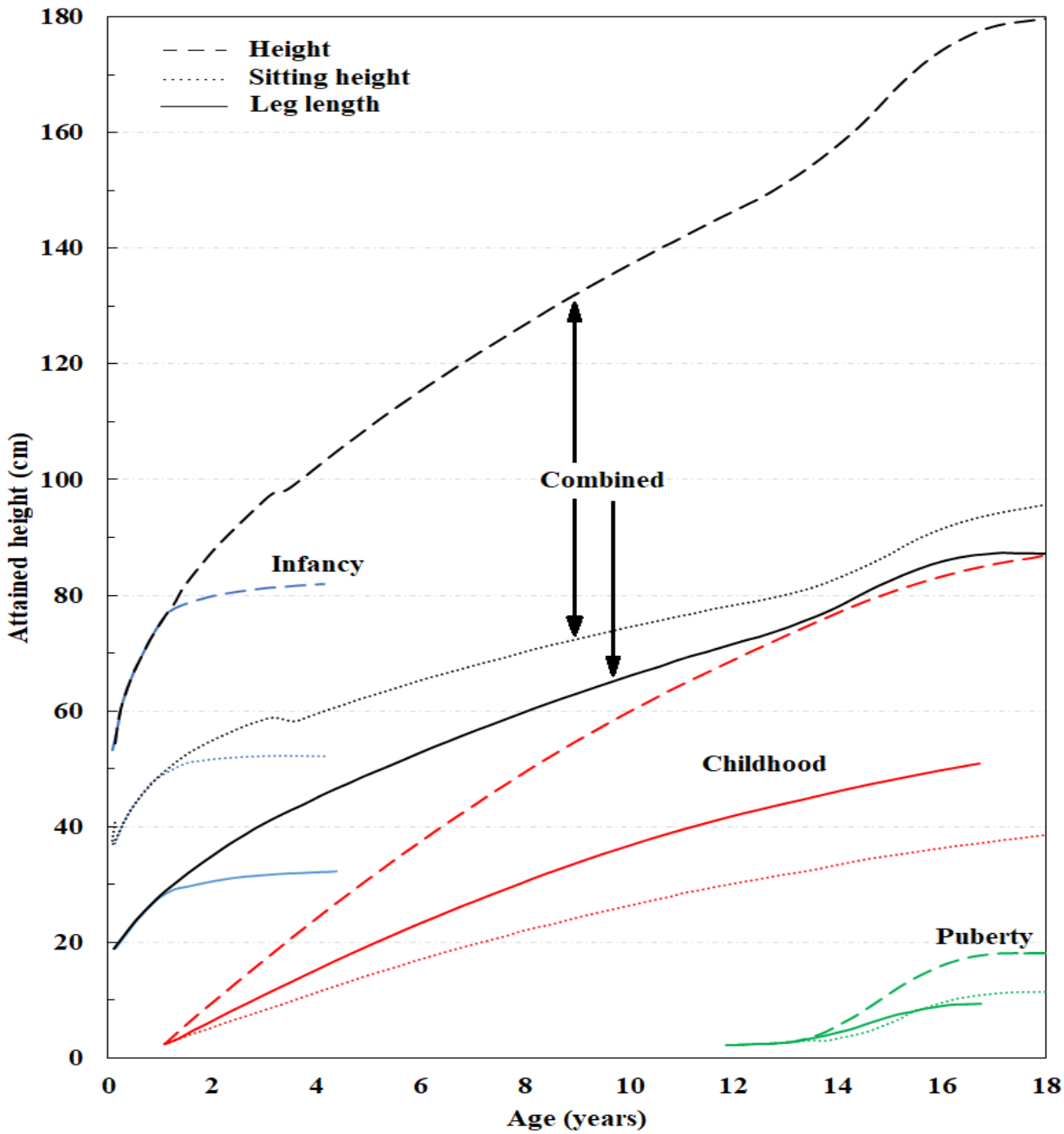

Figure 86: Karlberg ICP model illustrating growth rates for height (dashed), sitting height (dotted), leg length (solid), and their combined lengths through adolescence. Recreated from Karlberg (1989).

Table 9. Participant anthropometric characteristics

	Male (n = 55)	**Female (n = 52)**
Age (years)	12.29 (1.23)	12.77 (1.18)
Height (cm)	154.18 (10.83)	157.92 (8.1)
Mass (kg)	44.62 (10.65)	48.04 (9.63)
PHV offset (years)	-1.82 (1.2)	0.63 (1.04)

Group means ± (standard deviations)

Table 10: CI results across sex and testing sessions for each drill

	Female		Male	
Drill	**Pre**	**Post**	**Pre**	**Post**
40yd	6.98 (0.91)	7.11 (1.03)	6.95 (1.03)	7.08 (0.96)
5-10-5	4.94 (0.82)	5.08 (0.97)	5.32 (0.9)	5.25 (0.87)
Broad	3.16 (1.28)	3.37 (1.27)	3.15 (1.28)	3.37 (1.3)
DNB	6.39 (1.31)	6.25 (1.4)	6.15 (1.43)	6.45 (1.35)
M-L	5.63 (0.94)	5.78 (0.95)	5.68 (0.84)	5.78 (1.02)
M-R	5.49 (0.93)	5.79 (0.94)	5.61 (0.92)	5.66 (0.92)

Group means ± (standard deviations)

Table 11: CI model comparisons for 40yd dash drill

	NULL	**Model 1**	**Model 2**	**Model 3**
(Intercept)	6.971***	6.989***	6.952***	6.917***
	(0.079)	(0.085)	(0.123)	(0.131)
PHV		0.030	0.052	0.052
		(0.048)	(0.071)	(0.071)
SEX (Male)			0.099	0.099
			(0.237)	(0.237)
SESSION (Post-season)				0.071
				(0.088)
SD (Intercept SUBJECT)	0.684	0.686	0.690	0.690
SD (Observations)	0.641	0.641	0.641	0.642
n	214	214	214	214
R^2 Marg.	0.000	0.003	0.004	0.005
R^2 Cond.	0.532	0.535	0.539	0.538
AIC	552.2	558.1	561.0	565.3
BIC	562.3	571.6	577.8	585.5
ICC	0.5	0.5	0.5	0.5
RMSE	0.52	0.52	0.52	0.51

Fixed effects coefficient estimates reported for null and iterative models with standard errors in parentheses. n = number of observations; SD (Intercept SUBJECT) = standard deviation of random intercepts; SD (Observations) = standard deviation of model residual error; R^2 Marg. = marginal R^2; R^2 Cond. = conditional R^2; AIC = Akaike information criteria; BIC = Bayesian information criteria; ICC = intraclass correlation coefficient; RMSE = Root-mean-squared error; + $p < 0.1$, * $p < 0.05$, ** $p < 0.01$, *** $p < 0.001$

Table 12: CI model comparisons for 5-10-5 drill

	NULL	**Model 1**	**Model 2**	**Model 3**
(Intercept)	4.946***	4.907***	4.797***	4.805***
	(0.075)	(0.080)	(0.114)	(0.122)
PHV		-0.063	0.004	0.004
		(0.045)	(0.066)	(0.066)
SEX (Male)			0.299	0.299
			(0.222)	(0.222)
SESSION (Post-season)				-0.016
				(0.089)
SD (Intercept SUBJECT)	0.625	0.621	0.617	0.616
SD (Observations)	0.640	0.640	0.640	0.643
n	210	210	210	210
R2 Marg.	0.000	0.014	0.026	0.026
R2 Cond.	0.489	0.492	0.496	0.492
AIC	528.9	533.3	534.7	539.7
BIC	538.9	546.7	551.4	559.8
ICC	0.5	0.5	0.5	0.5
RMSE	0.52	0.52	0.52	0.52

Fixed effects coefficient estimates reported for null and iterative models with standard errors in parentheses. n = number of observations; SD (Intercept SUBJECT) = standard deviation of random intercepts; SD (Observations) = standard deviation of model residual error; R^2 Marg. = marginal R^2; R^2 Cond. = conditional R^2; AIC = Akaike information criteria; BIC = Bayesian information criteria; ICC = intraclass correlation coefficient; RMSE = Root-mean-squared error; + $p < 0.1$, * $p < 0.05$, ** $p < 0.01$, *** $p < 0.001$

Table 13: CI model results for Broad Jump drill

	NULL	**Model 1**	**Model 2**	**Model 3**
(Intercept)	3.162***	3.179***	3.139***	2.993***
	(0.093)	(0.099)	(0.144)	(0.160)
PHV		0.028	0.052	0.052
		(0.056)	(0.084)	(0.084)
SEX (Male)			0.109	0.109
			(0.277)	(0.277)
SESSION (Post-season)				0.291*
				(0.141)
SD (Intercept SUBJECT)	0.607	0.612	0.618	0.631
SD (Observations)	1.048	1.048	1.048	1.033
n	214	214	214	214
R2 Marg.	0.000	0.001	0.002	0.017
R2 Cond.	0.251	0.255	0.260	0.284
AIC	690.2	695.9	698.5	698.4
BIC	700.3	709.4	715.3	718.5
ICC	0.3	0.3	0.3	0.3
RMSE	0.94	0.93	0.93	0.91

Fixed effects coefficient estimates reported for null and iterative models with standard errors in parentheses. n = number of observations; SD (Intercept SUBJECT) = standard deviation of random intercepts; SD (Observations) = standard deviation of model residual error; R^2 Marg. = marginal R^2; R^2 Cond. = conditional R^2; AIC = Akaike information criteria; BIC = Bayesian information criteria; ICC = intraclass correlation coefficient; RMSE = Root-mean-squared error; + $p < 0.1$, * $p < 0.05$, ** $p < 0.01$, *** $p < 0.001$

Table 14: CI model results for left M-drill

	NULL	**Model 1**	**Model 2**	**Model 3**
(Intercept)	5.782***	5.771***	5.714***	5.710***
	(0.072)	(0.077)	(0.111)	(0.121)
PHV		-0.016	0.018	0.018
		(0.043)	(0.065)	(0.065)
SEX (Male)			0.154	0.154
			(0.214)	(0.214)
SESSION (Post-season)				0.008
				(0.097)
SD (Intercept SUBJECT)	0.546	0.550	0.552	0.550
SD (Observations)	0.709	0.709	0.709	0.712
n	214	214	214	214
R2 Marg.	0.000	0.001	0.004	0.004
R2 Cond.	0.372	0.376	0.380	0.377
AIC	552.2	558.5	561.2	566.0
BIC	562.3	571.9	578.0	586.2
ICC	0.4	0.4	0.4	0.4
RMSE	0.60	0.60	0.60	0.60

Fixed effects coefficient estimates reported for null and iterative models with standard errors in parentheses. n = number of observations; SD (Intercept SUBJECT) = standard deviation of random intercepts; SD (Observations) = standard deviation of model residual error; R^2 Marg. = marginal R^2; R^2 Cond. = conditional R^2; AIC = Akaike information criteria; BIC = Bayesian information criteria; ICC = intraclass correlation coefficient; RMSE = Root-mean-squared error; + $p < 0.1$, * $p < 0.05$, ** $p < 0.01$, *** $p < 0.001$

Table 15: CI model results for right M-drill

	NULL	**Model 1**	**Model 2**	**Model 3**
(Intercept)	5.494***	5.503***	5.481***	5.387***
	(0.071)	(0.076)	(0.110)	(0.118)
PHV		0.014	0.028	0.028
		(0.043)	(0.064)	(0.064)
SEX (Male)			0.059	0.059
			(0.212)	(0.212)
SESSION (Post-season)				0.187*
				(0.084)
SD (Intercept SUBJECT)	0.582	0.586	0.590	0.596
SD (Observations)	0.627	0.627	0.627	0.616
n	214	214	214	214
R2 Marg.	0.000	0.001	0.001	0.013
R2 Cond.	0.463	0.467	0.470	0.490
AIC	523.1	529.4	532.6	532.9
BIC	533.2	542.9	549.4	553.1
ICC	0.5	0.5	0.5	0.5
RMSE	0.52	0.52	0.52	0.50

Fixed effects coefficient estimates reported for null and iterative models with standard errors in parentheses. n = number of observations; SD (Intercept SUBJECT) = standard deviation of random intercepts; SD (Observations) = standard deviation of model residual error; R^2 Marg. = marginal R^2; R^2 Cond. = conditional R^2; AIC = Akaike information criteria; BIC = Bayesian information criteria; ICC = intraclass correlation coefficient; RMSE = Root-mean-squared error; + $p < 0.1$, * $p < 0.05$, ** $p < 0.01$, *** $p < 0.001$

Table 16: CI model results for DNB drill

	NULL	**Model 1**	**Model 2**	**Model 3**
(Intercept)	6.144***	6.100***	6.255***	6.170***
	(0.110)	(0.117)	(0.172)	(0.186)
PHV		-0.069	-0.160	-0.160
		(0.066)	(0.099)	(0.099)
SEX (Male)			-0.406	-0.406
			(0.330)	(0.330)
SESSION (Post-season)				0.171
				(0.138)
SD (Intercept SUBJECT)	0.874	0.873	0.870	0.871
SD (Observations)	1.005	1.005	1.005	1.003
n	210	210	210	210
R2 Marg.	0.000	0.008	0.018	0.022
R2 Cond.	0.430	0.434	0.438	0.442
AIC	702.5	707.0	707.9	710.5
BIC	712.6	720.4	724.6	730.6
ICC	0.4	0.4	0.4	0.4
RMSE	0.84	0.84	0.84	0.83

Fixed effects coefficient estimates reported for null and iterative models with standard errors in parentheses. n = number of observations; SD (Intercept SUBJECT) = standard deviation of random intercepts; SD (Observations) = standard deviation of model residual error; R^2 Marg. = marginal R^2; R^2 Cond. = conditional R^2; AIC = Akaike information criteria; BIC = Bayesian information criteria; ICC = intraclass correlation coefficient; RMSE = Root-mean-squared error; + $p < 0.1$, * $p < 0.05$, ** $p < 0.01$, *** $p < 0.001$

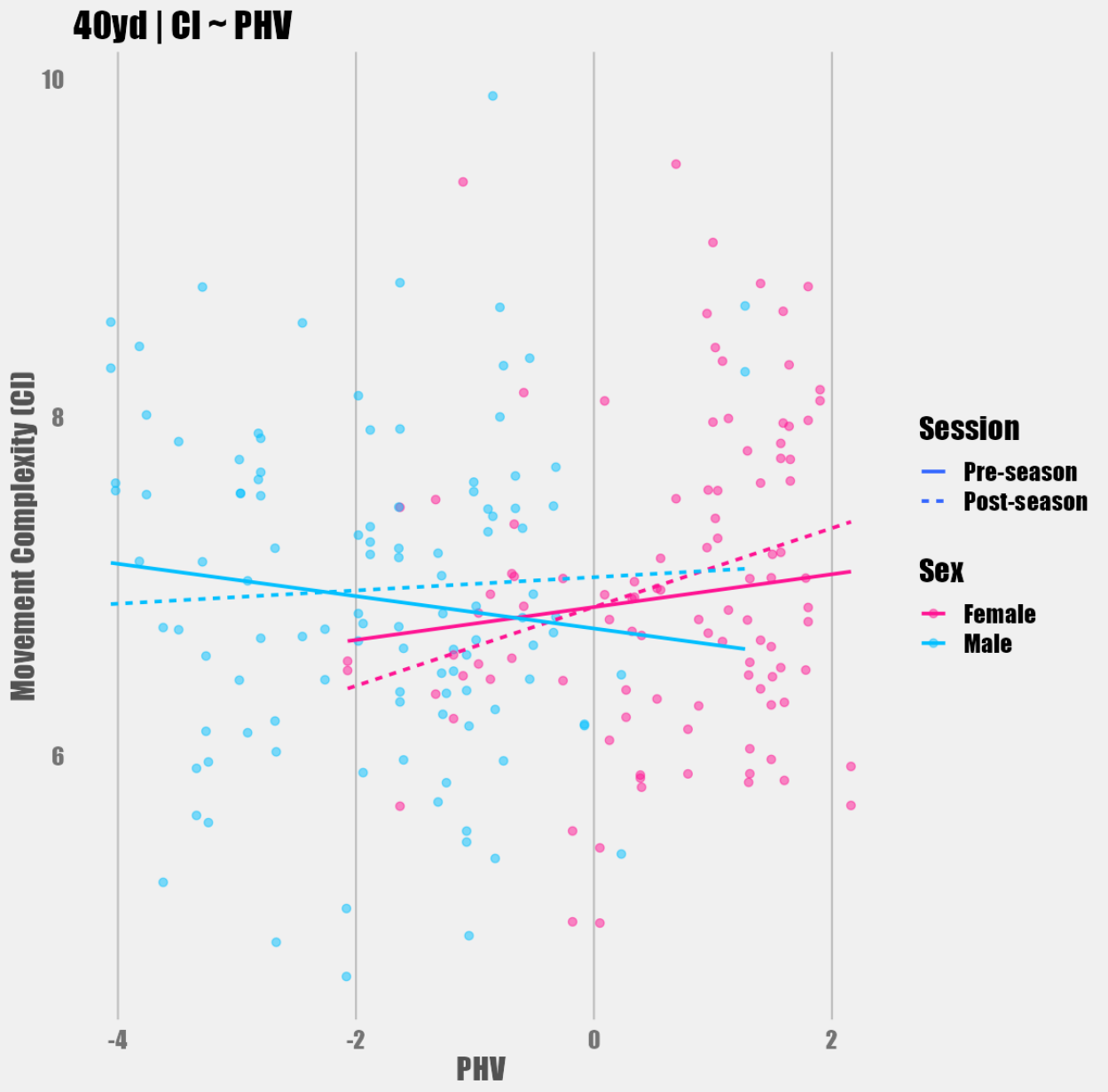

Figure 87: CI (arbitrary units) across PHV, sex, and testing session for the 40yd dash.

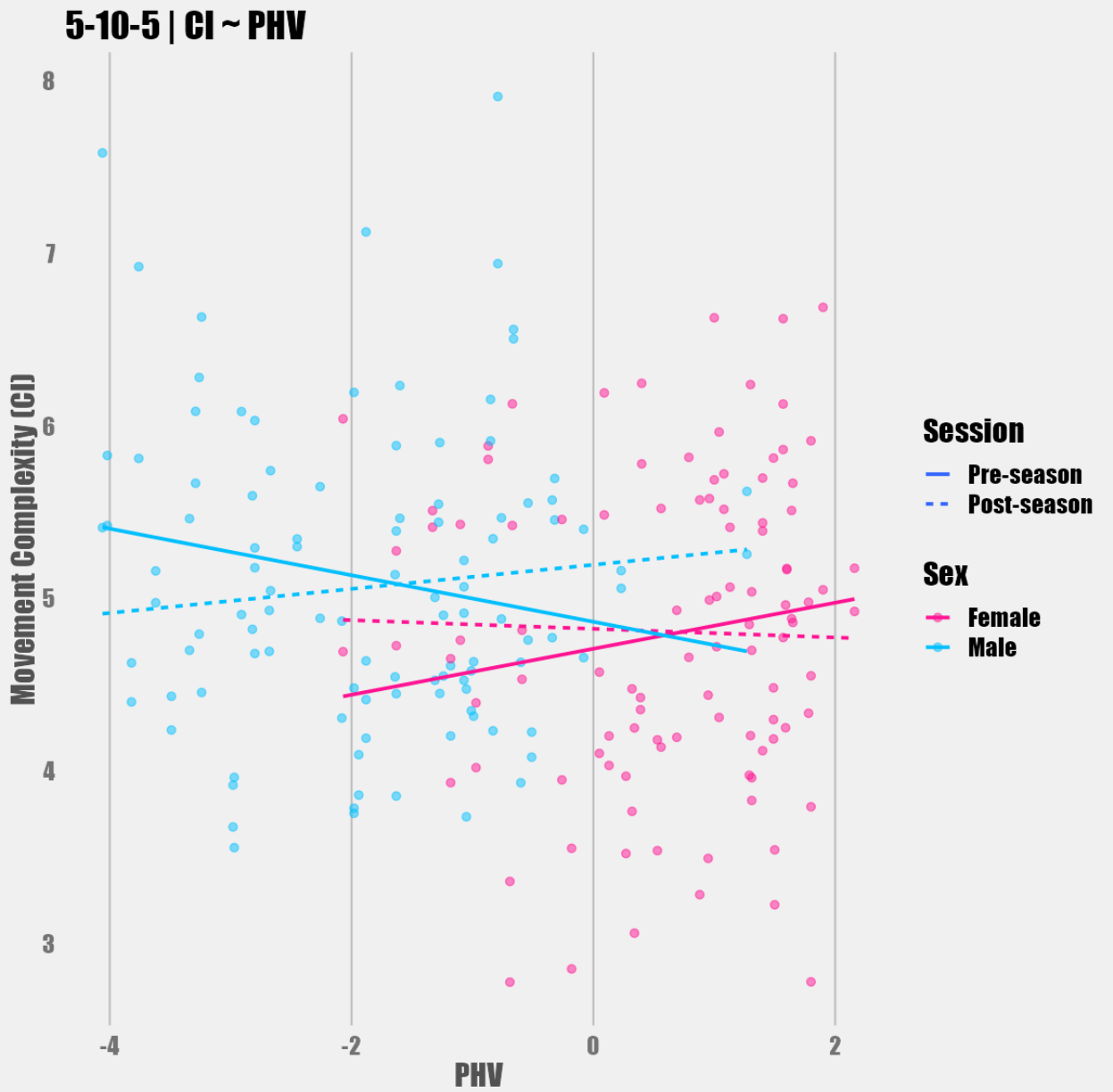

Figure 88: CI (arbitrary units) across PHV, sex, and testing session for the 5-10-5 shuttle drill.

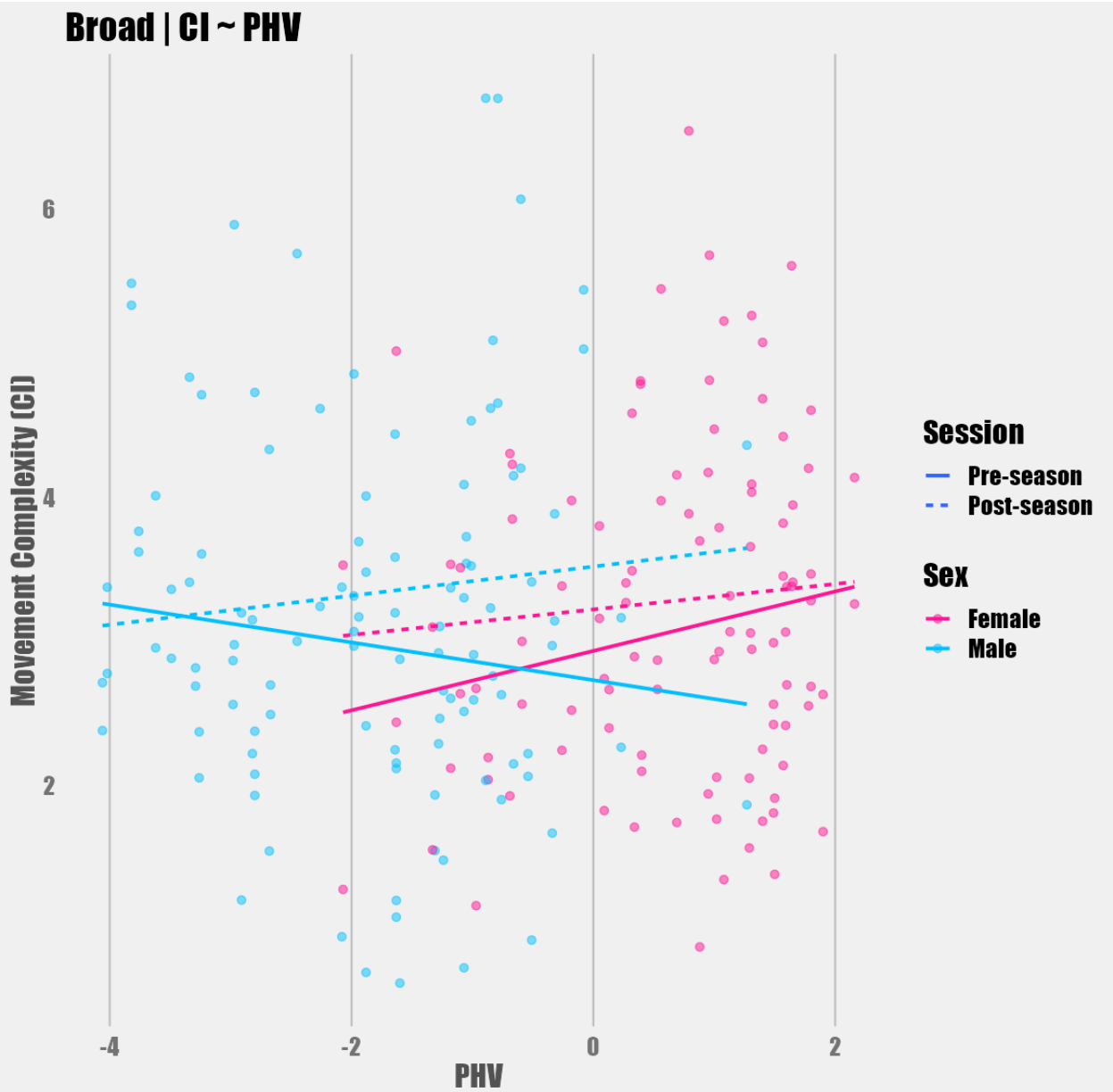

Figure 89: CI (arbitrary units) across PHV, sex, and testing session for the broad jump drill.

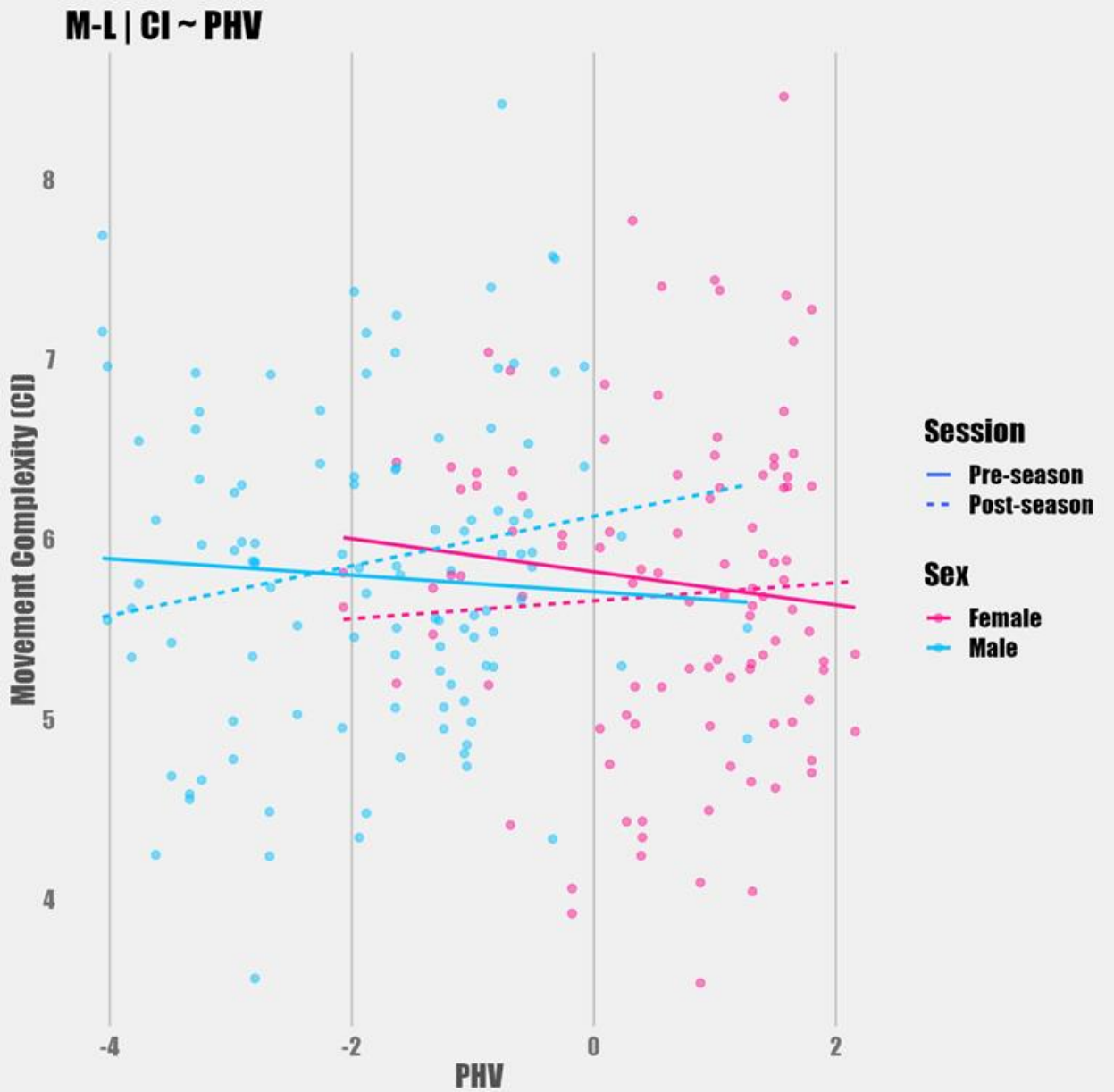

Figure 90: CI (arbitrary units) across PHV, sex, and testing session for the left M-drill.

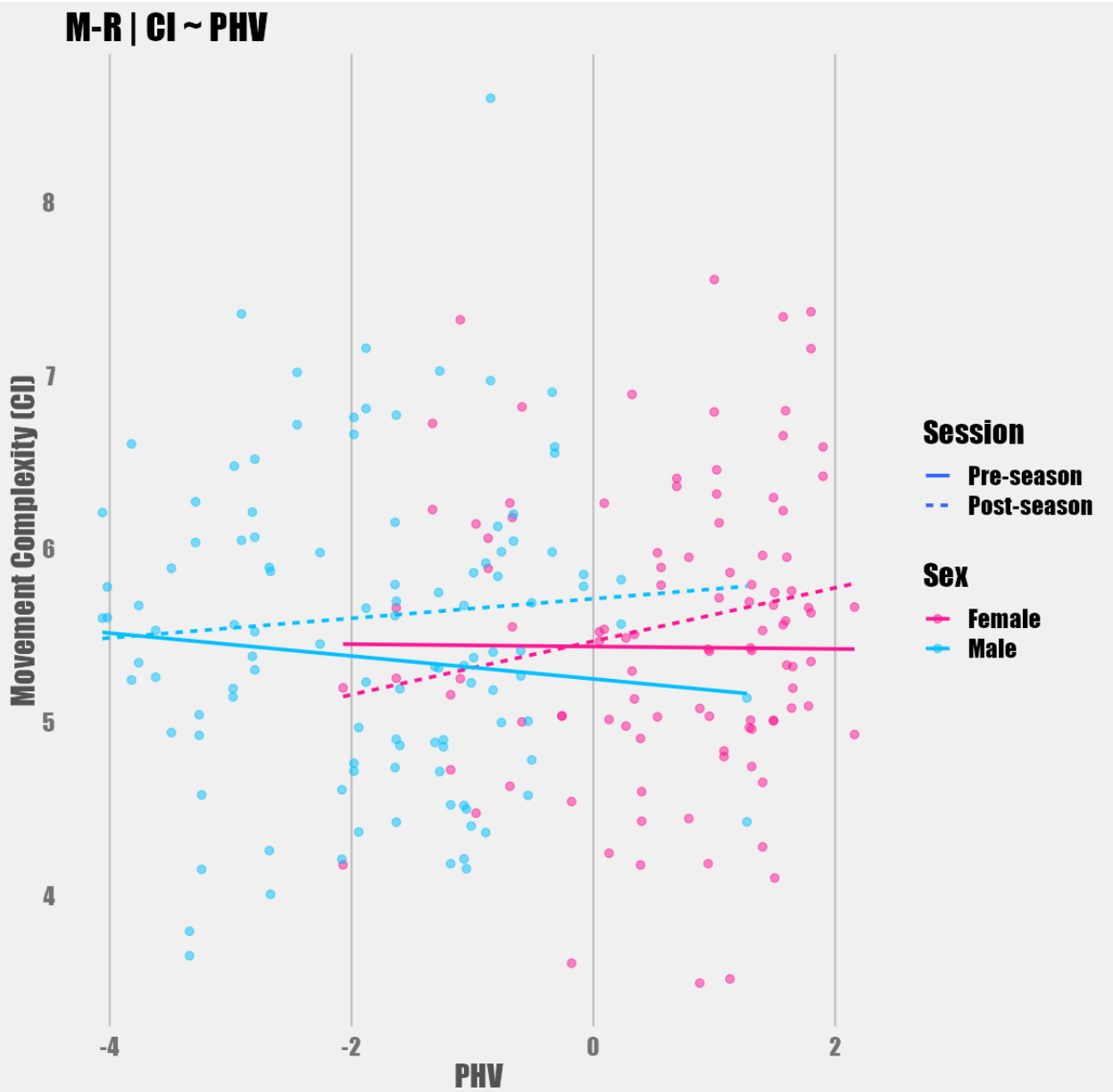

Figure 91: CI (arbitrary units) across PHV, sex, and testing session for the right M-drill.

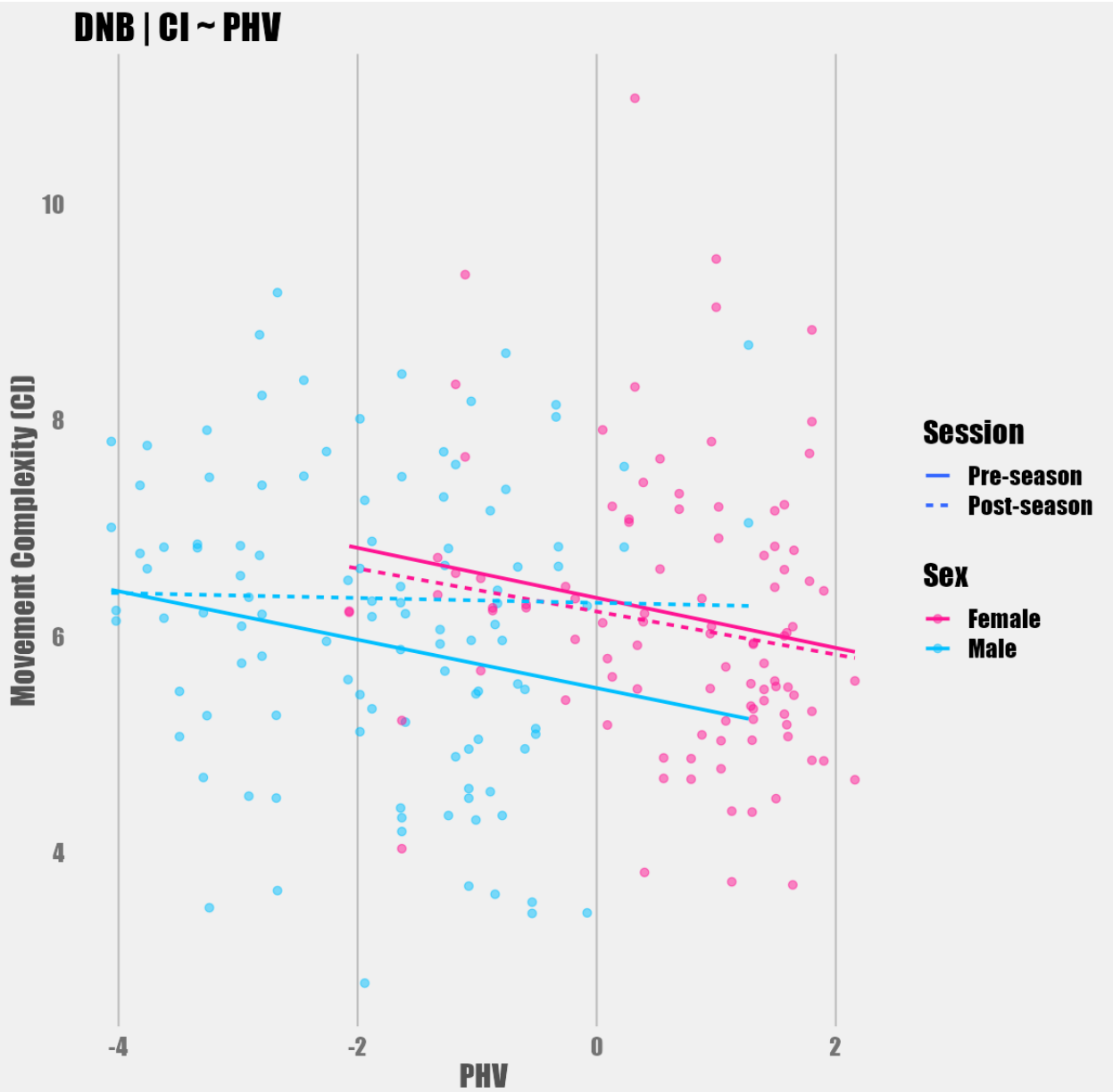

Figure 92: CI (arbitrary units) across PHV, sex, and testing session for the down-and-back jog.

Table 17: Acceleration peaks and integral results across sex and testing sessions for each drill

	Peaks				**Integrals**			
	Female		**Male**		**Female**		**Male**	
	Pre	**Post**	**Pre**	**Post**	**Pre**	**Post**	**Pre**	**Post**
40yd	41.45 (9.12)	40 (7.9)	42.36 (7.7)	41.56 (7.26)	61775 (9766)	59540 (7623)	61886 (7679)	60840 (8012)
5-10-5	25.17 (5.78)	24.41 (6.18)	24.77 (6.77)	23.91 (5.36)	39479 (5605)	38514 (5474)	42604 (7426)	38889 (5961)
Broad	45.69 (15.35)	46.78 (15.26)	46.67 (14.64)	46.93 (19.15)				
DNB	17.82 (5.91)	17.83 (6.11)	15.72 (6.14)	16.86 (6.37)	25328 (4500)	23987 (5069)	22140 (6284)	23665 (4770)
M-L	26.61 (5.82)	25.43 (5.29)	28.81 (5.27)	29.76 (6.16)	39046 (5368)	37895 (5424)	41547 (5957)	40571 (5927)
M-R	27 (6.04)	26.22 (5.71)	29.56 (5.19)	29.3 (5.5)	38995 (5491)	37184 (4062)	41140 (5333)	40322 (5761)

Group means ± (standard deviations)

Table 18: Acceleration peaks model comparisons for 40yd dash

	NULL	**Model 1**	**Model 2**	**Model 3**
(Intercept)	6.971***	6.989***	6.952***	6.917***
	(0.079)	(0.085)	(0.123)	(0.131)
PHV		0.030	0.052	0.052
		(0.048)	(0.071)	(0.071)
SEX (Male)			0.099	0.099
			(0.237)	(0.237)
SESSION (Post-season)				0.071
				(0.088)
SD (Intercept SUBJECT)	0.684	0.686	0.690	0.690
SD (Observations)	0.641	0.641	0.641	0.642
n	214	214	214	214
R^2 Marg.	0.000	0.003	0.004	0.005
R^2 Cond.	0.532	0.535	0.539	0.538
AIC	552.2	558.1	561.0	565.3
BIC	562.3	571.6	577.8	585.5
ICC	0.5	0.5	0.5	0.5
RMSE	0.52	0.52	0.52	0.51

Fixed effects coefficient estimates reported for null and iterative models with standard errors in parentheses. n = number of observations; SD (Intercept SUBJECT) = standard deviation of random intercepts; SD (Observations) = standard deviation of model residual error; R^2 Marg. = Marginal R^2; R^2 Cond. = Conditional R^2; AIC = Akaike information criteria; BIC = Bayesian information criteria; ICC = intraclass correlation coefficient; RMSE = Root-mean-squared error; + $p < 0.1$, * $p < 0.05$, ** $p < 0.01$, *** $p < 0.001$

Table 19: Acceleration peaks model comparisons for 5-10-5 shuffle drill

	NULL	**Model 1**	**Model 2**	**Model 3**
(Intercept)	24.913***	25.245***	24.518***	25.017***
	(0.588)	(0.624)	(0.891)	(0.933)
PHV		0.535	0.973+	0.973+
		(0.350)	(0.519)	(0.519)
SEX (Male)			1.979	1.979
			(1.735)	(1.735)
SESSION (Post-season)				-0.998+
				(0.550)
SD (Intercept SUBJECT)	5.313	5.270	5.260	5.276
SD (Observations)	4.027	4.027	4.027	3.983
n	210	210	210	210
R^2 Marg.	0.000	0.018	0.028	0.033
R^2 Cond.	0.635	0.638	0.641	0.649
AIC	1342.7	1342.7	1340.4	1338.5
BIC	1352.8	1356.1	1357.2	1358.6
ICC	0.6	0.6	0.6	0.6
RMSE	3.15	3.15	3.15	3.09

Fixed effects coefficient estimates reported for null and iterative models with standard errors in parentheses. n = number of observations; SD (Intercept SUBJECT) = standard deviation of random intercepts; SD (Observations) = standard deviation of model residual error; R^2 Marg. = Marginal R^2; R^2 Cond. = Conditional R^2; AIC = Akaike information criteria; BIC = Bayesian information criteria; ICC = intraclass correlation coefficient; RMSE = Root-mean-squared error; + $p < 0.1$, * $p < 0.05$, ** $p < 0.01$, *** $p < 0.001$

Table 20: Acceleration peaks model comparisons for Broad Jump drill

	NULL	**Model 1**	**Model 2**	**Model 3**
(Intercept)	47.134***	47.063***	45.909***	46.008***
	(1.363)	(1.466)	(2.114)	(2.302)
PHV		-0.112	0.576	0.576
		(0.826)	(1.228)	(1.228)
SEX (Male)			3.091	3.091
			(4.074)	(4.074)
SESSION (Post-season)				-0.197
				(1.822)
SD (Intercept SUBJECT)	10.528	10.616	10.654	10.615
SD (Observations)	13.268	13.268	13.268	13.330
n	214	214	214	214
R^2 Marg.	0.000	0.000	0.004	0.004
R^2 Cond.	0.386	0.390	0.394	0.390
AIC	1803.6	1804.1	1800.9	1799.9
BIC	1813.7	1817.6	1817.7	1820.1
ICC	0.4	0.4	0.4	0.4
RMSE	11.25	11.22	11.20	11.23

Fixed effects coefficient estimates reported for null and iterative models with standard errors in parentheses. n = number of observations; SD (Intercept SUBJECT) = standard deviation of random intercepts; SD (Observations) = standard deviation of model residual error; R^2 Marg. = Marginal R^2; R^2 Cond. = Conditional R^2; AIC = Akaike information criteria; BIC = Bayesian information criteria; ICC = intraclass correlation coefficient; RMSE = Root-mean-squared error; + $p < 0.1$, * $p < 0.05$, ** $p < 0.01$, *** $p < 0.001$

Table 21: Acceleration peaks model comparisons for left M-drill

	NULL	**Model 1**	**Model 2**	**Model 3**
(Intercept)	27.174***	26.891***	25.498***	25.451***
	(0.461)	(0.489)	(0.682)	(0.748)
PHV		-0.447	0.384	0.384
		(0.276)	(0.396)	(0.396)
SEX (Male)			3.733**	3.733**
			(1.314)	(1.314)
SESSION (Post-season)				0.093
				(0.617)
SD (Intercept SUBJECT)	3.550	3.502	3.294	3.280
SD (Observations)	4.495	4.495	4.495	4.516
n	214	214	214	214
R^2 Marg.	0.000	0.017	0.064	0.064
R^2 Cond.	0.384	0.388	0.391	0.387
AIC	1342.0	1342.1	1333.9	1335.0
BIC	1352.1	1355.6	1350.7	1355.2
ICC	0.4	0.4	0.3	0.3
RMSE	3.82	3.82	3.85	3.86

Fixed effects coefficient estimates reported for null and iterative models with standard errors in parentheses. n = number of observations; SD (Intercept SUBJECT) = standard deviation of random intercepts; SD (Observations) = standard deviation of model residual error; R^2 Marg. = Marginal R^2; R^2 Cond. = Conditional R^2; AIC = Akaike information criteria; BIC = Bayesian information criteria; ICC = intraclass correlation coefficient; RMSE = Root-mean-squared error; + $p < 0.1$, * $p < 0.05$, ** $p < 0.01$, *** $p < 0.001$

Table 22: Acceleration peaks model comparisons for right M-drill

	NULL	**Model 1**	**Model 2**	**Model 3**
(Intercept)	28.368***	28.026***	26.839***	27.500***
	(0.487)	(0.515)	(0.727)	(0.782)
PHV		-0.541+	0.168	0.168
		(0.290)	(0.422)	(0.422)
SEX (Male)			3.182*	3.182*
			(1.400)	(1.400)
SESSION (Post-season)				-1.322*
				(0.576)
SD (Intercept SUBJECT)	4.011	3.939	3.817	3.863
SD (Observations)	4.298	4.298	4.298	4.214
n	214	214	214	214
R^2 Marg.	0.000	0.023	0.056	0.068
R^2 Cond.	0.466	0.469	0.472	0.494
AIC	1343.9	1343.1	1337.5	1333.6
BIC	1354.0	1356.6	1354.3	1353.8
ICC	0.5	0.5	0.4	0.5
RMSE	3.55	3.55	3.57	3.47

Fixed effects coefficient estimates reported for null and iterative models with standard errors in parentheses. n = number of observations; SD (Intercept SUBJECT) = standard deviation of random intercepts; SD (Observations) = standard deviation of model residual error; R^2 Marg. = Marginal R^2; R^2 Cond. = Conditional R^2; AIC = Akaike information criteria; BIC = Bayesian information criteria; ICC = intraclass correlation coefficient; RMSE = Root-mean-squared error; + $p < 0.1$, * $p < 0.05$, ** $p < 0.01$, *** $p < 0.001$

Table 23: Acceleration peaks model comparisons for DNB drill

	NULL	**Model 1**	**Model 2**	**Model 3**
(Intercept)	17.446***	17.247***	19.301***	19.218***
	(0.506)	(0.540)	(0.749)	(0.806)
PHV		-0.316	-1.511***	-1.511***
		(0.302)	(0.428)	(0.428)
SEX (Male)			-5.361***	-5.361***
			(1.435)	(1.435)
SESSION (Post-season)				0.166
				(0.594)
SD (Intercept SUBJECT)	4.206	4.203	3.830	3.819
SD (Observations)	4.282	4.282	4.282	4.301
n	210	210	210	210
R^2 Marg.	0.000	0.008	0.095	0.095
R^2 Cond.	0.491	0.495	0.497	0.494
AIC	1324.2	1325.7	1311.9	1313.0
BIC	1334.2	1339.1	1328.6	1333.1
ICC	0.5	0.5	0.4	0.4
RMSE	3.50	3.50	3.55	3.56

Fixed effects coefficient estimates reported for null and iterative models with standard errors in parentheses. n = number of observations; SD (Intercept SUBJECT) = standard deviation of random intercepts; SD (Observations) = standard deviation of model residual error; R^2 Marg. = Marginal R^2; R^2 Cond. = Conditional R^2; AIC = Akaike information criteria; BIC = Bayesian information criteria; ICC = intraclass correlation coefficient; RMSE = Root-mean-squared error; + $p < 0.1$, * $p < 0.05$, ** $p < 0.01$, *** $p < 0.001$

Table 24: Acceleration integral model comparisons for 40yd dash

	NULL	**Model 1**	**Model 2**	**Model 3**
(Intercept)	61504.631***	61483.088***	61040.309***	62050.013***
	(641.984)	(690.303)	(996.581)	(1086.649)
PHV		-34.084	230.161	230.161
		(389.089)	(579.043)	(579.043)
SEX (Male)			1186.332	1186.332
			(1920.570)	(1920.570)
SESSION (Post-season)				-2019.407*
				(866.332)
SD (Intercept SUBJECT)	4815.681	4858.758	4885.825	4970.226
SD (Observations)	6466.618	6466.618	6466.618	6336.672
n	214	214	214	214
R^2 Marg.	0.000	0.000	0.002	0.018
R^2 Cond.	0.357	0.361	0.365	0.392
AIC	4432.8	4421.1	4405.7	4387.0
BIC	4442.9	4434.5	4422.6	4407.2
ICC	0.4	0.4	0.4	0.4
RMSE	5543.39	5526.80	5513.39	5351.44

Fixed effects coefficient estimates reported for null and iterative models with standard errors in parentheses. n = number of observations; SD (Intercept SUBJECT) = standard deviation of random intercepts; SD (Observations) = standard deviation of model residual error; R^2 Marg. = Marginal R^2; R^2 Cond. = Conditional R^2; AIC = Akaike information criteria; BIC = Bayesian information criteria; ICC = intraclass correlation coefficient; RMSE = Root-mean-squared error; + $p < 0.1$, * $p < 0.05$, ** $p < 0.01$, *** $p < 0.001$

Table 25: Acceleration integral model comparisons for 5-10-5 shuffle drill

	NULL	**Model 1**	**Model 2**	**Model 3**
(Intercept)	40886.200***	40573.136***	40166.604***	41373.255***
	(518.771)	(548.924)	(787.525)	(855.511)
PHV		-504.942	-259.968	-259.968
		(308.092)	(458.959)	(458.959)
SEX (Male)			1106.296	1106.296
			(1533.300)	(1533.300)
SESSION (Post-season)				-2413.302***
				(668.440)
SD (Intercept SUBJECT)	3896.776	3838.494	3855.396	4025.963
SD (Observations)	5113.339	5113.339	5113.339	4843.308
n	210	210	210	210
R^2 Marg.	0.000	0.017	0.020	0.055
R^2 Cond.	0.367	0.371	0.375	0.441
AIC	4254.2	4240.2	4225.2	4199.9
BIC	4264.2	4253.6	4241.9	4220.0
ICC	0.4	0.4	0.4	0.4
RMSE	4366.19	4370.60	4360.72	4049.75

Fixed effects coefficient estimates reported for null and iterative models with standard errors in parentheses. n = number of observations; SD (Intercept SUBJECT) = standard deviation of random intercepts; SD (Observations) = standard deviation of model residual error; R^2 Marg. = Marginal R^2; R^2 Cond. = Conditional R^2; AIC = Akaike information criteria; BIC = Bayesian information criteria; ICC = intraclass correlation coefficient; RMSE = Root-mean-squared error; + $p < 0.1$, * $p < 0.05$, ** $p < 0.01$, *** $p < 0.001$

Table 26: Acceleration integral model comparisons for left M-drill

	NULL	**Model 1**	**Model 2**	**Model 3**
(Intercept)	38993.755***	38569.977***	38012.538***	38419.491***
	(429.377)	(446.879)	(641.852)	(738.371)
PHV		-670.475**	-337.803	-337.803
		(251.883)	(372.935)	(372.935)
SEX (Male)			1493.539	1493.539
			(1236.951)	(1236.951)
SESSION (Post-season)				-813.908
				(729.979)
SD (Intercept SUBJECT)	2332.452	2090.285	2070.818	2078.625
SD (Observations)	5345.400	5345.400	5345.400	5339.336
n	214	214	214	214
R^2 Marg.	0.000	0.036	0.044	0.048
R^2 Cond.	0.160	0.164	0.168	0.173
AIC	4306.8	4289.0	4273.5	4259.2
BIC	4316.9	4302.5	4290.3	4279.4
ICC	0.2	0.1	0.1	0.1
RMSE	4953.44	5002.28	4996.69	4975.23

Fixed effects coefficient estimates reported for null and iterative models with standard errors in parentheses. n = number of observations; SD (Intercept SUBJECT) = standard deviation of random intercepts; SD (Observations) = standard deviation of model residual error; R^2 Marg. = Marginal R^2; R^2 Cond. = Conditional R^2; AIC = Akaike information criteria; BIC = Bayesian information criteria; ICC = intraclass correlation coefficient; RMSE = Root-mean-squared error; + $p < 0.1$, * $p < 0.05$, ** $p < 0.01$, *** $p < 0.001$

Table 27: Acceleration integral model comparisons for right M-drill

	NULL	**Model 1**	**Model 2**	**Model 3**
(Intercept)	39746.233***	39150.267***	38818.482***	39622.081***
	(395.241)	(392.399)	(565.734)	(661.078)
PHV		-942.901***	-744.896*	-744.896*
		(221.175)	(328.708)	(328.708)
SEX (Male)			888.946	888.946
			(1090.259)	(1090.259)
SESSION (Post-season)				-1607.198*
				(684.014)
SD (Intercept SUBJECT)	1915.880	1157.581	1177.311	1383.786
SD (Observations)	5107.730	5107.730	5107.730	5003.129
n	214	214	214	214
R^2 Marg.	0.000	0.082	0.085	0.106
R^2 Cond.	0.123	0.127	0.131	0.169
AIC	4279.5	4252.0	4237.5	4219.2
BIC	4289.6	4265.4	4254.3	4239.4
ICC	0.1	0.0	0.1	0.1
RMSE	4809.29	4965.14	4950.29	4790.53

Fixed effects coefficient estimates reported for null and iterative models with standard errors in parentheses. n = number of observations; SD (Intercept SUBJECT) = standard deviation of random intercepts; SD (Observations) = standard deviation of model residual error; R^2 Marg. = Marginal R^2; R^2 Cond. = Conditional R^2; AIC = Akaike information criteria; BIC = Bayesian information criteria; ICC = intraclass correlation coefficient; RMSE = Root-mean-squared error; + $p < 0.1$, * $p < 0.05$, ** $p < 0.01$, *** $p < 0.001$

Table 28: Acceleration integral model comparisons for DNB drill

	NULL	**Model 1**	**Model 2**	**Model 3**
(Intercept)	23833.434***	23473.741***	26095.674***	26050.219***
	(448.629)	(471.214)	(600.215)	(666.941)
PHV		-569.907*	-2095.469***	-2095.469***
		(263.467)	(343.002)	(343.002)
SEX (Male)			-6843.672***	-6843.672***
			(1149.294)	(1149.294)
SESSION (Post-season)				90.910
				(581.560)
SD (Intercept SUBJECT)	3512.487	3408.155	2549.284	2533.054
SD (Observations)	4194.179	4194.179	4194.179	4213.800
n	210	210	210	210
R^2 Marg.	0.000	0.030	0.202	0.202
R^2 Cond.	0.412	0.416	0.417	0.414
AIC	4182.4	4166.8	4122.1	4109.5
BIC	4192.4	4180.1	4138.8	4129.6
ICC	0.4	0.4	0.3	0.3
RMSE	3524.40	3537.45	3702.60	3714.80

Fixed effects coefficient estimates reported for null and iterative models with standard errors in parentheses. n = number of observations; SD (Intercept SUBJECT) = standard deviation of random intercepts; SD (Observations) = standard deviation of model residual error; R^2 Marg. = Marginal R^2; R^2 Cond. = Conditional R^2; AIC = Akaike information criteria; BIC = Bayesian information criteria; ICC = intraclass correlation coefficient; RMSE = Root-mean-squared error; + $p < 0.1$, * $p < 0.05$, ** $p < 0.01$, *** $p < 0.001$

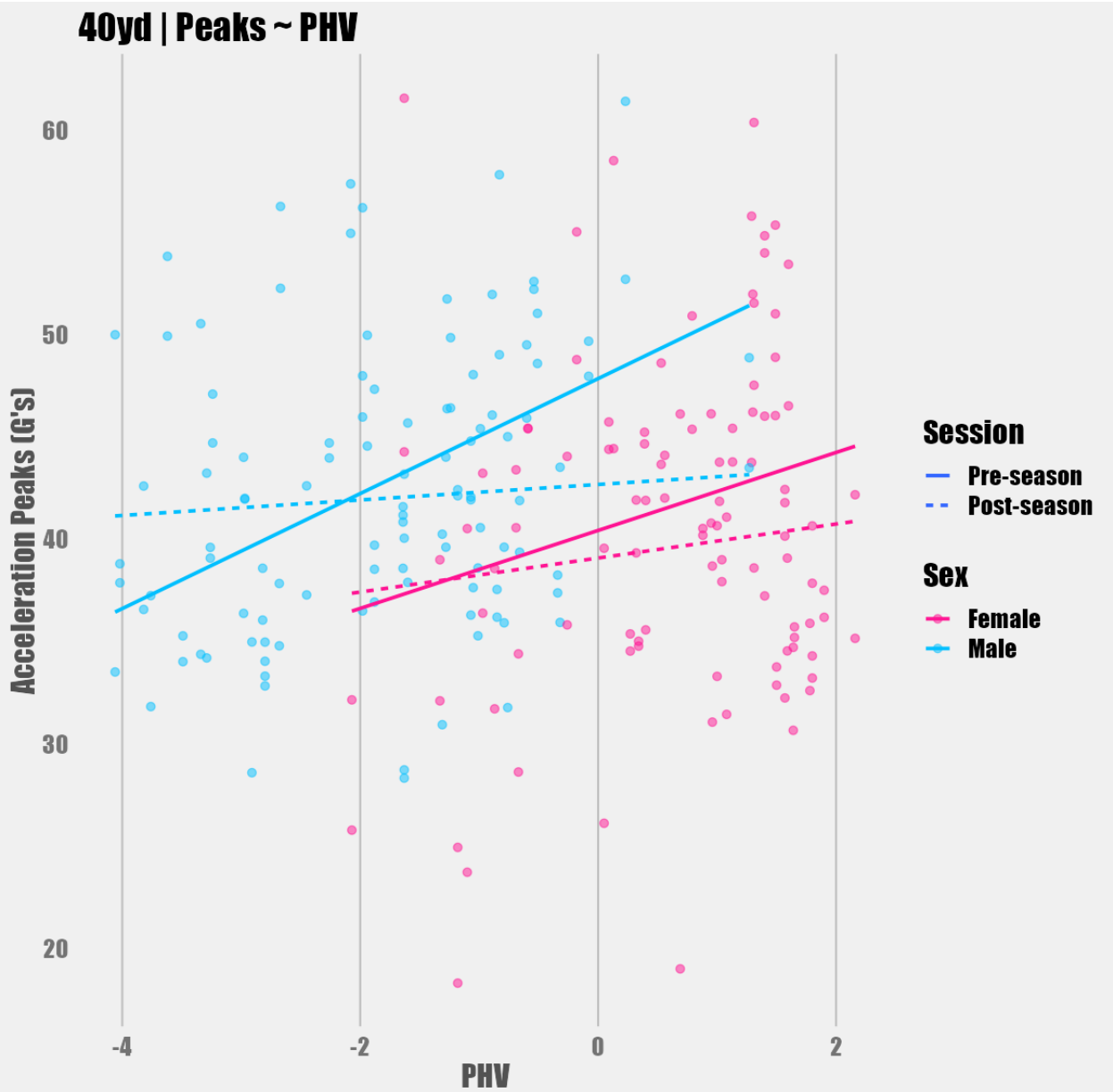

Figure 93: Acceleration peaks (G's) across PHV, sex, and testing session for the 40yd dash.

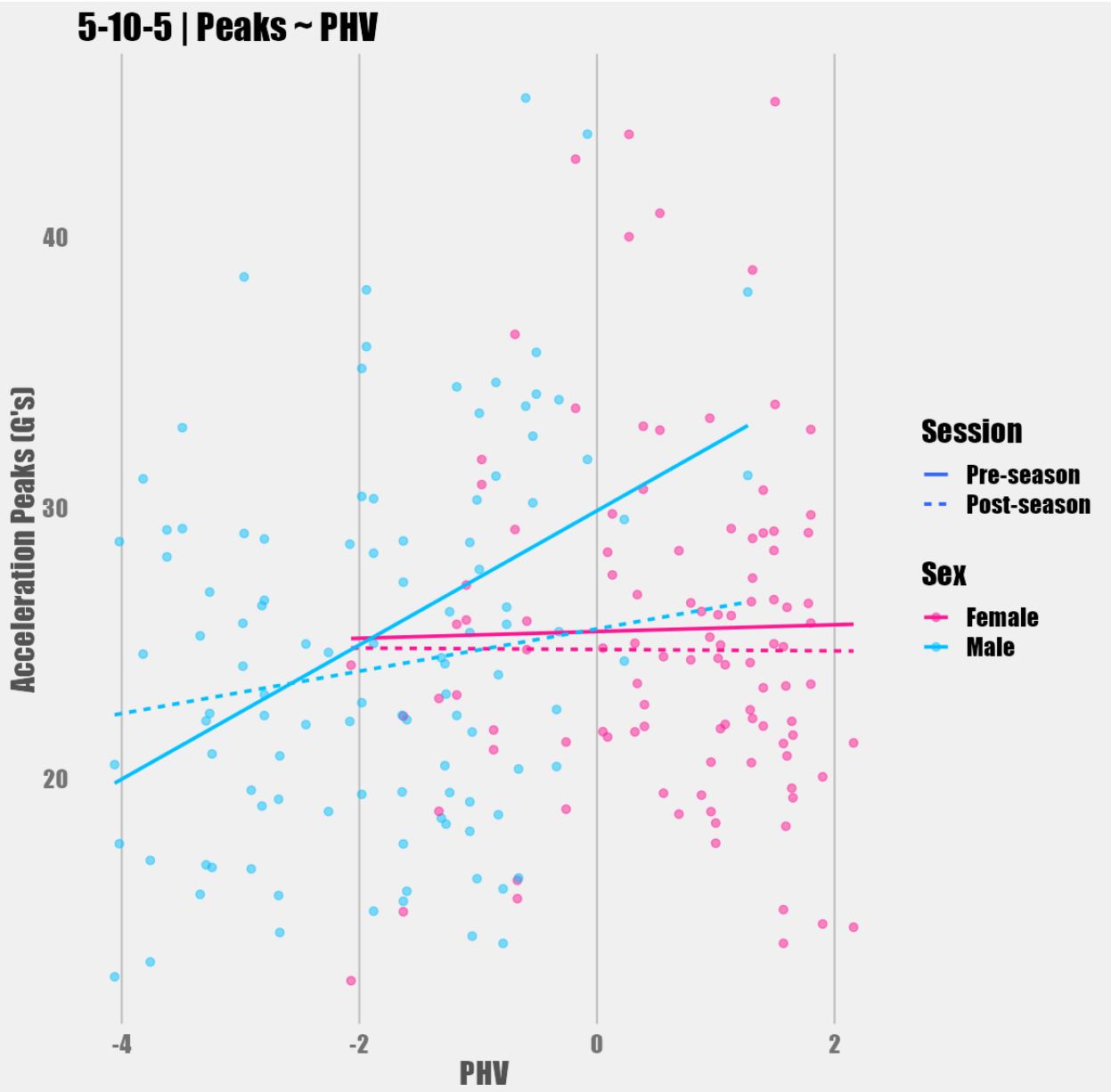

Figure 94: Acceleration peaks (G's) across PHV, sex, and testing session for the 5-10-5 shuttle drill.

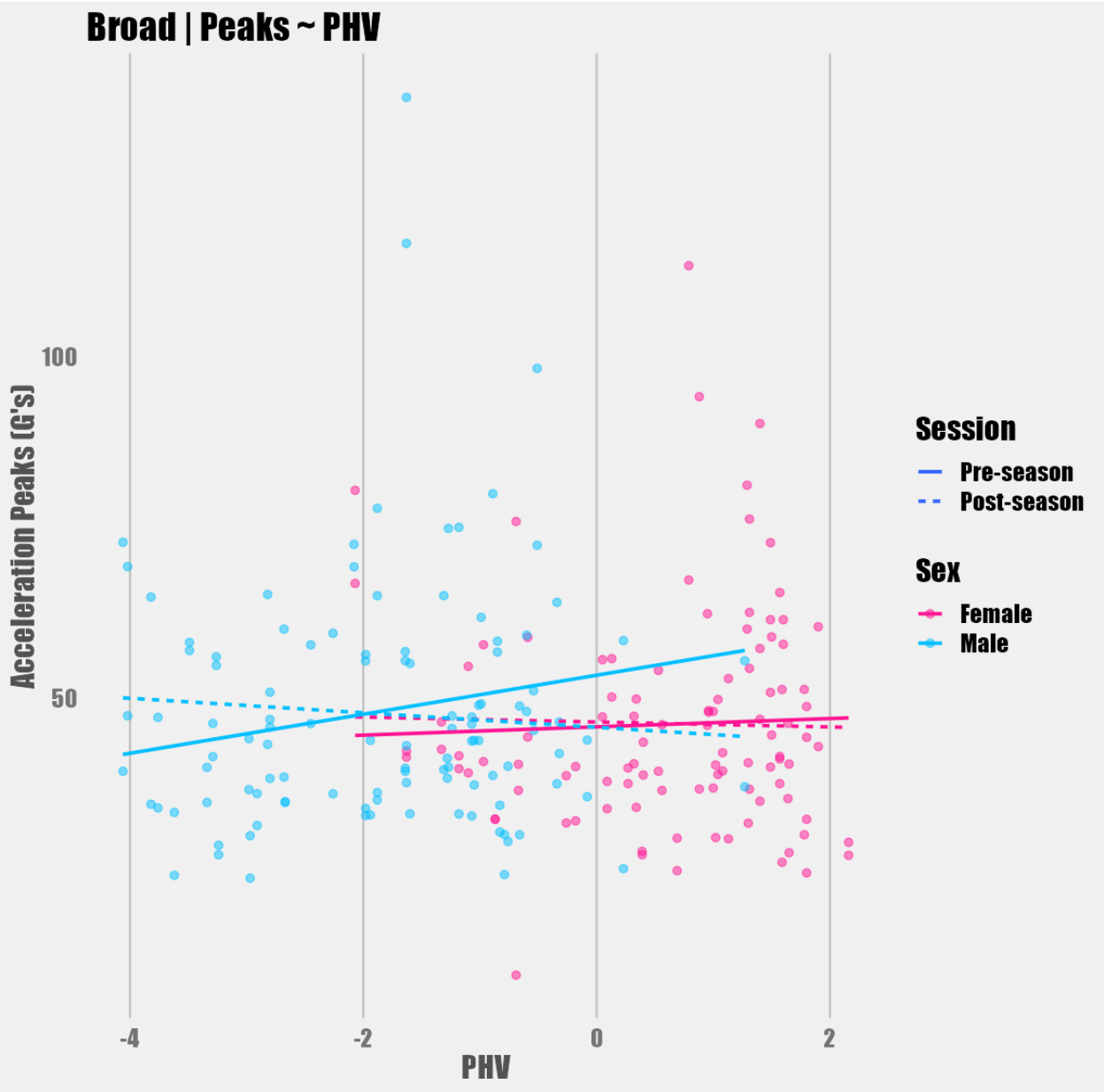

Figure 95: Acceleration peaks (G's) across PHV, sex, and testing session for the broad jump drill.

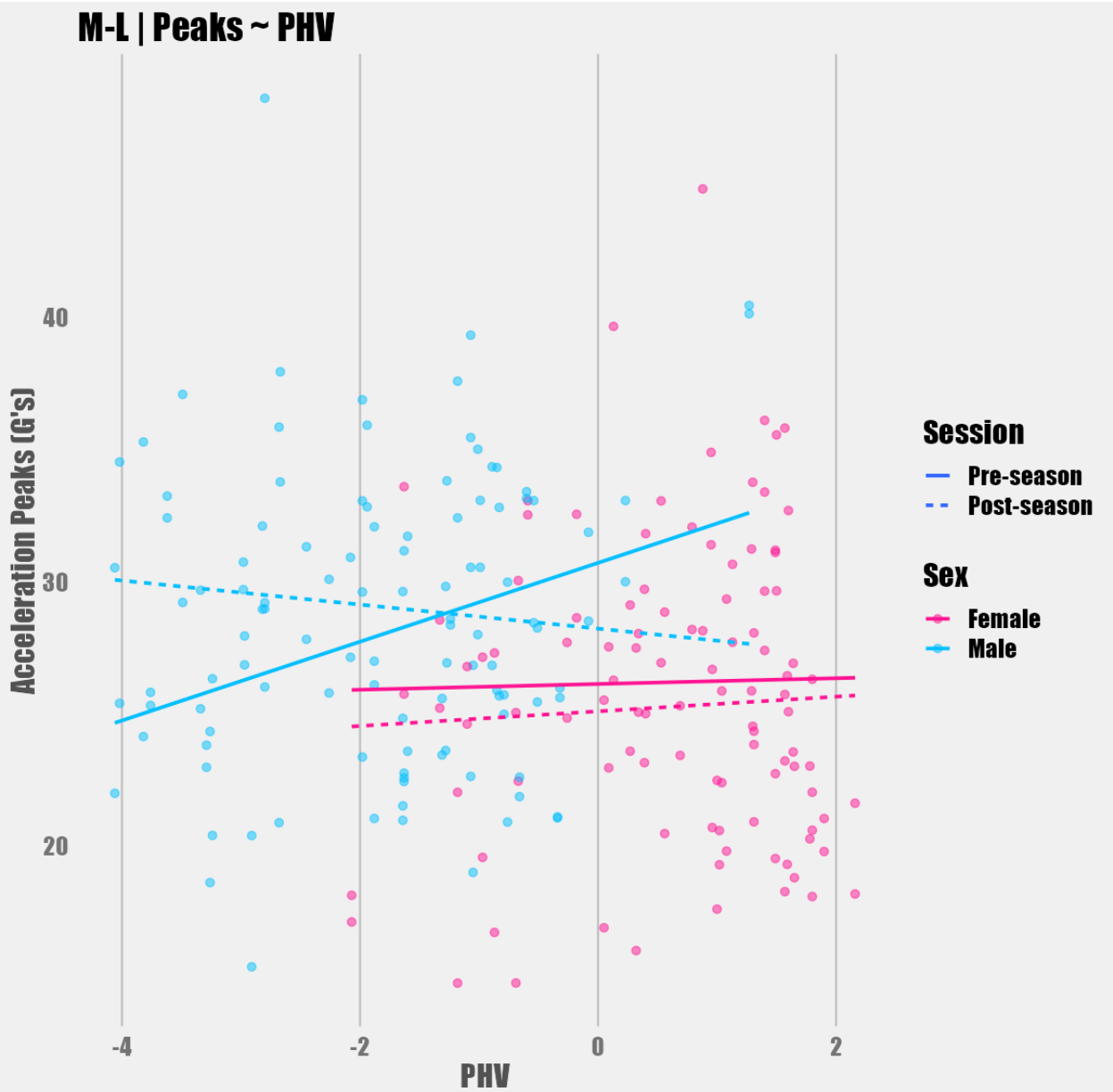

Figure 96: Acceleration peaks (G's) across PHV, sex, and testing session for the left M-drill.

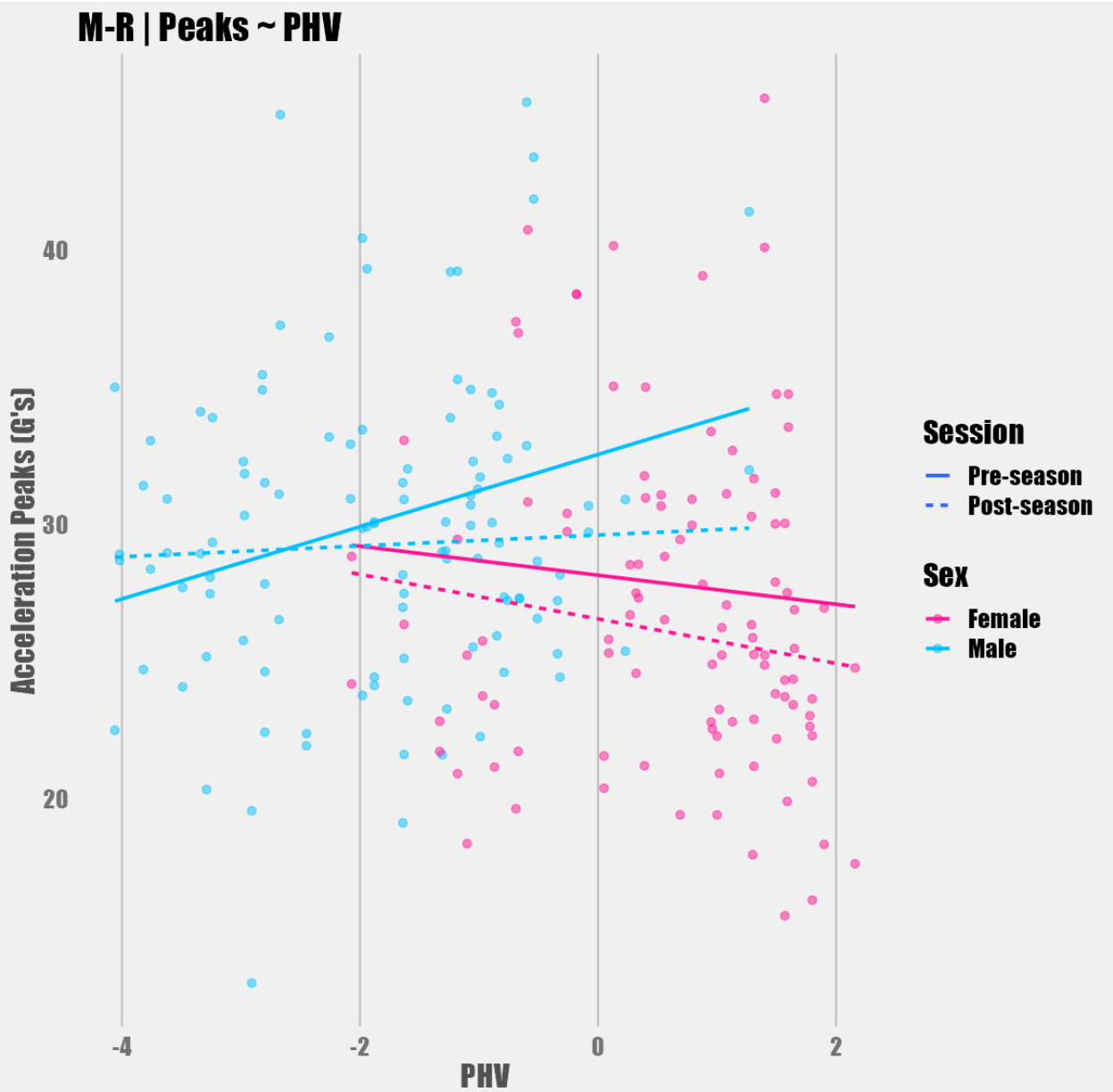

Figure 97: Acceleration peaks (G's) across PHV, sex, and testing session for the right M-drill.

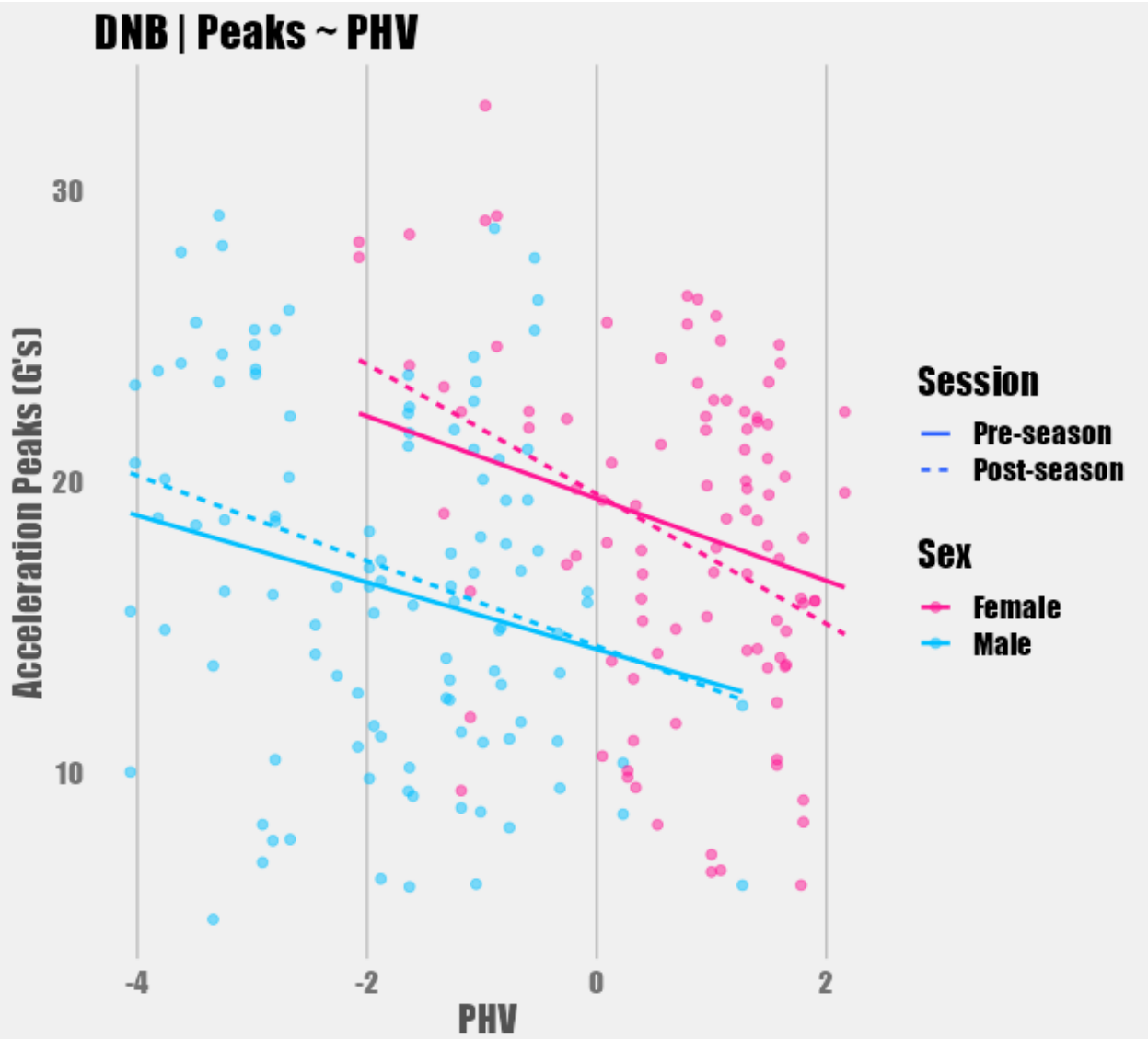

Figure 98: Acceleration peaks (G's) across PHV, sex, and testing session for the down-and-back jog.

Vita

Jake Melaro was born in Henderson, TN in 1993 and is the son of Joseph and Laura Melaro. He is the oldest of three children, with younger, less attractive siblings, Noah and Cami Melaro. Jake graduated from Chester County High School in Henderson, Tennessee in 2012 (shoutout to Bush Jr and the No Child Left Behind Act). After high school, Jake attended the University of Tennessee-Martin where he was conscripted into the Pi Kappa Alpha fraternity, got entangled in some shenanigans, and finally graduated with a Bachelors in Exercise Science and Wellness in 2017. Jake next fell ass-backwards into the University of Memphis where he earned his Master of Science degree in Health and Human Performance with a concentration in Exercise and Sports Science in 2019. Jake also "earned" a second Master's degree in Statistics during his time at the University of Tennessee, Knoxville in 2023. He completed his education at the University of Tennessee, Knoxville, earning a Doctor of Philosophy in Kinesiology and Sports Studies with a concentration in Biomechanics in 2023. Jake is a degenerate gambler who plans on using these degrees to get rich and retire to the beach with his girlfriend, Jenna, and their dog, Nala, well before he's earned the right to do so. He's still waiting for someone to thoroughly explain what entropy really is…